UNIVERSITY OF SOUTHAMPTON

Faculty of Medicine

Investigation of the Mechanisms Underlying the Effect of Oleic Acid and Docosahexaenoic Acid on DNA Methylation in Jurkat Cells

DOI: 10.5258/SOTON/T0013

by

José Eduardo Pérez Mojica

ORCID ID 0000-0003-4123-0649

Thesis for the degree of Doctor of Philosophy

March 2019

UNIVERSITY OF SOUTHAMPTON

ABSTRACT

FACULTY OF MEDICINE

Doctor of Philosophy

INVESTIGATION OF THE MECHANISMS UNDERLYING THE EFFECT OF OLEIC ACID AND DOCOSAHEXAENOIC ACID ON THE DNA METHYLATION IN JURKAT CELLS

by José Eduardo Pérez Mojica

There is evidence that olive oil, rich in oleic acid (OA), and fish oil, rich in docosahexaenoic acid (DHA), can modify the DNA methylation in human blood cells *in vivo*. However, the mechanisms underlying such effect are not well understood. To address this, a model to study DNA methylation changes was developed using the *in vitro* treatment of Jurkat cells with OA or DHA. Analysis showed that 15 μM OA or DHA treatment for eight days altered the DNA methylation of 563 or 1596 CpG sites (294 or 508 increased), respectively, using the Infinium MethylationEPIC BeadChip. Only 78 CpG sites were altered in common by both treatments. Further characterisation of 5 candidate CpG sites showed that DNA methylation changes were just significant after the 3rd day of DHA treatment which suggested and indirect mechanism. Pathway analysis of genes with at least one CpG site with altered DNA methylation by OA or DHA treatment (348 or 935, respectively) showed an enrichment of genes under the control of peroxisome proliferator-activated receptor alpha (PPARα) in DHA-treated cells only. PPARα has been reported to participate in the global hypermethylation of THP1 monocytes induced by arachidonic acid treatment. However, treatment of Jurkat cells with PPARα agonist GW7647 or PPARα antagonist GW6471 showed no difference in the DNA methylation of 5 candidate CpG sites analysed here by pyrosequencing. Therefore, other factors related to DNA methylation such as chromatin modification of histones and DNA motifs were investigated. Results showed that H3K4me3 was decreased in 5 candidate regions that changed DNA methylation status. Motif analysis indicated that sequences in the proximity of CpG sites that changed methylation were enriched in response elements including those for transcription factor SP1 and SP3. To further characterise the participation of transcription factors, transcriptome changes by OA or DHA were assessed using the HumanHT-12 v4 Expression BeadChip. Analysis showed that DHA, but not OA treatment, downregulated *SP3* mRNA and altered the activity of different transcription factors and enzymes. Together, results showed in this thesis suggest that DNA methylation changes by OA or DHA showed specificity, took more than three days to be established and may be associated with decrease H3K4me3 and the activity of different transcription factors and enzymes.

Contents

List of Figures

List of Tables

Declaration of Authorship

I, ……José Eduardo Pérez Mojica…….

declare that this thesis and the work presented in it are my own and has been generated by me as the result of my own original research.

INVESTIGATION OF THE MECHANISMS UNDERLYING THE EFFECT OF OLEIC ACID AND DOCOSAHEXAENOIC ACID ON THE DNA METHYLATION IN JURKAT CELLS.

I confirm that:

1. This work was done wholly or mainly while in candidature for a research degree at this University;

2. Where any part of this thesis has previously been submitted for a degree or any other qualification at this University or any other institution, this has been clearly stated;

3. Where I have consulted the published work of others, this is always clearly attributed;

4. Where I have quoted from the work of others, the source is always given. With the exception of such quotations, this thesis is entirely my own work;

5. I have acknowledged all main sources of help;

6. Where the thesis is based on work done by myself jointly with others, I have made clear exactly what was done by others and what I have contributed myself;

7. None of this work has been published before submission.

Signed: …….

Date: …….

Acknowledgments

The work and experiments carried out in the current thesis were possible thanks to several persons that help me out during this journey called PhD.

In the first place, my appreciation to The National Council of Science and Technology (CONACYT) (Mexico) and The Medical Research Council (United Kingdom) for the financial support to this project. I would like to thank all my supervisors Professor Graham C. Burdge, Professor Karen A. Lyllicrop, Professor Philip C. Calder and Professor Cyrus Cooper. They all taught me, directly and indirectly, many valuable things about research. The project, as it was, would not have been possible without their input in the different fields. I would like to specially thank my main supervisor Graham for giving me the opportunity to be part of his research group, the guidance through the whole PhD and the patience with me writing this thesis.

I also would like to thank all members of the research group that I was luckily part of. My appreciation to all of them which were accessible to clarify or discuss some of my doubts about experiments and results. They were available to help me whenever possible since the day I arrived at the lab up to the thesis writing process. Thanks to Dr Samuel Hoile, Dr Leonie Price, Dr Rebecca Clarke-Harris, Dr Robert Murray, Dr Eloïse Cook, Dr Mark Burton, Dr Elie Antoun, Miss Nevena Krstic and Dr Negusse Tadesse Kitaba. Particularly mentions to Dr Charlene Bailey for the induction to cell cultures and fatty acid determination by gas chromatography. Dr Annette West for the assistance in gas chromatography experiments. Dr Nicola Irvine and Dr Emma Garratt for the introduction and support in the evaluation of DNA methylation by pyrosequencing. Dr María Carmen de Andrés González for the counselling in all steps that are part of chromatin immunoprecipitation assays and Dr Faisal Rezwan for his advice in motif analysis when I was utterly lost in this field.

My acknowledgments extent not only to those persons that help me in the experimental work performed but to those that accompanied and motivated me in this journey. Good friendships were established indeed and were an essential part to keep me encouraged and stress out in the not too good moments. Big thanks to the ”taco representatives” Ana C. Aranda Jan, N. Alejandra Vergara Lope Gracia, Enrique Cuan Urquizo, Pedro García García, Anais Vermonden Thibodeau, Gregorio C. Martínez Jiménez; the ”pisco representatives” Carina A. Valenzuela Avendaño, Félix Catalán Arenas; the ”arepa representatives” L. Yurani Moreno Rueda, Lina M. Zapata Restrepo; and the ”scone representatives” Rose Owen and Luke Day. No doubts that apart from the knowledge acquired, this PhD was enriched in good experiences. I would like to thank specially to Reyna S. Peñailillo Escarate for her support since the day I started my PhD all the way until the end of it. All sciencing, talks, tea breaks

and shared experiences were lovely and with no doubt a great support. Definitely, these four years would have been very different without her.

Last but not least, I would like to give recognition to my family, which supported my decision to study a PhD abroad. To my brothers, Juan Manuel and Humberto to be there in their own particular way, and mostly to my mother, Julia. It was difficult for her to see me leave to another country to study. Huge thanks mom for always being there supporting me. You have always been an essential part of my life.

(Spanish translation of last paragraph) Por último, quisiera dar reconocimiento a mi familia la cual apoyo mi decisión de estudiar el doctorado en el extranjero. A mis hermanos, Juan Manuel y Humberto por estar ahí en su manera muy particular, y principalmente a mi madre, Julia. Fue difícil para ella verme partir para estudiar en otro país. Muchas gracias mamá por estar siempre ahí. Siempre has sido una parte esencial en mi vida.

Abbreviations

16:0	Palmitic acid
16:1n-7	Palmitoleic acid
18:0	Stearic acid
18:1n-9	Oleic acid
20:4n-6	Arachidonic acid
20:5n-3	Eicosapentaenoic acid
22:6n-3	Docosahexaenoic acid
5caC	5-carboxylcytosine
5fC	5-formylcytosine
5hmC	5-hydroxymethylcytosine
5mC	5-methylcytosine
AA	Arachidonic acid
ANOVA	Analysis of variance
ATP	Adenosine triphosphate
BER	Base excision repair
CFP1	CXXC finger protein 1
ChIP	Chromatin immunoprecipitation
CLA	Conjugated linoleic acid
CMV-IE	human cytomegalovirus immediate early
CO_2	Carbon dioxide
CoA	Coenzyme A
CpGi	CpG island
CpH	Non-CpG methylation
CTCF	CCCTC-binding factor
CYP4	Cytochrome P450 family 4
dH2O	Deionised water
DHA	Docosahexaenoic acid
DMPs	Differentially methylated positions
DMRs	Differentially methylated regions
DNA	Deoxyribonucleic acid
DNAm	DNA methylation
DNMT	DNA methyltransferase
DNMT1	DNA methyltransferase 1
DNMT3A	DNA methyltransferase 3 alpha
DNMT3B	DNA methyltransferase 3 beta
DNMT3L	DNA methyltransferase 3 like
DREME	Discriminative Regular Expression Motif Elicitation
EDTA	Ethylenediamine tetra-acetic acid
ELOVL	Elongation of very long chain fatty acid

ENCODE	The Encyclopedia of DNA Elements
EPA	Eicosapentaenoic acid
FA	Fatty acids
FADS2	Fatty acid desaturase 2
FAME	Fatty acids methyl esters
FASN	Fatty acid synthase
FDR	False discovery rate
gDNAm	Global DNA methylation
H19	noncoding RNA H19
H_2O	Water
H3K36me3	Histone H3 tri-methylated lysine 36
H3K4me0	Histone H3 unmethylated lysine 4
H3K4me3	Histone H3 tri-methylated lysine 4
HAT	Histone acetyltransferase
HDAC	Histone deacetylase
HDL	High-density lipoprotein
HEK293	Human embryonic kidney cells
HeLa	Henrietta Lacks endocervical adenocarcinoma cell line
HOCOMOCO	HOmo sapiens COmprehensive MOdel COllection
HOMER	Hypergeometric Optimisation of Motif EnRichment
HUVEC	Human umbilical vein endothelial cells
IBM SPSS®	International Business Machines, Statistical Package for the Social Sciences®
IGF2	insulin-like growth factor 2
IPA®	Ingenuity® Pathway Analysis
KLF	Krüppel-like factor
LDL	Low-density lipoprotein
LINE-1	Long interspersed nuclear elements 1
LTB_4	Leukotriene B4
LXR	liver X receptor
MCF-7	Human breast adenocarcinoma cell line
MeCP2	methyl-CpG-binding protein 2
MEFs	Mouse Embryonic Fibroblasts
MEME	Multiple EM (Expectation maximisation algorithm) for Motif Elicitation
$NADP^+$	Nicotinamide adenine dinucleotide phosphate
NADPH	Dihydronicotinamide-adenine dinucleotide phosphate
MUFA	Monounsaturated fatty acid
NCI-H460	Human lung carcinoma cell line
ncMMR	Non-canonical mismatch repair
NER	Nucleotide excision repair

O_2	Oxygen
OA	Oleic Acid
PBMCs	Peripheral blood mononuclear cells
PBS	Phosphate-buffered saline
PCA	Principal component analysis
PCR	Polymerase chain reaction
PEX7	Peroxisomal biogenesis factor 7
PG	Prostaglandins
PGE_1	Prostaglandins E1
PGE_2	Prostaglandins E2
$PGF_{2\alpha}$	Prostaglandins F2 alpha
PHYH	Phytanoyl-CoA 2-hydroxylase
PIC	protease inhibitor cocktail
PMSF	Phenylmethylsulfonyl fluoride
PPAR	Peroxisome proliferator-activated receptor
PPRE	Peroxisome proliferator-activated receptor response element
PTMs	Post-translational modifications
PUFA	Polyunsaturated fatty acid
PWWP	Pro-Trp-Trp-Pro motif
RAR	Retinoic acid receptor
RNA	Ribonucleic acid
RPMI-1640	Roswell Park Memorial Institute medium
RT-qPCR	Quantitative reverse transcription polymerase chain reaction
RXR	Retinoid X receptor
SAM	S-adenosyl methionine
SCD	Stearoyl-CoA desaturase
SIRT	Sirtuin
SP1	Specificity protein 1, transcription factor
SP3	Specificity protein 3, transcription factor
TAF	TATA-Box binding protein-associated factor
TDG	Thymine DNA glycosylase
TET	ten-eleven translocation
TP53	Tumour protein 53
TSS	Transcription start site
UHRF1	Ubiquitin-like, containing PHD and RING finger domains, 1
UTR	Untranslated region
WGBS	Whole-genome bisulphite-sequencing

Chapter 1

Introduction

1.1 Fatty acids

Fatty acids are hydrophobic organic compounds formed by carboxylic acid and an aliphatic chain that vary mainly from 4 to 28 carbons in nature[1]. Fatty acids belong to the lipid family that has been increasing in number as more lipids have been identified[2]. The current international classification of lipids incorporated eukaryotic and prokaryotic sources. Such classification includes in the same class fatty acids and their conjugates[2] (available in `http://www.lipidmaps.org`). For this thesis, only 2 out of the 17 subclasses are referred as fatty acids. This 2 subclasses are the commonly known saturated (straight chain fatty acids in the current nomenclature) and unsaturated fatty acids (Figure 1.1).

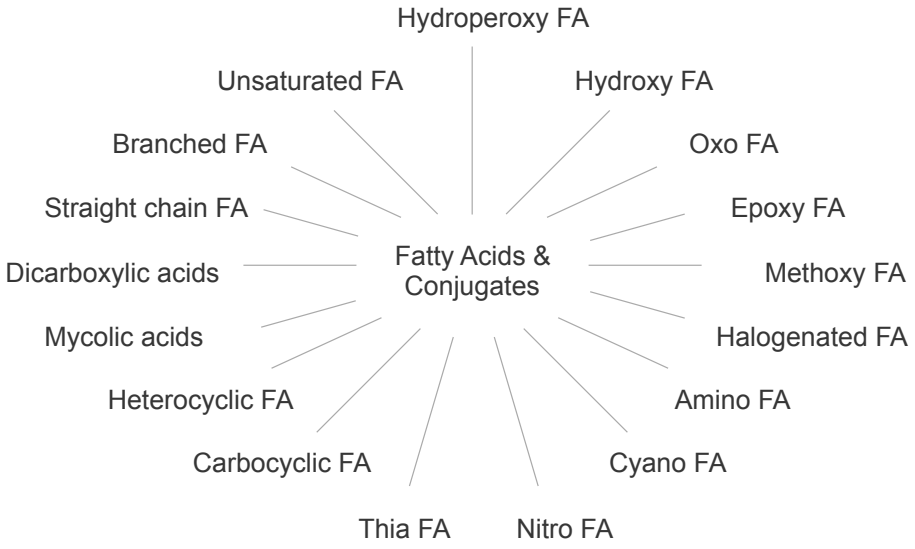

Figure 1.1: Current classification of fatty acids and conjugates includes 17 subclasses according to LIPID MAPS Lipidomics Gateway[2] (`http://www.lipidmaps.org`). FA, fatty acids.

Saturated fatty acids do not have any double bond in their structure whereas unsaturated fatty acids do. Depending on the number of double bonds, unsaturated fatty acids can be grouped as monounsaturated (MUFA), which have only one double bond; or polyunsaturated fatty acids (PUFA), that have more than one double bond. Alternatively, unsaturated fatty acids can be grouped according to the position of double bonds relative to the carboxylic group (Δ) or the methyl carbon end (ω or n)[3]. The most common groups of fatty acids by the position of double bonds are the n-3, n-6 and n-9 families, also known as omega-3, omega-6 and omega-9, respectively (Figure 1.2). Unsaturated fatty acids can also be classified in *cis* or *trans* fatty acids according to the chemical orientation of the double bond. Usually, the *trans* configuration is specified in fatty acids while the *cis* is assumed because it is the most recurring type of double bond in nature.

In addition to the number of double bonds, saturated and unsaturated fatty acids can be grouped depending on the total number of carbons which form the chain. Thus, short-chain ($<$ 8 carbons), medium-chain (6-8 to 12-14 carbons), long-chain (14-16 to 18-21 carbons) or very-long-chain fatty acids ($>$ 18-21 carbons) is a terminology commonly used in the literature[4–10]. The fatty acids included in each category may vary because there is not an official agreement among researchers.

A typical nomenclature for fatty acids is writing the number of carbons that constitute the fatty acid chain and the number of double bonds in the structure separated by a colon. In the case of unsaturated fatty acids, the number of double bonds may be followed by the correspondent omega ω / n family. For example, oleic acid which is an 18-carbon monounsaturated fatty acid with the double bond in omega-9 position is written as 18:1n-9. Docosahexaenoic acid which is a 22-carbon polyunsaturated fatty acid belonging to the omega-3 family is written as 22:6n-3 (Figure 1.2). In the case of the *trans* configuration, the location of the double bond with *trans* orientation can be specified after the fatty acid abbreviation. For example, the *trans* isomer of oleic acid, elaidic acid, can be written as 18:1 *trans*-9.

1.1.1 Fatty acid synthesis

Fatty acid synthesis *de novo* is a process widely spread in nature which is carried out by prokaryote and eukaryotes organisms[11]. This process has been shown to take place in two different subcellular compartments, the cytosol and mitochondrial matrix[12;13]. Fatty acid synthesis in the cytosol is referred as synthesis type I while that in the mitochondrial matrix as synthesis type II.

Type I fatty acid biosynthesis is well characterised in human cells. This process is carried out by a homodimer polypeptide coded by the fatty acid synthase gene (*FASN*)[14].

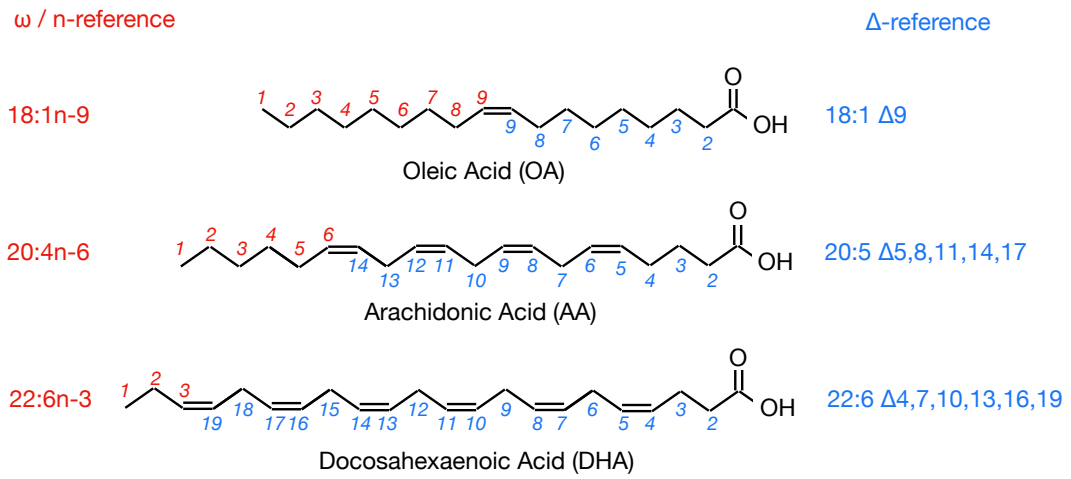

Figure 1.2: Examples of n-3, n-6 and n-9 families of unsaturated fatty acids are DHA, AA and OA, respectively. The n or ω reference (in red) and the Δ reference (in blue) are shown for each fatty acid.

FASN homodimer catalyses the condensation of acetyl-CoA with malonyl-CoA followed by further cyclic reactions to extend the fatty acid chain two carbons per cycle using as substrate malonyl-CoA[12]. *In vitro* fatty acid synthesis using radio-labelled [1-^{14}C]acetyl-CoA and [2-^{14}C]malonyl-CoA showed that the main product released from FASN homodimer was palmitic acid[15;16]. Such fatty acid may account for approximately 90% of the total fatty acids released[15;16]. The stoichiometry of type I fatty acid synthesis is summarised as follows[12].

$$[Acetyl-CoA] \; + \; 7\,[Malonyl-CoA] \; + \; 14\,[NADPH] \; + \; 14\,[H^+]$$

$$\downarrow$$

$$[Palmitic\ Acid] \; + \; 7\,[CO_2] \; + \; 8\,[CoA] \; + \; 14\,[NADP^+] \; + \; 6\,[H_2O]$$

Palmitic acid can be further elongated to produce long-chain and very-long-chain fatty acids by the action of different membrane-bonded elongases in the endoplasmic reticulum[17]. Besides, palmitic acid (16:0) and stearic acid (18:0) can be desaturated by stearoyl-CoA desaturase (SCD) in mammalian cells to produce palmitoleic acid (16:1n-7) and oleic acid (18:1n-9), respectively[18]. In humans, two isoforms of SCD gene have been characterized so far. *SCD1* that is present in metabolically active tissue (mainly adipose) and *SCD5* which mRNA expression has been shown to be lower or absent in some tissues compared with *SCD1*[19;20]. Oleic acid (18:1n-9), but not palmitoleic acid, has been shown to be further elongated to very long-chain monounsaturated fatty acids 20:1n-9, 22:1n-9, 24:1n-9 and $\geq$ 26:1. These are the only

unsaturated fatty acids that have been shown to be synthesized by mammalian cells *de novo*[17]. However, there is evidence that mammalian cells need polyunsaturated fatty acids to perform normal functions[21]. In humans, linoleic acid (18:2n-6) and α-linolenic acid (18:3n-3) are considered as essential[22;23] and they serve as substrates to synthesise other polyunsaturated fatty acids and lipid mediators by the cells[17]. A summary of the very-long-chain fatty acids synthesis in humans is shown in Figure 1.3.

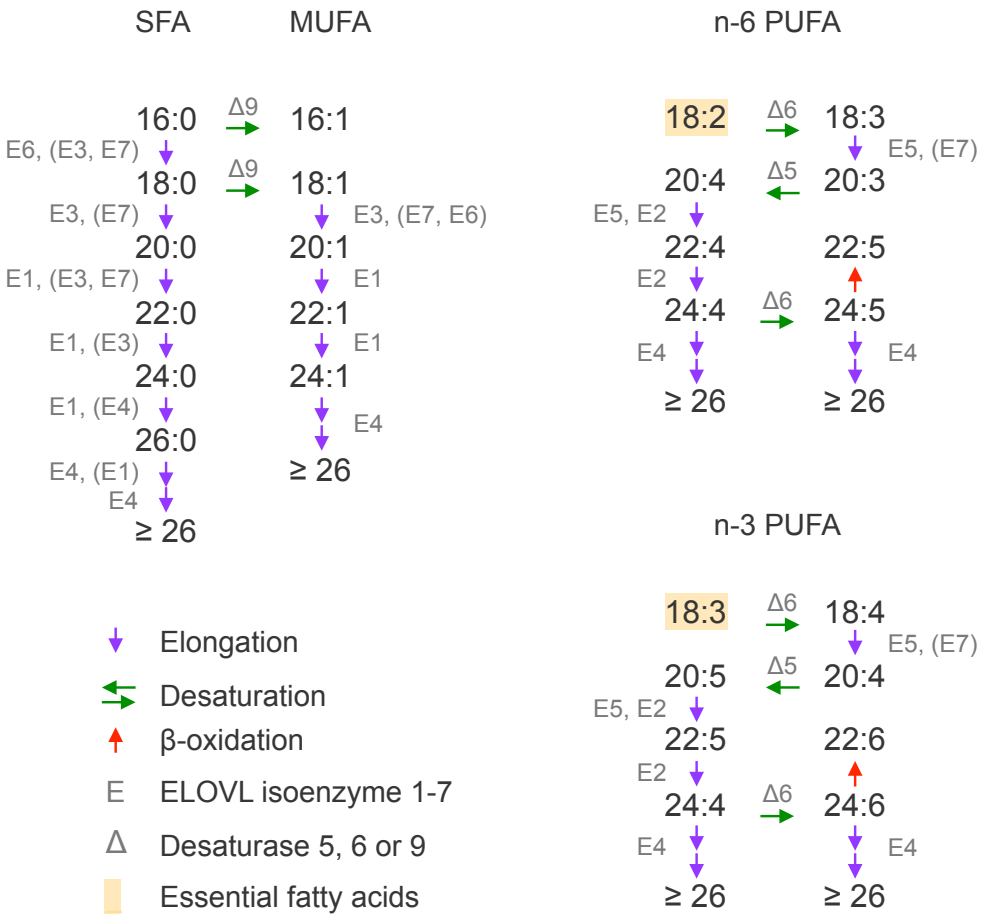

Figure 1.3: Synthesis of long-chain and very long-chain fatty acids in humans require different elongases and desaturases. Elongases in parentheses indicate weak catalytic activity in the reaction. Diagram modified from Sassa and Kihara, 2014[17]. FA, fatty acids; SFA, saturated FA; MUFA, monounsaturated FA; PUFA, polyunsaturated FA; ELOVL, Elongation of very long chain FA.

Type II fatty acid biosynthesis has been shown to produce fatty acids of length 6 to 18 carbons in *Neurospora crassa*, a member of the Kingdom Fungi[24]. At present, it is uncertain if type II fatty acid synthesis may take place and/or if this is metabolically relevant in mammalian cells.

1.1.2 Fatty acid oxidation

Fatty acid oxidation is the process of how fatty acids are broken down by the cells. Evidence has been shown that fatty acid oxidation can take place in the mitochondrial matrix and peroxisomes[25]. The oxidation of fatty acids has been shown to start by breaking down the α, β or ω bond. Such types of fatty acid oxidation are known as α-, β- or ω-oxidation, respectively. α- and ω-oxidation release one carbon while β-oxidation two carbons at a time because of the position of the double bonds that are broken down.

The study of α-oxidation has been associated with the phytanic acid accumulation identified in adults with the autosomal recessive Refsum disease[26]. Currently, the identification of human phytanoyl-CoA 2-hydroxylase (PHYH) which catalyzes the first step of phytanic acid oxidation[27;28]; the detection of a peroxisome targeted sequence in PHYH, that is recognized by peroxisomal biogenesis factor 7 (PEX7)[27] in peroxisomes; and the discovery that Refsum patients have mutations in *PHYH*[27;29;30] or *PEX7*[31;32] genes, suggests that α-oxidation is a process carried out exclusively by peroxisomes in humans. α-Oxidation of fatty acids other than that of phytanic acid has not been reported for humans.

In vitro experiments have been shown that fatty acids 12:0, 14:0, 16:0, 18:1n-9, 20:4n-6; leukotriene B_4 (LTB_4) and the phytyl tail of tocopherols and tocotrienols (vitamin E) can undergo ω-oxidation. This type of fatty acid oxidation has been shown to be catalysed by substrate-specific cytochrome P450 family 4 (CYP4) members using the human proteins expressed in *Escherichia coli*[33;34], microsomes from baculovirus-infected BTI-TN-5B1-4 cells[35] or cell cultures/suspensions[36;37]. Currently, *CYP4A11*, *CYP4A22*, *CYP4F3* and *CYP4F2* genes have shown ω-hydroxylase activity with specificity for individual fatty acids[33–36]. Other CYP4 members have been identified; however, the ω-hydroxylase activity of these orphans has not been characterised yet[38]. The biological function of ω-oxidation is unclear. It has been suggested that this may be a rescue pathway to metabolise certain fatty acids when α-oxidation is deficient such as phytanic acid in Refsum disease[38]. Supporting evidence is the identification of 3-methyladipic acid and 2,6-dimethyloctanedioic acid, both metabolites of phytanic acid ω-oxidation, in urine of patients with Refsum disease[39;40].

In comparison with α- and ω-oxidation, β-oxidation of fatty acids is well characterised in human cells[41]. In such process, fatty acids are broken down two carbons at a time inside the mitochondrial matrix or peroxisomes in the case of very long chain fatty acids. Each cycle of the β-oxidation involves sequential hydrogenation, hydration, a 2^{nd} hydrogenation and thiolysis by Acyl-CoA dehydrogenases, enoyl-CoA hydratases, 3-Hydroxyacyl CoA dehydrogenases and 3-ketoacyl-CoA thiolases, respectively. The specific enzymes catalysing such reactions dependent on the length of the fatty acid chain and sub-cellular localisation of the process (mitochondria or peroxisomes). One

difference between mitochondrial and peroxisomal β-oxidation is that the latter is not coupled with the generation of ATP through oxidative phosphorylation[42]. This is because electrons generated by peroxisomal β-oxidation are used to reduce O_2 generating H_2O_2 instead of delivering them to the respiratory chain[43]. The H_2O_2 in peroxisomes can be decomposed into $H_2O + O_2$ by the catalase and glutathione peroxidase to maintain an equilibrium between production and scavenging[42].

1.1.3 Fatty acid composition of human cells

Determination of the fatty acid composition of different tissues has been shown differences among cell types[44–46]. For example, oleic acid in human adults represents in average 18.5% of the total plasma lipids[44], 43.5% of white adipose tissue triglycerides[45] and 6.5% of brain phosphatidylethanolamine[46]. In comparison, docosahexaenoic acid constitutes the 1.3%[44] of the total plasma lipids, 0.4% of white adipose tissue triglycerides and 14% of brain phosphatidylethanolamine[46]. A list of the most abundant fatty acids in human plasma, adipose and brain tissue are shown in Table 1.1.

There is evidence that the fatty acid composition of cells can be modulated by exogenous fatty acids *in vivo*[47]. This suggests that the fatty acid composition of cells is a mixture of fatty acids synthesised by cells (endogenous) and those fatty acids taken up (exogenous) from the environment. Some *in vitro* work suggests that exogenous fatty acids are preferred over endogenous for membrane formation in proliferating human fibroblast, HeLa and NCI-H460 cells[48]. However, the proportion in which both endogenous and exogenous fatty acids contribute to the total lipids of cells is still unclear *in vivo*. Supplementation of individual fatty acids in the diet of healthy human volunteers has shown that they incorporate differently into different lipid fractions or tissues[49;50]. Besides, there is evidence that different tissues also take a different time to reach new constant levels of the fatty acids supplemented[45;49]. It seems that the new steady levels of fatty acids reached by supplementation are lost after stopping this in a lipid-fraction or cell-type specific manner too[4]. The importance of the fatty composition of cells is based on observations showing altered cell functions by a change in the fatty acid composition of cells[51;52]. To this respect, one of the best biological functions studied is the differential production of prostaglandins after incorporation of omega-6 or omega-3 fatty acids[53]. Some of the mechanisms and overall effects of fatty acids on human health are explained in the next section.

Table 1.1: Most abundant fatty acids in human plasma, adipose and brain tissue of adult humans.[44–46].

Trivial Name	Abbreviations		Plasma[a]	WAT[a]	Brain[a]
	Δ-reference	ω / n-reference			
Myristic	14:0	14:0	0.9	2.8	0.4
Palmitic	16:0	16:0	23	21.5	8.3
Palmitoleic	16:1Δ9	16:1n-7	1.9	7.2	0.2
Stearic	18:0	18:0	7	3.4	36.9
Oleic	18:1Δ9	18:1n-9	18.5	43.5	8.8
cis-Vaccenic	18:1Δ11	18:1n-7	1.86	ND	3
Linoleic	18:2Δ9, 12	18:2n-6	32	13.9	0.4
γ-linolenic	18:3Δ6, 9, 12	18:3n-6	0.8	0.8	ND
Gondoic	20:1Δ11	20:1n-9	0.1	ND	0.7
Dihomo-γ-linolenic	20:3Δ8, 11, 14	20:3n-6	1	0.2	1.6
Arachidonic	20:4Δ5, 8, 11, 14	20:4n-6	5.6	0.3	12.7
Adrenic	22:4Δ7, 10, 13, 16	22:4n-6	2.4	0.1	8.4
Osbond	22:5Δ4, 7, 10, 13, 16	22:5n-6	0.1	ND	2.7
DHA, Cervonic	22:6Δ4, 7, 10, 13, 16, 19	22:6n-3	1.3	0.1	14

[a] = % of total fatty acids in plasma or tissue.; Δ, carboxylic group; ω/n, omega; ND, no detected

1.2 Effects of fatty acids on human health

The first observations which began to show the impact that fatty acids have on health were reported in the early 1900's. McCollum and Davis described the effect that a diet prepared with or without lipids (either as egg's ether-soluble extracts or butter) had on the growth of rats. They showed that rats decreased weight during deprivation of lipids and partially recovered it when lipids were supplemented[54]. Sixteen years later, Burr and Burr showed that a fat-free diet starting at 21 days old induced skin lesions in feet and tail of rats at the age of ≈75 days[55]. Rats showed a further decline of weight at the age of ≈150 days and imminent death by the age of 253 days compared with lard-fed rats[55]. Detrimental effects of the fat-free diet were not avoided by daily supplementation of 0.65 gm of ether-soluble yeast extracts or with the non-saponifiable part of 70 mg cod liver oil. Only lard improved skin lesions and avoided animal death[55].

Another breakthrough that advanced understanding of the functions that fatty acids have on human health was the identification of prostaglandins (PG)[56]. These lipid mediators drove to the discovery of 18:2n-6 and 18:3n-3 essentiality by a serial number of experiments which described that 1) prostaglandins were derived from 20:3n-6, 20:4n-6 and 20:5n-3 fatty acids[57] and that in turn, 2) these fatty acids were synthesised from either linoleic acid (18:2n-6) or α-linolenic acid (18:3n-3)[58–60]. There is evidence that privation and later supplementation of essential fatty acids for at least five weeks can basically correct signs and symptoms observed by their deficiency in Wistar rats[61;62]. However, the administration of PGE_1, PGE_2 and $PGF_{2\alpha}$ up to 7 weeks has not shown to alleviate all symptoms of the essential fatty acid deficiency in the same Wistar rats[63]. The latter suggests that the "essential function" of 18:2n-6 and 18:3n-3 is not due to prostaglandins synthesis, at least in rats. The specific reason why 18:2n-6 and 18:3n-3 are essential in mammals remains to be established. In humans, deficiency of 18:3n-3 have been reported in patients undergoing gastric tube feeding or parental nutrition[22;23;64] and may not represent a problem for free-living subjects. Implementation of a dietary intervention in 428 infants showed that 18:2n-6 should represent at least 1.3% of the daily calories intake[65]. This is because 1.3% 18:2n-6 showed to avoid skin conditions and changes of the total fatty acids in serum observed in those infants that followed a diet with 0.04% or 0.07% of the calories provided by 18:2n-6[65]. In children and adults, it has been calculated using case-reports studies that 18:3n-3 should constitute 0.2-0.6% of total calories as these concentrations reverse symptomatology of deficiency in patients undergoing artificial nutrition support[22;23;64]. If such dietarian recommendations are enough for humans to reverse other possible effects that 18:2n-6 and 18:3n-3 deficiency may induce (e.g. altered fatty acid composition of the rat brain)[61] is unknown.

The detrimental effect of saturated fat on the cardiovascular system is one commonly known relationship that fatty acids have with human health[66]. Currently, this relationship is being revised and this is matter of debate as more recent meta-analysis studies have not found any significant association between increased saturated fat consumption and increased risk of coronary heart disease[67–69]. Instead, meta-analysis studies have shown that replacement of saturated fats by unsaturated fats is associated with decreased cardiovascular diseases[70–72]. Thus, it is possible that research in this subject may have been asking the wrong question and rather than a detrimental effect of saturated fat, a beneficial effect of polyunsaturated fatty acids may account for the link between saturated fat and cardiovascular disease identified in some studies. On the contrary, an association that has been continuously identified by different studies is the detrimental effect that *trans* fats have on cardiovascular health[66]. *trans* fats can be synthesized due to industrial processing of food such as hydrogenation of unsaturated fat, frying food using vegetable oil at high temperatures and bacterial biohydrogenation of unsaturated fatty acids inside ruminants' stomach[73]. Human clinical trials and meta-analysis have shown evidence that *trans* fats

increase up to 16% the risk of coronary disease[68;74] and alter low-density lipoprotein (LDL) cholesterol, high-density lipoprotein (HDL) cholesterol and triglyceride levels in human blood[75–77]. The effect that *trans* fats have on blood lipids has shown some specificity. For example, supplementation of *cis*-9, *trans*-11 conjugated linoleic acid (CLA) in healthy men reduced LDL cholesterol without any significant change in HDL levels[78]. On the contrary, *trans*-10, *cis*-12 CLA was found to decrease HDL cholesterol without changing LDL levels[78]. Other examples are the increased LDL and HDL by 18:1*trans*-11, increased LDL and decreased HDL (large subfraction only) by 18:1*trans*-9 and an absence of effect on LDL or HDL but decrease triglyceride levels by *cis*-9, *trans*-11 CLA identified in a double-blinded, randomised, crossover feeding trial[77]. Apart from clinical trials, there is evidence at population-level which has estimated a decrease in cardiovascular-related deaths after implementation of *trans* fat reduction policies in Argentina[79] and Denmark[80]. Analysis of the different types of public health policies, mostly in high-income counties, suggests that bans showed the stronger approach to reduce *trans* fats consumption[79].

Another effect that fatty acids have shown on human health is a decrease risk of cardiovascular disease by a diet rich in omega-3 fatty acids. The first trace of evidence was reported in 1972 which showed lower levels of total lipids, total cholesterol and triglycerides in 130 Greenland Eskimos (53 % females) compared with 130 (53 % females) Danish volunteers (including 25 female Greenland Eskimos living in Denmark)[81]. Greenland Eskimos were known to have a very low incidence of diabetes mellitus and ischaemic heart disease and, although limited in number, the study allowed comparison of female Eskimos living in Greenland (n = 35) and Denmark (n = 25)[81]. The latter suggested that the low incidence of ischaemic heart disease in Eskimos was not due to different genotype but environmental factors. Therefore, Greenland Eskimos diet was then analysed (n = 7) showing differences in the fatty acid composition, including 5.7 and 7.3 times more eicosapentaenoic acid (EPA) and DHA in Eskimos' diet, respectively[82]. EPA and DHA are omega-3 fatty acids that are found mainly in cold water fish such as salmon, mackerel, tuna and trout[83]. At present, there is more evidence that supports the hypothesis that omega-3 fatty acids can reduce the risk of cardiovascular disease than that which has shown no significant effects[84]. The lack of cardioprotection by omega-3 fatty acids found in some studies may be related to the already high fish consumption in the population studied[85;86]. The cardioprotective effect of omega-3 fatty acids has also been found in a meta-analysis[68]. Moreover, some studies indicate that EPA and DHA supplementation may reduce the death rate in patients with cardiovascular disease[87]. Such outcome suggests that besides prevention, these n-3 fatty acids may revert the cardiovascular damage[88]. However, these findings have not been replicated by others studies[87]. Currently, a beneficial effect of omega-3 fatty acids on cardiovascular health is widely accepted, although the effects on mortality associated with cardiovascular events are still unclear.

Efforts to elucidate the possible mechanisms underlying the effects of fatty acids in human health have been carried out. A brief overview of the current knowledge is summarised below.

1.2.1 Mechanisms

Fatty acids can modify cell functions by changing the composition and, consequently, the biophysical properties of the membrane bilayer[89;90], by providing substrates for the synthesis of second messengers including eicosanoids, diacylglycerol and phosphatidic acid[91] and by altering the transcription of target genes, primarily through the action of ligand-activated transcription factors of the peroxisome proliferator-activated receptor (PPAR) family[92;93]. The precise effect on cell function seems dependent on the structure of each fatty acid, and some of them may alter more cell functions than others[87].

1.2.1.1 Modulation of lipid-derived metabolites

The different production of prostaglandins and other lipid-derived metabolites by different fatty acids substrates is a well-described process in murine and human cells of the immune system. *In vitro* and *ex vivo* studies have shown that treatment of cells with omega-6 fatty acids induces a higher inflammatory response measured by increase pro-inflammatory lipid mediators and cytokines compared with an omega-3 fatty acid treatment[94–96]. Treatment of cells and mice with EPA and DHA have also shown to increase specific lipid mediators which have the capacity to assist in the resolution of inflammation such as resolvins, protectins and maresins[97;98]. These outcomes have been partially addressed and replicated *in vivo* in humans by clinical trials. Supplementation with EPA and DHA for 8 weeks showed to increase EPA and DHA-derived lipid metabolites levels in plasma and urine of healthy human volunteers (n = 19)[99]. There is *in vitro* evidence showing that increase EPA and DHA-derived lipid mediators leads to a decrease in those derived from AA as such fatty acids compete for the same enzymes[100]. A decrease in AA-derived lipid mediators has been shown in cancer patients whose showed a decrease in plasma PGE_2 levels after one 1-week supplementation with 2.4 g EPA and 1.2 g DHA daily[101]. PGE_2 is a pleiotropic prostaglandin that is considered to have a role in chronic inflammation[102]. Inflammation processes have been not only associated with cancer but also with other pathologies including diabetes and cardiovascular disease[103]. Thus, the current evidence supports that EPA- and DHA-derived lipid metabolites may account, at least partially, for the beneficial effects on human health observed in epidemiological studies.

There is evidence that altered lipid-derived metabolites levels observed *in vivo* after EPA + DHA supplementation are lost sometime after stopping supplementation[99].

The decrease in EPA- and DHA-derived metabolites is associated with the decreased levels of these fatty acids in cells after stopping the supplementation[4]. Therefore, evidence suggests that the possible beneficial effect on human health of EPA and DHA lipid-mediators may last as long as supplementation is continued.

1.2.1.2 Altered gene expression

The capacity of fatty acids to altered gene expression is well established. However, there is not a strong agreement about which genes are modulated by fatty acids *in vivo*. The study *in vivo* of altered gene expression by fatty acids in humans usually involves fatty acid supplementation in the diet followed by the collection of blood cells after a given time. The current evidence from clinical trials which have assessed genome-wide transcriptome changes by fatty acids in human leukocytes is not conclusive. Overall, altered transcripts by fatty acids do not show a specific pattern. A non-stringent analysis of twelve studies carried out in this work including men and women of all body mass index that followed supplementation during 1.5 to 6 months (one study for 6 hours[104]) and that assessed transcriptome changes in blood cells (mostly peripheral blood mononuclear cells (PBMCs)) identified a greater agreement in only 4 transcripts. The most recurrent transcripts changing in three out of the twelve studies analysed were triosephosphate isomerase 1 (TPI1, up-regulated)[105–107], CD40 (down-regulated)[106;108;109], microsomal glutathione s-transferase 1 (MGST1, down-regulated)[52;109;110] and hypoxia-inducible factor 1 alpha subunit (HIF1A, down-regulated)[105;109;111]. Such transcripts seem to be specifically regulated by n-3 fatty acids except for HIF1A which has been reported to change after a high-oleic acid sunflower oil in the same fashion as omega-3 fatty acids supplementation[111]. Gene expression changes by fatty acids in human blood cells that were reported in at least two out of the twelve studies analysed here are shown in Table 1.2.

Table 1.2: Gene expression changes by fatty acids in human blood cells. Observations from at least 2 out of 12 different clinical trials that have assessed genome-wide transcriptome changes in human leukocytes[52;104–115]

No apparent omega-3 specificity		
Up-regulated	ABCG1	ATP Binding Cassette Subfamily G Member 1
	CCL3L3	C-C Motif Chemokine Ligand 3 Like 3
	COX8A	Cytochrome C Oxidase Subunit 8A
	DDIT4	DNA Damage Inducible Transcript 4
	DGKQ	Diacylglycerol Kinase Theta
	DUSP1	Dual Specificity Phosphatase 1
	FOS	Fos Proto-Oncogene AP-1 Transcription Factor Subunit

	NDUFS6	NADH:Ubiquinone Oxidoreductase Subunit S6
	PCNA	Proliferating Cell Nuclear Antigen
	TSC22D3	TSC22 Domain Family Member 3
	UBA7	Ubiquitin Like Modifier Activating Enzyme 7
Down-regulated	ADAMTSL4	ADAMTS Like 4
	DUSP2	Dual Specificity Phosphatase 2
	HIF1A	Hypoxia Inducible Factor 1 Subunit Alpha
	LILRA2	Leukocyte Immunoglobulin Like Receptor A2

Apparent/possible omega-3 specificity		
Up-regulated	ALOX5AP	Arachidonate 5-Lipoxygenase Activating Protein
	ARID5B	AT-Rich Interaction Domain 5B
	BCL2	BCL2 Apoptosis Regulator
	CBR3	Carbonyl Reductase 3
	CBY1	Chibby Family Member 1 Beta Catenin Antagonist
	CCR5	C-C Motif Chemokine Receptor 5 (Gene/Pseudogene)
	CDC42SE2	CDC42 Small Effector 2
	CLK1	CDC Like Kinase 1
	CXCR3	C-X-C Motif Chemokine Receptor 3
	ECHDC1	Ethylmalonyl-CoA Decarboxylase 1
	ECI1	Enoyl-CoA Delta Isomerase 1
	FAM219B	Family With Sequence Similarity 219 Member B
	IVNS1ABP	Influenza Virus NS1A Binding Protein
	JUN	Jun Proto-Oncogene AP-1 Transcription Factor Subunit
	LOC80054	Uncharacterized
	MAP3K5	Mitogen-Activated Protein Kinase Kinase Kinase 5
	MAT2B	Methionine Adenosyltransferase 2B
	NFATC2IP	Nuclear Factor Of Activated T Cells 2 Interacting Protein
	PTGER4	Prostaglandin E Receptor 4
	THRA	Thyroid Hormone Receptor Alpha
	TPI1	Triosephosphate Isomerase 1
Down-regulated	ADAM9	ADAM Metallopeptidase Domain 9
	ADCY4	Adenylate Cyclase 4
	AHR	Aryl Hydrocarbon Receptor

ALDH4A1	Aldehyde Dehydrogenase 4 Family Member A1
BACH1	BTB Domain And CNC Homolog 1
BRF1	BRF1 RNA Polymerase III Transcription Initiation Factor Subunit
CD40	CD40 Molecule
CD55	CD55 Molecule (Cromer Blood Group)
CR1	Complement C3b/C4b Receptor 1 (Knops Blood Group)
CREB1	CAMP Responsive Element Binding Protein 1
CREB5	CAMP Responsive Element Binding Protein 5
CSF2RA	Colony Stimulating Factor 2 Receptor Alpha Subunit
CSF3R	Colony Stimulating Factor 3 Receptor
CYP51A1	Cytochrome P450 Family 51 Subfamily A Member 1
FADS1	Fatty Acid Desaturase 1
GCLM	Glutamate-Cysteine Ligase Modifier Subunit
GPX3	Glutathione Peroxidase 3
GSTP1	Glutathione S-Transferase Pi 1
HBEGF	Heparin Binding EGF Like Growth Factor
IL1R2	Interleukin 1 Receptor Type 2
KIAA0319L	KIAA0319 Like
LDLR	Low Density Lipoprotein Receptor
LIMK1	LIM Domain Kinase 1
MGST1	Microsomal Glutathione S-Transferase 1
NRAS	NRAS Proto-Oncogene GTPase
POLR1D	RNA Polymerase I And III Subunit D
PPARG	Peroxisome Proliferator Activated Receptor Gamma
RAB11FIP2	RAB11 Family Interacting Protein 2
RAMP2	Receptor Activity Modifying Protein 2
RSBN1L	Round Spermatid Basic Protein 1 Like
SCD	Stearoyl-CoA Desaturase
SERPINB9	Serpin Family B Member 9
SNORA12	Small Nucleolar RNA H/ACA Box 12
SNORD12C	Small Nucleolar RNA C/D Box 12C
SNORD13	Small Nucleolar RNA C/D Box 13
TGFA	Transforming Growth Factor Alpha
TLR2	Toll Like Receptor 2
VNN2	Vanin 2
ZNF669	Zinc Finger Protein 669
ZNF93	Zinc Finger Protein 93

The predicted pathways affected by fatty acid supplementation have been shown a better agreement than the individual transcripts with altered expression by fatty acids. Considering the same previous twelve studies, pathways affected by fatty acids on cells have been primarily related to energy flux (oxidative phosphorylation, β-oxidation and peroxisomal oxidation), ubiquitin-related protein modifications (ubiquitination, ubiquinone biosynthesis, protein folding and maturation) and nuclear receptors (PPARs). The greater agreement has been observed in immune response (chemokines and receptors, NFB signalling), inflammation, cell cycle, survival and apoptosis[52;104–112;114;115]. Apoptosis induced by fatty acids specifically in cancer cells by EPA or DHA is one of the main studied process. Growing evidence indicates that gene expression changes at mRNA and protein level are associated with the induced apoptosis of cancer cells by DHA treatment[116].

1.2.1.3 Epigenetic changes

Epigenetics is a relatively new field of research to understand how fatty acids induce some effects on cells. Epigenetics integrates the different pathways by which cells manage a control of RNA expression that is not related with changes on the DNA sequence. Such control of gene expression persist after mitosis, and sometimes after meiosis. The current knowledge about some epigenetic mechanisms is described in the next section and how these can be altered by fatty acids is addressed in section 1.3.3.

1.3 Epigenetics

Epigenetics study and refers to all those mechanisms that participate in the regulation of gene expression that are not related to the sequence of the DNA. In order to modulate gene expression, epigenetic mechanisms modify the instructions in the cell through specific signals or marks. The combination of epigenetic marks established in a particular cell is denominated epigenome. Alterations in the epigenome may be inherited through mitosis and/or meiosis. The heritable feature of the epigenetic marks has attracted much attention, and it is widely studied, although there is still much to understand[117].

Epigenetics includes different mechanism acting at transcriptional or post-transcriptional level. The most studied epigenetic modifications are DNA methylation, post-translational modifications (PTM) of histones and non-coding RNAs[118;119]. Current evidence shows that these epigenetic modifications are involved in differentiation, genome stability, genomic imprinting and inactivation of the X chromosome[120;121]. Changes in the usual epigenetic marks of cells have been associated with diseases[118]. For example, cancer presents marked epigenetic changes characterised by a global

DNA hypomethylation together with locus-specific DNA hypermethylation[118]. The current knowledge about DNA methylation is summarised next.

1.3.1 DNA methylation

DNA methylation is one of the epigenetic mechanisms which has shown to play a role in the expression of genes at the transcriptional level. This mark is heritable, at least mitotically, and could be regulated by environmental factors.

1.3.1.1 Establishment of DNA methylation

As its name indicates, DNA methylation describes the addition of a methyl group into the DNA. So far in some mammals, including humans, this modification has been shown to occur in adenine and cytosine nucleotides[122;123]. Relatively little is known about adenine DNA methylation while extensive experiments have been carried out on cytosine methylation. Cytosine methylation occurs only at the position 5 of the base (5-methylcytosine, 5mC). Most of the studies have focused on 5-methylcytosine that is preceded by a guanine nucleotide in 5' to 3' direction compared to other nucleotides. This locus is commonly known as CpG site which is the abbreviation of cytosine = C, phosphate = p and guanine = G. For this reason, DNA methylation in a CpG context is better understood compared to CpA, CpT or CpC methylation which are collectively referred to as non-CpG methylation or CpH.

Cytosine DNA methylation by bacterial DNA methyltransferase (DNMT) Hhal is a well described process that requires S-adenosyl methionine (SAM) as the universal donor of methyl groups. In summary, DNA methylation involves successive chain reactions that end when the cytosine's carbon at position 5 makes a nucleophilic attack on the methyl group of a SAM[124–128] (Figure 1.4). It is thought that the mechanism is similar for all DNMTs as catalytic domains share some homology[129]. In humans, there have been identified three DNMTs with catalytic activity coded by *DNMT1*, *DNMT3A* and *DNMT3B* genes[130]. Crystal structure of the catalytic domain of human DNMT3A showed to interact with the DNA similarly to bacterial Hhal DNMT which supports that DNA methylation reaction may be similar[131].

Northern blot analysis of *DNMT1*, *DNMT3A* and *DNMT3B* has been shown a similar pattern of mRNA expression in human adult heart, skeletal muscle, colon, kidney, liver, small intestine, placenta and PBMCs[133]. Because of this, it is believed that a common mechanism in differentiated cells regulates all three DNMTs. Some exceptions are brain, spleen and lung tissues showing *DNMT1* expression alone; and thymus tissue showing expression of *DNMT1* and *DNMT3B* only[133]. Different mRNA expression of DNMTs has also been identified throughout the cell cycle in human cells. The

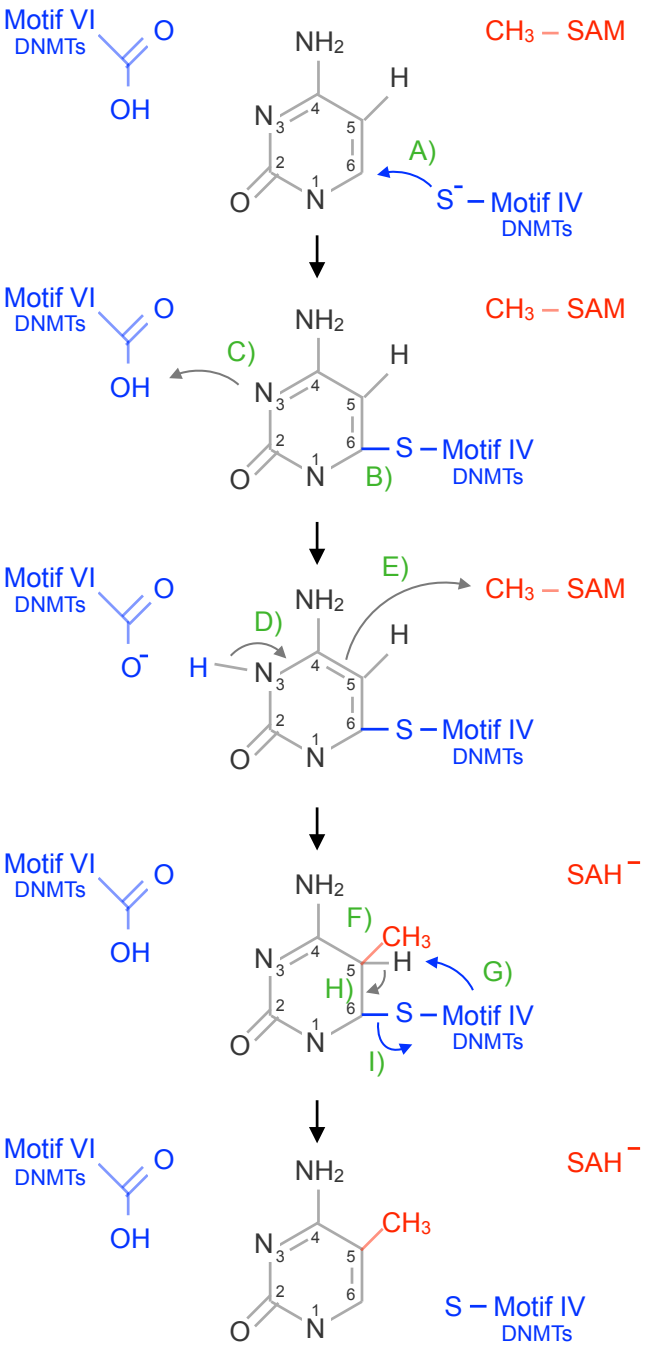

Figure 1.4: Catalysis of 5-methylcytosine by bacterial HhaI DNA methyltransferase (DNMT, in blue) requires as substrate cytosine and S-adenosylmethionine (SAM, in red) as co-factor. Biochemical evidence suggests that the sulfhydryl group of a cysteine in the catalytic motif IV of DNMTs performs a nucleofilic attack to cytosine's carbon 6 (A). This forms a covalent bond cytosine-DNMT (B) which induces protonation of cytosine's carbon 3 (C) using a glutamine residue in the catalytic motif VI of the DNMT. Protonation and deprotonation of cytosine's carbon 3 trigger a nucleophilic attack from cytosine's carbon 5 to SAM's methyl group (CH_3) (D, E). The covalent bond of the CH_3 with the cytosine (F) facilitates deprotonation of cytosine's carbon 5 (G) which resolves the covalent bond between cytosine-DNMT (H, I). After the reaction, SAM is converted to S-adenosylhomocysteine (SAH). References[124–126;132]

synchronisation and G1 arrest of T24 bladder tumour cells and normal bladder fibroblast LD98 showed that expression of DNMT1, and to a lesser extent DNMT3A and DNMT3B, peaked at S-phase[134]. The same synchronisation and G1 arrest of MCF7 breast cancer cells showed a similar high expression of DNMT1 and DNMT3B at S-phase while levels of DNMT3A remained constant[134]. This suggests that a higher expression of mainly DNMT1 is probably required at the S-phase to methylate newly synthesise DNA. Supporting this hypothesis is the preference that murine Dnmt1, but not Dnmt3a or Dnmt3b, have to methylate hemimethylated DNA compared with unmethylated DNA *in vitro*[135;136]. The preference of DNMT1 for hemimethylated DNA has also been observed *in vitro* using baculovirus-expressed human DNMT1[137]. DNMT1 is the only DNA methyltransferase that binds with ubiquitin-like, containing PHD and RING finger domains, 1 (UHRF1) which in turn, binds to hemimethylated DNA during S-phase[138]. UHRF1 is required to maintain normal CpG methylation as shown by a more than 70% decrease in DNA methylation of the intra-cisternal A-type particle (IAP) and 34% decreased in LINE-1 repetitive elements in mouse Uhrf1$^{-/-}$ embryonic stem cells[138]. Also, DNMT1 is the only DNA methyltransferase that binds to proliferating cell nuclear antigen (PCNA)[139]. However, DNMT1-PCNA binding rather than essential for copying the DNA methylation patterns in the newly synthesised DNA, only improves the efficiency of the process which was calculated in a two-fold increase using human HCT116 tumour cells[139]. Because of DNMT1 preference to methylate hemimethylated DNA and protein-protein interaction with UHRF1 and PCNA, DNMT1 is considered to mainly have a role in the maintenance of the DNA methylation patterns.

In contrast to Dnmt1, Dnmt3a and Dnmt3b have been shown similar efficiencies to methylate DNA templates that were either hemimethylated or unmethylated *in vitro*[135;136]. Both DNMT3A and DNMT3B can bind to DNMT3L, which sequence is homologous to the DNMT3 family but lacks the PWWP and the catalytic domain. DNMT3A and DNMT3B showed to increase their methyltransferase activity at least two-fold upon interaction with DNMT3L *in vivo* using co-transfection of expressing vectors in human 293 c18 kidney cells[140]. Human DNMT3B1 and DNMT3A2 were the isoforms that showed a more significant increase in activity when co-expressed with DNMT3L in comparison with DNMT3A or DNMT3B2[140]. Initial worked showed that murine Dnmt3L increased the affinity of Dnmt3a to bind DNA[141]. Currently, crystallography resolution of human DNMT3L have shown that two DNMT3L can bind to a DNMT3A homodimer (DNMT3L-DNMT3A-DNMT3A-DNMT3L)[131]. The catalytic domain of DNMT3A within the complex is maintained in an auto-inhibitory form until recognition of the H3K4me0 histone mark[131]. This mechanism is also supported by peptide interaction assays of DNMT3L with unmodified and modified histone tails which showed binding of DNMT3L only with H3K4me0, but not H3K4me1, H3K4me2 or H3K4me3[142]. In other words, DNMT3L-DNMT3A tetramer showed binding to chromatin when H3K4 was unmethylated (K_d = 2.1) and decreased when this residue

was methylated (H3K4me1 $K_d = 36.5$, H3K4me2 $K_d > 500$, H3K4me3 $K_d > 500$)[142]. The lack of recognition of methylated H3K4 by DNMT3L may explain the low DNA methylation levels in regions enriched with H3K4me2 *in vivo*[143]. The crystal structure of DNMT3L-DNMT3B-histone complex has not yet been resolved. However, because of the high homology between DNMT3B and DNMT3A, it is possible that a similar mechanism is involved.

Besides the methylation status of H3K4, emerging evidence shows that H3K36me3 may play a role in the direction of *de novo* DNA methylation in cells. Crystal structure of the PWWP domain of human DNMT3A and DNMT3B expressed in *Escherichia coli* have shown interaction with H3K36me3[144]. The genomic profiling of mouse Dnmt3a2, Dnmt3b1, H3K36me3 and RNA pol II occupancies have shown a global overlap[145]. This suggests that DNA methylation by Dnmt3 may be mediated by H3K36me3 marks, at least partially[145]. Further support for this hypothesis is the observation that regions deprived of the H3K36me3 in mouse stem cells, which become rich in H3K36me3 and transcriptionally active upon differentiation, also increase Dnmt3b occupancy[145].

The activity of all three Dnmts is essential for normal development as knockout mice of these enzymes fail to reach adult life. Dnmt1-specific knockout mice died during mid-gestation[146]. Similarly, Dnmt3b-specific knockout mice died at different stages before birth as a result of multiple developmental defects[147]. Dnmt3a knockout mice were the only ones that developed to term. However, mice did not reach more than four weeks of age[147]. Evidence from knockout mice suggests that each Dnmt has a specific and temporary role in the establishment of cytosine DNA methylation.

1.3.1.2 DNA demethylation

The removal of methyl groups from the DNA can be passively or actively accomplished. Passive DNA demethylation describes the loss of methyl groups by a failure in the copying of DNA methylation patterns in the newly synthesised DNA. This can be achieved by drugs, such as 5-azacytidine and 5-aza-2'-deoxycytidine, which are usually used for research purposes[148]. Currently, there are a few examples of passive DNA demethylation in mammalian cells. For instance, mouse embryos at two-, four- and eight-cell stages have shown approximately one-half decreased on DNA methylation. Such a decrease is observed only in the metaphase chromosomes of maternal origin using immunofluorescence for 5- methylcytosine[149]. A passive demethylation mechanism of the maternal genome is supported precisely by a decreased DNA methylation associated with cell division compared with the paternal genome which is rapidly demethylated by the first metaphase in mice[150]. DNA demethylation of the maternal genome in human embryos may not be passive as there has not been observed a progressively decreased in methylation between two- and eight-cell stages, nor significant

differences between DNA methylation of the paternal and maternal pronuclei[151].

In contrast to passive demethylation of the DNA, active demethylation is the process by which the activity of enzymes removes methyl groups. There are different possible mechanisms implicated in active demethylation, and they can be divided into two types for practicality. One type involves removal of the methylated cytosine alone and further insertion of an unmethylated cytosine by base excision repair (BER) mechanisms; or removal of several nucleotides, including the methylated cytosine, followed by insertion of new nucleotides by nucleotide excision repair (NER) or non-canonical mismatch repair (ncMMR) mechanisms. The second type of active DNA demethylation involves serial chemical modifications of the methylated cytosine starting by methylcytosine dioxygenases (TET family) enzymes that lead to removal of the methyl group without excision of the bases. There are examples of this type of active DNA demethylation in mammalian cells using *in vitro* experiments[152–154]. However, current evidence shows that the majority of DNA demethylation is a mixture of chemical modification of the methyl group followed by excision/mismatch repair.

BER, NER and MMR pathways are better known for repairing damaged DNA during all phases in the cell cycle. In this manner, BER, NER and MMR assured that DNA has no damaged bases or mismatches that could cause otherwise mutations or DNA breaks during DNA replication. The implication of these pathways on active DNA methylation in mammalian cells comes from evidence in plants[155]. However, BER, NER and MMR are currently not understood in the context of active DNA demethylation in mammalian cells. For reasons of clarity, only evidence from mammalian cells is reviewed below regarding active DNA demethylation.

BER pathway has shown to start by DNA glycosylases which achieve the removal of a damaged base primarily due to oxidation, deamination or alkylation[156;157]. In the context of DNA demethylation, human thymine DNA glycosylase (TDG) has shown to recognise and excise 5-formylcytosine (5fC) and 5-carboxylcytosine (5caC), but not 5-hydroxymethylcytosine (5hmC) *in vitro*. 5fC, 5caC and 5hmC are all modifications originated from 5-methylcytosine (5mC)[158;159]. Such evidence suggests that active demethylation by BER pathway is possible in human cells. Besides, single-turnover kinetics of TDG base excision activity showed that processing of guanine-5fC mismatch was 40% faster than guanine-thymine mismatch[159]. This suggests a possible main functional role of TDG on DNA demethylation.

NER pathway has also been implicated in active DNA demethylation. This is because the crystal structure of DNA with 5fC showed a change in the DNA's double helix compared with unmodified cytosine[160]. Such change in the DNA's structure suggested a helical underwinding[160] which is a type of DNA damage that may be resolved by NER[161]. So far, there is not a single clear example showing DNA demethylation mediated by NER mechanisms in mammalian cells.

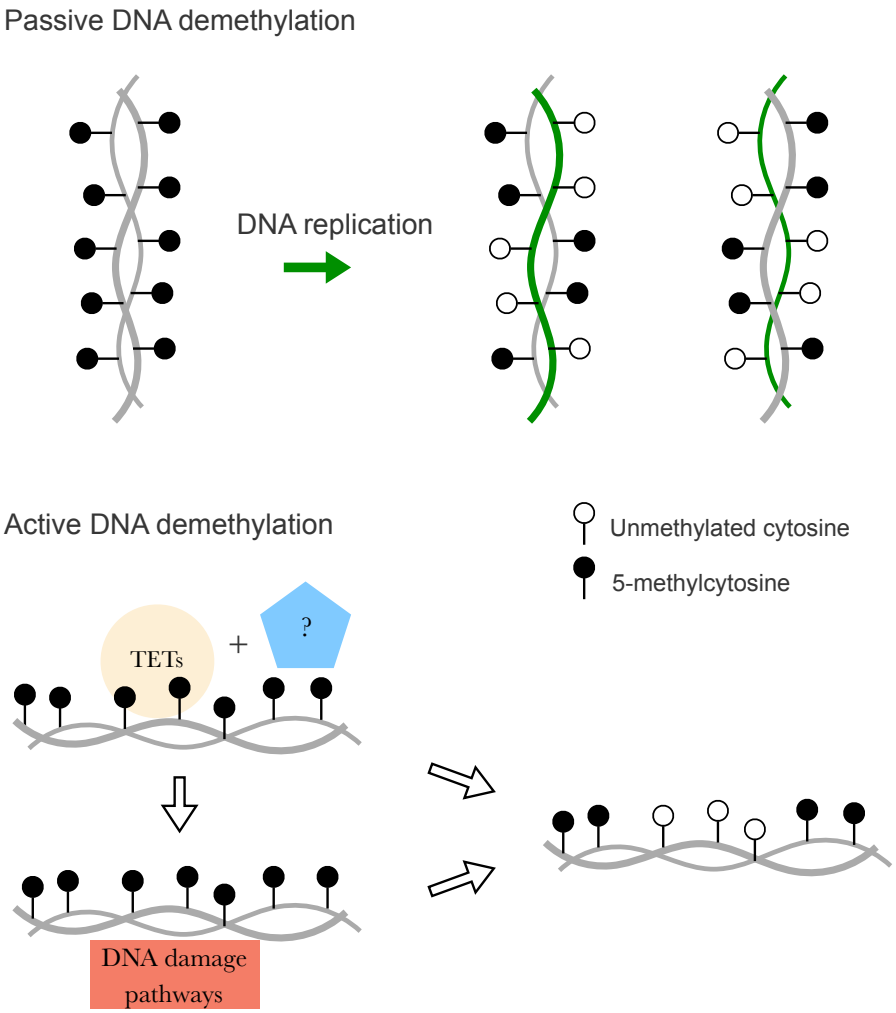

Figure 1.5: DNA demethylation in mammalian cells can be carried out by passive or active mechanisms. Passive DNA demethylation describes the failure in the copy of DNA methylation patterns in a newly synthesised DNA strand after replication. In comparison, active DNA demethylation refers to mechanisms independent of DNA replication. This type of demethylation can be achieved by chemical modification of the 5-methylcytosine by ten-eleven translocation (TETs) enzymes and possibly other proteins yet to be identified. Alternatively, 5-methylcytosine may be removed by DNA damage repair pathways and replaced by an unmethylated cytosine. At present, most of the DNA demethylation in mammalian cells seems to start with TET modification of the 5-methylcytosine and end with DNA damage repair pathways.

It has also been suggested that active DNA demethylation can be achieved through ncMMR[162]. In contrast to the canonical pathway, ncMMR is an S-phase-independent process which can be activated by N-methyl-N'-nitro-N-nitrosoguanidine (MNNG)[163]. This carcinogenic agent has shown to demethylate non-CpG cytosines in the telomerase reverse transcriptase (TERT) promoter using normal human gastric cells from a 42 old volunteer[164]. Although the study included a single sample and the mechanisms of TERT promoter demethylation were not addressed, this may represent the only association of ncMMR pathway with active DNA demethylation in human cells. At present, further experimental work needs to prove the involvement of a ncMMR pathway on active DNA methylation.

Active DNA demethylation by chemical modifications of the methylated cytosine was first reported in mammalian cells with the identification of human TET proteins function by Tahiliani *et al.,* in 2009[165]. Since then, different *in vitro* experiments showed that TETs mediates the conversion of 5mC to 5hmC, 5fC and 5caC[158;165–167]. The role of mammalian TET proteins in DNA demethylation was further supported by decreased or increased levels of 5hmC, 5fC and 5caC upon downregulation or upregulation of TETs proteins, respectively[165;167]. Regulation of TET proteins is still poorly understood. At present, there is evidence that vitamin C can change the effect that mouse Tet1 overexpression or deficiency have on MEFs' somatic cell reprogramming by an unknown mechanism[168]. Also, there has been identified that promoters of tumour suppressor genes of human solid-tumour samples were on average hypermethylated in hypoxic tumours compared with non-hypoxic ones[169]. *In vitro* experiments showed that hypoxia induced decreased TET activity which in turn resulted in hypermethylation of candidate gene promoters analysed[169]. Such results suggest that hypoxia in human and mouse tumours cells is another factor that may regulate TET activity.

There is some evidence showing that deamination mediated by activation-induced cytidine deaminase (AICDA or AID) may participate on DNA demethylation[162]. However, reported outcomes are contradictory and current evidence is not conclusive about the direct involvement of AICDA on DNA demethylation[162]. Spontaneous deamination of 5mC, but not unmethylated cytosine, leads to thymine[170] which may be then removed by TDG and followed the BER pathway. Further research needs to address if AICDA can actively deaminate 5mC which may followed then the BER pathway.

1.3.1.3 DNA methylation patterns and function in cells

In normal cells, the total amount of 5mC accounts for up to approximately 1% of all nucleotides in the human genome with some variations between tissues[171]. Besides tissue-specific methylation, 5mC is not randomly distributed in the DNA. Most of the

5-methylcytosine is observed on repetitive elements, which comprise more than 50% of the total CpG sites in humans[172–174]. Low levels of methylation (hypomethylation) of repetitive elements have shown to increase their expression and insertion into new genomic locations[175]. Therefore, DNA methylation is such sequences is believed to maintain chromosome structure and genome stability of normal cells[176].

Associations between cytosine methylation with gene expression have been described for intragenic regions, specifically gene bodies. Although the majority of intragenic regions are CpG-poor, methylation of these CpG sites frequently occurs[177]. Different studies have identified a positive correlation between intragenic DNA methylation with gene expression[178;179]. Therefore, it has been suggested that hypermethylation of the gene body may help to avoid spurious transcripts that may otherwise express[180]. In humans, such positive correlation seems to apply only to genes with low and medium-high levels of expression. The most highly expressed genes in humans show lower levels of intragenic methylation than medium-high expressed genes[177] (Figure 1.6).

Another association between DNA methylation and gene expression has been identified in clusters of CpG sites. These clusters are known as CpG islands (CpGi) and are usually unmethylated[181]. Although there is no general agreement, a CpGi can be defined as a sequence larger than 200 bp constituted mostly by cytosines and guanines with a CpG nucleotide frequency of more than 0.6 of the total C+G content[182]. CpGi are present in approximately 70% of human gene promoters[181]. Increased methylation (hypermethylation) of normally unmethylated CpGi in promoters has been related to decreased expression of such genes and vice-versa[183;184]. Therefore, it has been suggested that promoter methylation has an inverse relationship with transcription (Figure 1.6). However, evidence has also shown that the majority of CpGi remain unmethylated even when genes are not expressed or when they are located in intragenic regions[143;185]. Thus, it is possible that the relationship between promoter CpG methylation with gene expression may be due to the high number of genes with CpGi at promoter regions (70%[181]). At present, evidence suggests that CpG islands are protected from methylation in some way not well understood no matter their genomic location.

Cytosine methylation in a CpG context has been more studied than non-CpG methylation (or CpH) in cells. In human cells, it has been shown that both CpG and CpH methylation levels are cell-type specific. In average, reported CpG methylation varied from approximately 70% to 85% while CpH methylation from 0 to 8% using whole-genome bisulphite-sequencing (WGBS) of neuronal, brain and embryonic stem cells[179;186;187]. However, other studies have shown in general lower levels. Average CpG and CpH methylation varied from 55%-70% and 0%-3%, respectively, using reduce bisulphite sequencing representation of 20 human embryonic or induced stem cells lines and 10 different somatic cell types[188]. Such differences may arise due to

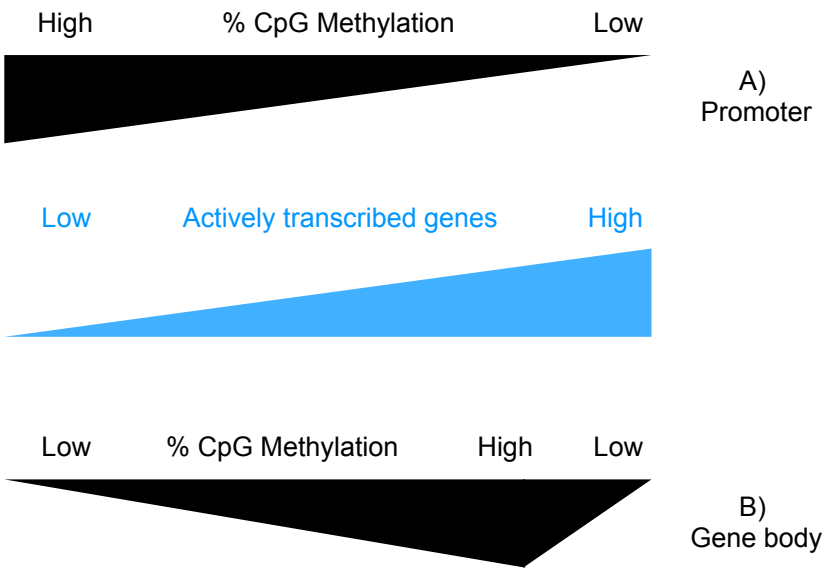

Figure 1.6: The relationship between expression of genes and 5-methylcytosine (5mC) of CpG sites at promoters shows that when one increases the other decreases (A). In contrast, 5mCpG at body regions increases while expression increases up to a medium-high level. After this, 5mCpG start to decrease while expression keep increasing (B).

the different methods[189] and cell types used. What seems clear is that averaged levels of CpH methylation are much lower than those in a CpG context. A more detailed analysis of the current evidence suggests that even when the average CpH methylation is much lower than that on CpG sites, the total number of CpH sites may be comparable or greater than the total number of methylated CpG sites[179;187]. For instance, WGBS of the human embryonic stem cell line H1 showed that 25% of the total 5-methylcytosines were in CpH context[179]. An even higher percentage has been identified in human oocytes which CpH number reached up to 60% of the total 5-methylcytosines at mature metaphase II using single-cell WGBS[187]. The reason underlying the low average CpH methylation and the moderate-to-high number of methylated CpH sites seems to be due to two factors. The first one is a higher number of CpH sites compared with the ≈28 million CpG sites in the haploid human genome[174]. The second one is that the majority of 5-methylcytosine in CpH sites have been shown to be hypomethylated (10-40% methylated) compared with CpG sites which are mostly hypermethylated (80-100%). Therefore, average methylation levels of CpG or CpH sites are just a reference, but not indicative of the genome-wide spreading of DNA methylation (Figure 1.7).

Although cytosine methylation in a CpG context has been studied for years, its biological function is still not entirely understood. In mammalian cells, most of the functions of DNA methylation derives from evidence on candidate genes or specific

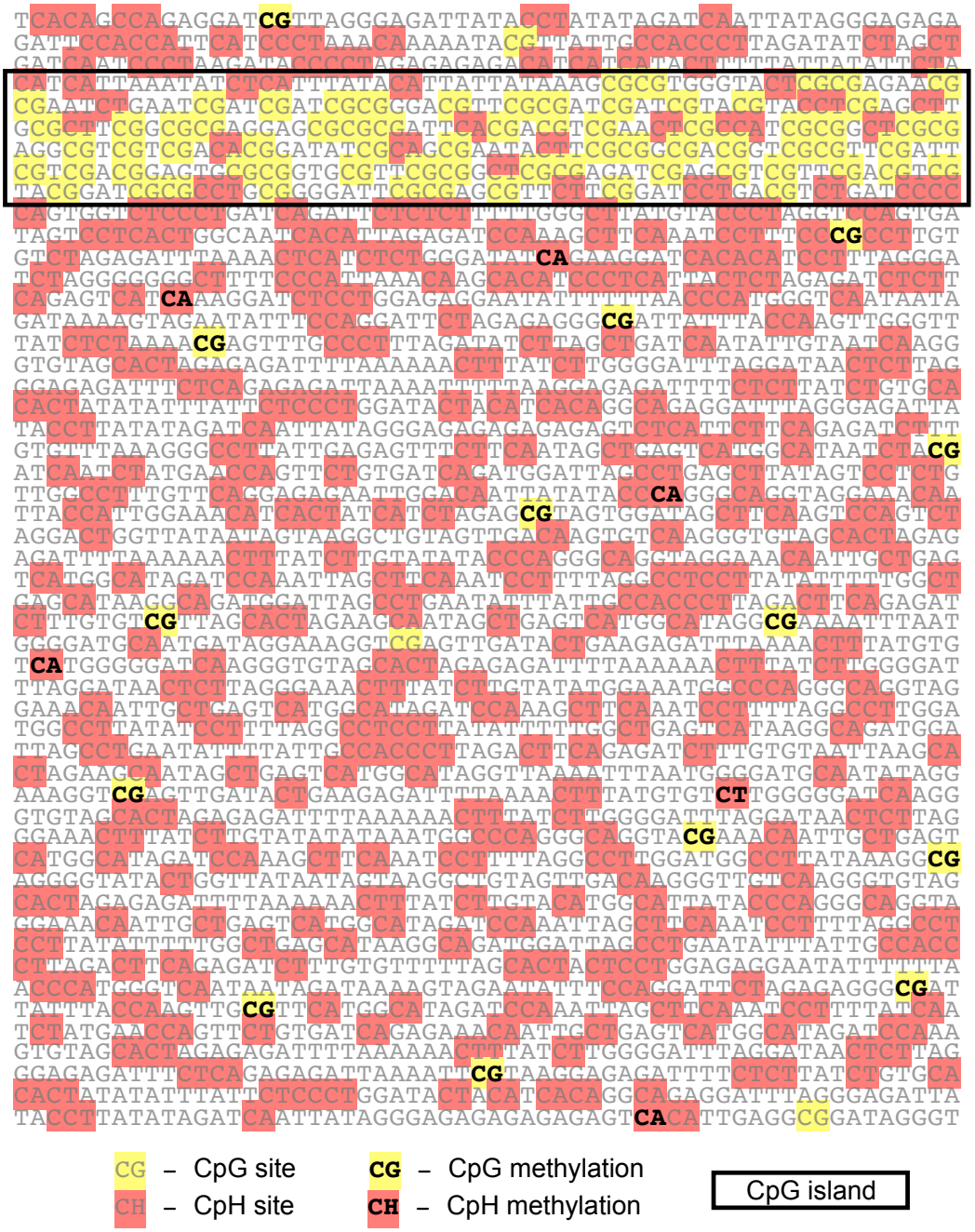

Figure 1.7: 5-Methylcytosine (5mC) patterns in the human genome show clusters of CpG sites (CpG islands) and a great number of CpH sites. Considering that the level of methylation is 100% in all 5mC, only one time the CpG island and 20 times the remaining sequence in the diagram, the DNA methylation profile would be as follows. 68% 5mCpG/CpG, 70% 5mCpG/total5mC, 1.4% 5mCpH/CpH, 30% 5mCpH/total5mC. Total number of CpG sites in such hypothetical sequence represents 0.8% of total nucleotides (410/53708). Total number of 5mC (5mCpG + 5mCpH) represents 0.7% of total nucleotides (400/53708). The DNA methylation pattern[179;186–188], total number of CpG sites[174] and total number of 5mC[171] of the hypothetical sequence is similar to what has been reported at the genome level for humans.

processes which relate DNA methylation with the expression of genes. One example is the participation of DNA methylation in the control of *IGF2* and *H19* expression. *In vitro* and *in vivo* experiments in mice have shown that *Igf2* and *H19* expression are under imprinted-control regions which depending on its methylation status allow the binding of CCCTC-binding factor (CTCF)[190–193]. The binding of CTCF modulates in turn enhancer activity to either *Igf2* or *H19* gene; thus, controlling their expression[191;194]. A similar mechanism has been described *in vitro* using human cells[195]. Besides, control of the imprinted region by DNA methylation is further supported by the hypomethylation or hypermethylation observed in Silver-Russell[196;197] or Beckwith-Wiedemann[198;199] syndromes which are characterised by undergrowth or overgrowth, respectively. It is clear that DNA methylation is not the only mechanism involved in such syndromes as not all patients showed a significant change in DNA methylation[196–199].

The consequence that altered DNA methylation of a single CpG site may have on cells illustrates the importance of DNA methylation changes and their effect on gene expression. An example is the *in vitro* regulation of krüppel-like factor 2 (KLF2) by low-density lipoproteins (LDL) using human umbilical vein endothelial cells (HUVEC)[200]. Experiments showed that 200 μM/ml LDL induced downregulation of *KLF2* mRNA; upregulation of *DNMT1* mRNA and DNMT1 activity; recruitment of methyl-CpG-binding protein 2 (MeCP2) into *KLF2* promoter; and displacement of myocyte enhancer factor-2 (MEF2) from *KLF2* promoter, which positively regulates *KLF2* transcription[200]. Sequence analysis of *KLF2* promoter showed that MeCP2 binding site overlapped with that of MEF2. MeCP2 has been shown to recognise and bind to a single methylated CpG pair[201]. Thus, although experiments did not address DNA methylation directly, Kumar *et al.,* showed evidence which suggested that the methylation status of a single CpG is associated with the control of *KLF2* expression[200]. Besides, the downregulation of *KLF2* mRNA, treatment with LDL induced downregulation of thrombomodulin (THBD), nitric oxide synthase 3 (NOS3) and upregulation of serpin family E member 1 (SERPINE1). As THBD and NOS3 are positively regulated while SERPINE1 negatively regulated by KLF2, evidence indicated that *KLF2* downregulation led to dysregulation of its target genes[200]. Such observations have shown the consequences that altered DNA methylation on a few CpG sites may have. In comparison, other *in vitro* experiments have been shown that the DNA methylation effect on gene expression is achieved until methylation is spread over several cytosines[202]. Therefore, the effect that DNA methylation has on cell functions depends on each specific case.

Altered DNA methylation have been shown a relationship with activity of some transcription factors. For instance, there is evidence that the dynamic interaction between SP1/SP3, TP53 and DNMT1 modulate the expression of the survivin gene *in vitro*[203;204]. Reported evidence showed that the luciferase gene coupled with the hu-

man survivin promoter increased reporter activity when SP1 or SP3 constructs were co-expressed in Drosophila SL2 cell line (naturally deficient in Sp proteins)[204]. The increased luciferase activity induced by SP1 or SP3 was repressed in cells expressing DNMT1 or TP53 constructs. Further characterisation of the system showed that stimulation of TP53 activity by doxorubicin increased TP53 occupancy and recruited DNMT1 into the proximal survivin promoter[203]. Doxorubicin treatment also showed to increase DNA methylation of survivin promoter which was dependent on TP53 expression because TP53 knockdown did not show the change in methylation[203]. Although there are still some gaps in how this system works, regulation of the survivin gene suggests that interaction between SP1/SP3, TP53 and DNMT1 may direct DNA methylation to specific regions.

The importance to study DNA methylation changes lay on associations showing altered DNA methylation in some diseases. For instance, the global DNA hypomethylation and locus-specific hypermethylation in cancer is a well described process[205]. Besides, other non-communicable diseases such as diabetes and atherosclerosis have shown different DNA methylation patterns compared with normal tissue[206;207]. If altered DNA methylation is mainly a cause or consequence of gene expression changes or the pathological condition itself is still unclear.

Overall, current evidence has shown that DNA methylation by its own does not generally control the expression of genes in cells[208;209]. The relationship between this epigenetic mark and gene expression should be interpreted within the particular genomic, epigenomic and cellular context. Other epigenetic marks which have shown an association with DNA methylation and gene expression are the post-translational modifications of histones. Some of these modifications are reviewed next.

1.3.2 Post-translational modification of histones

Post-translational modifications (PTM) of histones mainly include acetylation, methylation, phosphorylation, ubiquitination, sumoylation and ADP-ribosylation[210]. Such modifications are laid on different but specific positions of the N-terminal tails of histones[210]. Similar to DNA methylation, histone modifications have been associated with the expression of genes. Evidence shows that the combination of different PTMs, instead of a single type, is what creates a code that associates with transcription. For instance, actively transcribe genes show high levels of tri-methylation (me3) in the histone 3 at lysine 4 (H3K4) and H3K27 acetylation (ac). In contrast, inactive genes are enriched with H3K27me3 and show a lack of acetylation[210].

The most studied PTMs of histones are acetylation and methylation. The addition of acetyl groups in histones tails is only possible at lysine amino acids by histone acetyltransferase (HAT) enzymes. Different *in vitro* experiments have shown that hypera-

cetylation of histones disrupts chromatin structure, increases the rate of degradation by DNAse I enzyme and increases RNA polymerase transcription[211–214]. Disruption of the chromatin structure was only achieved when 100%, but not 23% of the lysine residues, were acetylated using purified core histones from HeLa cells[214]. Therefore, *in vitro* evidence supports that histone hyperacetylation allows a permissive chromatin structure that facilitates transcription possibly by neutralising the positive charge of lysine residues. On the contrary, histone deacetylase (HDAC) enzymes can deacetylate lysines within the histone tails. Histone deacetylation is thought to restore the positive charge of lysines in histone tails; thus, DNA is firmly attached to histones which have been shown to impair transcription[215]. Similar to acetylation, methylation of histones occurs only on certain amino acids, lysines and arginines. Histone methylation at lysine or arginine residues is mediated by lysine methyltransferases (KMT) and protein arginine methyltransferases (PMRT) families, respectively. The methylation marks are more diverse than acetylation as lysines or arginines may be mono-methylated, di-methylated or tri-methylated[216].

One of the features of histone modifications is that proteins with particular domains can identify specific marks. Histone acetylation may be recognised by proteins with a bromodomain while histone methylation by proteins with a chromodomain. For instance, chromo-ATPase/helicase-DNA-binding (CDH1) has two chromodomains that cooperate to interact with H3K4me3 in human cells[217]. CDH1 have been shown to be indispensable for pluripotency in mouse stem cells as this is required to keep the chromatin in an open state (euchromatin)[218]. The underlying mechanism how CDH1 induce an euchromatin state in mouse fibroblast and a possible connection with H3K4me3 is unknown.

Each histone modification has its own particular patterns in the genome. For this thesis, only H3K4me3 patterns will be addressed. It is widely accepted that H3K4me3 is an epigenetic mark associated with actively transcribed genes. The latter is because immunoprecipitation of H3K4me3 followed by sequencing of 46 different human cell types, including transformed and non-transformed cells showed an H3K4me3 enrichment around the transcription start site (TSS) of actively transcribed genes[219–221]. So far, *in vitro* experiments using human cells have identified five lysine methyltransferases and five lysine demethylases which can mediate methylation or demethylation of H3K4me3, respectively[222]. In addition to the enzymes that catalyse the methylation reaction, there is evidence that some other proteins are required for the establishment of H3K4me3 *in vivo*. For example, SET domain containing 1A (SETD1A) histone lysine methyltransferase has been recovered within a complex by immunoprecipitation of flagged CXXC finger protein 1 (CFP1) expressed in HEK293 cells[223]. Disruption of CFP1 expression has been shown to decrease global H3K4me3 levels in mouse embryonic stem cells[223;224]. Such evidence suggests a direct participation of CFP1 in the establishment of H3K4me3 mark. This is further supported by immuno-

precipitation of CFP1 or H3K4me3 and subsequent sequencing which showed similar occupancy of both proteins in the genome[224]. The genomic occupancy of CFP1 and H3K4me3 was significantly reduced, but not abolished, in CFP1$^{-/-}$ mouse embryonic stem cells, specially H3K4me3 levels of highly expressed genes[224]. The latter indicates that CFP1 is required for usual H3K4me3 patterns but not essential for the H3K4me3 establishment.

Although there is an evident association between H3K4me3 and actively transcribed genes, the H3K4me3 function is still unclear. Reduction of H3K4me3 levels by CFP1 depletion has shown little effect on gene expression in mouse cells[224]. CFP1 is a protein that physically interacts with SETD1A lysine methyltransferase and binds to only unmethylated CpG sites in double-stranded DNA *in vitro*[225]. Thus, it is possible that H3K4me3 association with actively transcribed genes is because CFP1 direction to gene promoters as the majority (70%) are CpG-rich[181] and are generally unmethylated[143;185]. In addition to CFP1, there is evidence that SETD1A interacts with WD repeat domain 82 (WDR82) protein[226]. WDR82, in turn, has a domain that interacts with RNA polymerase II[226]. Depletion of WDR82 by small interfering RNA has also been shown to reduce H3K4me3 levels which did not affect gene expression or RNA polymerase II occupancy on six candidate genes using HEK-293 cell line[226]. Overall, current evidence suggests that H3K4me3 at active promoters may result primarily as a consequence of SETD1A-containing complex interaction with RNA polymerase II and CFP1. It is not yet discarded the possibility that indeed H3K4me3 may facilitate transcription. There is experimental work that showed H3K4me3 recognition by TATA-Box binding protein-associated factor 3 (TAF3) using HeLa S3 cells[227]. TAF3 is a subunit of the transcription factor TFIID, and its binding to H3K4me3 showed to promote the formation of the preinitiation complex of transcription in a cell-free transcription system[228]. Further work is needed to verify if this may happen *in vivo* and if this may be a general feature or just applicable for some candidates genes as the reduction of H3K4me3 have shown no effect on gene expression at the genome-wide level[224].

1.3.3 Epigenetic changes by fatty acids

In vitro treatment of THP1 monocytes and HUVEC showed that 100 μM OA decreases whereas 100 μM arachidonic acid (AA) increases global DNA methylation of cells after 24 hours[229]. However, a tendency to decrease global DNA methylation has also been reported in HUVEC cells by 3 μM AA treatment[230;231]. Such differences may be due to the different methods employed to determine global DNA methylation. DNA hypermethylation by 100 μM AA was assessed by an antibody targeting 5mC[229] while the null effect or trend to decrease global DNA methylation by 3 μM AA was measured by HpaII restriction enzyme[230;231]. Antibody-based methods may

be a better approach for global DNA methylation as HpaII only provides the methylation status of 5'-CCGG-3' sequences. Therefore, the current evidence supports that AA induces DNA hypermethylation of cells.

DNA methylation changes by fatty acids have also been studied in candidate genes. *In vitro* treatment with 3 μM AA for 24 hours has also been shown to decrease DNA methylation in the promoter region of kinase insert domain receptor (KDR) using HUVEC[231]. Moreover, *ex vivo* treatment with 500 μM palmitate or 500 μM oleate for 48 hours increased promoter methylation of PPARγ coactivator 1 alpha gene in human primary monocytes compared with untreated cells[232]. Comparison of 100 μM OA or 100 μM EPA treatment showed that EPA, but not OA, demethylates a single CpG site within the promoter region of CCAAT enhancer binding protein delta (CEBPD)[233]. Demethylation by EPA treatment in CEBPD promoter showed to facilitate the binding of transcription factor Sp1[233]. These pieces of evidence suggest that similar to the modulation of prostaglandins and gene expression changes; there is some specificity in the altered DNA methylation induced by different fatty acids. In addition, these experiments show that epigenetic changes by fatty acids possibly have an impact in gene expression.

The effect of fatty acids on DNA methylation has also been studied *in vivo*. In rats, fish oil treatment for 9 weeks has shown to induce methylation changes in the liver fatty acid desaturase 2 (*Fads2*) gene, encoding Δ6 desaturase. Such changes correlated inversely with *Fads2* mRNA expression in the liver[234]. The DNA methylation and mRNA expression changes were reverted after 4-weeks of stopping fish oil treatment in adults rats[234]. However, offspring of dams that underwent the same fish oil treatment including 14 days preconception, 20 days of pregnancy and 28 days of lactation did not reverse the DNA methylation changes in *Fads2* gene after 11-weeks of stopping the treatment[234]. Such results indicated that epigenetic changes at developing stages by fish oil may possibly reprogramme expression patterns of *Fads2* in rats. Reprogramming of DNA methylation patterns in humans by fatty acids has been addressed experimentally in other candidate regions[235;236]. One study showed that 400 mg DHA/day supplementation from gestation week 18-22 to birth increased methylation ($< 1\%$) of long interspersed nuclear elements (LINE) in umbilical cord blood of smoker mothers[235]. Another study showed that 800 mg DHA/day supplementation from gestation week 20 to birth increase methylation of a single CpG in female ($< 3\%$), but not male children blood cells. However, there were raised some concerns about the results[237], essentially because changes in DNA methylation were small and may represent an artefact of the pyrosequencing[238] or the Illumina HumanMethylation-450K BeadChip used. At present, evidence of the reprogramming of DNA methylation patterns by any fatty acid in human cells is unclear.

To date, there are only three studies that provide direct evidence of an *in vivo* association of the fatty acids effect on the DNA methylation of human cells[239–241]. One

study showed an association between total saturated, monounsaturated or polyunsaturated fatty acids with the global DNA methylation of cells using peripheral blood in a cohort of 15 men[239]. Other study showed that supplementation for 12 weeks with either omega-3 fatty acids or olive oil altered the DNA methylation on specific CpG sites within the promoter region of *FADS2* and *ELOVL5* genes using PMBCs of healthy volunteers (n = 20)[240]. The effects observed were different between fatty acids and sex which suggested that DNA methylation was altered in a fatty-acid and sex-specific manner[240]. Furthermore, supplementation with 1.9-2.2g EPA plus 1.1g DHA daily for 6 weeks showed to change the DNA methylation of 308 CpG sites using blood leukocytes in a cohort of 36 overweight and obese volunteers[241]. Thus, evidence suggests that olive oil and omega-3 fatty acids modulate DNA methylation with specificity in humans.

There is another study that has also addressed *in vivo* DNA methylation changes by fatty acids in humans. However, volunteers followed hypercaloric diets that led to a difference in weight[242]. Changes in body weight have also been associated with DNA methylation changes in PBMCs[243] and adipose tissue[244]. Thus, it is difficult to evaluate if the effect reported is due to the fatty acids or the overfeeding.

At present, there is only one study reporting possible mechanisms by which fatty acids may alter the DNA methylation in cells. Silva-Martinez *et al.*, showed that altered DNA methylation induced by 100 μM arachidonic acid (AA) treatment was reduced by a 1-hour pre-treatment with 10, 100, and 200 μ M β-oxidation inhibitor etomoxir or inhibited by 0.5 μ M PPARα inhibitor GW6471, but not with PPARγ inhibitor GW9662 in THP1 cells[229]. The same pre-treatments with etomoxir, GW6471 or GW9662 did not reduce or inhibit the altered DNA methylation by 100 μM OA using the same THP1 monocytes[229]. The same study assessed the involvement of Situins on the DNA methylation induced by OA or AA treatment using wild-type mouse embryonic fibroblasts (MEFs), SIRT1$^{-/-}$, SIRT2$^{-/-}$ or SIRT6$^{-/-}$ MEFs. Results showed that only SIRT1 knockout essentially abolished the altered DNA methylation induced by both OA or AA in wild-type MEFs. Currently, *in vitro* evidence in human and mouse cells suggests that β-oxidation, PPARα and SIRT1 are involved in AA-induced global DNA hypermethylation while only SIRT1 is associated with OA-induced DNA hypomethylation. Participation of different proteins suggests that there may not be a single way how fatty acids induce changes in the DNA methylation. A summary of the evidence showing the fatty acids effect on DNA methylation in human cells is shown in Figure 1.8.

Some studies have also shown that fatty acids can modulate PTMs of histones such as acetylation[245]. At present, it is well accepted that short-chain fatty acids, foremost butyrate, increases global acetylation of histones through inhibition of histone deacetylases[245]. Also, there is evidence showing that β-oxidation of long-chain and very-long chain fatty acids can increase acetylation levels of proteins including histones by

generating more available acetyl groups[246;247]. *In vitro* acylation of histones including acetyl-, butyryl-, malonyl-, in the presence or absence of eukaryotic HATs showed that a proportion of the changes in histone were not mediated by HATs[247]. This suggests a certain level of unspecific effect of fatty acids on histone marks which seems to be different for diverse types of acylations of histones. In the specific case of acetylation, *in vitro* experiments have estimated that approximately 85% of the total acetylation is mediated by HATs[247].

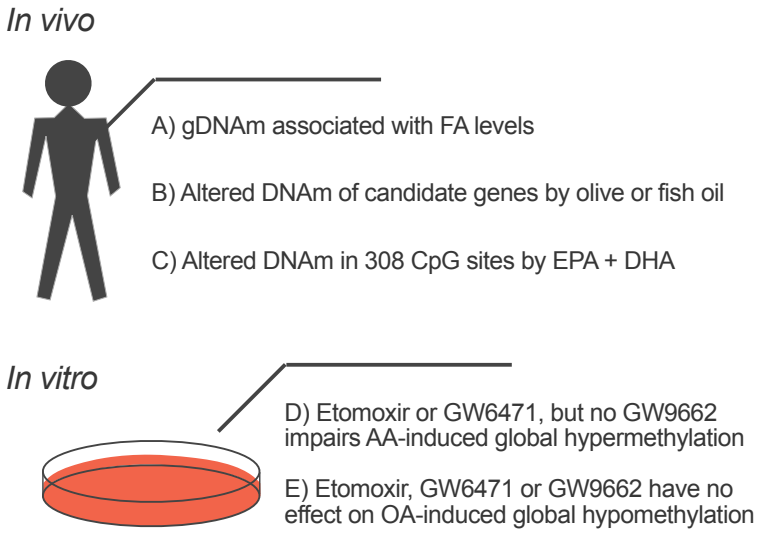

Figure 1.8: Current evidence of the effect of fatty acids on DNA methylation (DNAm) in human cells shows that global DNAm (gDNAm) has a relationship with total fatty acids (FA) in peripheral blood cells[239] (A). Human clinical trails have been shown that olive oil or omega-3 fatty acids EPA+DHA can induce altered DNA methylation on candidate genes in white blood cells[240;241] (B, C). *In vitro* experiments have been shown that etamoixir (a β-oxidation inhibitor) or GW6471 (a PPARα inhibitor), but not GW9662 (a PPARγ inhibitor), reduce or inhibit the effect of arachidonic acid (AA) on the global DNAm in THP1 monocytes. The same inhibitors have not been shown to reduce significantly the effect of oleic acid (OA) on DNA methylation in THP1 monocytes[229].

Besides global changes in acetylation of histones, information about the specific residues of the histone tails that are modified by fatty acids is currently limited. Incubation with 30 μM DHA for two days showed to increase acetylation levels of H3K4 and decreased methylation levels of H3K4, H3K9, H3K27M H3K36 and H3K79 in human neuroblastoma M17 cells[248]. Specific changes of histone marks are important because they have shown a different association with gene expression. The relationship between histone marks and DNA methylation induced by fatty acids has not yet been addressed.

1.4 Aims and rationale

Currently, the molecular mechanisms underlying the effect of fatty acids on the DNA methylation are not well understood. Therefore, this research project sought to elucidate such mechanisms using the *in vitro* treatment of Jurkat cells with OA or DHA. These two fatty acids were chosen as they are major components of olive oil and omega-3 fatty acids which have been shown to induce altered DNA methylation of human PBMCs *in vivo*[240]. Jurkat cell line was selected as growing conditions are similar to that of blood cells (suspension) and are T-cells which constitute a significant component of PBMCs.

1.5 Research hypotheses

1.5.1 Hypothesis 1; OA and DHA induce mainly different locus-specific DNA methylation changes at the genome-wide level

At the global level, treatment of THP1 cells with 100 μM AA showed to induce global DNA hypermethylation while 100 μM OA induced global DNA hypomethylation. In candidate genes, treatment with 100 μM EPA, but not OA, showed to alter DNA methylation status of CCAAT / enhancer-binding protein delta promoter in U937 cells[233]. Results of the only study addressing locus-specific DNA methylation changes at the genome-wide level did not reach statistically significance[229]. Therefore, the current evidence suggests specificity on the effect of fatty acids on the DNA methylation, but the degree of such specificity at the genome-wide level is still unclear. This work addressed such specificity with the hypothesis that OA and DHA induce mainly different locus-specific DNA methylation changes at the genome-wide level.

1.5.1.1 Aim 1

To develop a model for studying the fatty acid effect on DNA methylation using the human T-cell line Jurkat. Once a model was established, locus-specific DNA methylation changes induced by OA or DHA treatment at the genome-wide level were determined. Description of the data provided evidence of the similarities and differences (specificity) between the effect of OA or DHA treatment on the DNA methylation.

1.5.2 Hypothesis 2; PPARα participates in the DNA methylation changes induced by DHA

There is evidence showing that PPARα activity was required for the effect of AA on the global DNA methylation of THP1 monocytes[229]. On the contrary, the same study showed that PPARα activity was not required for the effect of OA on the global DNA methylation in the same cells[229]. The involvement of PPARα in the altered DNA methylation induced by other fatty acids such as DHA has not been previously tested. Therefore, we hypothesise that PPARα activity is required for the altered DNA methylation induced by DHA.

1.5.2.1 Aim 2

To assess if PPARα activity is required for the DNA methylation changes induced by DHA. In order to do so, Jurkat cells were treated with the PPARα agonist GW7647, PPARα inhibitor GW6471 and co-treated with PPARα inhibitor GW6471 plus DHA. After treatments, the DNA methylation was measured in candidate CpG sites identified here to change DNA methylation status by DHA treatment.

1.5.3 Hypothesis 3; transcription factors, other than from PPARα, are required for the effect of OA or DHA on the DNA methylation

In vitro treatment of THP1 cells with the PPARα inhibitor GW6471 showed to completely block the global DNA hypermethylation induced by 100 μM AA[229]. Similarly, treatment of THP1 cells with the β-oxidation inhibitor etomoxir showed to significantly decrease, but not block, the global DNA hypermethylation induced by 100 μM AA[229]. The same treatment using wild-type and Sirt1 knockout MEFs showed that Sirt1 knockout MEFs were not responsive to the global DNA hypermethylation induced by AA compared with wild-type MEFs[229]. Thus, current evidence suggests that the activity of different proteins and pathways may be required for the altered DNA methylation induced by fatty acids. This work attempt to look for proteins or pathways associated with the DNA methylation changes induced by OA or DHA.

1.5.3.1 Aim 3

To determine altered transcription factors and pathways by OA or DHA treatment. In order to do this, different approaches were covered. These included pathway analysis using the genes with altered DNA methylation or mRNA expression to provide evidence of a functional relationship between altered genes. Such analysis allowed to de-

termine if altered genes were under the control of a specific transcription factor. Additionally, *in silico* analysis of the sequences near CpG sites that changed DNA methylation were used to look for possible DNA motifs that may drive the recruitment of transcription factors.

1.5.4 Hypothesis 4; DNA methylation changes induced by fatty acids are associated with altered H3K4me3 enrichment

Treatment with 40 μM oleate plus 40 μM palmitate showed to alter H3K4me3 and H3K9me3 enrichment of C57BL/6J mice primary hepatocytes[249]. The effect of fatty acids on histone marks has also been observed *in vivo* using adipose tissue from offspring of dams that followed a high-fat diet[250]. Besides the evidence in mice, there is evidence that fatty acids can altered the enrichment of certain histone marks in human cells[248]. *In vitro* treatment with DHA for two days showed to increase acetylation of H3K4 and decrease methylation of H3K4, H3K9, H3K27 H3K36 and H3K79 residues in the neuroblastoma M17 cell line[248]. The occupancy of tri-methylated H3K4 is the only histone mark available in ENCODE for Jurkat cells. Therefore, we asked if DNA methylation changes induced by OA or DHA were associated with altered H3K4me3. The relationship between altered DNA methylation and altered H3K4me3 enrichment (or any other histone mark) induced by fatty acids has not been reported before.

1.5.4.1 Aim 4

To map all significantly altered CpG sites identified by the DNA methylation BeadArray with H3K4me3 occupancy in the Jurkat's genome. To further characterise such relationship chromatin immunoprecipitation of H3K4me3 and subsequent qPCR was carried out to know if H3K4me3 increased or decrease in candidate regions which showed altered DNA methylation by OA or DHA.

Chapter 2

Materials and General Methods

2.1 Materials

All reagents and chemical used in experiments and their correspondent supplier are shown in Table 2.1.

Table 2.1: List of reagents and chemicals used.

Reagent/chemical	Supplier
Agarose	Sigma-Aldrich, Dorset, UK
BlueJuice	Life Technologies, Renfrewshire, UK
Butyrated hydroxytoluene	Sigma-Aldrich, Dorset, UK
ChIP-IT Control Kit - Human	Active Motif, La Hulpe, Belgium
ChIP-IT Express Enzymatic kit	Active Motif, La Hulpe, Belgium
Chloroform	Sigma-Aldrich, Dorset, UK
Cignal PPAR Reporter (luc) Kit	Qiagen, Manchester, UK
CpGenome universal methylated DNA	Millipore, Watford, UK
DNA- and RNA-free water	Fisher Scientific, Loughborough, UK
DNase I kit	Sigma-Aldrich, Dorset, UK
Docosahexaenoic acid (DHA)	Sigma-Aldrich, Dorset, UK
Dual-Luciferase® Reporter Assay System	Promega, Southampton, UK
Eicosapentaenoic acid (EPA)	Sigma-Aldrich, Dorset, UK
EpiTect Control DNA	Qiagen, Manchester, UK
Ethanol	Fisher, Leicestershire, UK
EZ DNA Methylation-Gold™ Kit	Cambridge Bioscience, Cambridge, UK
Fetal bovine serum	Life Technologies, Renfrewshire, UK

Formaldehyde (16%, w/v), methanol-free	Life Technologies, Renfrewshire, UK
FuGENE HD Transfection Reagent	Promega, Southampton, UK
GE Healthcare streptavidin sepharose™ high-performance (34 μm)	Fisher Scientific, Loughborough, UK
GelRed™ 10 000X in water	VWR International, Leicestershire, UK
geNorm	Primer Design, Chandler's Ford, UK
Glycerol	Sigma-Aldrich, Dorset, UK
Glycine	Bio-Rad, Watford, UK
GW6471, PPARα antagonist	Bio-Techne, Oxfordshire, UK
GW7647, PPARα agonist	Bio-Techne, Oxfordshire, UK
Hexane	Sigma-Aldrich, Dorset, UK
Histone H3K4me3 antibody (pAb)	Active Motif, La Hulpe, Belgium
HotStarTaq DNA Polymerase	Qiagen, Manchester, UK
KAPA2G Robust HotStart ReadyMix	KAPA Biosystems, London, UK
L-glutamine	Sigma-Aldrich, Dorset, UK
M-MLV Reverse Transcriptase Kit	Promega, Southampton, UK
Methanol	Sigma-Aldrich, Dorset, UK
mirVana™ miRNA Isolation Kit with phenol	Life Technologies, Renfrewshire, UK
Sodium chloride (NaCl) 1 M	Sigma-Aldrich, Dorset, UK
Nonadecanoic acid	Sigma-Aldrich, Dorset, UK
O'GeneRuler 1 kb ladder Plus DNA Ladder	Life Technologies, Renfrewshire, UK
Oleic acid (OA)	Sigma-Aldrich, Dorset, UK
Opti-MEM™ Reduced Serum Medium	Life Technologies, Renfrewshire, UK
Penicillin and streptomycin	Sigma-Aldrich, Dorset, UK
Phosphate-buffered saline (PBS)	Sigma-Aldrich, Dorset, UK
Potassium bicarbonate (KHCO3)	Sigma-Aldrich, Dorset, UK
Potassium carbonate (K2CO3)	Sigma-Aldrich, Dorset, UK
Primers (own design)	Eurofins Genetic Services, Wolverhampton, UK
Primers (QuantiTect)	Qiagen, Manchester, UK
PyroMark annealing buffer	Qiagen, Manchester, UK
PyroMark binding buffer	Qiagen, Manchester, UK
PyroMark Gold Q96 Reagents	Qiagen, Manchester, UK
PyroMark Gold Q96 Reagents	Qiagen, Manchester, UK
PyroMark Q96 Capillary Tip	Qiagen, Manchester, UK
PyroMark Q96 Reagent Tip	Qiagen, Manchester, UK

PyroMark wash buffer	Qiagen, Manchester, UK
QIAamp DNA Blood Mini Kit	Qiagen, Manchester, UK
QuantiFast SYBR Green I PCR Kit	Qiagen, Manchester, UK
Random nonamers	Sigma-Aldrich, Dorset, UK
RNase A	Sigma-Aldrich, Dorset, UK
RPMI-1640 medium	Sigma-Aldrich, Dorset, UK
Sodium Acetate (3 M, pH 5.2)	Sigma-Aldrich, Dorset, UK
Sulphuric acid (H2SO4)	Sigma-Aldrich, Dorset, UK
Supelco® 37 Component FAME Mix	Sigma-Aldrich, Dorset, UK
Toluene	Sigma-Aldrich, Dorset, UK
Tris-acetate-EDTA (TAE)	Life Technologies, Renfrewshire, UK
Trypan Blue	Sigma-Aldrich, Dorset, UK

2.2 Cell culture management

2.2.1 Cell culture and treatments

Jurkat cells, a human T-lymphocyte cell line, were maintained in RPMI-1640 medium supplemented with 9% (v/v) foetal bovine serum, 2 mM L-glutamine, 100 U/ml penicillin and 100 μg/ml streptomycin in a 5% (v/v) CO_2 atmosphere at 37 °C. Cell density was invariably maintained lower than 1x10^6 cells/ml. Cell cultures were treated with either OA or DHA dissolved in 90% (v/v) ethanol. Concentrations used in fatty acid treatments were 15 μM OA or 15 μM DHA, otherwise specified. Jurkat cells were also treated with a peroxisome proliferator-activated receptor alpha (PPARα) agonist (0.2 μM GW7647), a PPARα antagonist (2 μM GW6471) and co-treated with 2 μM GW6471 PPARα antagonist plus 15 μM DHA. PPARα agonist and antagonist were dissolved in absolute ethanol. Concentration of GW7647 or GW6471 used in experiments has shown to activate or abolish PPARα activity, respectively[251;252]. Control treatment in all experiments consisted in addition of only the vehicle, ethanol, at same concentration used in fatty acid or PPARα treatments. The final concentration of ethanol in cell cultures was $< 0.05\%$ (v/v) in all experiments carried out. Cells were treated for eight days, otherwise specified. Culture cell media was replaced every 72 hrs with fresh treatment media in all experiments performed.

2.2.2 Cell proliferation

Cell proliferation was assessed by the fold change in cell count during treatments. Cell counting was conducted using Coulter Counter (Z1; Coulter Electronics, Luton, UK).

The cell pellet was obtained after a 5 minute centrifugation at 212 g. Pellet was re-suspended in cell media three times with micropipette and 10 μl were pipette into diluvial (Elkey Laboratory, UK). 10 ml of Isoton were then added to diluvial (1:1000 dilution) using a bottle-top dispenser to disaggregate the cells. Standard manufacturer's instructions and calculi were carried out as follows. Two reads were combined to obtain the number of cells in 1 ml of the 1:1000 dilution as each read by Coulter Counter was the total number of particles ($>$ 6 μm $<$ 24 μm) in 500 μl. This number was then multiplied by the dilution factor (1000) and by the volume in ml of the re-suspension of the pellet to obtain the total number of cells. Formula used to obtain total number of cell per ml was:

$$Cells/ml \;=\; (1^{st} + 2^{nd}\; read) \times \left(\frac{isoton\;(\mu l)}{cell\;aliquot\;counted\;(\mu l)}\right) \times total\;cell\;suspension\;(ml) \tag{2.1}$$

When the difference between the first and second read in the Coulter Counter was higher than 100, isoton dilution was shaken to ensure the break down of cell aggregates. Samples were then read until a difference less than 100 between the two reads was archived. Fold change was obtained dividing the number of cells/ml after treatment by the number of cells/ml seeded.

$$Fold\;change\;in\;cell\;count \;=\; \left(\frac{cells/ml\;after\;treatment}{cells/ml\;seeded}\right) \tag{2.2}$$

2.2.3 Cell viability

Cell viability was assessed by the Trypan Blue exclusion method. This method was based on the principle that cell membrane integrity changed following cell death[253]. After cell suspension was mixed with Trypan Blue, live cells with an integrate cell membrane remained unstained while death cells allowed the take-up of the dye. Cell pellet was obtained after a 5 minutes centrifugation at 212 g. Pellet was then resuspended in cell media three times with micropipette and a 10 μl aliquot was pipette into a microtube. 90 μl of Trypan Blue stain were added to the aliquot (1:10 dilution) and mixed by pipetting five times. Mixture was incubate for 1-2 minutes at room temperature. 15 μl of this mixture were then added to each chamber of a hemocytometer. Cells in both chambers of the haemocytometer were counted using a hand tally counter (Fisher Scientific) and Olympus light microscope with the Olympus SPlan 10x objective lens. The mean of unstained and stained cells in both chambers was then calculated. Unstained cell number was divided by the total number of cells and multiply by 100 to obtain cell viability percentage. The formula used was:

$$Cell\;viability \;=\; \left(\frac{unstained\;cells}{total\;cells\;(unstained\;+\;stained)}\right) \times 100 \tag{2.3}$$

2.3 Nucleic acid analysis

2.3.1 RNA extraction

Total RNA was extracted using the mirVana™ miRNA Isolation Kit with phenol according to the manufacturer's instructions. The kit provided all reagents/supplies except for chloroform, ethanol and DNA- and RNA-free water. The protocol combined organic[254] and solid-phase extraction[255]. Frozen cell pellets were lysed with 600 μl Lysis/Binding buffer and 60 μl miRNA Homogenate Additive after a 10 minute incubation on ice. 600 μl of acid phenol:chloroform (1:1) were then added, samples mixed and centrifuged at 21130 g for 10 minutes at room temperature. The upper phase was then transferred to a new microtube and 1.25 volumes of absolute ethanol added and mixed. Mixture was pipette to the filter cartridge (containing silica glass) and centrifuged 15 seconds at 9408 g. Filter was washed once with 700 μl Wash Solution 1 and then twice with 500 μl Wash Solution 2/3. DNA- and RNA-free water was then added to the filters and incubated for 2 minutes. Samples were centrifuged for 20 seconds at 21130 g to obtain the total RNA, including very small RNA species. Samples were stored at $-80\,^{\circ}$C and maintained on ice when used, avoiding thaw-freezing cycles.

2.3.2 DNA extraction

DNA extractions were performed using QIAamp DNA Blood Mini Kit according to manufacturer's instructions. The kit provided all reagents/supplies except for phosphate-buffered saline (PBS, 10 mM PO_4^{3-}, 138 mM NaCl, 2.7 mM KCl, pH 7.4 at $25\,^{\circ}$C), RNase A (20 μl, 20 mg/ml), ethanol and DNA- and RNA-free water. Frozen cell pellets were resuspended and incubated for 2 minutes at room temperature with 180 μl PBS plus 20 μl RNase A to avoid any possible RNA contamination. Cells were then lysed by adding 20 μl Proteinase K (600 mAU/ml), 200 μl Buffer AL and a 10 minute incubation at $56\,^{\circ}$C. 200 μl absolute ethanol were then added, mixed and lysates loaded to columns. DNA was immobilised into columns after 1 minute centrifugation at 6000 g and then washed once with 500 μl Buffer AW1, repeating centrifugation. Samples were further washed with 500 μl Buffer AW2 and centrifuged at 21130 g for 3 minutes to completely remove wash solution. DNA- and RNA-free water was then added to columns. Samples were incubated for 5 minutes at room temperature prior centrifugation for 1 minute at 6000 g to elute DNA. Samples were stored at $4\,^{\circ}$C for short-term (up to 24 hrs), $-20\,^{\circ}$C for middle-term (up to 1 month), or $-80\,^{\circ}$C for long-term (up to 3 years).

2.3.3 Quantity and quality assessment of nucleic acids

RNA and DNA concentration and purity was assessed using a NanoDrop® ND-1000 full-spectrum (220-750nm) spectrophotometer (Thermo Scientific). Nucleic acid concentrations were calculated with a modified Beer-Lambert equation solved for concentration, which employed ultraviolet (UV) light absorbance of samples at 260 nm. All concentrations were calculated automatically by the default software in NanoDrop®. Nucleic acid purity was assessed by a 260 nm / 280 nm ratio of absorbance close to 1.8 for DNA and around 2.0 for RNA, whereas a 260 nm / 230 nm ratio of absorbance in the range of 2.0-2.2 was a target for both. Further RNA and DNA purity was evaluated by agarose gel electrophoresis.

2.3.4 Agarose gel electrophoresis

RNA, DNA and PCR amplicons were run on agarose gels to measure purity, integrity and quantity qualitatively. 1% gels (1 g agarose in 100 ml 1x Tris-acetate-EDTA (TAE)) were used for RNA and DNA samples, whereas 2% gels were used for PCR amplicons. Agarose was dissolved in 1x TAE by microwave heating and then cooled down at room temperature for a maximum of 5 minutes. 7 μl 100,000x GelRed in water were then added and mixed. Agarose was poured into a mould with combs inserted, and was let to gelatinise. Every electrophoresis was run with 1x TAE buffer using 4 uL O'GeneRuler 1 kb ladder Plus DNA Ladder as size reference. Samples were mixed with 1x BlueJuice (Bromophenol Blue) loading dye prior to load samples into gels. Agarose gels were run at 120 V for a maximum of 10 minutes in RNA samples or before the loading dye migrated the total length of the gel in DNA samples. RNA purity was assessed by the presence of mainly two bands corresponding to 28S and 18S rRNA when exposing gels to UV light. DNA and PCR amplicons purity was assessed by the presence of only one band when exposing gels to UV light. In all instances, integrity was assessed by the sharpness of bands, whereas quantity by the brightness of bands compared to each other (Figure 2.1).

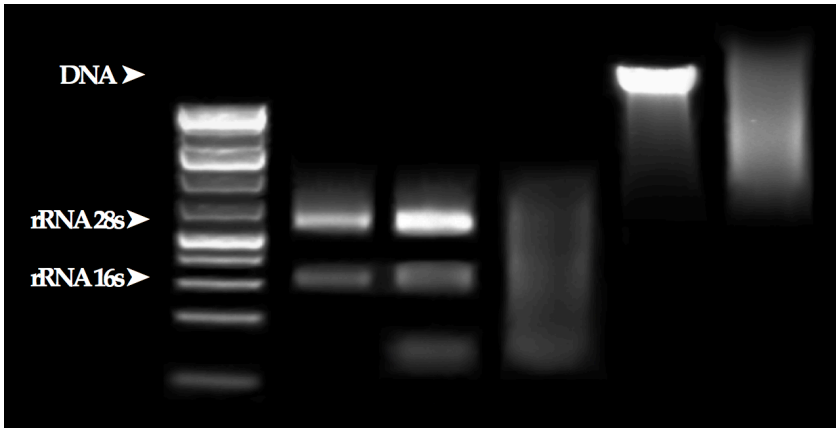

Figure 2.1: Nucleic acids on a typical agarose gel. Image shows, left to right, O'GeneRuler ladder, total RNA with no very small species of RNA, total RNA including very small species of RNA, degraded RNA, genomic DNA and degraded genomic DNA.

2.4 Standard and quantitative polymerase chain reaction

2.4.1 Primer design, synthesis and optimisation of annealing temperature

Bespoke primers were designed using the primer designing tool in The National Center for Biotechnology Information (NCBI) website. This tool used the free software Primer3 to design PCR primers. Primer3 calculated the melting temperatures, propensity to form harpins and dimers in candidate primers according to the user-specified constraints[256;257]. Once designed, primers were aligned to the NCBI human genome database and selected if they were potentially specific to the sequences of interest[258].

For ChIP-qPCR experiments, bespoke primers were designed using DNA as template and the Human Reference Sequence Build 37 (same as Infinium Human MethylationEPIC BeadChip). Details of all primers used for ChIP-qPCR and optimised annealing temperatures are shown in Table 2.2.

Table 2.2: Primers used for ChIP-qPCR.

Target DMP ID / gene	Primer Sequences (5'-3')	Temp[a]	Size[b] (bp)
cg17058565	Fwd TGCATCTGTGTTGTCCCTTTTGTA Rev TGAATGGTCACCGTTTTACGTTCAG	64 °C	69
cg15707568	Fwd GGCGGTGATAACATTCTTCGGT Rev AGCCTGGATGGAACCCTGAGA	64 °C	110
cg17016559	Fwd AGGACGCGCCCCTCTTTCTCA Rev GGACCTGTGTTGATGTGGCCGT	66 °C	92
cg07203320	Fwd AAGGCTGCGAAGAGACGCAC Rev AAGCTCTCAGCCCTCCCTCTG	68 °C	77
cg18492804	Fwd CTGCGTCACTGCCCTGCATC Rev CCAATGCGGTACCACCCCAAGA	64 °C	68

DMP; differential methylated position; Fwd, forward primer; Rev, reverse primer; [a] = annealing temperature; [b] = amplicon size. DMP ID according to 850k DNA MethylationEPIC BeadChip.

For RT-qPCR experiments, bespoke primers were designed using RNA as template and the Human Reference Sequence Build 38 (same reference as Illumina HumanHT-12 v4 Expression BeadChip) using spanning exon-exon junctions to avoid PCR artefacts. Details of all primers used for RT-qPCR (designed or purchased) and optimised annealing temperatures are shown in Table 2.3.

Table 2.3: Primers used for RT-qPCR.

Target Gene	Primer Sequences (5'-3')	Exon location	Temp[a]	Size[b] (bp)
CD79A	QT00998354	NA	60 °C	104
HMGCS1	QT00055531	4/5	60 °C	123
ID1	QT01002757	NA	60 °C	131
IGF2R	QT00080549	39/40	60 °C	105
MSMO1	QT01007986	NA	60 °C	93
PER2	QT01011892	18/19	60 °C	83
TOX2	QT01864380	NA	60 °C	88
RPL13A	QT00089915	5/6/7	60 °C	161
GZMA	Fwd TGTGCTGGGGCTTTGATTGC Rev TGACCTGGGACCTTTTGTTCA	2 2/3	60 °C	76
HMGCR	Fwd ACGTTTACCCTCGATGCTCT Rev AGCTGACGTACCCCTGACAT	6 6/7	60 °C	71
LSS	Fwd CGTTATTTGCAGAGTGCCCAG Rev CCTCGATGTCAGGATGCCG	20 20/21	60 °C	88
RPS18	Fwd ATTAAGGGTGTGGGCCGAAG Rev TGGCTAGGACCTGGCTGTAT	2/3 4/5	60 °C	205

Fwd, forward primer; Rev, reverse primer; [a] = annealing temperature; [b] = amplicon size; *CD79A*, CD79a Molecule; *HMGCS1*, 3-Hydroxy-3-Methylglutaryl-CoA Synthase 1; *ID1*, Inhibitor Of DNA Binding 1, HLH Protein; *IGF2R*, Insulin Like Growth Factor 2 Receptor; *MSMO1*, Methylsterol Monooxygenase 1; *PER2*, Period Circadian Clock 2; *TOX2*, TOX High Mobility Group Box Family Member 2; *RPL13A*, Ribosomal Protein L13a; *GZMA*, Granzyme A; *HMGCR*, 3-Hydroxy-3-Methylglutaryl-CoA Reductase; *LSS*, Lanosterol Synthase; *RPS18*, Ribosomal Protein S18. Sequences of purchased primers (QuantiTect®) were not available. NA; No available information.

For standard RT-PCR experiments, bespoke primers were designed same as RT-qPCR primers. Details of primers used and optimised annealing temperatures are shown in Table 2.4.

Table 2.4: Primers used for standard RT-PCR.

Target Gene	Primer Sequences (5'-3')	Exon location	Temp[a]	Size[b] (bp)
PPARα	Fwd GGTGTATGACAAGTGCGACC Rev AATCGCGTTGTGTGACATCC	5 5/6	54 °C	112

Fwd, forward primer; Rev, reverse primer; [a] = annealing temperature; [b] = amplicon size; *PPARα*, Peroxisome proliferator-activated receptor alpha.

All bespoke primers were synthesised by Eurofins Genomics using High Purity Salt-Free (HPSF) oligo purification. PCR annealing temperature for each primer was optimised by a PCR gradient using 10 ng/μl cDNA, 1.25 units HotStartTaq DNA Polymerase, 1x PCR buffer, 16 mM $MgCl_2$, 0.2 μM of each forward and reverse primer and 200 μM of each deoxynucleoside triphosphates (dNTP's) in a 25 μl final volume reaction. All reagents, except from dNTP's, were provided with the HotStartTaq DNA Polymerase. PCRs were carried out with an initial 95 °C incubation for 15 minutes to activate polymerase with subsequent amplification for 35 cycles using a Veriti Thermal Cycler (Applied Biosystems). Each cycle included denaturation at 95 °C for 45 seconds, annealing from 48 to 63 °C for 45 seconds and elongation at 72 °C for 60 seconds. A final incubation at 72 °C for 10 minutes was performed as final step. PCR amplicons were then run in an agarose gel as described previously (section 2.3.4) to assess specificity and the best annealing temperature.

2.4.2 cDNA or DNA qPCR

qPCR was carried out in a 10 μl final volume reaction using QuantiFast SYBR Green I PCR Kit, bespoke forward/reverse primers (0.3 μM/each) and 15 ng/μl cDNA or 15 ng/μl DNA for RT-qPCR or ChIP-qPCR experiments, respectively. Reactions were performed using a LightCycler® 480 Real-Time PCR System (F. Hoffmann-La Roche Ltd). To activate HotStarTaq Plus DNA Polymerase provided with SYBR Green I, pre-incubation at 95 °Cfor 5 minutes was performed prior 40 cycles amplification. Each cycle included denaturation at 95 °C for 10 seconds to separate double-stranded DNA (dsDNA) and a combined annealing/extension step at 60 °C for 30 seconds to prime template and synthesise the complementary strand. This two-step PCR was according to the SYBR Green I protocol. After each elongation step, SYBR Green I fluorescence was measured at 530 nm. As the fluorescence of SYBR Green I dye is enhanced up to 100-fold when intercalated into dsDNA, the fluorescence measured was proportional to the quantity of product synthesised by the primers.

To ensure that SYBR Green I fluorescence reads were reflecting specifically the PCR amplicon of interest, a melting curve was performed. This technique was based on the principle that every dsDNA product has a particular meting temperature[259]. Hence, the melting curve analysed all possible dsDNA products in samples (specific, non-specific and primer-dimers). When qPCR reactions were gradually heated up to 95 °C, all dsDNA products were separated into single-strands. This triggered a decrease in fluorescence that was measured and plotted as inverse. Specificity of qPCR reactions was assessed by the presence of a single peak in the melting curve which was achieved with all primers used, otherwise re-design or not used. Melting curves were obtained after denaturation at 95 °C for 15 seconds with a ramp rate of 4.8 °C/s and annealing at 60 °C for 1 minute with a ramp rate of 2.5 °C/s. Fluorescence data was

acquired twice every 1 °C change in temperature. Cycle threshold (Ct) values were given by default LightCycler® 480 software with the same manually fixed fluorescence background in all samples. All qPCR reactions were performed in duplicate (technical replicate).

2.4.3 Data analysis of ChIP-qPCR experiments

After qPCR was performed, the % input was then calculated using the Ct values. First, the adjusted input to 100% was obtained as follows.

$$Adjusted\ input\ =\ Duplicate\ average\ Ct\ value\ of\ input\ -\ \log_2(dilution\ factor) \tag{2.4}$$

$$where\ dilution\ factor\ =\ \frac{input\ used\ (\mu l)\ \times\ 100}{sample\ used\ (\mu l)} \tag{2.5}$$

Duplicated averaged Ct values of samples were then used to obtain the % input.

$$\%\ input\ =\ 100 \times 2^{(Adjusted\ input\ -\ duplicate\ averaged\ Ct\ of\ samples)} \tag{2.6}$$

The % input of H3K4me3 of cells treated with either vehicle ethanol (control), OA or DHA was then tested with IBM SPSS® version 22.0.0.0, 64-bit edition. Treatment means versus controls were compared by Student's T-test or one-way ANOVA with Dunnett's post hoc test. The selection of the statistical analysis was dependent on the number of groups involved in the analysis.

2.4.4 Data analysis of RT-qPCR experiments

mRNA levels were calculated using the Ct values by the standard curve method [260] and then normalised to *RPL13A* and *RPS18* expression (discussed in section 6.3.7). The standard curve for each gene was performed and included 5 known concentrations ranging from 4x (20 ng/μl) to 1/4x (1.25 ng/μl) the concentration of samples (1x = 5 ng/μl). After qPCR was carried out in the standard curve, the base 10 log-form of the concentrations in x-axis were plotted against the correspondent Ct values in the y-axis. Log-transformed concentration allowed a more symetrical data to apply linear regression. The equation of the slope of the linear regression was then obtained (Formula 2.7) and solved for x (concentration) (Formula 2.8). Data was raised to power 10

and the abundance of mRNA was obtained.

$$Y_i = \beta_1 X_i + \epsilon_i \tag{2.7}$$

where
Y_i= regressand or Ct value
X_i= regressors or abundance/expression of mRNA
β_1= parameter vector
ϵ_i = error term

$$Expression\ of\ mRNA\ of\ interest\ = 10^{\left(\frac{Ct\ value\ -\epsilon_i}{\beta_1}\right)} \tag{2.8}$$

The expression of the mRNA was then divided by the square root of *RPL13A* expression multiplied by *RPS18* expression (Formula 2.9). This relative expression reduced the possible variability of the mRNA of interest due to different amounts of template in samples and variations in RT efficiency.

$$relative\ expression\ of\ mRNA\ of\ interest\ = \left(\frac{concentration\ of\ mRNA\ of\ interest}{\sqrt{RPL13A \times RPS18}}\right) \tag{2.9}$$

Relative expression of mRNA in cells treated with either control vehicle, OA, EPA or DHA were tested with IBM SPSS® version 22.0.0.0, 64-bit edition. Treatment versus control means were compared by one-way ANOVA with Dunnett's post hoc test on the log transformed data as gene expression have shown to be not normally distributed[261].

2.5 Pyrosequencing

Measurement of DNA methylation by pyrosequencing involved several steps as describe elsewhere[234]. DNA was bisulphite treated to serve as a template for PCR amplification of a region of interest using bespoke primers. PCR amplicons were then sequenced through a light-base method (pyrosequencing). As unmethylated cytosines, but not methylated ones, changed with bisulphite treatment. Changes observed in the sequences were proportional to the changes in DNA methylation.

2.5.1 Primer design

Primer design was performed using 500 bp up- and downstream the CpG site of interest and PyroMark Assay Design version 2.0.1.15 (Qiagen). The 1002 bp sequence

corresponded to the same strand and genome build of probes in the MethylationEPIC BeadChip. Designed primer sets included a 5' biotin-label forward or reverse primer, its complement and a sequencing primer. Primer synthesis was carried out by Eurofins Genomics using High Purity Salt-Free (HPSF) and High-performance liquid chromatography (HPLC) purification methods for non- and biotin-label primers, respectively. Details of primers used for pyrosequencing are shown in Table 2.5.

Table 2.5: Primers used for pyrosequencing.

Target Cytosine ID	Primer Sequences (5'-3')	Temp[a]	Size[b] (bp)
cg26292058	Fwd TGTATATATTTGATAGGAGGGAAAGT Rev BIO-ACACCCCTTAAAATCATCCTATATATTAC Seq TTTAAGGTGTGTGTTAGA	57 °C	162
cg05475386	Fwd GTGTTTTTTGAGAGGAAATGGGTGATAAT Rev BIO-TACATTACACAAACCTTATTAAACATTACC Seq GGTTTTTTAATAGAAGGA	57 °C	121
cg27188282	Fwd AGGGTAAAGTTTGAGGGTATTTGT Rev BIO-ATCTTCTTCCCAAAACATCTTCTC Seq TGTTTTTGTGATTTAATTTATTATTTAAG	62 °C	165
cg06989443	Fwd BIO-TTAGGTAGATGGGGGAGTTGG Rev ACAAACAAACAAATAATTCCCCCTTACA Seq CTAAAAACAACTATTTATTCCCT	57 °C	246
cg22518417	Fwd BIO-TTTTGTTATTATTTAGATTGTGGTTTGG Rev ACCCAACCTTCTAATCTTTTCATAA Seq AAAAAACATTAATACTTATATACT	57 °C	79

Fwd, forward primer; Rev, reverse primer; Seq, sequencing primer; BIO-, biotin-labeled primer; [a] = annealing temperature; [b] = amplicon size.

2.5.2 Bisulphite conversion of DNA

DNA samples (1 μg) were bisulphite converted using EZ DNA Methylation-Gold™ Kit according to the manufacturer's instructions. Additionally, 1 μg of human unmethylated (EpiTect Control DNA) and methylated DNA (CpGenome universal methylated DNA) were also treated with bisulphite as control. The reaction involved denaturation of DNA, bisulphite treatment (sulphonation and deamination) and desulfonation. In this manner, unmethylated cytosines turned into uracils whereas methylated cytosines remained the same after bisulphite treatment. Samples were eluted in 60 μl elution buffer provided by the kit and store at $-80\,^{\circ}$C.

2.5.3 PCR

PCR was carried out in a 25 μl final volume reaction using 2 μl of bisulphite treated DNA (< 12.5 ng/μl), 12.5 μl KAPA2G Robust HotStart ReadyMix Kit and 1 μl of primers (10 μM/each). The reaction was performed using a Veriti 96 well Thermal Cycler (Applied Biosystems). PCR started with a 95 °C incubation for 3 minutes to activate polymerase with subsequent amplification for 45 cycles. Each cycle included denaturation at 95 °C for 15 seconds, annealing at a specific temperature for 15 seconds and elongation at 72 °C for 30 seconds. Annealing temperatures were selected after a PCR gradient and pyrosequencing optimisation was performed (Table 2.5). PCR products were stored at 4 °C until further processing.

2.5.4 DNA pyrosequencing

Pyrosequencing was carried out using GE Healthcare streptavidin sepharose high-performance beads (34 μm), PyroMark binding buffer, 1x PyroMark wash buffer, 96-well plates, 70% (v/v) ethanol, denaturation solution (8 g NaOH / 1 l dH_2O), PyroMark Q96 HS Sample Prep Thermoplate, PyroMark annealing buffer, PyroMark Q96 HS tips and PyroMark Gold Q96 Reagents which included deoxythymidine (dTPP), deoxyadenosine alfa-thio triphosphate (dATPαSs), deoxycytosine (dCTP), deoxyguanine (dGTP) triphosphates, enzyme and substrate.

In a 80 μl final volume reaction, 2 μl beads, 38 μl binding buffer, 10 μl PCR product and 30 μl dH2O were mixed for a minimum of 5 minutes using a plate shaker. The process bond double-stranded biotin-labeled PCR amplicon to beads which strands were then separated using a Vacuum Workstation (Biotage) following the manufacture's instructions. The separation of strands included the capture of double-stranded biotin-labeled PCR amplicon with a vacuum tool and serial flushes with 70% (v/v) ethanol, denaturation solution and wash buffer. The now single-strand biotin-labeled PCR amplicon was annealed after 80 °C incubation for 2 minutes using 12 μl annealing buffer with sequencing primers (0.3 μM) on a thermoplate. Samples were cooled down for a minimum of 5 minutes at room temperature prior pyrosequencing was carried out using a PyroMark MD instrument (Biotage). The final output was analysed using Pyro Q-CpG version 1.0.9 software (Biotage). Percent methylation of CpG sites of interest was determined by comparison of peak's height between dTPP or dATPαS and dCTP or deoxyguanine dGTP. This depended if sequencing primer amplification was on the forward or reverse strand, respectively. dTPP and dATPαS peaks represented unmethylated cytosines while dCTP and dGTP methylated ones. An example of each case is shown in Figure 2.2.

Human unmethylated, methylated DNA, NTC and bisulphite conversion controls were run and used in each pyrosequencing run. An additional bisulphite conversion effi-

ciency control was used and consisted in the measurement of DNA methylation of a cytosine that was not followed by a guanine (CpG), and therefore, expected to be totally unmethylated. Bisulphite conversion efficiency in samples was indicated by the absence of a peak in the pyrogram after adding dCTP or dGTP (Figure 2.2). Cut-offs to consider a pyrosequencing run successful were unmethylated control showing $< 10\%$ methylation, methylated control $> 70\%$ methylation and bisulphite conversion efficiency $> 95\%$.

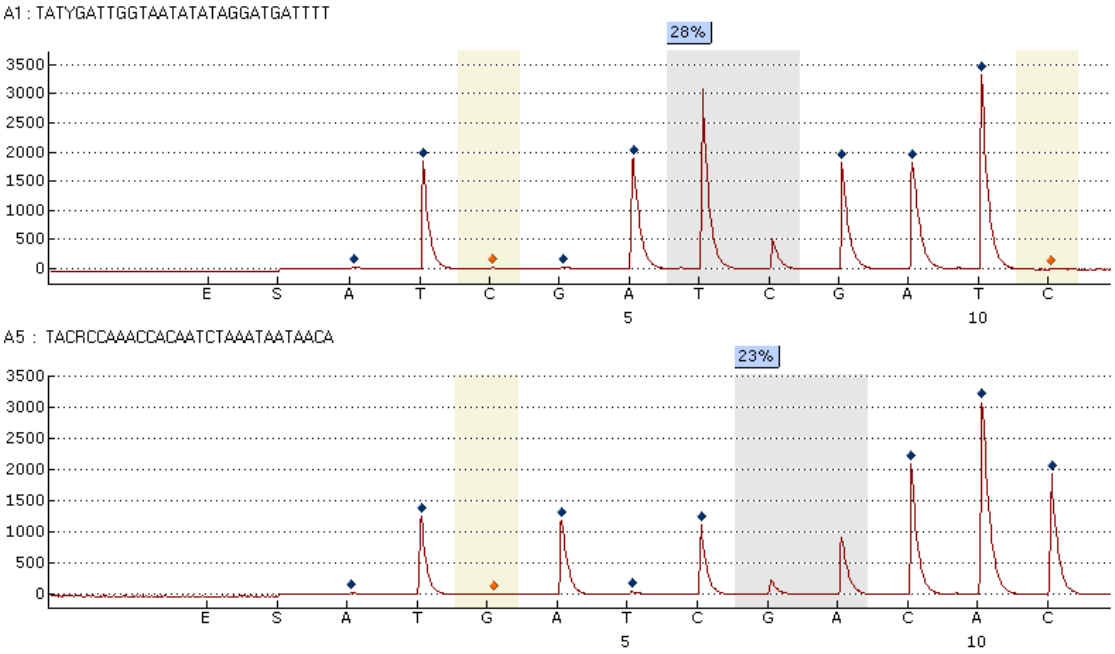

Figure 2.2: A typical pyrogram. Intensity of light is shown in the y-axis whereas nucleotide dispensation order in the x-axis, starting with enzyme (E) and substrate (S) signals. DNA methylation of the CpG site of interest and bisulphite conversion efficiency control is shown with a grey or yellow background, respectively. Pyrosequencing was performed using sequencing primers to amplify forward (top) or reverse (bottom) strands. T or A was expected when cytosines were unmethylated otherwise C or G. Comparison between un- and methylated signals indicated methylation percentage in the CpG site of interest (blue box).

2.6 Pathway analysis

Pathway analysis was carried out using Ingenuity® Pathway Analysis (IPA®, QIAGEN Bioinformatics) built version: 400896M, content version: 28820110 (release date: 2018-09-24). Such analyses were carried out to identify possible pathways altered in OA or DHA-treated cells using all significant transcriptome or DNA methylome changes identified by BeadArrays. Analyses were performed using annotated genes in IPA® database, all node types (e.g. ligand-dependent nuclear receptor, microRNA), all data sources (e.g. protein-protein interactions, Gene Ontology) with experimentally reported data in humans only. IPA® predicted activation and/or inhibition of canonical pathways, toxicity-related categories (ToxList), upstream regulators and downstream effects on biological functions of cells.

Predictions carried out using IPA® were based on the enrichment of significantly altered genes in a specific pathway and the agreement of the direction of change on gene expression compared with published data. Enrichment was determined by a p-value whereas agreement by a z-score. The p-values were calculated by Fisher's exact test right-tailed. This test examined if the overlap of significantly altered genes and the genes associated within a specific pathway/function in IPA® database was due to chance[262]. A minus logarithm (-log) p-value greater than 1.3 (equivalent to p-value < 0.05) was considered significant. The use of the -log(p-value) rather than p-value values was obtained by default in the software and was maintained for displaying purposes. The z-score of the significant pathways/functions was then calculated. The z-score was determined by the likelihood of the directional effect of one molecule to another in the dataset of interest. This was according to all information found in the software database. Positive z-scores indicated a possible activation while a negative value designated a possible inhibition. The more distant a z-score was from zero, the stronger the prediction was[262]. In this work, a z-score higher or lower than 1 or -1 was considered as a significantly activation or inhibition, respectively. A representation of the analyses performed in IPA® is shown in Figure 2.3.

2.6.1 Gene expression changes

To explore altered pathways by gene expression changes, duplicated transcripts regardless variants were removed. In addition, some transcripts that were not recognised by IPA® software were also discarded from analysis. The direction of change of genes (up- and downregulated) was included in the analysis. The final dataset that was used to predict molecules and pathways related to expression changes consisted of 82 transcripts (37 up-regulated) in OA treatment and 445 transcripts (218 up-regulated) in DHA treatment.

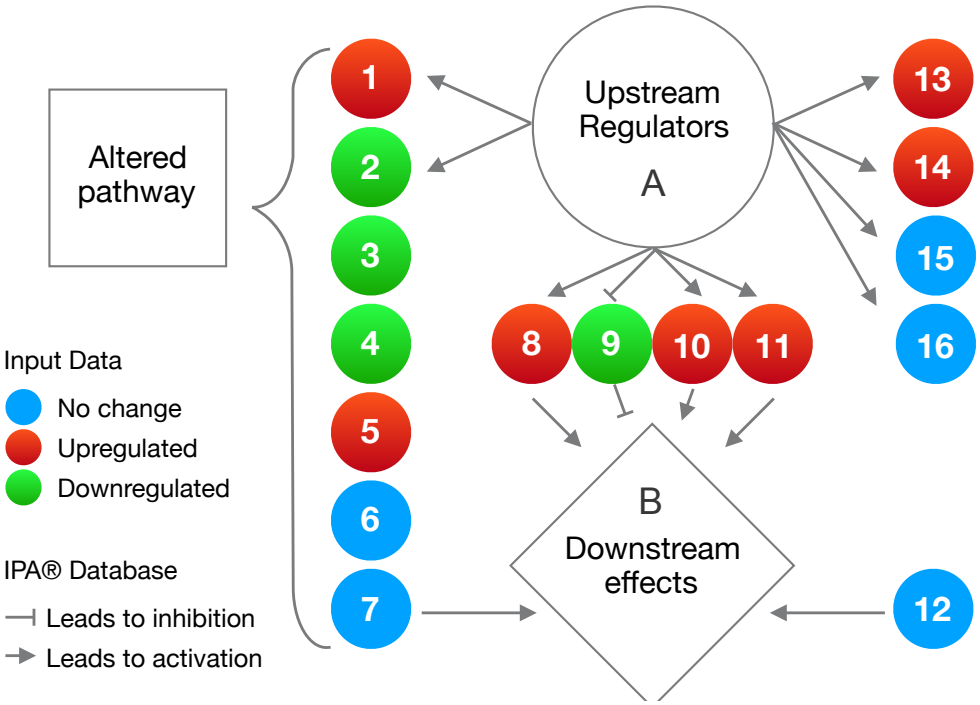

Figure 2.3: Overview of pathway analysis performed in IPA®. Significantly altered pathways were calculated according to enrichment of genes in a specific pathway/category with a -log(P-value) > 1.3 from Fisher's exact test. In addition, IPA® calculated a z-score based on the direction of change of published data compared with the input genes. The z-score accounted for similarities/discrepancies of the input data (altered transcripts by OA or DHA) with the experimental evidence in the IPA® database. Positive z-scores indicated a possible activation while negative values suggested a possible inhibition of the pathway. The same Fisher's exact test and z-scores were used to predict upstream regulators and downstream effects of altered transcripts on cells. The diagram shows hypothetical genes downregulated (green circles), upregulated (red circles) or genes that did not change expression (blue circles) by the treatments. For example, if reported evidence has been shown that a upstream regulator only lead to activation (arrows), but the input data showed a downregulation (gene 2 in group of genes 1-2) or a lack of effect in target genes (genes 15 and 16 in group of genes 13-16), the possibility of such gene to be an upstream regulator was low (z-score close to 0). In the perfect scenario, an upstream regulator that has been reported to activate genes 8, 10 and 11 while inhibiting gene 9 would find the same information in the input data (A). Similarly, the downstream effects were predicted. Assuming that a particular biological function (downstream effect) is under control of genes 7-12 (B). The ideal scenario would be that expression of genes that inhibit (blunt arrows) that biological function should be downregulated (gene 9) or not change (gene 7 and 12), while genes that induce a particular effect should be upregulated (gene 8, 10 and 11).

2.6.2 DNA methylation changes

Only DNA methylation changes in intragenic regions were considered to explore altered pathways by DNA methylation changes. Intragenic regions consisted of all genomic locations that form part of gene. These locations included promoter regions (up to 1500 bp), 5' UTRs, exons, introns and 3' UTRs. When a single gene changed DNA methylation in more than one CpG site within the same gene, this was considered as one altered gene. When a single CpG site was part of two genes, both genes were included in the analysis. Any duplicate gene regardless variants and some others that were not recognised by IPA® database were discarded from analysis. The direction of change was not included in the analysis (increased or decreased DNA methylation). Only a list of genes significantly changing DNA methylation in each treatment was used. The final dataset that was used to predict pathways and upstream regulators related to genes with altered DNA methylation by fatty acids consisted of 348 genes in OA treatment and 935 genes in DHA treatment.

Chapter 3

A Model to Investigate the Effects of OA or DHA on DNA Methylation in Cells

3.1 Introduction

The main aim of the current work was to understand how fatty acids alter the DNA methylation of human cells. The capacity of fatty acids to alter the DNA methylation has been identified in candidate genes using PBMCs from human volunteers after supplementation with olive oil or omega-3 fatty acids for 8 or 12 weeks[240]. Since OA and DHA are major constituents of olive oil or omega-3 fatty acids, respectively, they were selected to study their effects on the DNA methylation. In order to investigate the underlying mechanisms, a robust model such as a cell culture was needed. Therefore, Jurkat cells were selected because they are an immortalized human cancer cell line that grows fast (they duplicate cell number approximately every 30 hours). Besides, they are lymphocytes which are the major component of PBMCs[263] and their growing conditions are similar to those of PBMCs during fatty acid supplementation in humans (a cell suspension exposed to fatty acids in media).

The concentrations of OA and DHA in plasma lipids of healthy adults are on average 1285 μM and 88 μM, respectively[44]. Such physiological concentrations have been shown to decrease the viability of different human cancer cell lines *in vitro*[264;265]. In the specific case of Jurkat cells, no significant effect on viability has been detected after 1-day treatment with concentrations lower than 200-250 μM OA or 15-50 μM DHA[264;266–268]. However, those concentrations could reduce the cell viability if the duration of treatment is increased[267]. Available evidence suggests that the effects of fatty acids on cell viability is determined by the concentrations used, the type of fatty acid treatment, the duration of treatment and the cell type[264;266;267;269;270]. There-

fore, different concentrations and different duration of treatments were tested to expose the cells to OA or DHA with the highest dose and time without affecting cell survival.

In vitro treatment of cells with fatty acids has also shown to modify the fatty acid composition of treated cells[4]. Such changes are reported to be dependent of the time, cell-type and dose of the treatment until treated fatty acids reach a new steady state of concentration[4;53]. The increment of particular fatty acids may also increase the concentration of their derivative fatty acids by conversion or retro-conversion depending on the cell type[271]. Incorporation of fatty acids into cell membranes is needed for most of the fatty acid effects on cells[4]. The same may also be true for their effects on the DNA methylation. However, this is unknown.

The experiments in this chapter aimed to establish a working model to study the effect of fatty acids on DNA methylation. Since the effects of fatty acids on cell viability may represent a confounding factor, different concentrations of fatty acids were tested to avoid this. The fatty acid changes in cell media and cells were analysed to asses the effectiveness of the treatments used.

3.2 Materials and methods

Treatment of Jurkat cells with OA or DHA was carried out as described in section 2.2.1. Cell viability was determined by Trypan Blue exclusion (section 2.2.3). Measurement of fatty acids in cell media and cells was carried out by gas chromatography (GC, section 3.2.1).

3.2.1 Gas chromatography

3.2.1.1 Extraction, methylation and resolution of fatty acids

Cells ($8x10^6$) were washed three times with PBS and resuspended in 0.8 ml of 0.9% (w/v) NaCl. 1 M NaCl (1.0 ml) and 2:1 (v/v) chloroform:methanol[272] (5.0 ml) containing butylated hydroxytoluene antioxidant (50 mg/l) were added to the cell suspension or to 0.8 ml RPMI-1640 medium containing 9% (v/v) FBS, 2 mM L-glutamine, 100 U/ml 10 penicillin and 100 μg/ml streptomycin. Nonadecanoic acid was added as internal standard for medium (5 μg) and cells (15 μg). Samples were vortexed and then centrifuged at 753 g for 10 minutes at room temperature. The lower phase was recovered and dried under nitrogen. The dried extract was dissolved in toluene, and fatty acids methyl esters (FAME) were synthesised by incubation with 2% (v/v) sulphuric acid in methanol at 50 °C for 2 hours[273]. The reaction was neutralised by adding 1 ml of a solution containing 0.25 M $KHCO_3$ (25.03 g/l) and 0.5 M K_2CO_3

(69.10 g/l). 1 ml hexane was then added, samples mixed and then centrifuged at 188 g for 2 minutes at room temperature. The upper phase (hexane) was transferred to a glass tube and dried under nitrogen. FAME were resuspended in 75 μl of hexane and resolved on a BPX-70 fused silica capillary column (32 m $\times$ 0 $\cdot$ 25 mm $\times$ 25 μm; SGE Analytical Science) using an Agilent 6890 gas chromatograph equipped with flame ionisation detection (Agilent Technologies Ltd). The fatty acid composition of all samples at specific time points was determined in a single run when possible. At the beginning of each GC run, a blank sample and authentic FAME standards were run as controls (Supelco® 37 Component FAME Mix).

3.2.1.2 Analysis of data

Chromatograms obtained from GC were analysed using Chemstation software. An example chromatogram of Jurkat cells is shown in Figure 3.1. Fatty acids were identified by their retention times peaks compared with authentic standards. Automated integration was used and was checked manually. The area of all peaks in chromatograms was quantified; however, only peaks detected in more than 95% of all samples were included in the analyses. These peaks were considered as the total lipids in samples and were used to calculate fractional concentration (%) of each fatty acid using equation 3.1.

$$Fractional\ concentration\ (\%)\ =\ \left(\frac{area\ of\ peak\ of\ interest}{\sum\ area\ of\ all\ peaks}\right) \times 100 \tag{3.1}$$

To calculate the amount of each fatty acid (μg) in 8x10^6 cells, the area of the peak of the internal control added (15 μg nonadecanoic acid) was used as the reference (Equation 3.2).

$$Fatty\ acid\ (\mu g)\ =\ \left(\frac{area\ of\ peak\ of\ interest}{area\ of\ internal\ standard}\right) \times internal\ standard\ added\ (\mu g) \tag{3.2}$$

Finally, to calculate the fatty acid concentration in cell media (μM) the amount of the fatty acid of interest was calculated using Equation 3.2 (5 μg nonadecanoic acid as reference) followed by the Equation 3.3.

$$Concentration\ (\mu M)\ =\ \frac{fatty\ acid\ of\ interest\ (\mu g) \times \left(\frac{1}{volume\ of\ sample\ (l)}\right)}{Molecular\ weight\ of\ fatty\ acid\ of\ interest\ (g/mol)} \tag{3.3}$$

The amounts of internal standard used for cells (15 μg) or medium (5 μg) were selected after optimisation to obtain an area of the peak of the internal standard similar to the area of peaks of fatty acids in samples.

3.2.2 Statistical analysis

All statistical analyses were carried out using IBM SPSS® version 22.0.0.0, 64-bit edition. In 1-day treatments, the Student's T-test was used to compare the viability between control and OA or DHA-treated cells at the different concentrations tested. In 8-days and 10-days treatments, two-way ANOVA with Dunnett's post hoc test was used to compare the viability and proliferation of OA or DHA-treated cells versus controls. The Student's T-test was used to compare the fatty acid composition changes between control, OA or DHA-treated cells and treatment media.

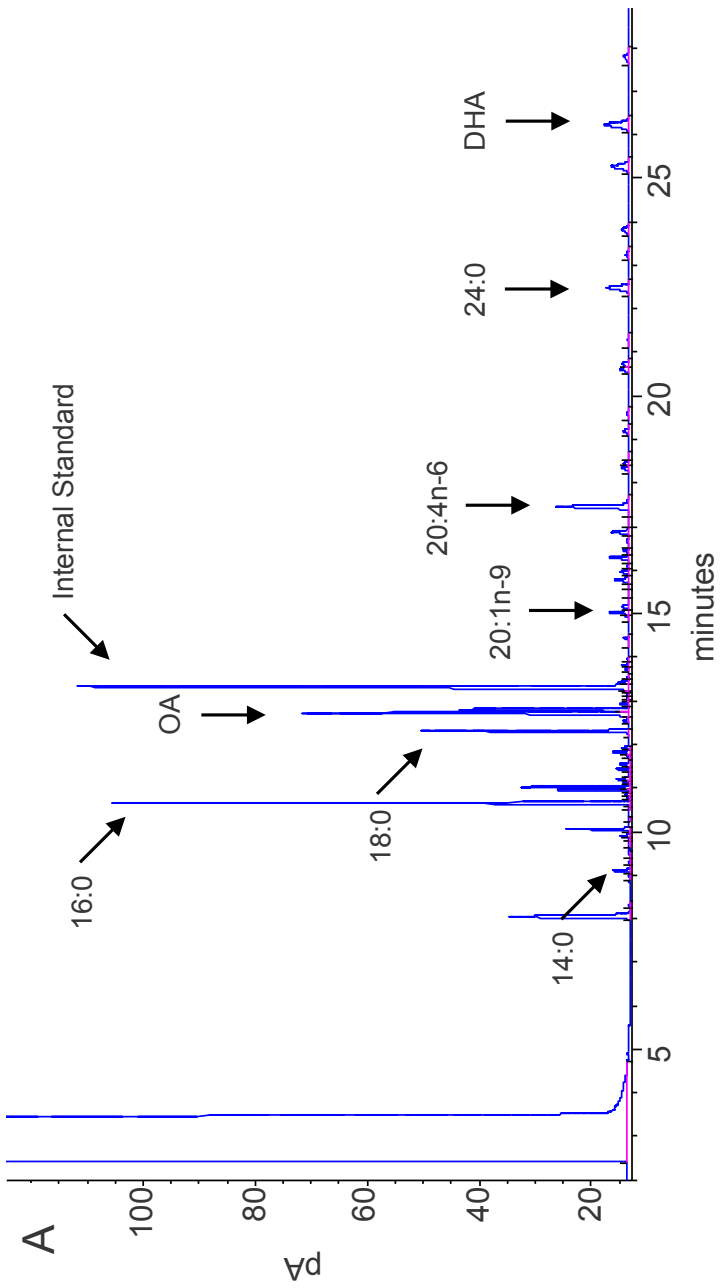

Figure 3.1: An example chromatogram of Jurkat cells. Each peak represented a different fatty acid according to their retention time in minutes (x axis), whereas the area of peak was proportional to the mass of each fatty acid (y-axis). Identification of fatty acids are indicated by arrows.

3.3 Results

3.3.1 The effect of OA or DHA on the cell viability and proliferation

Treatment of cells with OA at the concentrations tested (7.5 to 30 μM) did not alter cell viability significantly after 1 day of treatment compared with the control treatment (vehicle ethanol $< 0.01\%$ (v/v)). Similarly, there was no significant effect on cell viability by incubation with 7.5 μM or 15 μM DHA. However, incubation with 22.5 μM or 30 μM DHA induced a significant decrease in cell viability after 1 day of treatment (4 to 9% points) compared with controls (Figure 3.2). Therefore, in order to ensure the greatest effect of fatty acids on cells without reducing cell viability, the 15 μM concentration was selected for subsequent experiments.

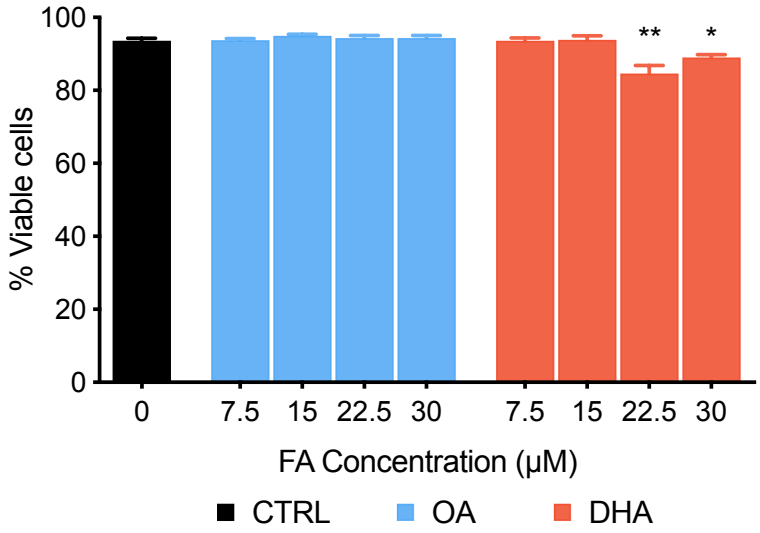

Figure 3.2: Viability of Jurkat cells after OA or DHA treatment for 1 day at different concentrations ranging from 7.5 μM to 30 μM. Data are the mean % of viable cells $\pm$ standard error of the mean (n = 3 per concentration per treatment). Controls versus treatments means were compared by one-way ANOVA with Tukey HSD post-hoc test per treatment and those which differed significantly are indicated by *P < 0.05, **P < 0.01 or ***P < 0.001. FA, fatty acid.

Cells were incubated then with 15 μM OA or 15 μM DHA for 10 days. Treatment of cells with 15 μM OA did not alter cell viability during a 10-day incubation. In contrast, DHA treatment induced a significant decrease in cell viability after the 5^{th} day of treatment ($> 4\%$ points). The viability of cells decreased by 15% to 19% points compared with controls between day 9 and 10 (Figure 3.3).

Same to cell viability, 15 μM OA treatment did not alter cell proliferation during a 10-day incubation. However, 15 μM DHA treatment induced a time per treatment effect on proliferation of cells (Figure 3.4).

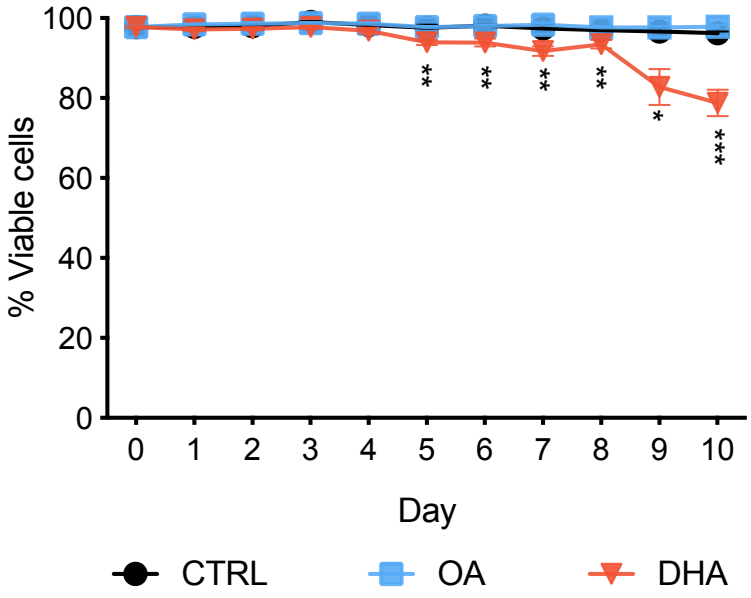

Figure 3.3: Viability of Jurkat cells during 15 μM OA or 15 μM DHA treatment for 10 days. Data are mean ± standard error of the mean (n = 3 replicates per treatment per time point). Control versus treatments means were compared by two-way ANOVA with time as a repeated measure and treatment as a fixed factor. Means that differed significantly are indicated by *P $<$ 0.05, **P $<$ 0.01 and ***P $<$ 0.001.

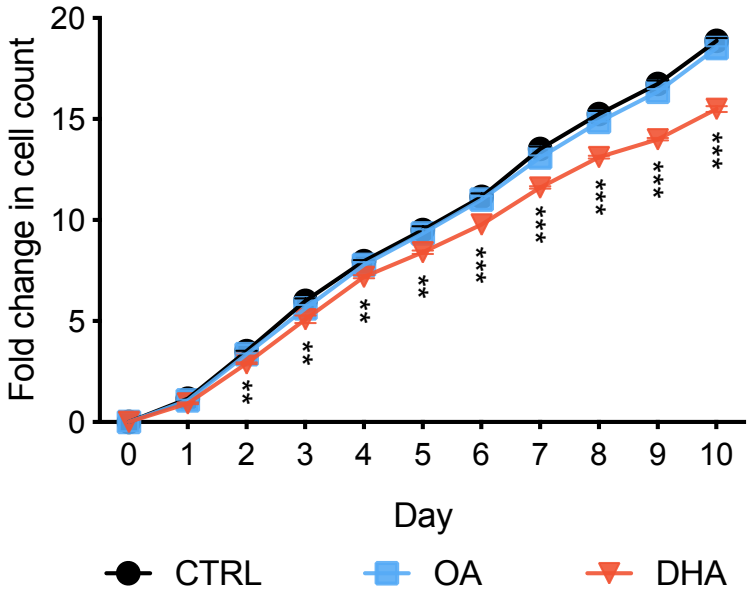

Figure 3.4: Proliferation of Jurkat cells during 15 μM OA or 15 μM DHA treatment for 10 days. Data are mean ± standard error of the mean (n = 3 replicates per treatment per time point) of the fold change in cell count between cells seeded and cells harvested. Control versus treatments means were compared by two-way ANOVA with time as a repeated measure and treatment as a fixed factor. Means that differed significantly are indicated by *P $<$ 0.05, **P $<$ 0.01 and ***P $<$ 0.001.

Because cell viability decreased three times more at day 9 (15% points) compared with day 8 (4% points) in DHA-treated cells, a period of 8 days was selected for further experiments. 15 μM OA or 15 μM DHA treatments were performed again for 8 days increasing the number of cultures replicates (n = 12 per treatment). Similar to previous experiments, the viability decreased significantly only in DHA-treated cells. After the 8th day of incubation with 15 μM DHA the cell viability decreased significantly 4% points compared with vehicle control (Figure 3.5). DHA treatment, but not OA treatment, decreased the fold change in cell count between cells seeded and cells harvested compared with the control treatment (Figure 3.6).

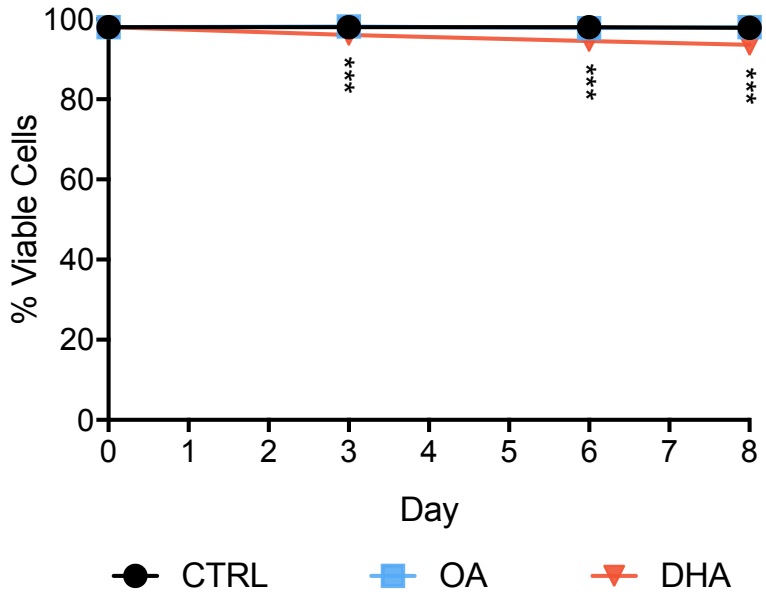

Figure 3.5: Viability of Jurkat cells during 15 μM OA or 15 μM DHA treatment for 8 days. Data are mean ± standard error of the mean (12 replicates per treatment per time point). Control versus treatments means were compared by two-way ANOVA with time as a repeated measure and treatment as a fixed factor. Means that differed significantly are indicated by *P $<$ 0.05, **P $<$ 0.01 and ***P $<$ 0.001.

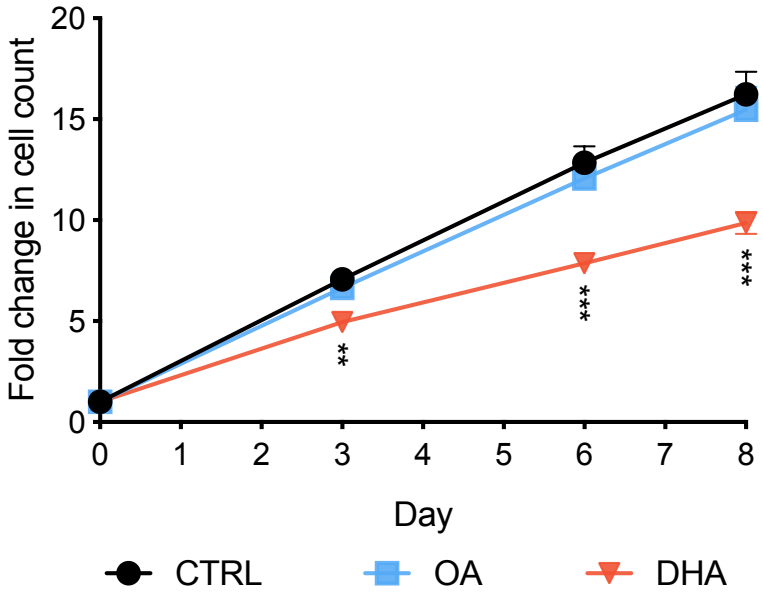

Figure 3.6: Proliferation of Jurkat cells during 15 μM OA or 15 μM DHA treatment for 8 days. Data are mean $\pm$ standard error of the mean (12 replicates per treatment per time point) of the fold change in cell count between cells seeded and cells harvested. Control versus treatments means were compared by two-way ANOVA with time as a repeated measure and treatment as a fixed factor. Means that differed significantly are indicated by *P $<$ 0.05, **P $<$ 0.01 and ***P $<$ 0.001.

3.3.2 The effect of OA or DHA treatment on the fatty acid composition of cells

Fatty acids in treatment media were measured to corroborate the concentrations used. OA treatment media increased the amount of OA (17 μM, 2.2 fold) while DHA treatment media increased the amount of DHA (14 μM, 6.1 fold) compared with control media (Figure 3.7).

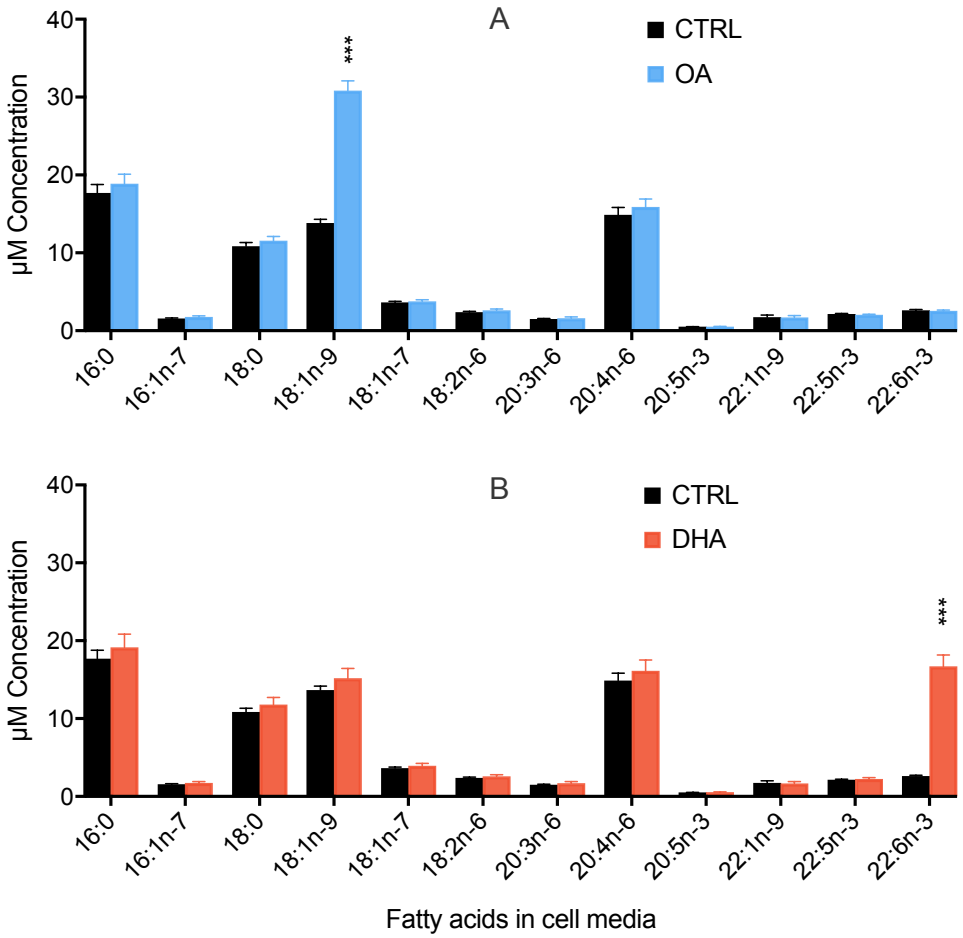

Figure 3.7: Fatty acid composition of control (black bars), OA (A) or DHA (B) treatment media (n = 18 / treatment). Data are mean ± standard error of the mean. Control versus treatments means were compared by Student's T-test per time point and those which differed significantly indicated by *P $<$ 0.05, **P $<$ 0.01 and ***P $<$ 0.001.

To test the effectiveness of fatty acid treatments the total cell lipids were measured after the 3rd and 8th day of incubation. OA treatment induced a significant increase in the amount of OA (2.9 fold), 16:0 (1.2 fold) and 20:1n-9 (4.4 fold) after 3 days of incubation. This was accompanied by decreased amounts of 16:1n-7 (-1.3 fold). Except for 16:0, all significant differences identified at the 3rd day remained the same after 8 days

of incubation with OA (Figure 3.8).

DHA treatment induced a significant increase in the amount of DHA (11.9 fold), 16:0 (1.5 fold), 18:0 (1.4 fold), 20:3n-6 (2.1 fold), 20:5n-3 (3.8 fold) and 22:5n-3 (2.2 fold) after 3 days of incubation. This was accompanied by decreased amounts of 16:1n-7 (-1.26 fold), 18:1n-9 (-1.1 fold) and 18:1n-7 (-1.26 fold), although this only reached significance after 8 days of incubation with DHA (Figure 3.8).

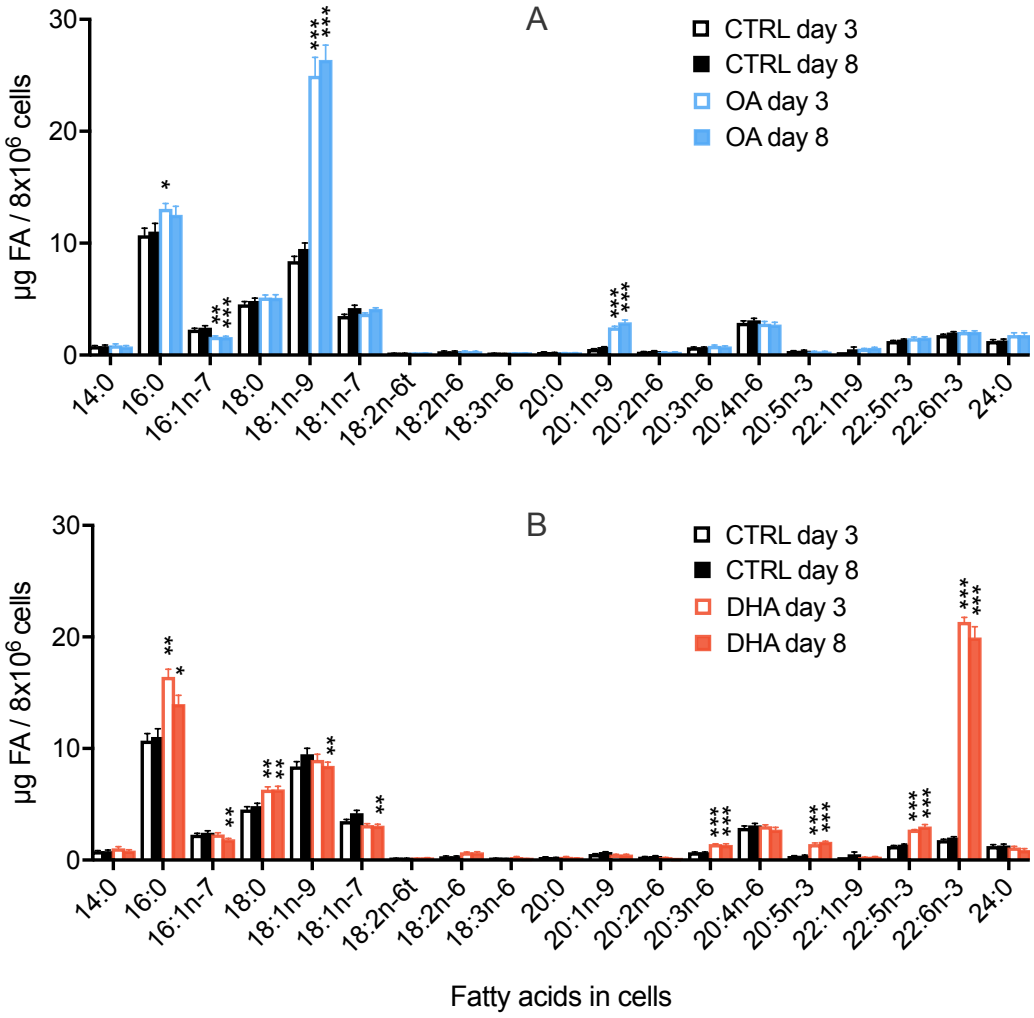

Figure 3.8: Changes in fatty acid composition of Jurkat cells by 15 μM OA (A) or 15 μM DHA (B) after 3 (n = 4 replicate cultures) or 8 (n = 7 replicate cultures) days of incubation. Data are mean ± standard error of the mean. Control versus treatments means were compared by Student's T-test per time point and those which differed significantly indicated by *P $<$ 0.05, **P $<$ 0.01 and ***P $<$ 0.001. FA, fatty acid.

3.4 Discussion

In order to study the mechanisms of how fatty acids alter the DNA methylation, a robust model was needed. Treatment of Jurkat cells with OA or DHA was tested as a model of study. Different concentrations and times of treatment were explored to avoid cytotoxic effects of fatty acids and at the same time to induce the major effect possible on cells. The fatty acid composition of cells was then measured to asses the effectiveness of OA or DHA treatment.

3.4.1 The effect of OA or DHA on cell viability and proliferation

The results agreed with several studies that have been shown a decrease survival of different human tumour cells and cell lines in a dose and time-dependent manner by an *in vitro* treatment with DHA, but not OA at the same concentration[269;274;275]. After testing different concentrations and duration of treatments, 15 μM OA or DHA for 8 days were selected as working conditions. Although this concentration and time significantly decreased the viability of DHA-treated cells ($<$ 5% points), the overall viability of Jurkat cells was not affected ($>$ 90% viable cells).

Several mechanisms to explain the cell death of cancer cells by DHA have been described. They include an increase in lipid peroxidation[276], induction of procaspase-3 clavage[277], lower production of prostaglandin E_2[101;275;278] and altered expression of genes that control the cell cycle[116]. These mechanisms are still not completely understood and were not assessed mainly because they were beyond the scope of the current work and because the cell viability dropped less than 5% points. Such small decrease may restrict the experimental measurement of the different process possibly altered by DHA. Reports addressing the mechanisms of cell death induced by DHA generally show a reduction in the cell viability of more than 40% points[276;277].

DHA, but not OA treatment, decreased the number of cells that were harvested in comparison with the control treatment. This suggested that DHA treatment decreased cell proliferation, which is in agreement with reported evidence[266]. Cell cycle arrest by DHA has been associated with increased ceramide formation and cyclin-dependent kinase (CDK) inhibitor 1A protein expression, together with decreased phosphorylation of RB transcriptional corepressor 1, CDK2 activity and cyclin A2 protein levels[266]. The latter in a time-dependent manner. Results in this work support the time-dependent effect on Jurkat cells' proliferation as there was identified a significant time-dependent decrease in the cell count after DHA treatment. The effect on cell proliferation specifically by DHA, but not OA treatment, suggests that different molecular mechanisms were altered. Therefore, there is a possibility that such differences may trigger or influence different changes in cells, including DNA methylation changes. This is currently unknown.

3.4.2 The effect of OA or DHA treatment on the fatty acid composition of cells

OA or DHA treatment increased the concentration of the fatty acid supplemented in Jurkat cells (Figure 3.8). In addition to these, the amounts of other fatty acids were also altered by the fatty acid treatments. Such changes were observed since the 3rd day of treatment and remained virtually unchanged after the 8th day.

Treatment with OA decreased the total amount (μg) of 16:1n-7 in cells. This monounsaturated fatty acid, together with OA, are products of 16:0 and 18:0 desaturation by stearoyl-CoA desaturase (SCD), respectively[18]. There is evidence that OA can decrease *SCD1* mRNA expression using mice hepatocytes[279]. Thus, it is possible that the decreased amounts of 16:1n-7 in OA-treated cells were due to an end-product inhibition of SCD1 by the increased amounts of OA. Further analysis of the transcriptome changes in chapter 6 support this (Appendix B). Changes in the expression of *SCD1* by OA treatment using human cells are not usually tested in studies addressing gene expression changes by OA. Because of this, it was not possible to compare the findings observed in this work.

OA-treated cells also showed an increment in the amount of 20:1n-9. In mammalian cells, OA can undergo two-carbon elongation to synthesise 20:1n-9 mainly by elongation of very long chain (ELOVL) 3 enzyme[280]. The approximately 4.5 fold increase in 20:1n-9 concentration and the 30% decrease in the OA|20:1n-9 ratio (μg|μg) in OA-treated cells suggested a possible activation of the elongation process presumably by activation of ELOVL3 (Figure 3.9).

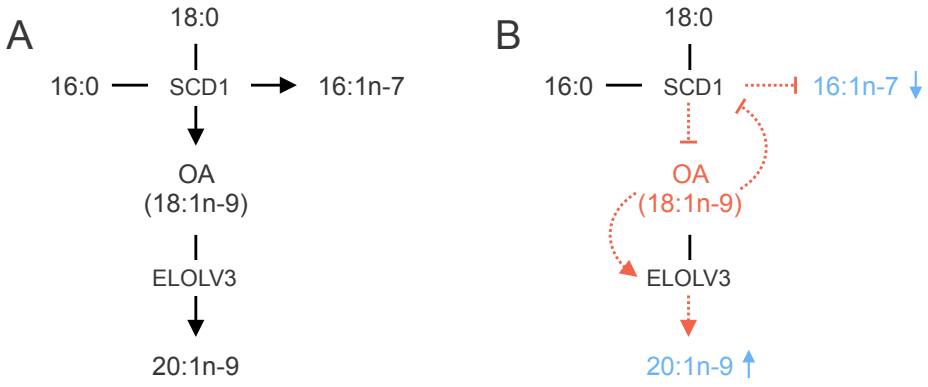

Figure 3.9: Model to explain changes in the amount of fatty acids (blue arrows) induced by OA treatment in Jurkat cells (B) compared with control treatment (A). Possible mechanisms (red dotted lines) underlying such alterations may include activation (red dotted arrows) and inhibition (red dotted blunt arrows) of ELOVL3 and SCD1, respectively.

Treatment with DHA increased the amount of 20:5n-3 and 22:5n-3 in cells. One possible explanation is that some DHA was retroconverted to 20:5n-3 and 22:5n-3. Retroconversion of DHA has been described in a few human cell cultures as it is not usually reported[271;281]. Taking into account the increased amount of DHA in cells, it was calculated that this was retroconverted to 22:5n-3 by 7% and to 20:5n-3 by 6%. In both instances, DHA had to lose a double bond plus two carbons in the case of 20:5n-3 retroconversion. The widely accepted mechanisms of DHA biosynthesis in mammalian cells has been shown that DHA retroconversion is a peroxisomal function[281;282]. Besides, DHA treatment has been shown to increase elongation and the number of peroxisomes using human fibroblasts deficient in peroxisomal enzymes acyl-CoA oxidase 1 or 2-enoyl-CoA hydratase/D-3- hydroxyacyl-CoA dehydrogenase, bifunctional protein[283]. Thus, evidence suggests that DHA may stimulate peroxisome function that led to peroxisomal retroconversion of DHA. However, it is difficult to conclude on the possible mechanisms that were activated or inhibited to achieve DHA retroconversion considering only the fatty acid composition changes in Jurkat cells.

DHA incorporation into cell phospholipids has been widely described to occur with a concomitant decrease of arachidonic acid (AA)[284]. An altered level of AA has implications in cellular functions as it is the primary precursor to produce eicosanoids[284]. In the current experiments, there were no changes in the amounts of AA in both, OA or DHA-treated cells. Differences between the literature and results in this work may arise because the majority of reports have been analysed the fractional concentration (%)[284–286] instead of amounts reported here. Net increase of any fatty acid can lead to an apparent reduction in the proportion of others which concentration remained the same. Alternatively, the current work analysed total lipids in cells which may not reflect the specific decreased AA levels reported in cell phospholipids.

Finally, there was identified a different increase in the amounts of OA or DHA in treated cells in spite of the same concentration added to treatment media (15 μM OA or DHA). Such differences were not entirely explained by the corresponding amounts of fatty acids in treatment media. For example, DHA treatment media, which was supplemented with 15 μM DHA, showed a similar total concentration of OA, AA and DHA. However, the amount of DHA in DHA-treated cells was 2 times more than OA and 5 times more than AA. Besides this, the total amount of OA and DHA in cells were different before fatty acid treatments. Both, different fatty acid uptake and unequal initial concentration of fatty acids may influence the higher fold increase in DHA identified in DHA-treated cells compared with the fold increase in OA observed in OA-treated cells. A different fold change increase in OA or DHA in Jurkat cells may potentially influence fatty acid effects on cells such as DNA methylation changes. This is currently unknown and future experimental work should consider the differential uptake and initial concentration of fatty acids in cell media to address this.

Overall, fatty acids treatments are in agreement with evidence showing that composi-

tion of cells can be modulated accordingly to exogenous fatty acids treated or supplement[4]. The time required to incorporate fatty acids into cells has been shown to be cell type specific. In our experimental conditions, fatty acids changes in cells reached new steady-state levels before the 3rd day of treatment which remained constant until the 8th day.

3.5 Conclusions

15 μM OA or 15 μM DHA for 8 days showed to be the highest concentration and longest time to treat Jurkat cells without compromising the cell viability ($>$ 90% viable cells). OA and DHA were incorporated, elongated, or retroconverted to others fatty acids which reached new steady-state levels before the 3rd day of treatment. Changes in the fatty acid composition of cells indicated that treatments worked, therefore, this suggested that such treatments were appropriate for studying the effects of fatty acids on cells. One effect of particular interest in the current project is the impact that OA or DHA may have on the DNA methylation. Altogether, results suggested that 15 μM OA or 15 μM DHA treatment for 8 days using the Jurkat cell line was a suitable model to study the effects of fatty acids on the DNA methylation. Understanding the effect of OA or DHA on the DNA methylome may help to elucidate the underlying mechanisms of such effects.

Chapter 4

The Effect of OA or DHA Treatment on DNA Methylation in Jurkat Cells

4.1 Introduction

The effect of fatty acids on the DNA methylation has been investigated mainly on candidate genes showing specificity[231–233;240]. The specific effect of individual fatty acids on such candidates genes may not be representative of the genome. One of the main difficulties to carry out whole-genome analysis is a large number of loci (≈28,000,000) that can be potentially methylated in the human genome[174]. Nevertheless, genome-wide studies using BeadArrays are an alternative. To date, only four studies have reported the effects of fatty acids on the DNA methylation of human cells using BeadArrays technology[229;241;242;287]. Two of them included a single fatty acid treatment, therefore, results were unable to provide evidence about the specificity of effects by different fatty acids[241;287]. Another study analysed the *in vivo* effect of palm and sunflower oil on human adipose tissue[242]. However, besides the different fatty acid composition, these oils have also different bioactive components[288] which may have an impact on the results obtained. In addition, volunteers followed a hypercaloric diet that led to a difference in weight[242]. Changes in body weight have also been associated with DNA methylation changes[243], thus, complicating the evaluation of the actual effect of fatty acids. The only study that have addressed the specificity of DNA methylation changes by individual fatty acids found no statistically significant effects by BeadArrays, although a difference on DNA methylation was identified by pyrosequencing in selected loci[229]. Therefore, there is still uncertainty about the fatty acids specificity to induce altered DNA methylation of cells at the genome level.

The experiments in this Chapter aimed to determine the effect of OA and DHA on the DNA methylome using DNA methylation BeadArrays. All significantly altered loci were analysed in the first instance to obtain the global changes on DNA methylation. Then, pathways analysis was performed using CpG sites within genic regions to investigate any possible functional relationship of the genes that showed altered DNA methylation by OA or DHA treatment. Finally, the time required for fatty acids to establish DNA methylation changes was addressed. BeadArrays results were validated by pyrosequencing.

4.2 Materials and methods

Cultures and treatments of Jurkat cells were carried out as described in section 2.2.1. DNA extractions were performed according to section 2.3.2. Quality and quantity of DNA was assessed by NanoDrop and agarose gel electrophoresis, respectively (sections 2.3.3 and 2.3.4). BeadArray hybridisation and analysis was carried out as described in section 4.2.1. Pathway analysis was performed according to section 2.6. Pyrosequencing was done as indicated in section 2.5.

4.2.1 BeadArray analysis of DNA methylation

DNA methylation was determined using the Illumina Human MethylationEPIC BeadChip covering more than 850,000 methylation loci per sample. An overview of the analysis that was carried out is shown in Figure 4.1.

4.2.1.1 Samples & BeadChip hybridisation

After DNA extraction, samples from different cell culture replicates treated with vehicle control, OA or DHA for 8 days were selected (n = 4 per treatment group) according to the highest DNA yield obtained. DNA samples were diluted to 50 ($\pm$5) ng/μl and sent for 850k MethylationEPIC analysis to Dr Michael Kobor's laboratory in the Centre for Molecular Medicine and Therapeutics, BC Children's Research Hospital (BCCHR) Institute, University of British Columbia, Vancouver, Canada. To avoid batch effects, the samples were distributed to a specific position between and within BeadChips[289] (Figure 4.2). In accordance with Dr Michael Kobor's laboratory quality control procedures, the DNA samples were bisulphite converted using the zymo EZ DNA Methylation Kit (Zymo Research, D5002) with the incubation conditions that manufacturer recommended to use for the Illumina Methylation BeadArray (incubation of samples in a thermocycler at 95 °C for 30 seconds, 50 °C for 60 min for

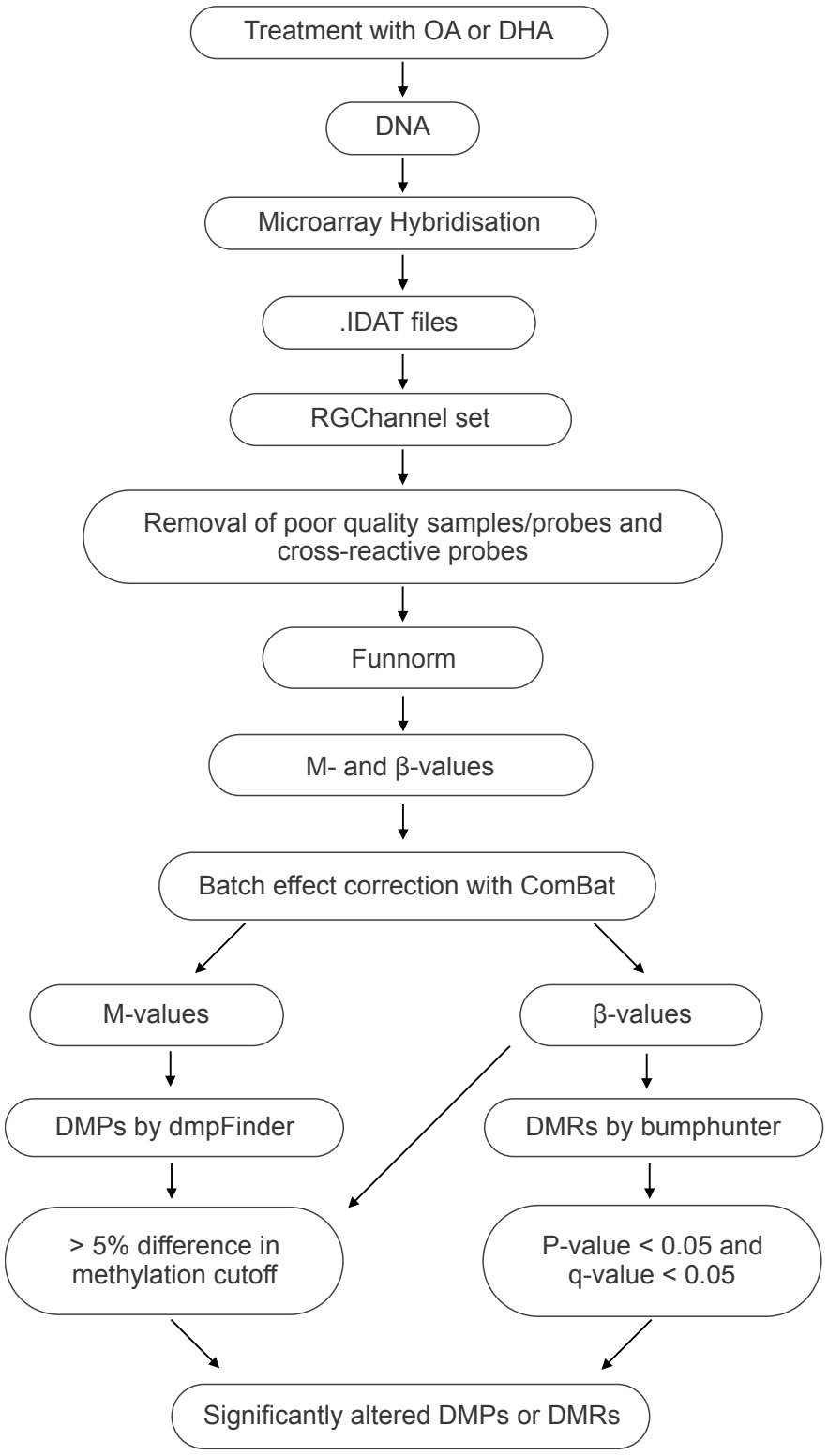

Figure 4.1: MethylationEPIC BeadArray; overview of analysis workflow using R package minfi. Funnorm, Functional Normalisation; DMPs, differentially methylated position; DMRs, differentially methylated regions.

16 cycles). Bisulphite-converted DNA was then hybridised to beads on BeadChip followed by a single-base extension using labelled dideoxynucleotides triphosphates (ddATP, ddTTP, ddCTP, ddGTP) which inhibited DNA polymerase once added. Cy3-Green fluorophore was used for ddCTP and ddGTP whereas Cy5-Red for ddATP and ddTTP. The correspondent green and red intensities in each bead allowed the quantification of DNA methylation. In type I probes, the red and green channels corresponded to both unmethylated and methylated loci, respectively. In type II probes, the red channel corresponded to methylated whereas the green channel to unmethylated loci[290]. Red and green channels intensities were analysed in-house.

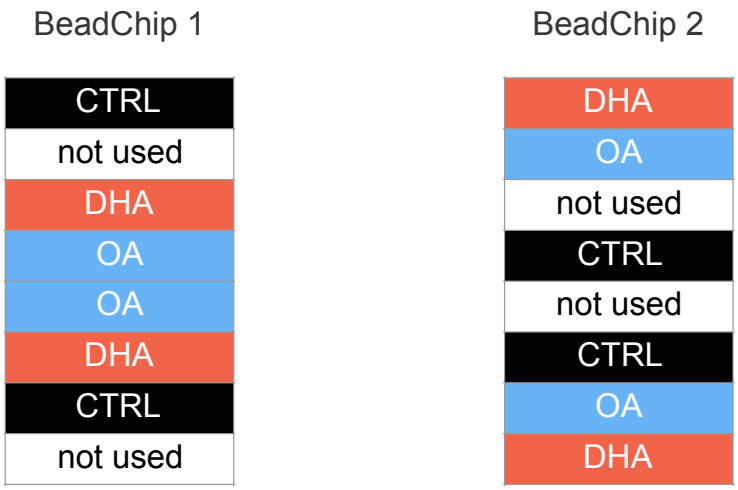

Figure 4.2: MethylationEPIC BeadArray; sample distribution on BeadChip to avoid batch effects.

4.2.1.2 Quality controls & normalisation

Raw data were analysed using the R package minfi version 1.18.6[291] with MethylationEPIC annotation ilm10b2.hg19_0.3.0 and the R version 3.3.0 of the IRIDIS 4 High-Performance Computing Facility at the University of Southampton, Southampton, UK. Standard quality controls and normalisation procedures were followed for the data pre-processing. The first step was reading the raw data (.IDAT files) to obtain a dataset containing the raw fluorescence in the green and red channels (RGChannel set). Poor quality samples/probes were excluded from the analysis according to a mean detection p-value > 0.05 at sample/probe level of the absolute signal (methylated + unmethylated) compared with background[292]. The list of cross-reactive probes reported by Chen *et al.*,[293] were also excluded from the analysis. Quality controls were given by adequate bisulphite conversion of DNA, extension and hybridisation controls. Moreover, the relationship of $\log^2$ median intensities of the total methylated and unmethylated signals was evaluated to asses an overall quality of samples as proposed by Aryee *et al.*[291]. Normalisation was carried out using functional normali-

sation (Funnorm) which has shown to perform better than others by reducing batch effects[294]. Funnorm pre-processing started with the coupling of the RGChannel set to Infinium I or Infinium II probes. This process transformed the green and red fluorescence signals in the RGChannel set to raw unmethylated and methylated signals (Methyl set). This Methyl set was further processed to normalise raw methylation signals across all probes into a number that was proportional to the degree of methylation in each locus (Ratio set). Such number ranged between 0 to 1 in case of the β-values (representing 0% to 100% DNA methylation, respectively) or between - infinity to + infinity in case of M-values. The Ratio set was then mapped to the genome to add genomic coordinates to each locus (Genomic Ratio Set). The β-values and M-values were further corrected for any possible batch effect using ComBat function in Surrogate Variable Analysis (SVA) R package version 3.22.0. ComBat correction has been shown to be particularly robust in experiments with small sample sizes ($n < 10$)[295] such as the current study.

4.2.1.3 Statistical analysis of DNA methylation BedChip

OA or DHA samples were individually compared with controls using the function dmpFinder within the R package minfi to obtain differentially methylated positions (DMPs). dmpFinder computed significant DMPs using an F-test of the M-values between treatment groups (categorical phenotype). The M-values were used to obtain all DMPs as they have more detection power and higher true positive rate in low and high methylated locus[296]. All significant P-values were corrected by multiple testing using the Benjamini and Hochberg False Discovery Rate (FDR)[297] which gave a q-value. To further increase confidence in the results a cutoff greater than 5% change in DNA methylation (> 0.05 β-value) was also used. In summary, the cutoffs to consider a DMPs significant in the present work were a P-value < 0.05, a q-value < 0.05 and a β-value > 0.05.

OA or DHA samples were also compared individually with controls using the function bumphunter within the R package minfi to obtain differentially methylated regions (DMRs). bumphunter function computed DMRs using a t-statistic test of β-values[298] and 100 permutations at each genomic location. The β-values were used to obtain significant DMRs as there was no option available to perform analysis with the M-values. The cutoffs to consider a DMRs significant were a P-value < 0.05 and a q-value < 0.05 within each genomic region.

4.2.1.4 Validation of results

DMPs were validated by pyrosequencing as described in section 2.5.

4.3 Results

4.3.1 Quality control of samples and BeadArray processing

DNA samples showed an average 260/280 ratio of 1.8 (±0.1) and 260/230 ratio of 2.2 (±0.2) which indicated an absence of protein, phenol or other contaminants in the samples. There were no signs of DNA degradation according to agarose gel electrophoresis. Also, DNA fragments in samples were ≥ 2 Kb which fulfilled requirements by the BeadChip manufacturer, Illumina. (Figure 4.3).

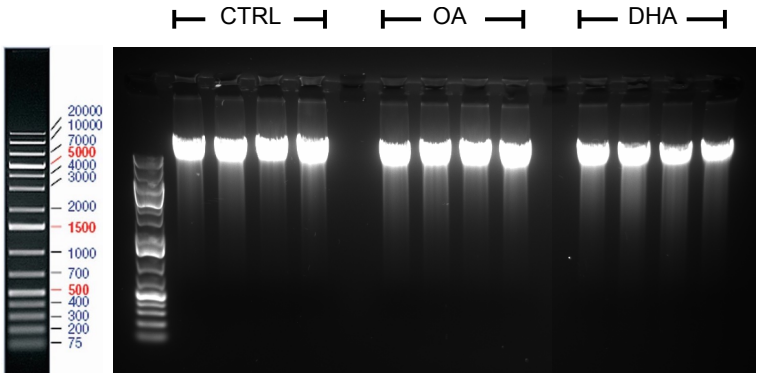

Figure 4.3: MethylationEPIC BeadArray; DNA integrity of samples used as per 250 ng/μl DNA from control (CTRL), OA or DHA-treated cells (n = 4 culture replicates per treatment) run in a 1% agarose gel alongside 1 Kb ladder (3 μl) for 30 min at 120 volts.

DNA samples were sent off for DNA analysis using MethylationEPIC BeadArray and raw data returned. In-house analysis showed that there were no outlier samples identified by a detection p-value > 0.05. Poor quality probes (1,038 and 1,047) and cross-reactive probes (28,928 and 28,931) were removed from datasets which left a total number of 836,870 and 836,858 probes for analysis in OA or DHA group, respectively. Extension and hybridisation controls were similar across samples as expected. The $\log^2$-transformed median intensities of unmethylated signals plotted against methylated signals showed a good sample index as proposed by Aryee[291] (Figure 4.4).

Raw array signals were normalised using Funnorm which clustered together the β-densities of all samples as expected (Figure 4.5). Normalised signals were used to carry out a principal component analysis (PCA) to identify any factor related to the DNA methylation signals of samples. PCA identified a clustering of samples by the BeadChip used for analysis, thus, suggesting a batch effect (Figure 4.6 B). Because of this, ComBat tool was implemented to lose such batch effect. PCA carried out after ComBat was applied showed that the batch effect was effectively removed from the data (Figure 4.6 C). Adjusted DNA methylation signals were then used to identify significantly changes on DNA methylation of OA or DHA-treated cells compared with controls.

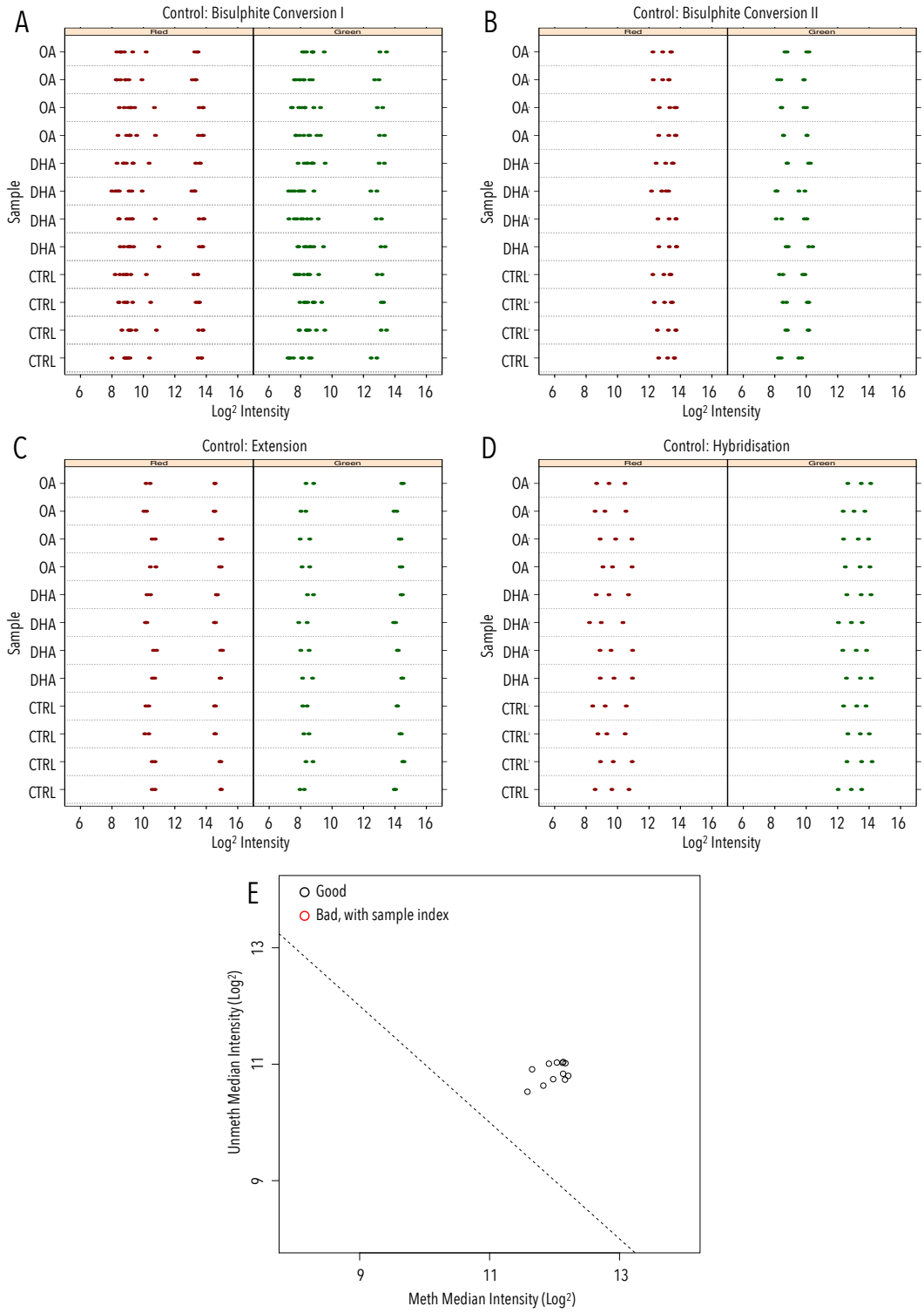

Figure 4.4: MethylationEPIC BeadArray; quality report showing bisulphite conversion (A, B), extension (C) and hybridisation (D) controls in each sample. The $\log^2$ median intensities of total methylated and unmethylated signals (E) showed that all samples were above the cutoff threshold (dotted line).

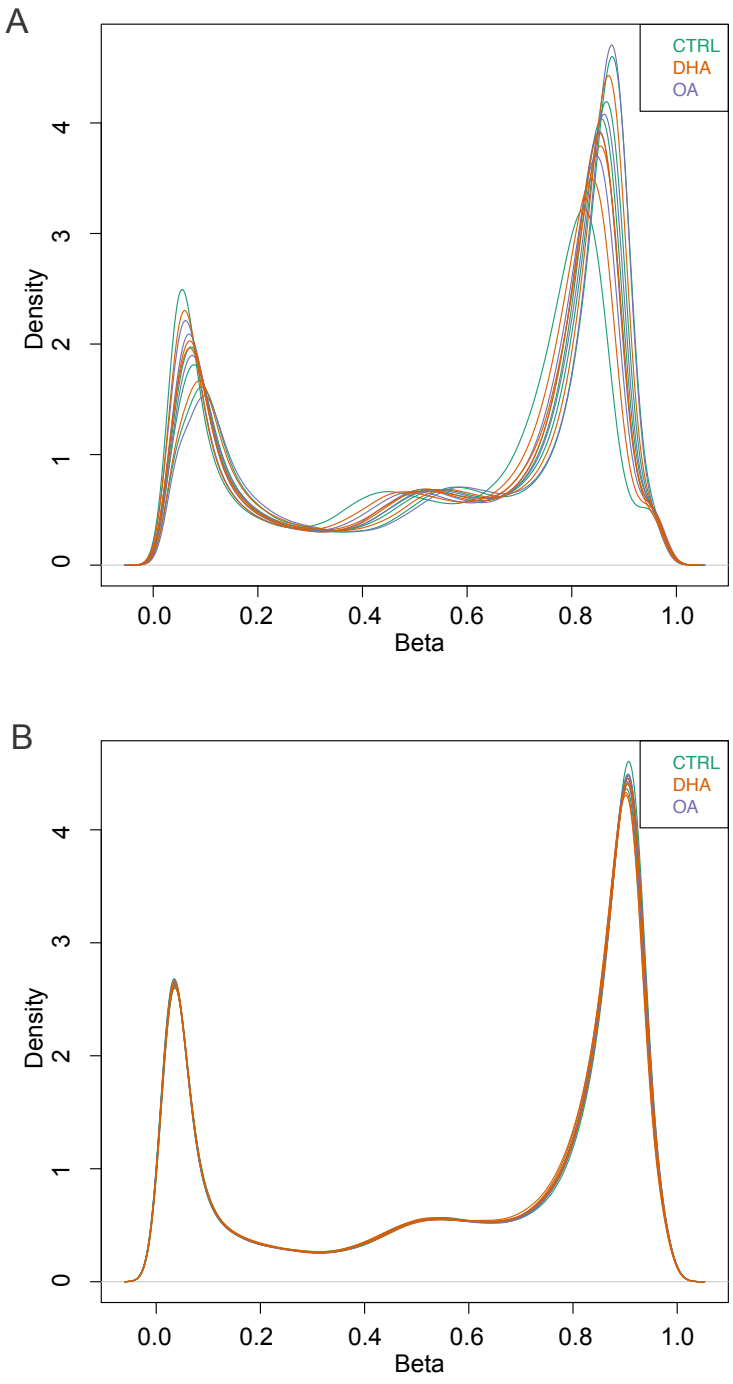

Figure 4.5: MethylationEPIC BeadArray; β-density distribution before (A) and after (B) normalisation using Funnorm pre-processing within minfi R package.

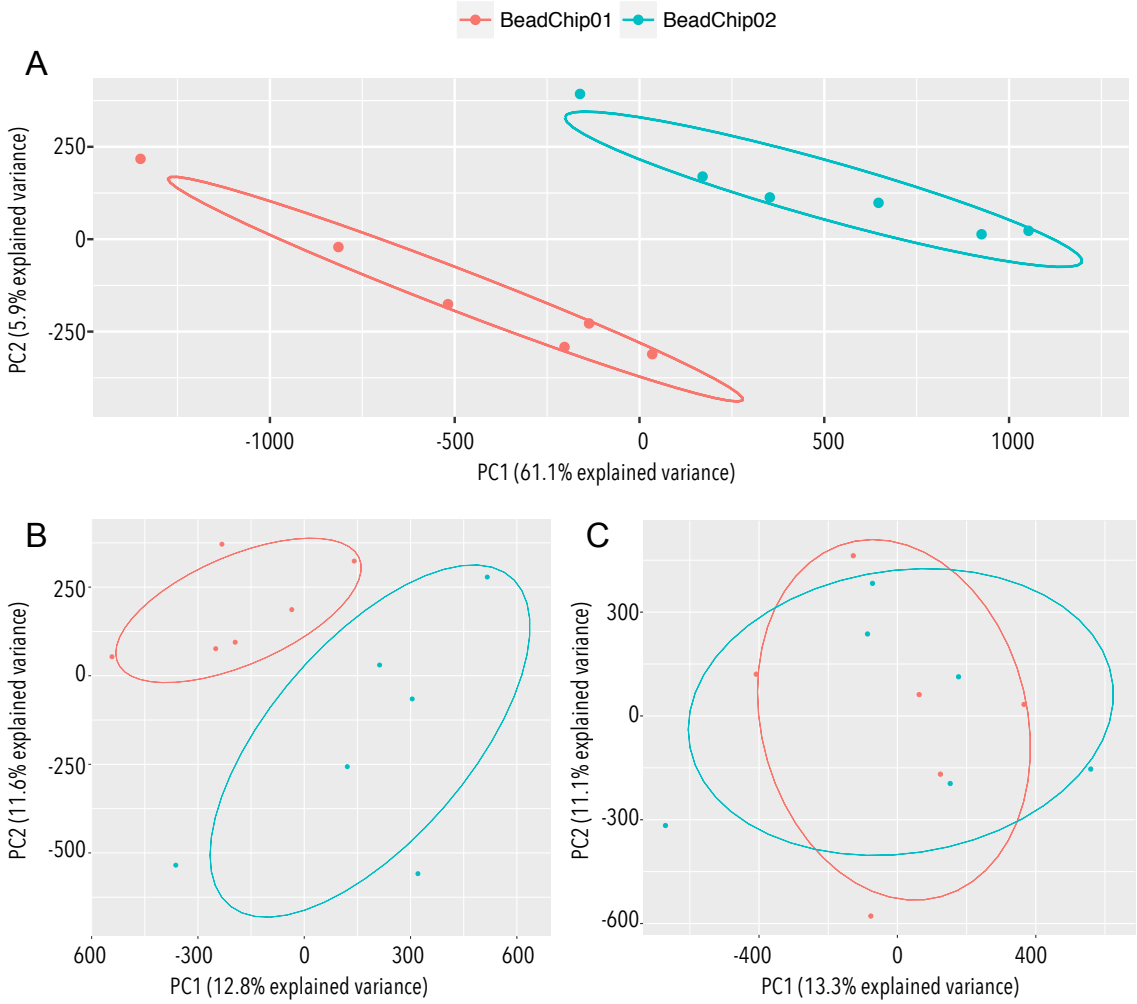

Figure 4.6: MethylationEPIC BeadArray; principal component analysis (PCA) showed a batch effect on the raw signals of samples (A). The batch effect was partially corrected after Funnorm pre-processing (B) and was lost after application of the Combat tool (C).

4.3.2 Do OA or DHA treatment induce the same effect on the DNA methylome?

An unsupervised principal component analysis dendrogram using all analysed cytosines (> 836,857) failed to show a complete divergence between treatment groups (Figure 4.7 A). Nevertheless, the same analysis using only cytosines which DNA methylation was significantly altered by 15 μM OA or 15 μM DHA treatment ($P < 0.05$, q-value < 0.05, $\Delta\beta > 0.05$) showed a complete clustering of samples. This indicated that although DNA methylation changes represented a small fraction of the cytosines analysed, they were enough to cluster all biological replicates to the correspondent treatment without any outliers (Figure 4.7 B).

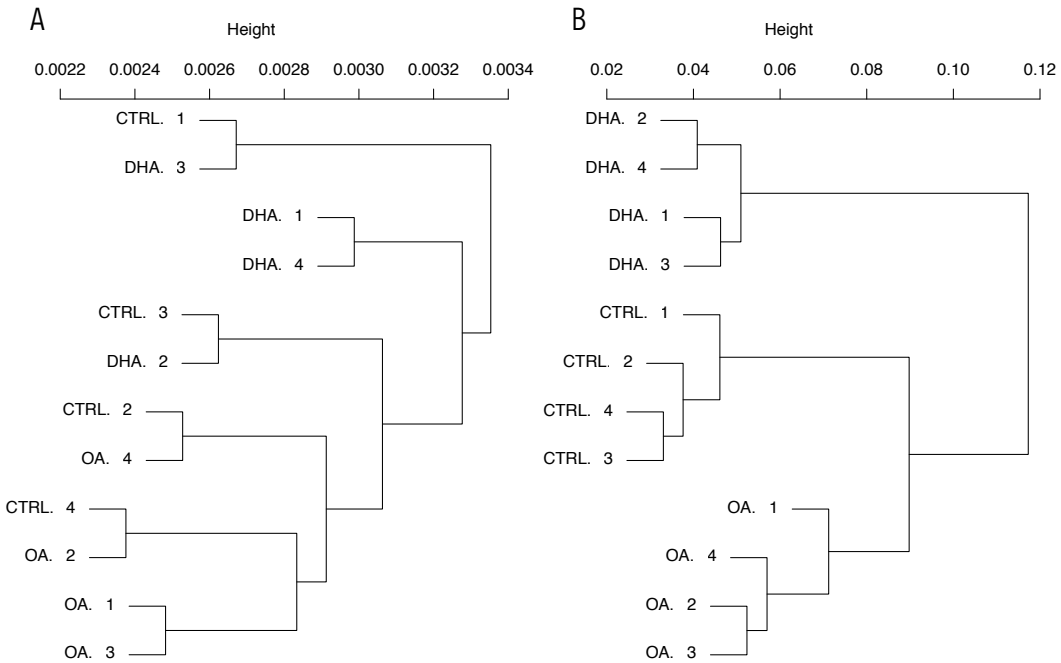

Figure 4.7: MethylationEPIC BeadArray; cluster dendogram of samples using M-values of all (> 836,857) cytosines analysed in BeadArray (A) or only those cytosines which DNA methylation was significantly altered by 15 μM OA or 15 μM DHA treatment after 8 days of incubation (B).

Treatment with 15 μM OA significantly altered the DNA methylation levels of 563 CpG sites. The 52% (294/563) of the altered loci showed increased methylation (Figure 4.8).

Treatment with 15 μM DHA significantly altered the DNA methylation levels of almost three times more CpG sites (1596) compared with OA (563). Of these, 32% (508/1596) showed increased methylation (Figure 4.8).

Only 78 CpG sites showed altered DNA methylation levels by both treatments. This represented 14% (78/563) of total changes induced by OA or 5% (78/1596) by DHA treatment. All 78 loci showed altered DNA methylation with the same direction of change, either increase or decreased, by OA or DHA. The 33% (26/78) of the altered CpG sites by both treatments showed increased methylation, while the methylation level of the remaining 67% (52/78) was decreased.

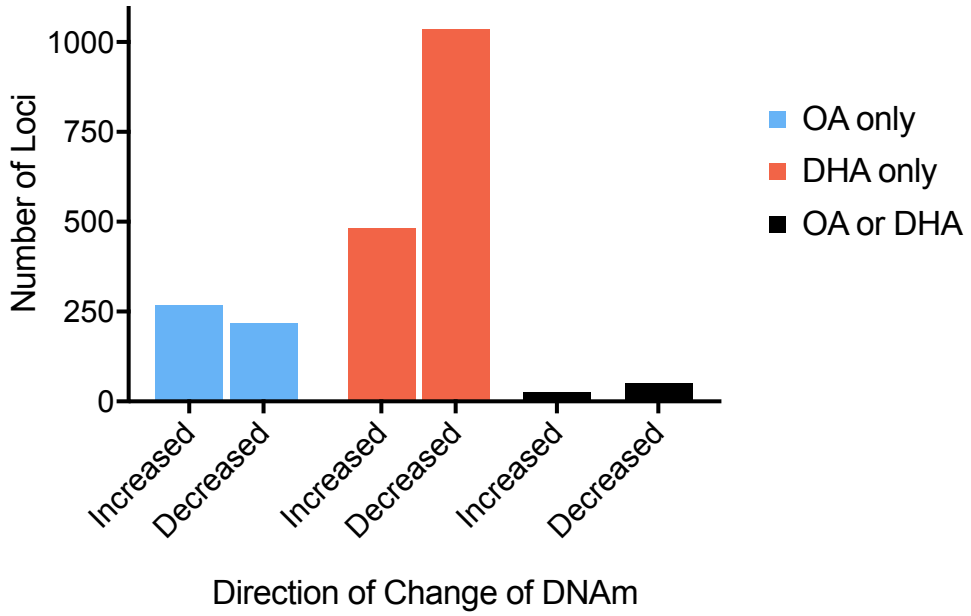

Figure 4.8: Number and direction of change of CpG sites with significantly altered DNA methylation (DNAm) after treatment with OA or DHA for 8 days ($P < 0.05$, $q < 0.05$, $\Delta\beta > 0.05$). OA or DHA alone increased DNAm of 268 or 482 CpG sites whereas decreased DNAm of 217 or 1036 CpG sites, respectively. Both treatments increased DNAm of 26 CpG sites and decreased DNAm of 52 CpG sites.

The genomic location and magnitude of change in methylation (%) of all significantly altered loci by OA or DHA are shown in Appendix A.

4.3.3 Do OA or DHA treatment induce DNA methylation changes in specific regions in the genome?

In addition to the differentially methylated positions (DMPs or CpG sites), analysis of DNA methylation data was performed to identify possible differentially methylated regions (DMRs) by OA or DHA treatments. None of the possible DMRs passed the FDR cutoff ($q < 0.05$). Therefore, all significantly DMPs were grouped and analysed according to their location in the genome to evaluate a possible pattern.

The majority of DNA methylation changes induced by OA treatment were located in intergenic regions (Figure 4.9 A). This was in comparison with changes in genic regions defined hereafter as sequences from -1,500 bp of the transcription start site (TSS) until the 3' untranslated region (UTR) of genes. All the significantly altered loci were also analysed according to the location of CpG islands (CpGi), their shores and shelves. These three genomic locations were collectively defined as CpGi-related regions. Analyses showed that the majority of DNA methylation changes induced by OA treatment were located outside CpGi-related regions (Figure 4.9 B).

Same as OA treatment, the majority of DNA methylation changes induced by DHA treatment were located in intergenic regions compared with changes in genic regions (Figure 4.9 A). Analysis of all the significant DNA methylation changes by DHA according to CpG islands also showed that the majority of altered CpG sites were located outside CpGi-related regions (Figure 4.9 B).

The same analyses were then carried out grouping all significantly altered CpG sites according to the change on DNA methylation, either increase or decrease. Analyses showed that CpG sites that increased DNA methylation by OA or DHA were mainly located within intergenic regions and outside CpGi-related regions (Figure 4.9 C, D). In the same manner, CpG sites that showed decreased DNA methylation by OA or DHA treatment were also primarily located within intergenic regions and outside CpGi-related regions (Figure 4.9 E, F).

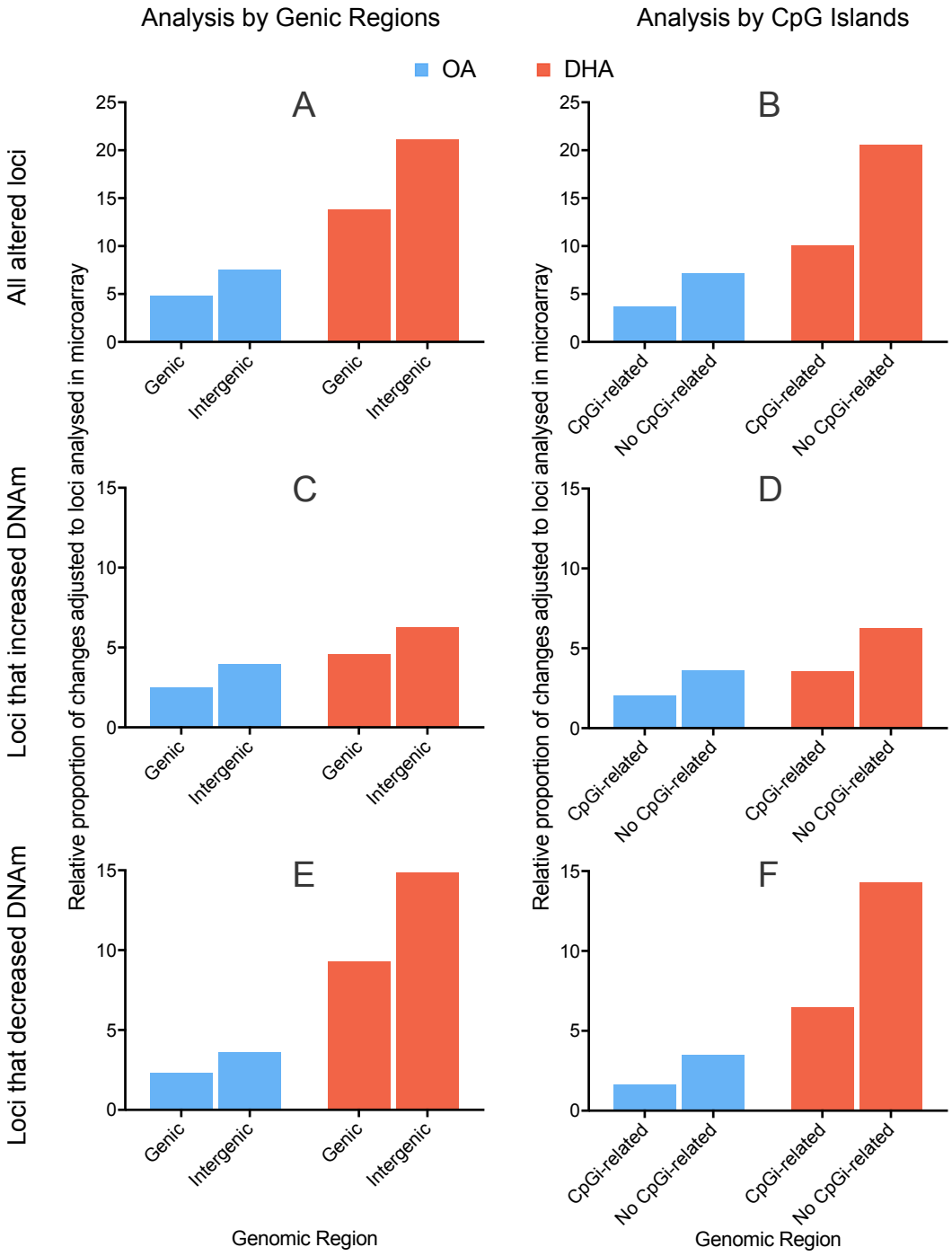

Figure 4.9: Genomic location of CpG sites that showed altered DNA methylation (DNAm) by OA or DHA treatment according to genic/intergenic regions (A, C, E) or to CpG islands (CpGi)-related regions (B, D, F). The total number of significantly altered CpG sites (A, B), only those that showed increased methylation (C, D) or only those that showed decreased methylation (E, F) were primarily located within intergenic regions and outside CpGi-related regions.

4.3.4 Do OA or DHA treatment alter the same genes?

Treatment with 15 μM OA for 8 days changed the DNA methylation status of at least one CpG site of 345 different genes. In comparison, treatment with 15 μM DHA for 8 days changed the DNA methylation status of at least one CpG site of almost three times more genes (n = 988). Only 52 genes were altered by both treatments which represented the 15% of total genes altered by OA (52/345) and the 5% of total genes altered by DHA (52/988) (Figure 4.10). A gene was defined as the genomic region from -1,500 bp of the transcription start site (TSS) until the 3' untranslated region (UTR) of an annotated gene.

Lists with the top ten genes with altered DNA methylation by OA or DHA treatment are shown in Table 4.1 and Table 4.2, respectively.

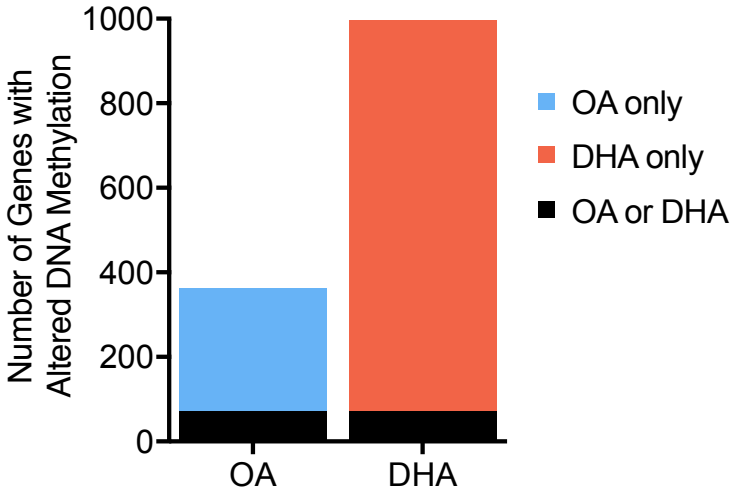

Figure 4.10: Number of genes with at least one CpG site that showed altered DNA methylation by OA (blue bar), DHA (red bar) or both treatments (black region).

Table 4.1: Top 10 genes with altered DNA methylation by OA treatment

ID	Change in DNAm	Gene Symbol	Gene Region
cg10841253	-17	CLNK	Body
cg17175279	-14	MTAP	TSS1500
cg07548325	-12	No Consensus[a]	No Consensus[b]
cg04310488	-12	SLC22A2	Body
cg07091719	-11	TBX15	Body
cg04390689	12	EGLN1	Body
cg17446583	13	BCAT1	Body
cg19336448	14	KSR2	Body
cg21970086	16	PRUNE2	Body
cg07372659	16	CDKAL1	Body

CLNK, cytokine dependent hematopoietic cell linker; MTAP, methylthioadenosine phosphorylase; KSR2, kinase suppressor of ras 2; SLC22A2, solute carrier family 22 member 2; TBX15, T-box 15; EGLN1, egl-9 family hypoxia inducible factor 1; BCAT1, branched chain amino acid transaminase 1; KSR2, kinase suppressor of ras 2; PRUNE2, prune homolog 2; CDKAL1, CDK5 regulatory subunit associated protein 1 like 1. [a] = STON1-GTF2A1L readthrough or stonin 1 (STON1), [b] = 5'UTR or TSS1500

Table 4.2: Top 10 genes with altered DNA methylation by DHA treatment

ID	Change in DNAm	Gene Symbol	Gene Region
cg25254444	-17	IFNA8	TSS1500
cg17564498	-15	EXOC4	Body
cg26292058	-14	RGS1	TSS1500
cg05475386	-13	MSRB3	Body
cg10841253	-12	CLNK	Body
cg04730456	11	HSPBAP1	Body
cg05060085	12	TMEM18	Body
cg03435901	13	IL17RD	3'UTR
cg25576961	13	TTC23	Body
cg14348664	19	CDKN2A	No Consensus[a]

IFNA8, interferon alpha 8; EXOC4, exocyst complex component 4; RGS1, regulator of G protein signaling 1; MSRB3, methionine sulfoxide reductase B3; CLNK, Cytokine Dependent Hematopoietic Cell Linker; TMEM18, Transmembrane Protein 18; IL17RD, Interleukin 17 receptor D; TTC23, tetratricopeptide repeat domain 23; HSPBAP1, HSPB1 associated protein 1. [a] = 3'UTR or body

4.3.5 Do altered genes are related to particular pathways or biological functions?

The total number of genes with altered DNA methylation by OA or DHA were analysed using Ingenuity® Pathway Analysis (IPA®) to determine a biological relationship between altered genes. From the total number of altered genes by OA or DHA (345 or 988) 348 and 935 different genes were mapped by the software and used for pathways analysis, respectively.

4.3.5.1 OA pathways

The genes with altered DNA methylation induced by OA were significantly enriched (-log(P-value) > 1.3) in "Amyotrophic Lateral Sclerosis Signalling", "Aryl Hydrocarbon Receptor Signalling" and "Clathrin-mediated Endocytosis Signalling" canonical pathways, among others (Figure 4.11). The analysis of the same genes using as reference molecular associations of clinical pathology endpoints (ToxList) showed that "Aryl Hydrocarbon Receptor Signalling", "Xenobiotic Metabolism Signalling" and "RAR Activation" categories were also significantly enriched (Figure 4.12). Ultimately, the genes with altered DNA methylation by OA treatment were also analysed to identify possible downstream effects on cells accordingly to the functions of the altered genes. Analysis showed that the genes with altered DNA methylation induced by OA treatment were enriched in genes which functions were related to "Stimulation of Natural Killer Cells", "Hematopoiesis of Leukemia Cell Lines" and "Trafficking of lymphocytes" downstream effects, among others (Figure 4.12).

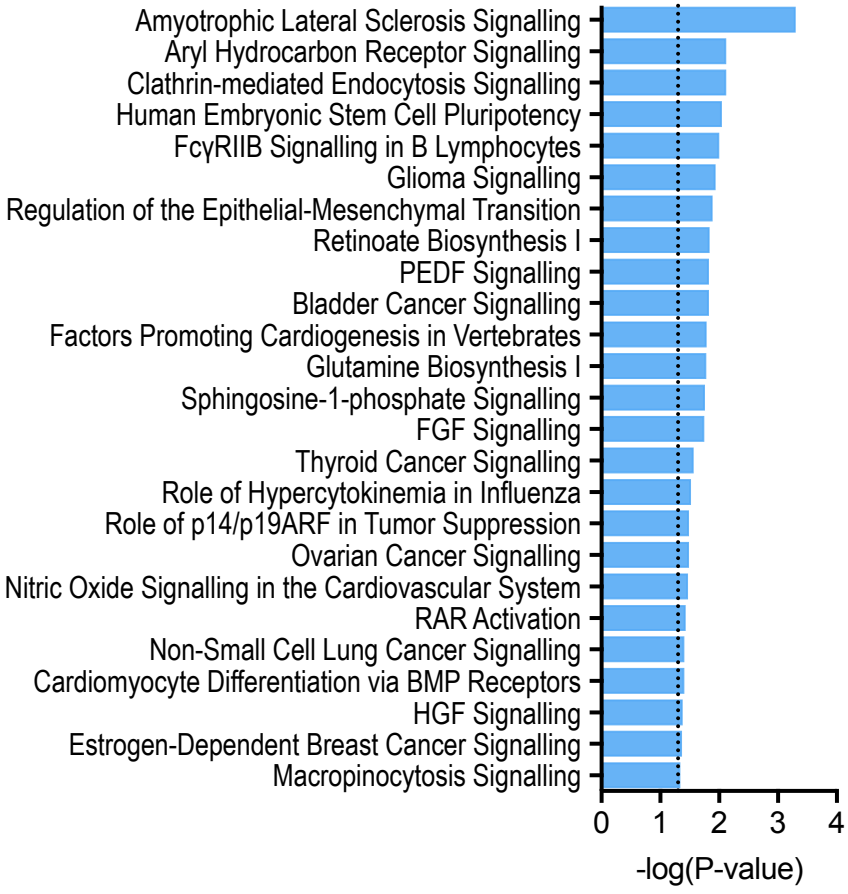

Figure 4.11: Canonical pathways related to genes with altered DNA methylation by OA treatment. The level of significance (dotted line) was according to an enrichment of genes in a specific pathway with a -log(P-value) > 1.3 from Fisher's exact test using IPA®.

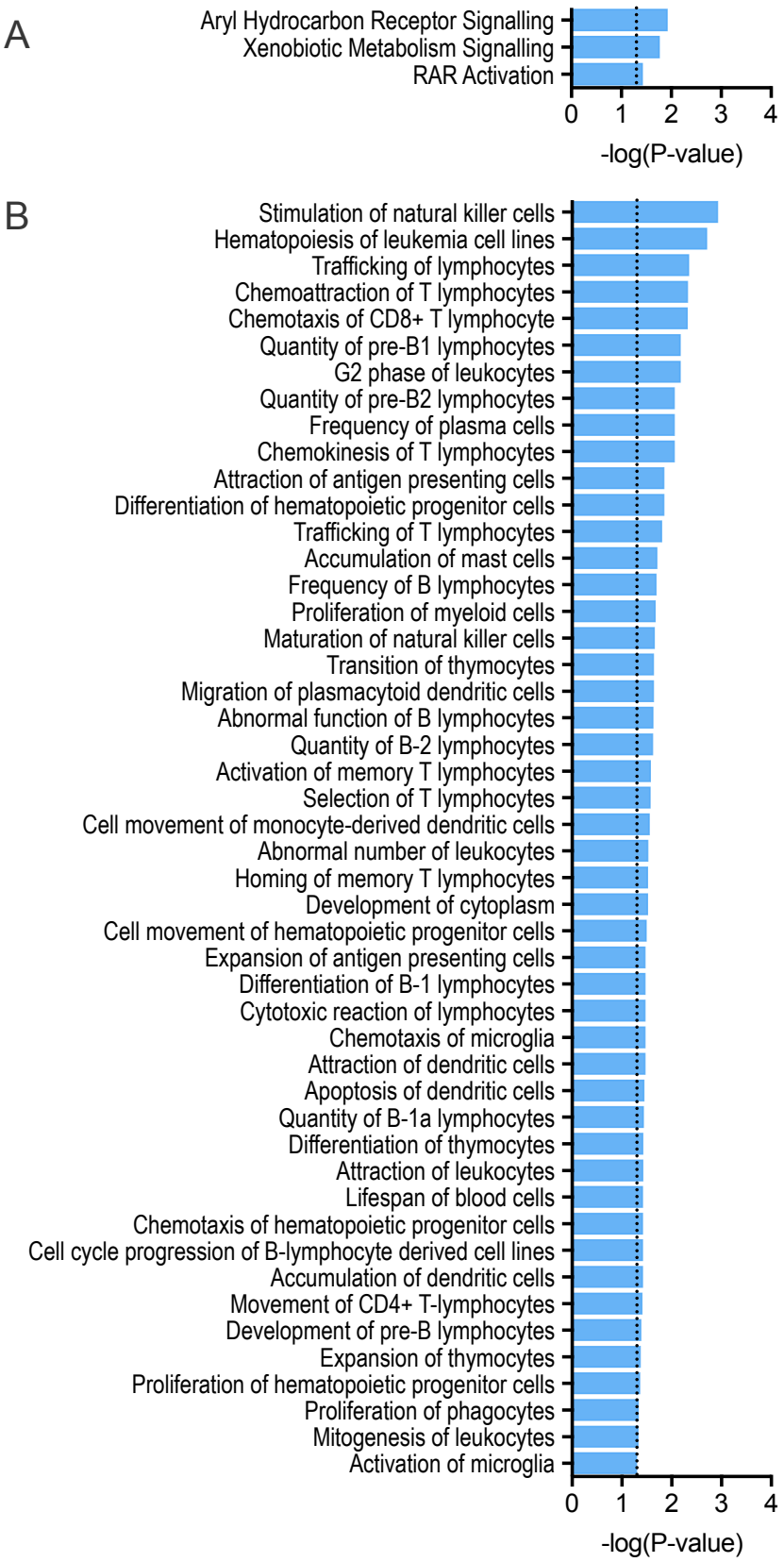

Figure 4.12: ToxList (A) and downstream effects (B) related to genes with altered DNA methylation by OA treatment. The level of significance (dotted line) was according to an enrichment of genes in a specific category/effect with a -log(P-value) > 1.3 from Fisher's exact test using IPA®.

4.3.5.2 DHA pathways

The genes with altered DNA methylation induced by DHA were significantly enriched in "Synaptic Long-Term Potentiation", "Synaptic Long-Term Depression" and "Protein Kinase A Signalling" canonical pathways, among others (Figure 4.13). The analysis of the same genes using as reference molecular associations of clinical pathology endpoints (ToxList) showed that "Cardiac Hypertrophy", "Cardiac Fibrosis" and "PPARα/RXRα Activation" categories were also significantly enriched (Figure 4.14). The genes with altered DNA methylation induced by DHA treatment were also enriched in genes which functions were related to "Leukemogenesis", "Rett Syndrome" and "Proliferation of pro-T3 thymocytes" downstream effects, among others (Figure 4.14).

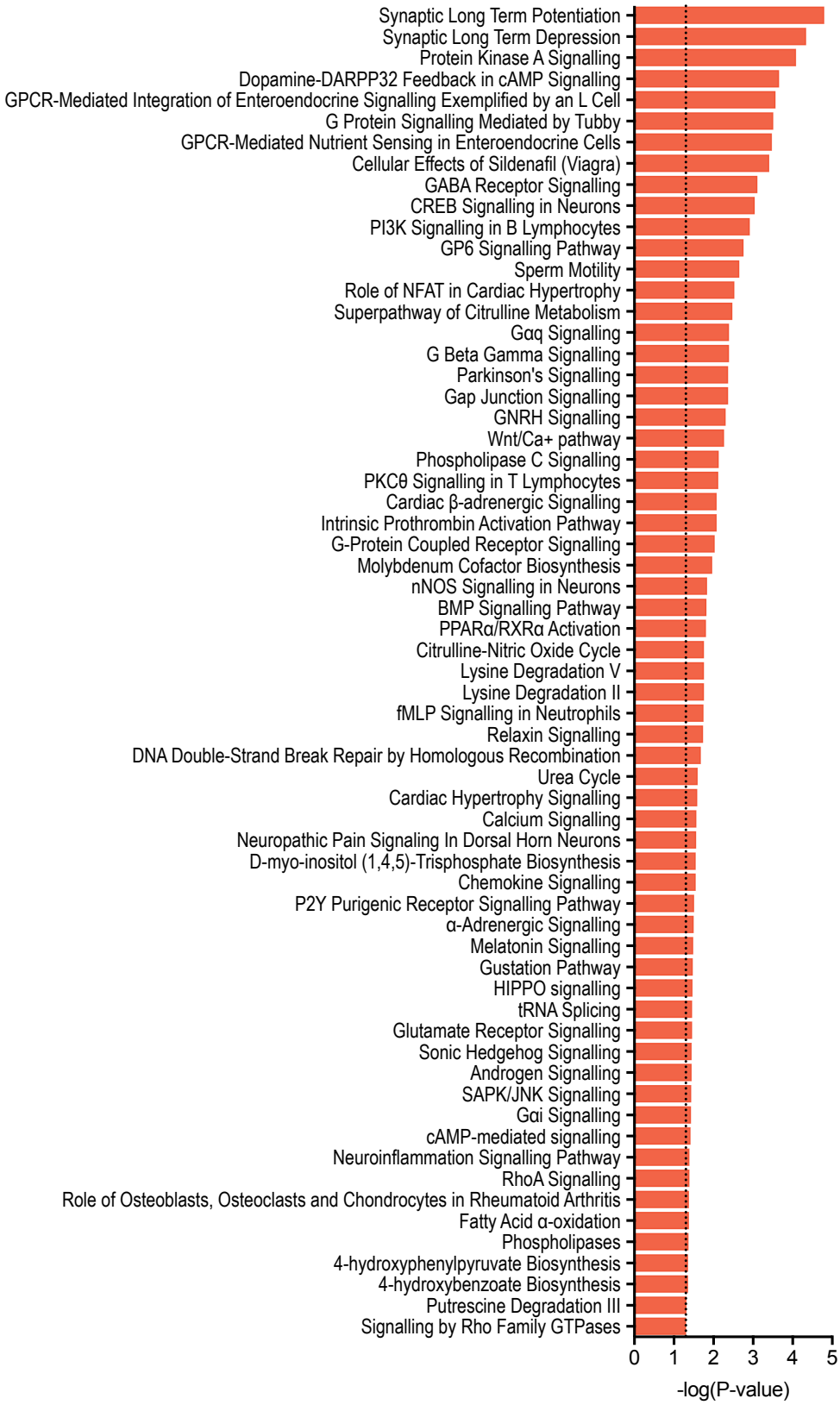

Figure 4.13: Canonical pathways related to genes with altered DNA methylation by DHA treatment. The level of significance (dotted line) was according to an enrichment of genes in a specific pathway with a -log(P-value) > 1.3 from Fisher's exact test using IPA®.

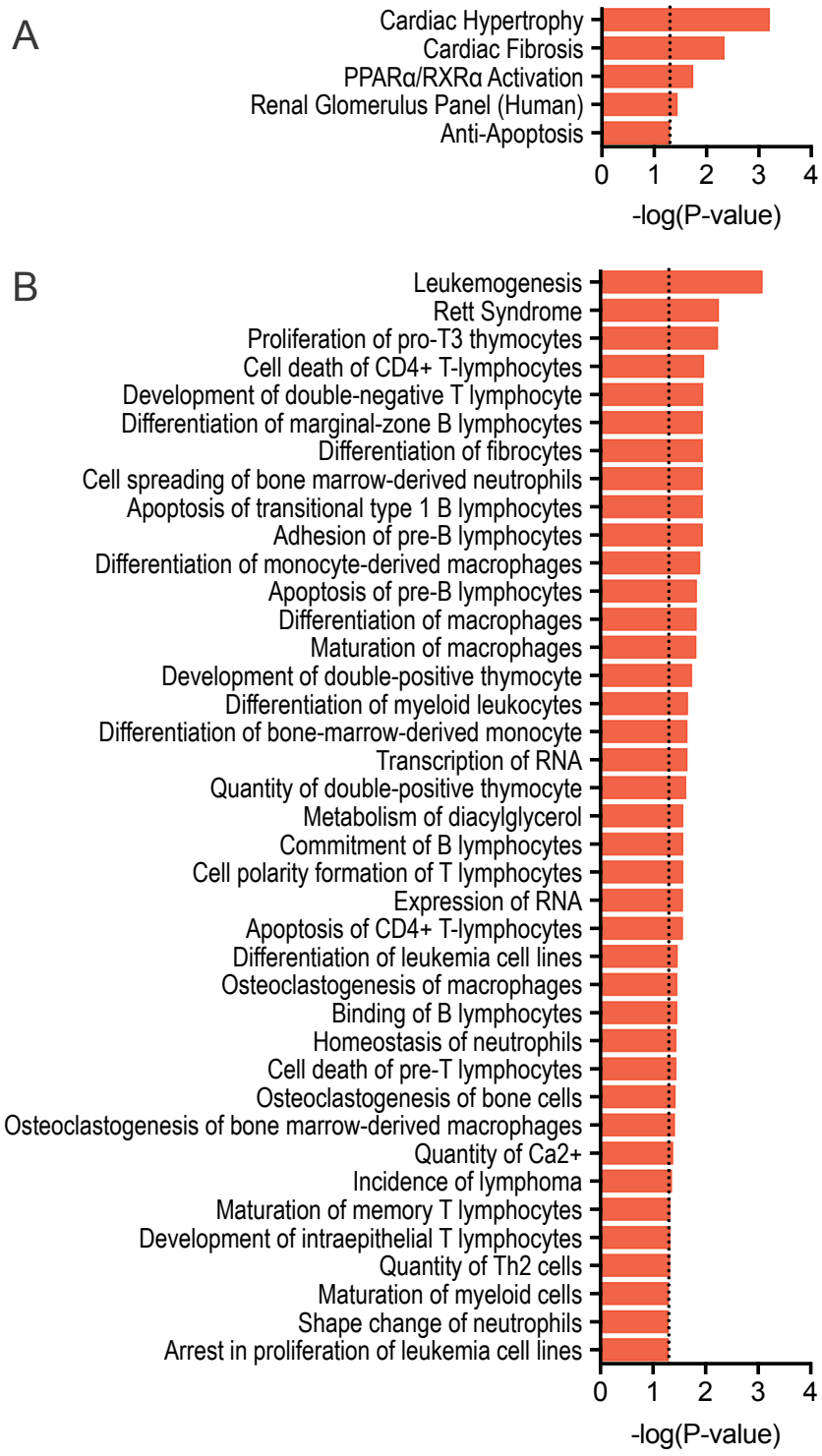

Figure 4.14: ToxList (A) and downstream effects (B) related to genes with altered DNA methylation by DHA treatment. The level of significance (dotted line) was according to an enrichment of genes in a specific category/effect with a -log(P-value) > 1.3 from Fisher's exact test using IPA®.

4.3.5.3 OA and DHA common pathways

The genes with altered DNA methylation induced by both, OA or DHA treatment, were significantly enriched in "Opioid Signalling Pathway", "S-methyl-5'-thioadenosine Degradation II" and "Axonal Guidance Signalling" canonical pathways, among others (Figure 4.15). In contrast, ToxList analysis did not show any significantly altered category by both treatments. Analysis of downstream effects showed that the genes with altered DNA methylation induced by both OA or DHA treatments were enriched in genes with functions related to "Chemotaxis of B-lymphocytes derived cell lines", "Abnormal morphology of plasma cells", "Accumulation of natural killer cells" and "Abnormal quantity of lymphocytes" (Figure 4.15).

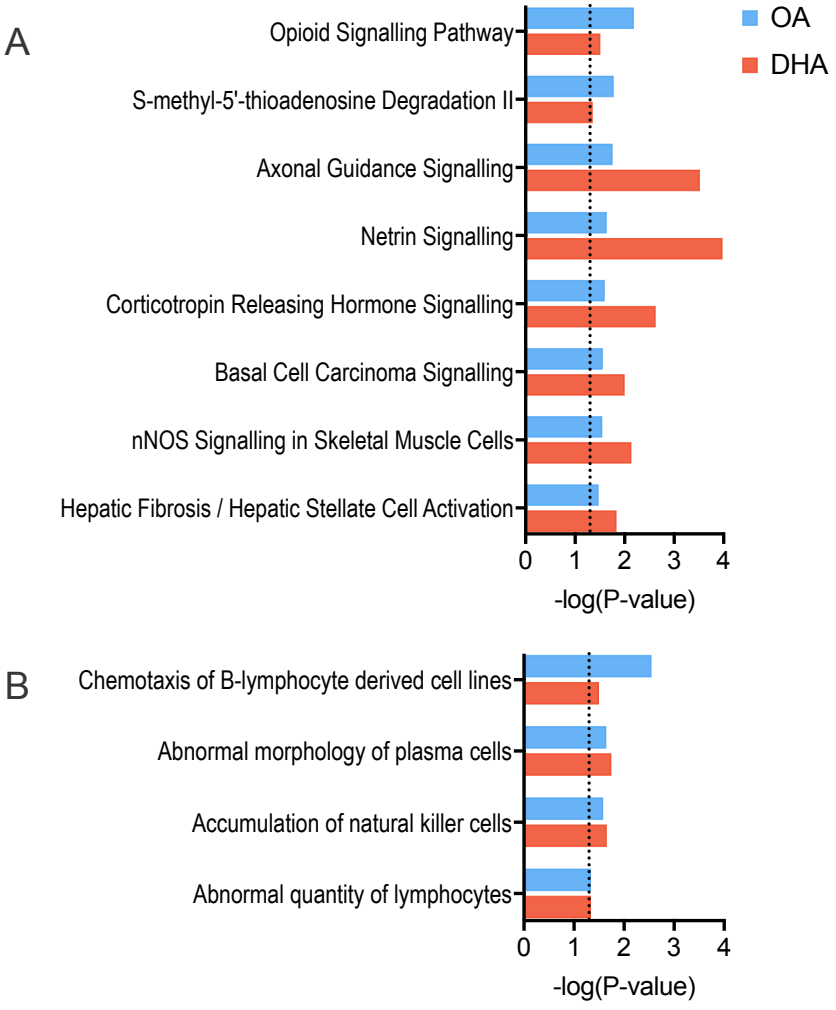

Figure 4.15: Canonical pathways (A) and downstream effects (B) related to genes with altered DNA methylation by both, OA or DHA treatment. The level of significance (dotted line) was according to an enrichment of genes in a specific pathway/effect with a -log(P-value) > 1.3 from Fisher's exact test using IPA®.

4.3.6 Validation of the MethylationEPIC BeadChip

The measurement of DNA methylation status of candidate CpG sites was carried out by pyrosequencing to validate BeadArray results. Pyrosequencing was performed targeting 5 CpG sites that showed a significant change in DNA methylation levels by DHA, as the magnitude of changes with this treatment showed to be greater compared with OA. Selected CpGs included three that decreased (ID cg26292058, cg05475386 and cg27188282) and two that increased (IDs cg06989443 and cg22518417) DNA methylation by DHA treatment. Such CpG sites were within the top twenty changing DNA methylation and were chosen by a sequence context that allowed primer design to perform pyrosequencing. Locus ID cg26292058 was also significantly altered by OA treatment, although the change in DNA methylation was the half (-7%) of that induced by DHA (-14%) according to BeadArray results.

Pyrosequencing of the 5 CpG sites showed that DNA methylation in DHA-treated cells was significantly altered in the same direction of change as BeadArray results (Figure 4.16). DNA methylation in OA-treated cells showed decreased levels on CpG ID cg26292058, same as BeadArray results, although this did not reach statistical significance (Figure 4.16 A). In line with BeadArray results, all other CpG sites analysed in OA-treated cells did not show any significant change on DNA methylation (Figure 4.16 B, C, D, E).

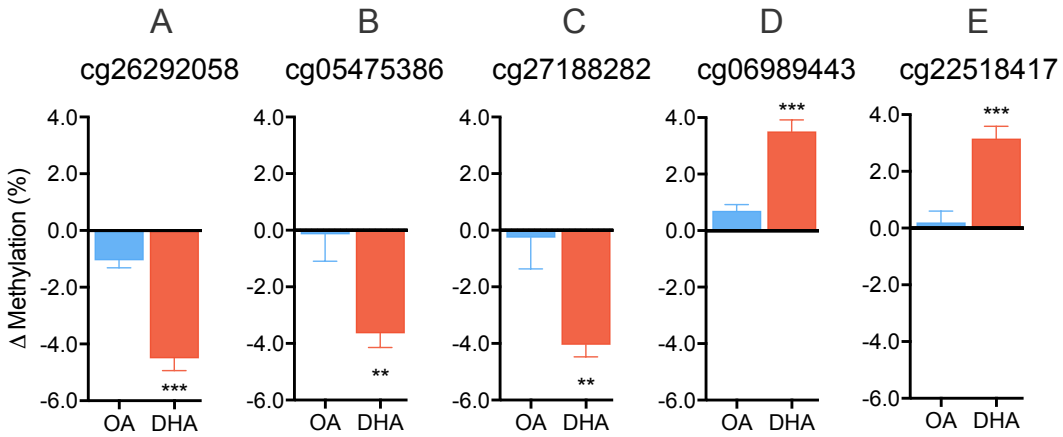

Figure 4.16: Pyrosequencing of 3 CpG sites that decreased (A = ID cg26292058, B = ID cg05475386, C = ID cg27188282) and 2 CpG sites that increased (D = ID cg06989443, E = ID cg22518417) DNA methylation by DHA after 8 days of treatment (n = 6 biological replicates per treatment) according to BeadArray analysis. Data are the mean difference (Δ) in the absolute change in DNA methylation (% points) between treatments and controls ± standard error of the mean. Treatment versus control means were compared by Student's T-test and those which differed significantly are indicated by *P < 0.05, **P < 0.01 or ***P < 0.001.

Significant changes in the absolute difference of DNA methylation between treatments and controls by pyrosequencing (Δ Methylation (%)) were smaller than those observed in the BeadArray analysis. Different methods have different sensitivities/specificities to detect changes in samples with a specific variability of the method itself. Therefore, 10 technical replicates of a single sample were carried out in each pyrosequencing assay to assure that DNA methylation changes by pyrosequencing, although small, were reliable. Results showed that the standard error of the mean (SEM) of the 10 technical replicates were at least 6 times lower than the difference observed by fatty acid treatments (pyrosequencing ΔMet (%); Table 4.3). This indicated that DNA methylation changes measured by pyrosequencing were not due to variability of the method. BearArray ΔMet (%) of the 5 CpG sites analysed were similar to pyrosequencing DNA methylation measurements only when results form the latter were analysed as a percentage of controls (Table 4.3).

Table 4.3: Validation of DNA Methylation Bead Array by pyrosequencing

ID	BeadArray	Pyrosequencing		Tech. Rep.	Treatment
	ΔMet (%)	% of Control	ΔMet (%)	SEM	
cg26292058	-7	-3	-1.2	0.38	OA
cg26292058	-15	-16	-4.5	0.38	DHA
cg05475386	-13	-14	-3.6	0.36	DHA
cg27188282	-11	-7	-4.0	0.59	DHA
cg06989443	12	17	3.5	0.17	DHA
cg22518417	11	14	3.2	0.19	DHA

Comparison of DNA methylation measurements between bead array and pyrosequencing. The standard deviation of the mean (SEM) of 10 technical replicates in each pyrosequencing assay is shown. ΔMet = difference in DNA methylation.

4.3.7 At what time during the 8 days of treatment are the DNA methylation changes induced?

Pyrosequencing of the same CpG sites used for the BeadArray validation was carried out after the 3rd and 6th day of treatment to assess the time when DNA methylation changes were established.

DHA-treated cells failed to show any significant change in the DNA methylation levels of all 5 CpG sites analysed at the 3rd day of treatment when compared with controls. Pyrosequencing of the 5 CpG sites showed the same direction of change in methylation as BeadArray results by the 6th day of treatment, although only three reached statistical significance (Figure 4.17 A, B, D). The methylation levels of the remaining two CpG sites showed to be significantly different just until the 8th day of treatment (Figure 4.17 C, E). In all 5 CpG sites analysed, the mean methylation levels after the 8th day showed the greatest decrease or increase on DNA methylation compared with the respective methylation levels after the 6th day of treatment. In summary, results showed that the DNA methylation changes by DHA were established after the 3rd day of treatment in three loci (Figure 4.17 A, B, D) and after the 6th day of treatment in two loci (Figure 4.17 C, E).

OA-treated cells failed to show any significant change on DNA methylation levels of all 5 CpG sites at the 3rd, 6th or 8th day of treatment when compared with controls (Figure 4.17). Nevertheless, significant changes on DNA methylation were observed in two CpG sites by the 6th day compared with the methylation levels at the 3rd day of the same OA treatment (Figure 4.17 A, D). The remaining loci analysed did not show any significant change in the DNA methylation by OA treatment in any day (Figure 4.17 B, C, E).

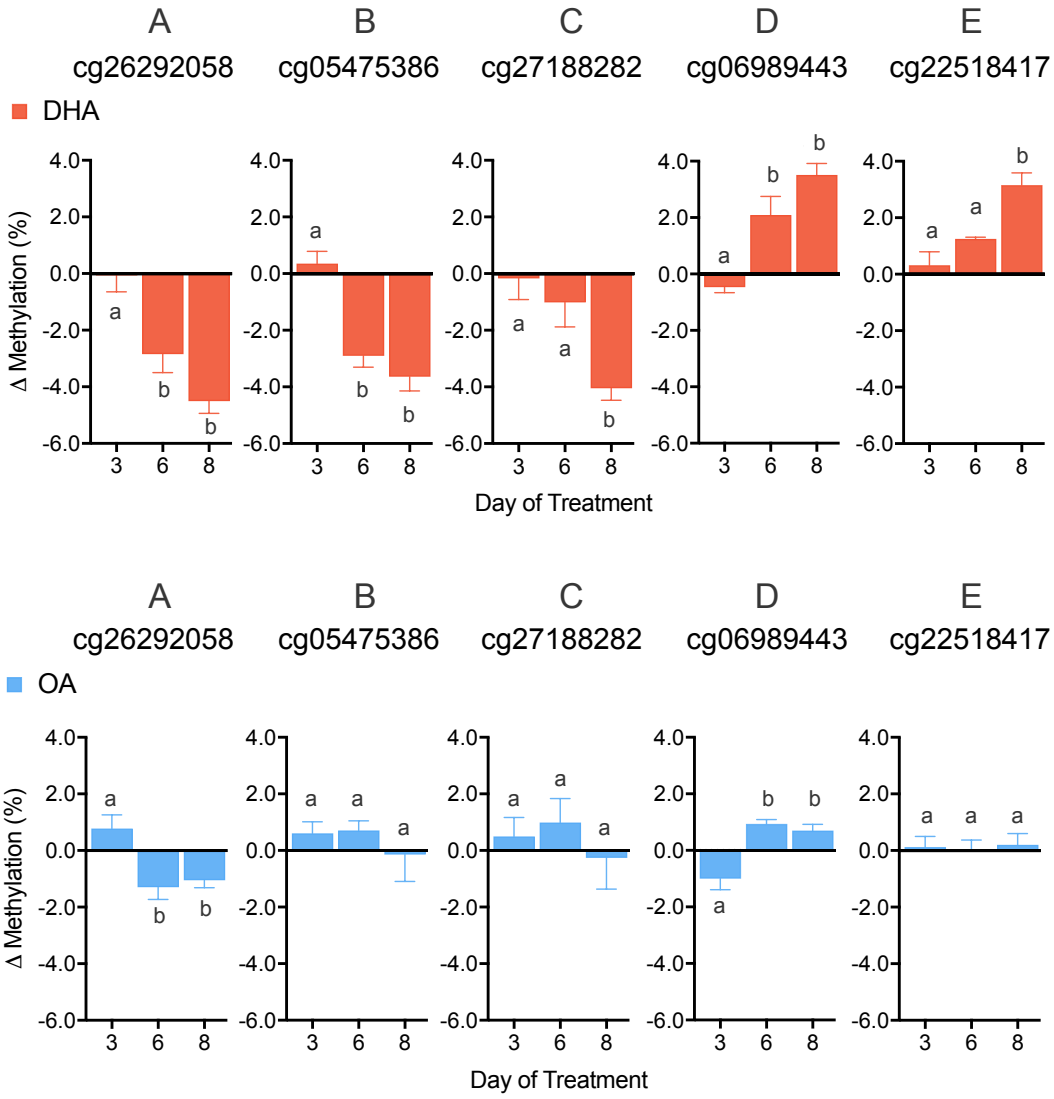

Figure 4.17: Pyrosequencing of 5 candidate CpG sites at the 3rd (n = 8 biological replicates per treatment), 6th (n = 8 biological replicates per treatment) and 8th (n = 6 biological replicates per treatment) day of treatment. Data are the mean difference (Δ) in the absolute change in DNA methylation (% points) between treatments and controls $\pm$ standard error of the mean. The methylation levels in each treatment were compared by one-way ANOVA with Tukey post-hoc test. Those which differed significantly to each other ($P < 0.05$) are indicated by a different letter.

4.4 Discussion

DNA methylation changes induced by 15 μM OA or 15 μM DHA treatment were evaluated using the Infinium MethylationEPIC BeadChip and results validated by pyrosequencing. CpG sites with altered methylation showed specificity and a greater proportion of them were located within intergenic regions. Results suggested that the DNA methylation changes by DHA were induced between the 3rd and 8th day of treatment.

4.4.1 OA or DHA specificity on the DNA Methylome

In this work, the effects of OA or DHA on the DNA methylome agreed with current evidence showing that different fatty acids have different capacities to alter DNA methylation levels[229;230;233;240]. Differential effects between OA and DHA were identified in the number of altered CpG sites, the direction of change in the DNA methylation of such CpG sites, the number of genes that changed DNA methylation and the biological function of the altered genes.

OA treatment showed to alter the DNA methylation of a lower number of CpG sites and genes compared with DHA. Therefore, this suggests that the epigenetic effect of OA was smaller than that of DHA. Such differences may be related to the lower degree/number of effects that OA induces on cells compared with DHA at the same concentration[100;111;264;299–302]. These include lower gene expression changes[111], lower immunomodulatory effects[299;300], lower cell membrane rafts disruption[301;302], absence to affect eicosanoid production[100] and absence to alter cell proliferation or cell viability of cancer cells[264]. Except for the decreased global DNA methylation in THP1 monocytes[229], the effects of OA on the DNA methylome has not been well described. Only a few studies have reported the modest or null effect that OA has on some candidate loci compared with other fatty acids[233;303]. One of the main observations in the current work was the specificity that OA showed concerning CpG sites, genes and biological functions that were altered. At the time this thesis was written, there was not found in the literature evidence to explain the enrichment of genes with altered DNA methylation in all canonical pathways, ToxList categories and downstream effects. However, some possible explanations based on indirect relationships will be discussed.

OA treatment, but not DHA, showed to change the DNA methylation of genes related to "Retinoic Acid Receptor (RAR) Activation" pathway. RARα works as a heterodimer with Retinoid-X Receptor α (RXRα) to modulate the transcription of genes[304]. Upon treatment with 1 μM all-*trans* retinoic acid, native RARα has shown to interact with SIRT1 *in vivo* using H1299 cells. Besides RARα, SIRT1 has shown to interact with DNA methyltransferase 1 (DNMT1) and modulate its activity[305;306]. Because OA can bind to human RXRα[307], there is a possibility that such event may alter

RARα/RXRα heterodimer which in turn may in some way induced RARα-SIRT1-DNMT1 interaction (Figure 4.18). A possible recruitment of DNMT1 to genes under the control of RARα may explain the enrichment of genes with altered DNA methylation in the RAR activation pathway identified in this work. At present, the possible interaction of RARα-SIRT1-DNMT1 in the same complex has not been reported.

RAR/RXR activation has also been shown to alter transcription through the displacement of DNMT3A alongside TETs recruitment to carry out active demethylation on a candidate gene using mouse embryonic fibroblast [308]. Therefore, there is a possibility that activation of RAR/RXR, presumably by OA treatment, may induce active DNA demethylation on RAR/RXR regulated genes. Such a hypothesis has not been addressed here or elsewhere. A model proposed to explain DNA methylation changes induced by OA is shown in Figure 4.18.

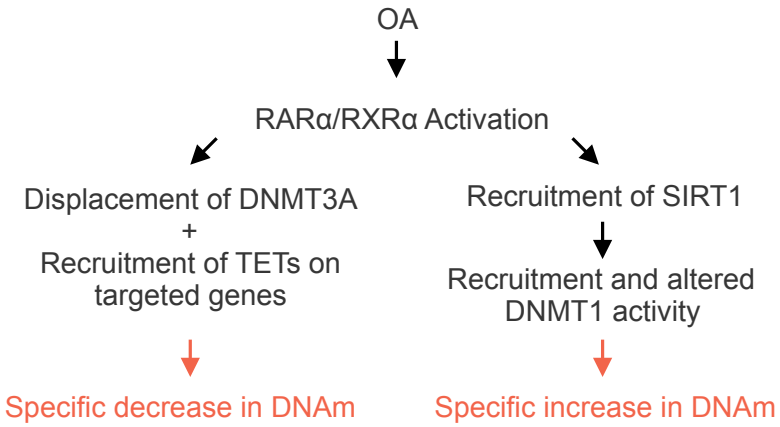

Figure 4.18: Possible mechanisms involved in the altered DNA methylation (DNAm) induced by OA in Jurkat cells may be related to RARα/RXRα activation. The diagram shows the current evidence (in black) coupled with the possible relationship with DNA methylation changes induced by OA (in red). RARα, retinoic acid receptorα; RXRα, retinoid-X receptor α; DNMT1, DNA methyltransferase 1; DNMT3A, DNA methyltransferase 3A; SIRT1, Situin 1; TETs, ten-eleven translocation proteins.

DHA treatment decreased the DNA methylation of the majority of CpG sites that were altered. Thus, this suggested that DHA treatment mainly activated DNA demethylation processes in cells. Active DNA demethylation can be achieved by either direct removal of the methylated base (BER) or region (NER or ncMMR) and enzymatic chemical modifications of the methylated base to remove the methyl group by specific enzymes (e.g. TETs). BER, NER and ncMMR are DNA repair mechanisms that are activated upon DNA damage. There is evidence that DHA can induce DNA damage specifically in cancer cells by accumulation of reactive oxygen species (ROS) [309]. Moreover, DHA treatment has also been shown to decrease gene expres-

sion of DNMTs[310]. Therefore, it is possible that the marked decrease on DNA methylation by DHA may be a consequence of the failure of *DNMTs* to establish usual DNA methylation patterns following DNA damage and DNA repair, at least in some extent (Figure 4.19 A). This may be related to the time-dependent decreased in cell proliferation identified only in DHA-treated cells (discussed in Chapter 3). DNA damage may decrease cell proliferation due to a cell-cycle arrest to allow time to repair such DNA damage[311]. Thus, it is possible that a higher need for DNA repair mechanisms in DHA-treated cells may induce a loss of DNA methylation.

DNA demethylation as a consequence of DNA damage is further supported by the time required for DHA to induce ROS accumulation and altered DNA methylation. ROS accumulation has been shown to take place after a 24-hour treatment with 25 μM DHA in MCF-7 cells[312], a breast cancer adenocarcinoma cell line. Meanwhile, the DNA methylation was shown to be significantly altered only after the 3rd day of treatment in the present work. However, the time required for the 5 CpG sites analysed may not be representative of all significant changes. Besides, pyrosequencing results suggested that altered DNA methylation may change at different rates in different CpG sites. This hampers the formation of a clear time course of the DNA methylation changes to suggest that they were a consequence of DNA repair mechanisms. Furthermore, the downregulation of DNMTs induced by DHA has not always been observed and even upregulation have been reported in some cell types[310].

The probable decrease on DNA methylation as a consequence of DNA damage, DNA repair and consecutive failure to copy DNA patterns would not explain per se the observed increase in DNA methylation by DHA. However, it has been shown that oxidative damage induced by 2 mM H_2O_2 treatment can relocate DNMT1 occupancy to GC-rich regions in HCT116 cells[306]. Therefore, relocation of DNMT1 by DHA treatment would explain both an increase and decrease of DNA methylation in specific CpG sites (Figure 4.19 A). Oxidative stress can occur by concentrations $>$ 100 nM H_2O_2 according to Sies[313]. If DHA can induce H_2O_2 concentrations able to trigger oxidative stress and relocate DNMT1 occupancy is currently unknown.

Besides DNA damage and DNMT1 relocation, the current results do not discard the possibility that decreased or increased DNA methylation were a consequence of diverse effects that DHA may have on cells. For instance, DHA treatment altered DNA methylation of genes related to apoptosis and cell death. In the previous Chapter, it was discussed how DHA treatment had a slight effect on cell death ($<$ 5%), which was not enough to compromise the viability of cells ($>$ 90% viable cells). Therefore, results in this work suggest that DNA methylome changes may be associated with a small decrease in cell viability. Currently, there is evidence suggesting that DHA may decrease cell viability of cancer cells through gene expression changes[116]. If DNA methylation changes were involved in altered expression of genes related to cell viability and cell death will be assessed and discussed in Chapter 6.

Genes that significantly changed DNA methylation by DHA were also enriched in genes that form part of the "PPARα / RXRα Activation" pathway. Of all significantly enriched pathways that were identified, only PPARα has been involved in the DNA methylation changes induced by fatty acids[229;303]. However, there has not been reported a participation of PPARα in the altered DNA methylation induced by DHA so far. DHA can bind and activate both PPARα and RXRα nuclear receptors[307;314]. Similar to the suggested model for OA, it is possible that specificity of the effect of DHA was mediated by PPARα/RXRα activation, the direction of the heterodimer to response elements and further recruitment of TET1 enzyme to the complex (Figure 4.19 B). Such a mechanism has been identified for PPARγ/RXRα heterodimer in a candidate region[303] and would explain the genome-wide specificity of altered loci by different fatty acids. A hypothesis proposed to explain altered DNA methylation by DHA is that this fatty acid may activate PPARα/RXRα and recruit TET proteins on site. This hypothesis may explain the decrease, but no the increase in DNA methylation (Figure 4.19 B).

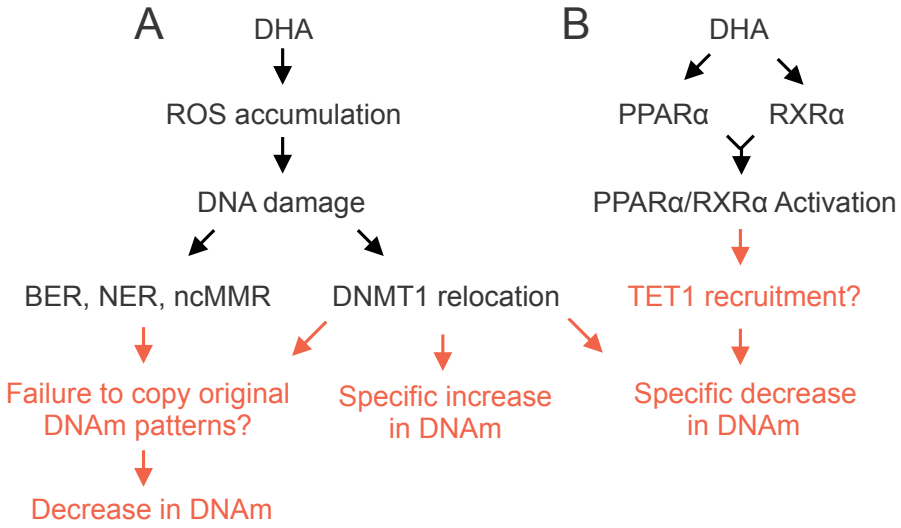

Figure 4.19: Possible mechanisms involved in the DNA methylation (DNAm) changes induced by DHA in Jurkat cells may be related to reactive oxygen species (ROS) accumulation (A) and PPARα/RXRα activation (B) triggered by the same DHA treatment. The diagram shows the current evidence (in black) couple with the possible relation to DNA methylation changes by DHA (in red). BER, base excision repair; NER, nucleotide excision repair; ncMMR, non-canonical mismatch repair; DNMT1, DNA methyltransferase 1; TET1, ten-eleven translocation; PPARα, peroxisome proliferator-activated receptor alpha; RXRα, retinoid X receptor alpha.

4.4.2 Biological significance of OA or DHA effect on the DNA Methylome

Associations between DNA methylation and gene expression have been described when DNA methylation is established at the promoter or body region of genes[178;179;183;184]. However, the results indicated that the majority of DNA methylation changes by OA or DHA were located within intergenic regions. This observation was conserved even when altered loci were analysed separately by those that decreased or those that increased DNA methylation. Intergenic regions contain regulatory elements[315] such as enhancers[316], silencers[317], differentially methylated regions[191], and a broad range of different non-coding RNAs that can modulate gene expression[318]. Therefore, it is possible that fatty acids treatments may affect some of these regulatory elements. Currently, there is still uncertainty about how to locate regulatory elements using only bioinformatic methods. For this reason, once regulatory elements are predicted they should be validated experimentally[316]. An approached base on DNA motifs will be explored and discussed in the following Chapter.

Analysis of altered CpG sites according to CpG islands showed that there was a higher proportion of DNA methylation changes in genomic regions outside such regions. This is in agreement with studies showing that CpG islands are, at least in part, resistant to methylation[319]. It is believe that such protection is given by the DNA sequence rich in CpG dinucleotides, although the exact mechanism remains unknown[319].

Downstream effects analysis showed that the second most probable effect in cells treated with DHA was "Rett Syndrome". This neurological and developmental disorder is originated by mutations on the methyl-CpG-binding protein 2 (MEPC2) gene[320]. There is evidence showing that omega-3 supplementation (EPA + DHA) improves clinical severity, oxidative stress and inflammation markers in patients with Rett Syndrome[321;322]. Further studies are needed to address the impact that altered DNA methylation induced by DHA may have on genes associated with Rett Syndrome.

4.4.3 Limitations of DNA methylation analysis

Pathways and biological functions related to genes with altered DNA methylation by OA or DHA treatment were predicted using IPA®. This software used a knowledge database that was designed for mRNA expression changes. However, DNA methylation changes alone should not be taken as an indicator for gene expression. The location of altered CpG sites[175;178;179], the number of altered CpG sites, the degree of change in methylation[233] and the interplay between other epigenetic marks influence the modulation of the mRNA gene expression through DNA methylation. It is difficult to interpret pathway analysis in isolation as DNA methylation alone does not imply changes in expression, activity or function of the genes/pathways.

The coverage of the 850k DNA MethylationEPIC BeadArray only represents < 3% of the total CpG sites in the human genome[174] that potentially may alter their DNA methylation status by fatty acids. Thus, it is possible that the number of loci and genes altered by OA and DHA reported here were bias by the BeadArray coverage. Besides, it is not discarded the possibility that DNA methylation changes can have a different distribution across the genome instead of the one reported in the current work (intergenic > genic).

Overall, the tendency of OA or DHA to mainly alter intergenic regions and CpG sites outside CpGi-related regions needs to be confirmed by experiments with higher coverage of the human DNA methylome. The number of genes, pathways and biological functions related to genes that altered their DNA methylation status by OA or DHA should be taken with caution, just as a hint for further investigation.

4.5 Conclusions

Treatment with 15 μM OA or 15 μM DHA for 8 days altered the DNA methylation of individual CpG sites in a treatment-specific manner. Nevertheless, both fatty acids seemed to alter preferentially intergenic regions and CpG sites that were not related to CpG islands. DNA methylation changes required more than 3 days to be established and they were associated with activity of different pathways and transcriptional factors, including PPARα in DHA-treated cells. Therefore, evidence suggests that activation of diverse pathways and transcription factors may be part of the mechanisms by which fatty acids may alter the DNA methylation of cells. To address such hypothesis, the possible participation of PPARα and other transcription factors in the altered DNA methylation induced by OA or DHA was explored in the next Chapter.

Chapter 5

Mechanisms Underlying The Effect of OA or DHA Treatment on DNA Methylation in Jurkat Cells

5.1 Introduction

Different fatty acids have been shown to modify the DNA methylation of cells[229;233;240]. However, the underlying mechanisms are not well understood. In the previous Chapter, the genes whose methylation was altered by DHA, but not OA, showed enrichment in the "PPARα/RXRα Activation" pathway. PPARα is a nuclear receptor that can be activated by fatty acids[314]. Thus, this suggested that activation of PPARα may be a mechanism by which fatty acids may alter the DNA methylation of cells. This hypothesis has previously been tested by Silva-Martinez *et al.,* using THP1 monocytes treated with OA or AA and PPARα or PPARγ inhibitors[229]. Experiments showed that only PPARα inhibitor significantly impaired the effect of AA, but not OA, on the global DNA methylation[229]. Whether PPARα can also mediate the effect of DHA on DNA methylation has not been tested before.

In contrast to DHA, pathways analysis of genes with altered DNA methylation induced by OA did not identify an enrichment of genes under PPARα control. Such results are in agreement with the current evidence suggesting that a PPARα does not mediate the altered DNA methylation induced by OA[229]. This also indicates that there may be more than one transcription factor or pathway underlying the effect of fatty acids on the DNA methylation of cells. Recently, it has been hypothesised that some short DNA sequences may modify the usual methylome patterns through

cell-type specific proteins[323]. However, if DNA motifs are associated with the DNA methylation induced by fatty acids has not been addressed. Besides, if such putative DNA motifs may recruit specific transcription factors it is unknown.

In addition to transcription factors, we hypothesised that other factors such as chromatin modifications were associated with the altered DNA methylation induced by OA or DHA treatment. Such hypothesis was based on evidence that has shown increased acetylation of H3K4 and decreased methylation of H3K4, H3K9, H3K27 H3K36 and H3K79 by 30 μM DHA treatment for 2 days using human M17 cell line[248]. Of all these residues, methylation of H3K4[324;325], H3K9[208;326;327] or H3K36[144;328] and global acetylation of H3 have shown an interplay with DNA methylation[329]. Currently, the occupancy of H3K4me3 is the only histone mark available for Jurkat cells in ENCODE. Therefore, H3K4me3 was selected to carry out experiments that sought to elucidate if DNA methylation changes induced by OA or DHA had a relationship with the local enrichment of this histone mark. Understanding the effect of OA or DHA treatment on H3K4me3 levels may provide evidence about the epigenetic context and mechanisms involved on the DNA methylation changes induced by fatty acids.

The experiments in this Chapter aimed to characterise three possible ways through which fatty acids may accomplish to alter DNA methylation of cells. Firstly, PPARα involvement in the altered DNA methylation induced by DHA was tested using treatments with PPARα agonists or PPARα antagonists. Secondly, it was sought if DNA methylation changes by OA or DHA were associated with specific DNA motifs or other transcription factors using motif analysis. Finally, experiments assessed if CpG sites with altered DNA methylation also changed H3K4me3 enrichment using chromatin immunoprecipitation assays.

5.2 Materials and methods

Cell culture and treatment of Jurkat cells was carried out as described in section 2.2.1. DNA extractions were performed according to section 2.3.2. Quality and quantity of DNA was assessed by NanoDrop and agarose gel electrophoresis, respectively (sections 2.3.3 and 2.3.4). Luciferase reporter assay was carried out as described in section 5.2.1. Pyrosequencing was conducted as indicated in section 2.5. Motif analysis was carried out as described in section 5.2.2. Chromatin immunoprecipitation was performed according to section 5.2.3.

5.2.1 Luciferase reporter assay

Luciferase reporter assay was carried out to confirm the activation of PPARα by agonist GW7647 in Jurkat cells. An overview of the method followed is shown in Figure 5.1.

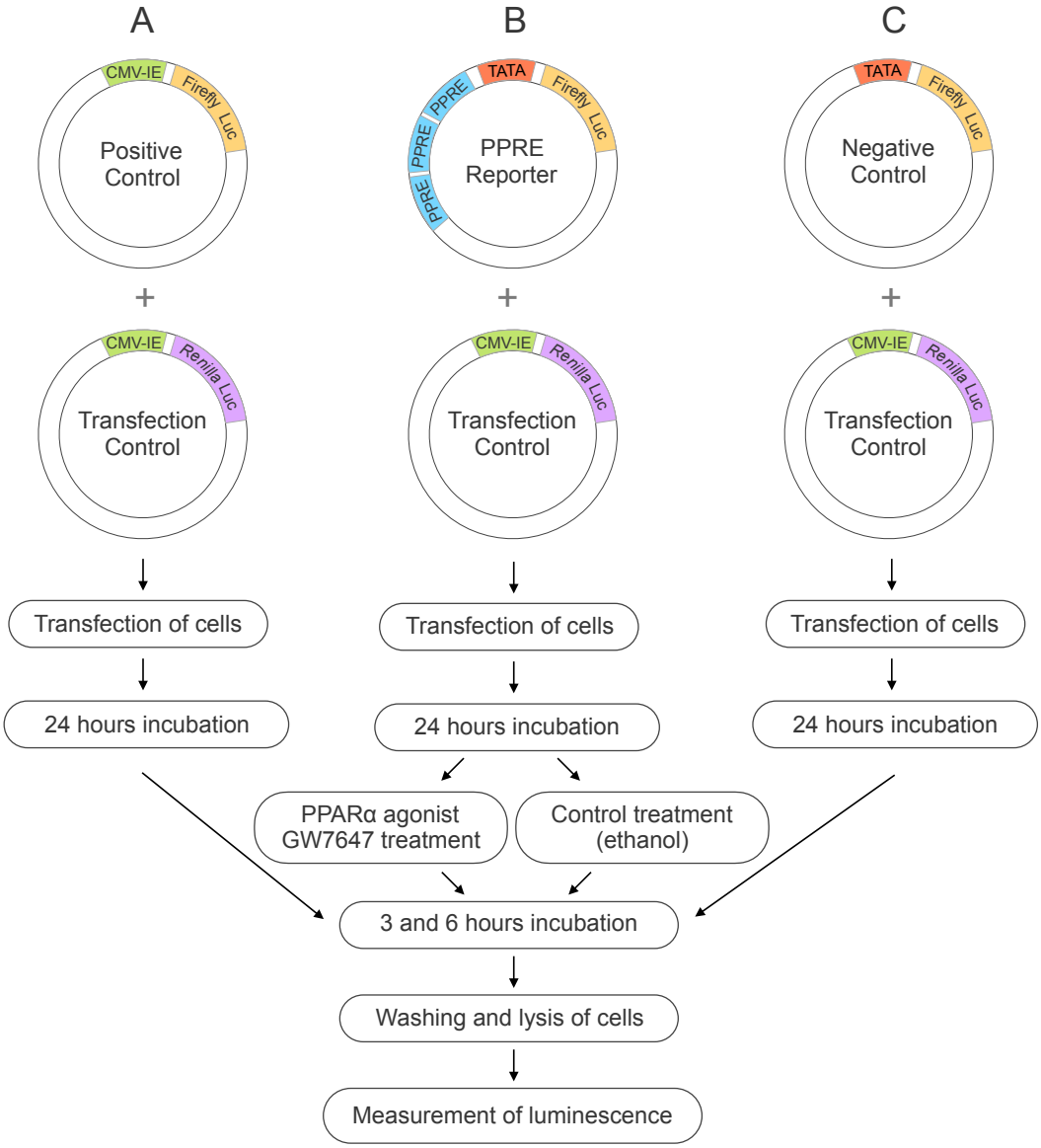

Figure 5.1: Overview of luciferase reporter assay. Diagram of the firefly luciferase gene under the control of the a human cytomegalovirus immediate early (CMV-IE) enhancer/promoter[330] (A) or under the control of tandem repeats of the PPAR response element (PPRE) and a TATA-box (B) or under the control of TATA-box only (C). The construct with the firefly luciferase gene was co-transfected with a construct containing the *Renilla* luciferase gene under the control of CMV-IE enhancer/promoter in all instances as indicator of transfection efficiency.

5.2.1.1 Transfection and treatment of cells

Cells were transfected using FuGENE HD Transfection Reagent, Opti-MEM™ Reduced Serum Medium and Cignal PPAR Reporter (luc) Kit following manufacturers' instructions. The recommended FuGENE-reagent:plasmid-DNA ratio for Jurkat cells of 6:1 (v/w) at 0.05 μg DNA developed by Promega was used and implemented as follows. Transfection complexes were prepared with 0.05 μg of either positive (100 ng/μl, n = 6), negative (100 ng/μl, n = 6) or PPRE plasmid (100 ng/μl, n = 12) in Opti-MEM:FuGENE HD (15.5:1, v/v) to a final volume of 5 μl per transfection. Complexes were incubated for a minimum of 30 minutes at room temperature before they were added to 3x10^3 cells in 100 μl of growth medium using 96-well conical bottom plates. Cells were then incubated for 24 hours in a 5% (v/v) CO_2 atmosphere at 37 °C. A further incubation for 3, and 6 hours was carried after cells were treated with either 0.2 μM PPARα agonist GW7647 dissolved in absolute ethanol. Ethanol at the same concentration was used in the positive and negative controls. In all instances, transfection complexes included a *Renilla* luciferase gene plasmid under the control of a human cytomegalovirus immediate early (CMV-IE) enhancer/promoter[330] which served as the internal control of transfection. The firefly luciferase gene in the transfection complexes was either under inducible control of a TATA box and a PPAR response element (PPRE) (reporter); or under constitutive control of a TATA-box and CMV-IE enhancer/promoter (positive control); or under non-inducible control of a TATA-box only (negative control). The Dual-Luciferase® assay was then performed.

5.2.1.2 Dual-Luciferase® assay

Luciferase reporter experiments were performed using the Dual-Luciferase® Reporter Assay System following the manufacturer's instructions. This kit provided all reagents except for PBS, 70% (v/v) ethanol and dH2O. Cells were recovered from a 96-well plate and pipetted into microtubes. A 10 μl aliquot was then obtained from each sample to test cell viability as described in section 2.2.3. The remaining cells were centrifuged at 212 g for 3 minutes at room temperature and the cell medium discarded. Cell pellets were washed twice with PBS before 20 μl of 1x lysis buffer was added. Cells were then lysed by mixing with a pipette up and down 10 times, an incubation for 15 minutes at room temperature and 3 freeze/thaw cycles using dry ice. Lysed cells were placed into a white opaque 96-well plate to read the luciferase activity on the Varioskan flash luminometer (Thermo Fisher Scientific) as follows. Luminometer's injectors were washed with 1.5 ml of 70% (v/v) ethanol and further 1.5 ml of dH2O. After 100 μl of 1x firefly luciferase assay reagent II (LARII) was added to each plate, the luminescence was measured. The firefly luciferase luminescence was then quenched with concomitant activation of the *Renilla* luciferase using 100 μl of 1x Stop and Glo® reagent. All steps by the Varioskan flash luminometer were automated.

5.2.1.3 Data analysis

The luminescence in each sample was adjusted for the transfection efficiency by dividing the firefly luciferase luminescence by the *Renilla* luciferase luminescence. The relative luminescence of the PPRE construct is shown in Equation 5.1 as an example of the calculi.

$$Relative\ PPRE\ activity\ =\ \left(\frac{firefly\ luminescence}{Renilla\ luminescence}\right) \times PPRE\ luminescence \tag{5.1}$$

The relative luminescence of all constructs was adjusted to the mean of the relative luminescence of PPRE construct with control treatment (vector ethanol). After this adjustment, the mean values of cells transfected with the PPRE construct treated with PPARα agonist GW7647 versus control treatment were compared by Student's T-test. The relative firefly luciferase luminescence of the positive and negative control was assessed but not considered by statistical analysis. The mean cell viability between the positive control, negative control and PPARα agonist GW7647 was compared by one-way ANOVA with Tukey HSD post-hoc test.

5.2.2 DNA motif analysis

Motif analysis was carried out to assess a possible enrichment of DNA motifs proximal to CpG sites that were differentially methylated by the fatty acid treatments. An overview of the steps followed is shown in Figure 5.2.

5.2.2.1 DNA sequences used

DNA sequences next to a CpG site that significantly changed DNA methylation (p-value < 0.05, q-value < 0.05, β-value > 0.05) by OA or DHA treatment were used for motif analysis. All sequences analysed were 122 base pairs (bp) in length and included 60 bp upstream and 60 bp downstream the CpG site of interest. Such length was selected in order to find motifs that may be directly associated with altered DNA methylation. All sequences were grouped and analysed either by treatment and direction of change in methylation or by treatment, the direction of change in DNA methylation and genomic location (promoter region, gene body and intergenic region). Sequences allocated to the promoter region included those CpG sites with altered DNA methylation up to 1500 bp upstream the transcription start site whereas sequences allocated to the gene body included CpG sites from the 5'UTR to the 3'UTR. The sequences that overlapped over two genomic locations were discarded from the analysis. The number of sequences in each group is shown in Table 5.1. Control sequences used

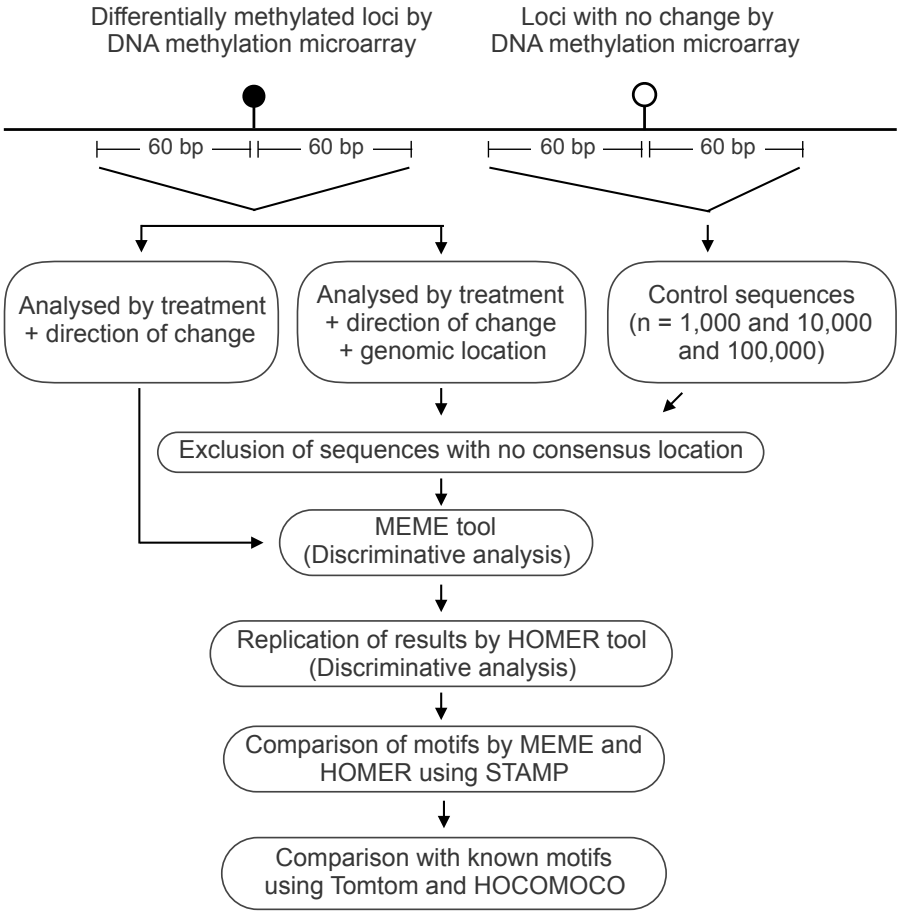

Figure 5.2: Overview of motif analysis workflow carried out in sequences where specific loci showed to significantly change DNA methylation by fatty acid treatments. MEME, Multiple Expectation maximisation algorithm for Motif Elicitation; HOMER, Hypergeometric Optimisation of Motif EnRichment; STAMP, similarity, tree- building, and alignment of DNA motifs and profiles; HOCOMOCO, HOmo sapiens COmprehensive MOdel COllection.

were the same length (122 bp) that did not change DNA methylation significantly (p-value > 0.05) in response to fatty acid treatment. Control sequences were randomly selected from the same genomic location (promoter, gene body or intergenic region) as the target sequences analysed.

5.2.2.2 Identification of DNA motifs

DNA motif analysis was carried out using Multiple EM (Expectation maximisation algorithm) for Motif Elicitation (MEME) and Hypergeometric Optimisation of Motif EnRichment (HOMER), both tools publicly available. *De novo* motif discovery was performed using discriminative analysis with ZOOPS scoring (zero or one occurrence per sequence). This compared sequences within the DNA methylationEPIC BeadChip that changed DNA methylation significantly (target sequences) with those which did not change (control sequences). Both tools analysed the most frequent DNA sequence patterns to predict an ungapped motif using different algorithms components. MEME used expectation maximisation, maximum likelihood ratio based and greedy search while HOMER a cumulative binomial distribution. Putative ungapped DNA motifs were then compared with control sequences which assigned a score or P-value that was then corrected for multiple testing. The resulted Expect value (E-value) indicated the number of times that the identified motifs in target sequences were expected to match as well or better in the control sequences. The lower the E-value, the lower expectancy of a motif that was associated with methylation change being present in control sequences[331–333].

MEME analysis was carried out using online MEME Suite Version 4.11.4 (`http://meme-suite.org`) with a background model of second order, without random subsampling, a motif length restriction to 6 and 30 nucleotides and a search not restricted to palindromes. Discriminative Regular Expression Motif Elicitation (DREME) analysis was also carried out as part of the tools available in the MEME Suite. DREME employed a Fisher's Exact Test to calculate the P-value and correspondent E-value which evaluated the enrichment of short motifs (up to 8 bases) in target sequences relative to the control sequences[333]. The cutoff to consider a motif significantly enriched by both MEME and DREME analyses was an E-value $\geq 1\text{x}10^{-10}$.

HOMER analysis was performed using Version 4.9 with homer2 executable, the denovo command, cumulative binomial distribution and a motif length restriction same as the significant motifs identified by MEME. The cutoff to consider a motif significantly enriched was an E-value $\geq 1\text{x}10^{-10}$.

Table 5.1: Groups and number of DNA sequences used in the DNA motif analysis.

	Treatment	Direction of Change	Genomic Location	# of Sequences Analysed
Groups by treatment and direction of change	OA	⇓	Any	269
	OA	⇑	Any	294
	DHA	⇓	Any	1088
	DHA	⇑	Any	508
Groups by treatment, direction of change and genomic location	OA	⇓	Promoter	40
	OA	⇑	Promoter	40
	OA	⇓	Gene body	111
	OA	⇑	Gene body	130
	OA	⇓	Intergenic region	104
	OA	⇑	Intergenic region	114
	DHA	⇓	Promoter	127
	DHA	⇑	Promoter	54
	DHA	⇓	Gene body	476
	DHA	⇑	Gene body	254
	DHA	⇓	Intergenic region	427
	DHA	⇑	Intergenic region	181

⇓ indicates a decrease in DNA methylation; ⇑ indicates an increase in DNA methylation. Sequences which genomic location was not specific for only one were excluded from the analysis

5.2.2.3 Comparison of DNA motifs between MEME, HOMER and known motifs

The motifs identified by MEME and HOMER were compared using similarity, tree-building, and alignment of DNA motifs and profiles (STAMP) tool[334;335]. The comparison of motifs was performed using the recommended default parameters. These were column comparisons with Pearson's correlation coefficient using an ungapped Smith-Waterman algorithm with the iterative refinement option for the alignment. The ungapped Smith-Waterman method aligned first the core of motifs without the allowance of gaps and then the edges of the motif using the Smith-Waterman algorithm[336] (Figure 5.3). Once an alignment was constructed, it was removed from the current alignment and added again to the remaining sequence to be aligned. This iterative refinement was employed to avoid any influence of the nearby sequence (local minima) in the alignment[334], which is a common problem[337]. The Pearson's correlation coefficient then measured the agreement in the covariance of the nucleotides in the sequences[334] derived from the alignments (Figure 5.3). The Pearson's correlation coefficient has been shown to perform better than normalised Euclidean distance, Spearman rank correlation and the sum of products[338].

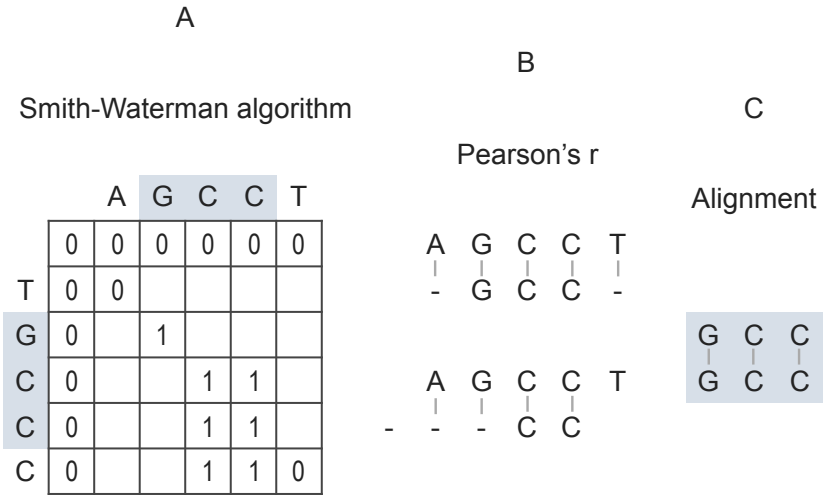

Figure 5.3: Diagram of DNA motif comparison/alignment. Sequences of different lengths were aligned and scored according to the matches in nucleotides (hypothetical score 0 = not aligned, 1 = aligned) as shown in A. Alignments constructed were removed from the sequences and put back in a different position to avoid influences from the local environment (iterative refinement). The multiple alignments were transformed into position specific scoring matrices (PSSMs) which were then compared by Pearson's correlation coefficient (data not shown). Essentially, this means that Pearson correlation measured the agreement of the nucleotides in the sequences (B). The best fit in the alignments, if any, was then obtained (C) (E-value < 0.05).

The motifs identified by MEME and HOMER that were significantly similar to each other using STAMP tool (E-value < 0.05) were then compared individually to known motifs using the Tomtom tool[339] and the core collection of the HOmo sapiens COmprehensive MOdel COllection (HOCOMOCO) v11[340] (available in `http://meme-suite.org/tools/tomtom`). The similarity of significant motifs with HOCOMOCO motifs was carried out using the Pearson's correlation coefficient to score even the unaligned nucleotides (columns) in both, the input and HOCOMOCO motifs. This resulted in a single score of all nucleotides included in a motif by an E-value. In addition to the E-value, Tomtom computed the q-values for each match as a second type of multiple-testing correction. The cutoff to consider a motif comparison significant was an E-value < 0.05 and q-value < 0.05.

5.2.3 Cross-linked chromatin immunoprecipitation coupled with qPCR

Cross-linked chromatin immunoprecipitation coupled with qPCR was carried out to investigate if CpG sites that showed altered DNA methylation by OA or DHA treatment were associated with altered H3K4me3 enrichment. An overview of the method is shown in Figure 5.4.

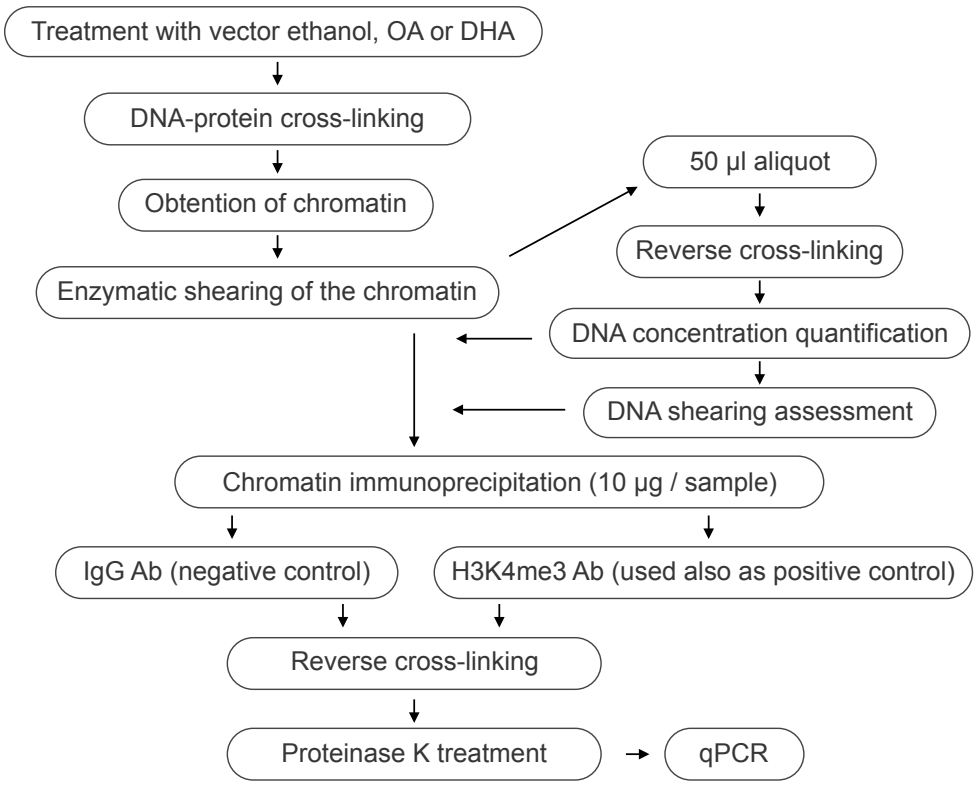

Figure 5.4: Overview of cross-linked chromatin immunoprecipitation coupled with qPCR. Ab, antibody; qPCR, quantitative polymerase chain reaction.

5.2.3.1 DNA-protein cross-linking

Cross-linking of samples was performed following protocols used by the ENCODE Consortium[341]. After treatment with fatty acid vector (ethanol), OA or DHA (n = 8 cultures replicates per treatment) for 8 days, $2x10^7$ cells in cell media were made up to 1.5 ml with 1x PBS in 2.2 ml microcentrifuge tubes. 100 μl of 16% methanol-free formaldehyde (w/v) was added to obtain a final concentration of 1% formaldehyde. Samples were then incubated for 10 minutes on a roller mixer at room temperature to cross-link DNA with proteins[342]. The reaction was stopped after 1-minute incubation with glycine at a final concentration of 0.125 M at room temperature[343]. Samples were then centrifuged (376 g, 2 minutes, 4 °C) and the supernatant discarded. Cell pellets were washed with 2 ml cold (4 °C) 1x PBS, repeating centrifugation and the discard of the supernatant. Cell pellets were snap-frozen in liquid nitrogen and stored at −80 °C until further used.

5.2.3.2 Preparation of chromatin

An enzymatic method was preferred over sonication to shear the chromatin in order to minimise systematic variation. Enzymatic shearing of the chromatin has shown to be a reliable option[344]. Nevertheless, enzymes preferentially target sequence-specific locations[345;346], which possibly could lead to a bias in nucleosome positioning studies[344]. As this is not the purpose of the current project, the enzymatic method presented no disadvantage.

The isolation and shearing of the chromatin were carried out using ChIP-IT Express Enzymatic kit following manufacturer's instructions. The kit provided all reagents needed except for glycine. Frozen cell pellets were prepared for lysis by addition of 1 ml 1x Lysis Buffer supplemented with 5 μl protease inhibitor cocktail (PIC) and 5 μl of 100 mM phenylmethylsulfonyl fluoride (PMSF). PIC and PMSF were mixed by gently pipetting and samples incubated on ice for 30 minutes. The cell lysis was then carried out by freeze-thaw cycles using liquid nitrogen to freeze samples and a water bath at 40 °C to thaw samples. A minimum of 8 freeze-thaw cycles were carried out or more until the samples turned cloudy, which indicated the cell membrane disruption. The samples were then centrifugated at 2352 g for 10 minutes at 4 °C, the supernatant discarded and the pelleted nuclei resuspended in 350 μl Digestion Buffer supplemented with 1.75 μl PIC and 1.75 μl PMSF. Samples were then incubated for 5 minutes at 37 °C. 17 μl Enzymatic Shearing Cocktail (200 U/ml) in 50% (w/v) glycerol was added to samples and mixed by vortex. The samples were incubated for another 20 minutes at 37 °C period in which they were mixed by vortex approximately every two minutes. The shearing of the chromatin was stopped by adding 7 μl of 0.5 M EDTA followed by a 10-minute incubation on ice. The samples were

then centrifuged at 21130 g for 10 minutes at 4 °C to pellet the cell debris. The supernatant (sheared chromatin) was recovered and pipetted into a new microcentrifuge tube. 50 μl of each sample was placed into a new PCR tube to assess the shearing of the chromatin (size of fragments) and the DNA concentrations (section 5.2.3.3) before proceeding with the immunoprecipitation (section 5.2.3.4). Samples were stored at −80 °C until further use.

5.2.3.3 Reverse cross-linking of aliquots to assess DNA concentrations

Reverse cross-linking to asses DNA concentrations was performed using the same reagents provided by ChIP-IT Express Enzymatic kit plus phenol Tris-EDTA (TE)-saturated (10 mM Tris (HCl-adjusted), 1 mM EDTA, pH 8), chloroform, 3 M Sodium Acetate pH 5.2, ethanol and DNA- and RNA-free water. 150 μl dH2O followed by 10 μl 5 M NaCl were added to each 50 μl aliquot (from section 5.2.3.2). Samples were incubated overnight at 65 °C using a Veriti Thermal Cycler (Applied Biosystems) to reverse the cross-links. Once nucleic acids and proteins were separated, 1 μl of RNase A (10 μg/μl) was added and samples incubated for 15 minutes at 37 °C to degrade any possible RNA in samples. Protein degradation was then carried out by the addition of 10 μl of Proteinase K (0.5 μg/μl) and incubation for 90 minutes at 42 °C. After this, samples were placed in 1.5 microcentrifuge tubes to isolate the DNA (clean-up) using a phenol/chloroform method provided in the kit as follows. 200 μl of 1:1 phenol-TE-saturated:chloroform was added to samples, vortex mixed and centrifuged at 21130 g for 5 minutes. The supernatant was transferred into a new 1.5 microcentrifuge tube. 20 μl 3 M sodium acetate pH 5.2 and 500 μl 100% ethanol were then added. Samples were vortex mixed, incubated at −80 °C for 2 hours and then centrifuged at 21130 g for 10 minutes at 4 °C. The supernatant was discarded, 500 μl of 70% (v/v) ethanol added to samples and centrifugation repeated for just 5 minutes. The supernatant was discarded again, the pellet air-dried and then resuspended in 20 μl DNA- and RNA-free water. Chromatin shearing was assessed by agarose gel electrophoresis as described in section 2.3.4. DNA concentration was assessed as described in section 2.3.3 and concentrations used to back-calculate the concentration of the sheared chromatin in samples using Equation 5.2.

$$Chromatin\ (ng/\mu l)\ =\ \left(\frac{DNA\ after\ clean-up\ (ng/\mu l)\ \ \times\ \ Resuspension\ volume\ (\mu l)}{Volume\ of\ aliquot\ used\ for\ clean-up\ (\mu l)}\right) \quad (5.2)$$

5.2.3.4 Chromatin immunoprecipitation and reverse cross-linking of samples

ChIP was carried out using reagents and a magnet provided by the ChIP-IT Express Enzymatic Kit and ChIP-IT Control Kit-Human following manufacturers' instructions. The latter kit provided an RNA polymerase II mouse monoclonal antibody (mAb) as a positive control, a bridging antibody (Ab) (1 μg/μl) to facilitate binding of RNA polymerase II to magnetic beads, a mouse immunoglobulin G (IgG) Ab as a negative control and glyceraldehyde 3-phosphate dehydrogenase (GAPDH) primers to carry out a control PCR amplification. In addition, histone H3K4me3 polyclonal antibody (pAb) (isotype IgG, host rabbit) was used to target the histone mark of interest.

Frozen samples containing the sheared chromatin were thawed on ice. 20 μl were then transferred to a PCR tube (input DNA) while 10 μg of sheared chromatin were transferred to another PCR tube for the immunoprecipitation. ChIP reaction was carried out using 25 μl protein G magnetic beads, 20 μl ChIP buffer 1, 61 to 150 μl (10 μg) of sheared chromatin, 2 μl PIC, up to 197 μl dH2O and 3 μl H3K4me3 pAb (1 μg/μl) added last for a final volume reaction of 200 μl. Negative control reactions were prepared as previously described using 190 μl dH2O and 10 μl IgG (0.2 μg/μl).

After ChIP reactions were prepared, the PCR tubes were placed into 50 ml tubes to immobilise them and to allow samples to mix on a roller mixer during an overnight incubation at 4 °C. The PCR tubes were centrifuged to collect drops on lids and the beads were then collected on the tubes side using a magnetic bar. The supernatant was removed, discarded and serial washes performed as follows. The first 3 times with 200 μl ChIP Buffer 1 and then 2 times with 200 μl ChIP Buffer 2. The washed beads were resuspended in 50 μl Elution Buffer AM2 and incubated 15 minutes at room temperature on a roller mixer. 50 μl of Reverse Cross-linking Buffer were then added and mixed by pipetting. The magnetic beads were collected again using the magnetic bar and the supernatant transferred to a new PCR tube. The sheared chromatin was placed on ice while 88 μl of ChIP Buffer 2 and 2 μl 5 M NaCl were added to the 20 μl input DNA aliquot. Both, the ChIP samples and DNA input aliquot were incubated for 15 minutes at 95 °C using a Veriti 96 well Thermal Cycler (Applied Biosystems). 2 μl Proteinase K (0.5 μg/μl) were then added, mixed and samples incubated for 60 minutes at 37 °C. Reaction was stopped by adding 2 μl of Proteinase K Stop Solution. Samples were stored at −20 °C until further use.

5.2.3.5 Mapping of H3K4me3 and selection of regions

All CpG sites that significantly changed DNA methylation by OA or DHA were mapped to the genome in order to look for any overlap with H3K4me3 mark. The mapping of CpG sites and H3K4me3 mark was carried out using the WashU Epigenome Browser[347]

v46.1 (available in `https://epigenomegateway.wustl.edu`) which is part of the Roadmap Epigenomics Project. The mapping was performed using the human *hg19* assembly from ENCODE, same as MethylationEPIC BeadArray. The cutoff to consider an overlap valid was a difference > 10 between the ChIP-seq input DNA raw signals and the ChIP-seq H3K4me3 raw signals. 5 candidate regions with the top difference located in promoter regions were selected for analysis. Bespoke primers were designed using the primer design tool in the NCBI website as described (section 2.4.1). Primer sets for ChIP-qPCR were named after the ID of probes in the DNA methylation BeadArray. A diagram of the sequences analysed is shown in Figure 5.5.

5.2.3.6 qPCR and statistical analysis

qPCR was carried out as described in section 2.4.2.

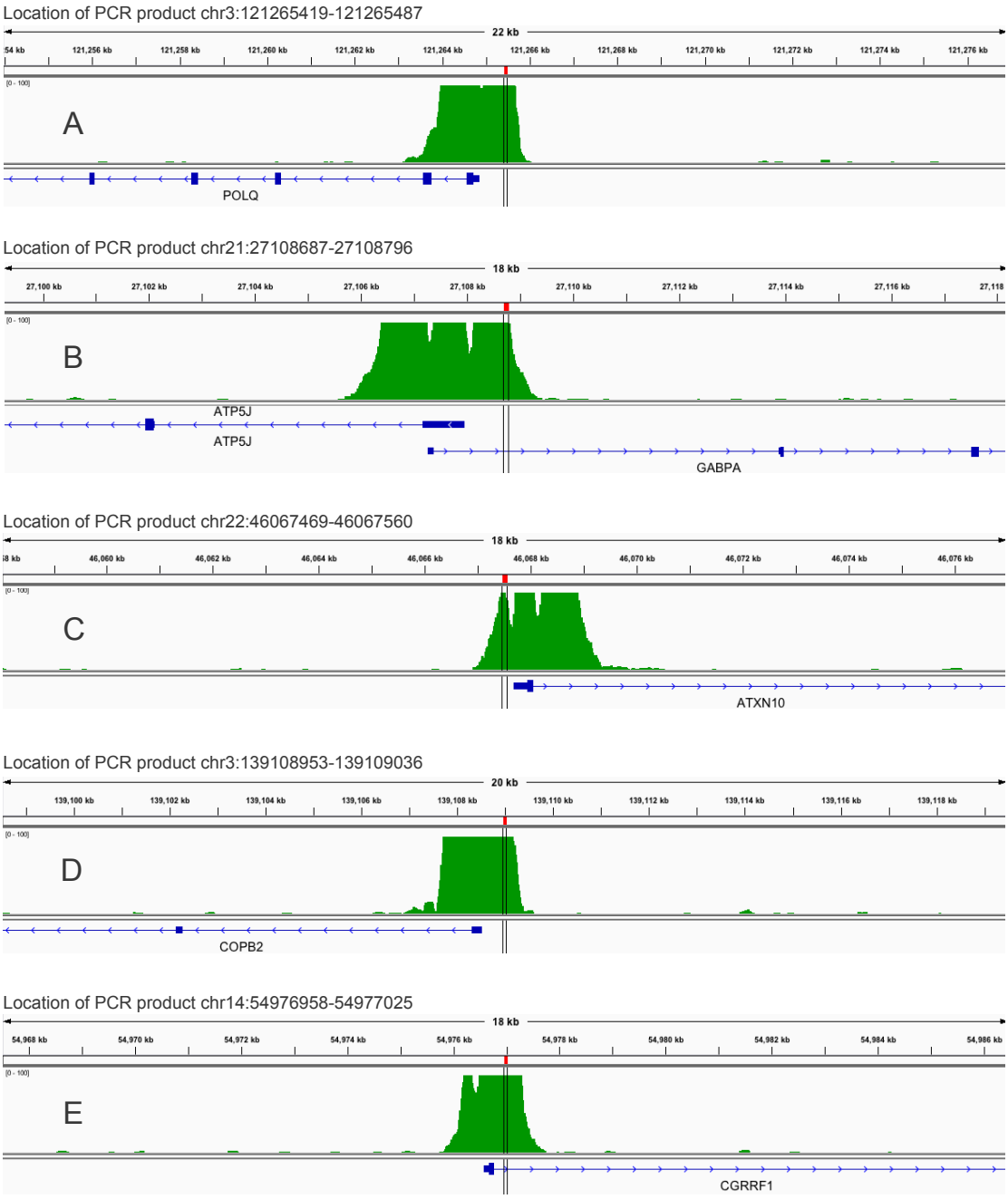

Figure 5.5: Genomic locations of primers ID cg17058565 (A), cg15707568 (B), cg17016559 (C), cg07203320 (D), cg18492804 (E) used for ChIP-qPCR. The diagram shows the raw signal peaks of H3K4me3 occupancy in Jurkat cells (in green) and the genes (in blue) near the regions that were amplified by each primer set (black parallel lines). Genomic locations, H3K4me3 occupancy and genes according to assembly *hg19* from ENCODE using Integrative Genomics Viewer version 2.3.91[348] available in `http://www.broadinstitute.org/igv`.

5.3 Results

5.3.1 Does PPARα mediate the altered DNA methylation induced by DHA?

The involvement of PPARα on DNA methylation changes induced by DHA has not been tested before. Therefore, this work sought to address this using PPARα agonist/antagonists treatments. To conduct such experiments, it was first tested the gene expression of PPARα in Jurkat cells. PCR using bespoke primers for PPARα showed that cells expressed this transcription factor (Figure 5.6).

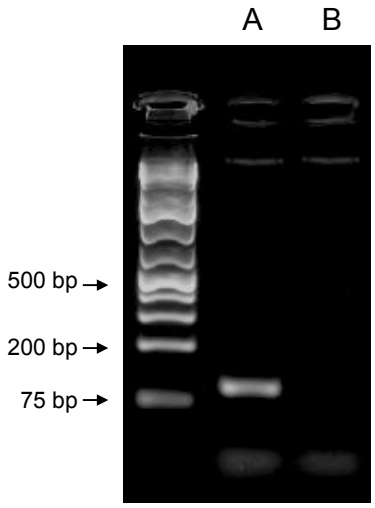

Figure 5.6: Representative 2% agarose gel after a PCR using primers for PPARα (112 bp expected amplicon size) and Jurkat cells cDNA (A) or reverse transcriptase control (B).

After verifying PPARα mRNA expression in cells, it was tested if PPARα agonist GW7647 efficiently increased the activity of PPARα. For this purpose, Jurkat cells were transfected with a luciferase reporter construct under the control of PPAR response element (PPRE) tandem repeats. Transfected cells treated with 0.2 μM PPARα agonist GW7647 showed to induce a 2-fold increase in luciferase activity after 3 hours incubation compared with transfected cells treated with vector ethanol (Figure 5.7 A). There was not identified a further change in luciferase activity in transfected cells after 6 hours of treatment with 0.2 μM PPARα agonist GW7647 (Figure 5.7 B). The transfection of Jurkat cells with the different constructs and subsequent treatments did not show any statistical difference in cell viability between controls and treatments (Figure 5.8). Therefore, results suggested that the treatment of Jurkat cells with 0.2 μM PPARα agonist GW7647 was adequate to study the participation of PPARα agonist in DHA-induced DNA methylation changes.

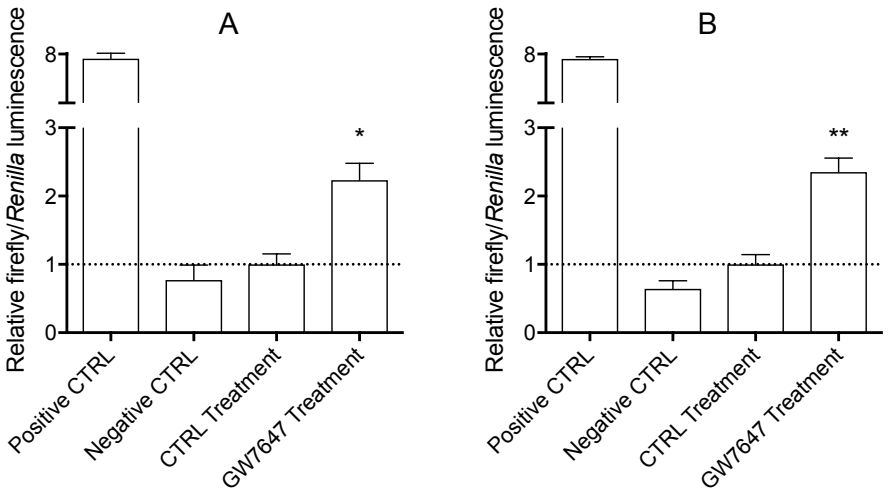

Figure 5.7: Relative firefly / *Renilla* luciferase gene luminescence (n = 3 culture replicates per group) after treatment with PPARα agonist GW7647 showed a 2.2 or 2.3 fold change increase compared with control (CTRL) treatment (vector ethanol) at the 3rd (A) or 6th hour (B) of incubation, respectively. Data are the relative luminescence values adjusted to the mean luminescence values of cells transfected with the PPRE construct and treated with the vector ethanol ± standard error of the mean. Treatment versus control means were compared by Student's T-test and those which differed significantly are indicated by *P $<$ 0.05, **P $<$ 0.01 or ***P $<$ 0.001.

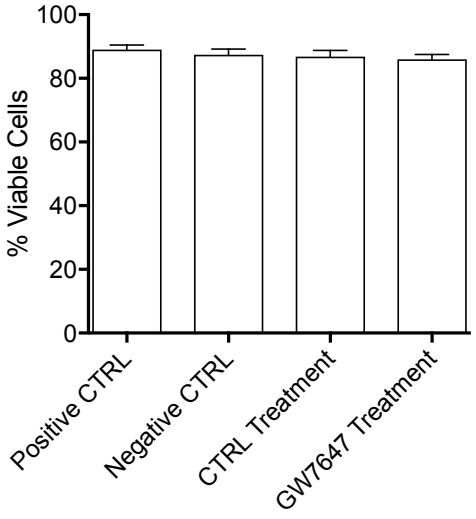

Figure 5.8: Cell viability after transfection of constructs and treatment with 0.2 μM PPARα agonist GW7647 or vector ethanol. Data are the mean % of viable cells after 3 and 6 hours of incubation (n = 6 culture replicates per group) ± standard error of the mean. The means of all groups were compared by one-way ANOVA with Tukey HSD post-hoc test and those which differed significantly are indicated by *P $<$ 0.05, **P $<$ 0.01 or ***P $<$ 0.001.

Jurkat cells were then treated with 15 μM DHA, 0.2 μM PPARα agonist GW7647, or 2 μM PPARα antagonist GW6471 for 8 days. Cells were also co-treated with 15 μM DHA plus 2 μM PPARα antagonist GW6471 for the same period of time. The concentrations used for treatments with PPARα agonist GW7647 or antagonist GW6471 were higher than the EC_{50} value according to manufacturer's (0.006 μM and 0.24 μM, respectively). After 8 days of incubation, there was no significant difference in the cell viability between controls (vector ethanol), 0.2 μM PPARα agonist GW7647 and 2 μM PPARα antagonist GW6471 treatment. Jurkat cells showed a statistically significant decreased in cell viability only after 15 μM DHA treatment (3.6% Δ points) or 15 μM DHA plus 2 μM PPARα antagonist GW6471 co-treatment (4.2% Δ points) after the 8^{th} day of treatment (Figure 5.9).

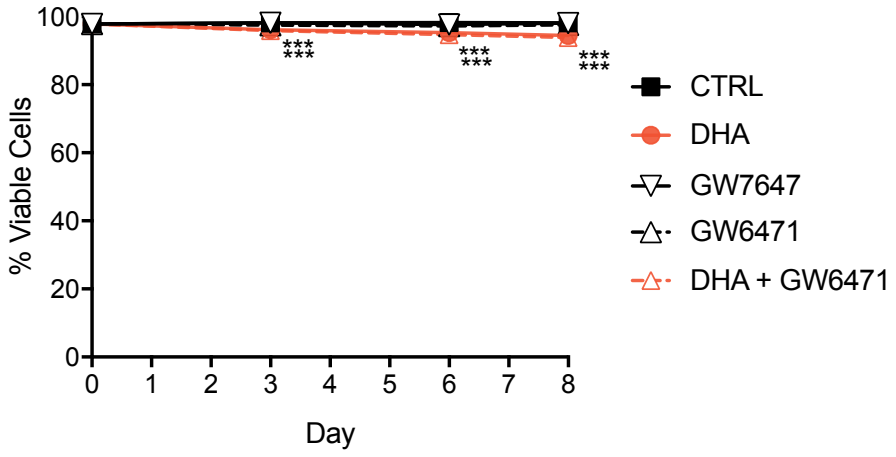

Figure 5.9: Cell viability after treatment with 0.2 μM PPARα agonist GW7647, 2 μM PPARα antagonist GW6471, 15 μM DHA or 15 μM DHA plus 2 μM PPARα antagonist GW6471 for 8 days. Data are the mean of cell viability absolute % points $\pm$ standard error of the mean using Typan blue exclusion. Treatment versus control means were compared by one-way ANOVA with Dunnett's post hoc test and those which differed significantly are indicated by *P $<$ 0.05, **P $<$ 0.01 or ***P $<$ 0.001.

After dismissing any effect on cell viability by PPARα agonist or antagonist, the DNA methylation was measured in the same 5 CpG sites analysed for BeadArray validation (previous Chapter). Treatment with 15 μM DHA or co-treatment with 2 μM PPARα antagonist GW6471 showed to significantly alter the DNA methylation of the 5 CpG sites analysed (Figure 5.10). In contrast, treatment with 0.2 μM PPARα agonist GW7647 or 2 μM PPARα antagonist GW6471 did not induce any significant change on DNA methylation of any CpG site analysed (Figure 5.10).

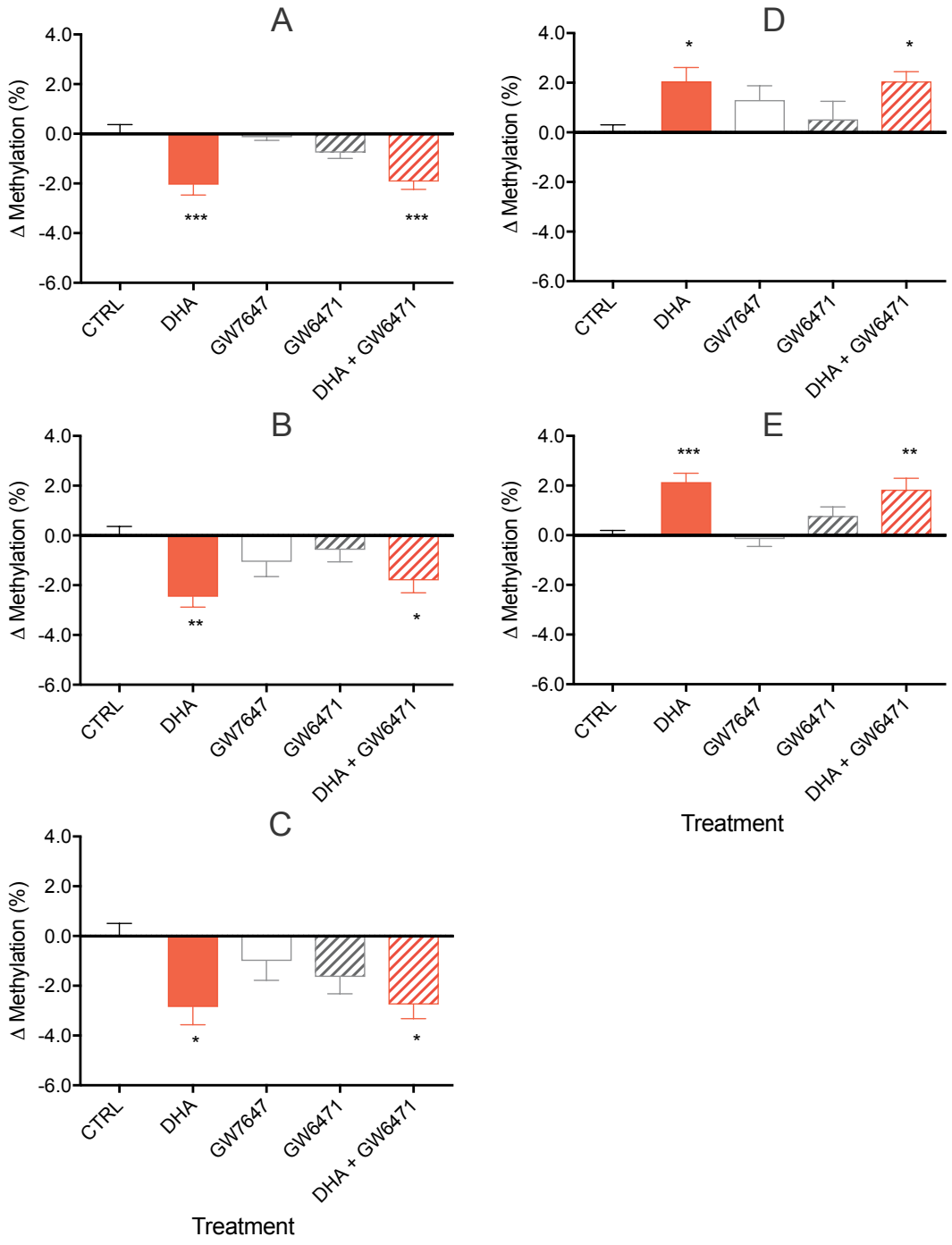

Figure 5.10: The effect of PPARα agonist GW7647 and PPARα antagonist GW6471 on 5 candidate CpG sites (A = ID cg26292058, B = ID cg05475386, C = ID cg27188282, D = ID cg06989443, E = ID cg22518417) that showed altered DNA methylation by DHA after 8 days of treatment. Data are the mean difference (Δ) in the absolute change on DNA methylation (% points) between treatments and controls (n = 8 culture replicates per treatment) $\pm$ standard error of the mean. Treatment versus control means were compared by one-way ANOVA with Dunnett's post hoc test and those which differed significantly are indicated by *P $<$ 0.05, **P $<$ 0.01 or ***P $<$ 0.001.

5.3.2 Do DNA motifs mediate the DNA methylation induced by OA or DHA?

There were identified DNA motifs in the proximity of CpG sites (60 bp upstream and 60 bp downstream) that significantly changed DNA methylation by OA treatment using MEME tool. Nevertheless, the three most significant motifs identified using $1x10^3$ control sequences were different from those motifs identified using $1x10^4$ or $1x10^5$ control sequences (Table 5.2). Analysis of the same sequences grouped by the direction of change on DNA methylation (decrease or increase) also showed enrichment of specific motifs. Again, the three most significant motifs were not the same when using $1x10^3$, $1x10^4$ or $1x10^5$ control sequences (Table 5.2).

Similar to OA treatment, there were identified DNA motifs in the proximity of CpG sites that significantly altered DNA methylation status by DHA treatment (122 bp long) using MEME tool. The significant motifs identified using $1x10^3$ control sequences were different from those motifs identified using $1x10^4$ or $1x10^5$ control sequences. Two motifs that were identified using $1x10^4$ control sequences were also identified using $1x10^5$ control sequences (Table 5.2). Analysis of the same sequences grouped by the direction of change on DNA methylation (decrease or increase) also showed enrichment of DNA motifs. Again, identified motifs using $1x10^3$ control sequences were different from those motifs that were identified using $1x10^4$ or $1x10^5$ control sequences. The most significant motifs using $1x10^4$ or $1x10^5$ control sequences were the same (Table 5.2).

The MEME tool used for motif analysis was specialised in the identification of long DNA motifs (up to 30 bp). In order to look for shorter DNA motifs, the DREME tool (part of the MEME Suite) was also employed. DREME analysis specialised in the identification of short DNA motifs (up to 8 bp). DREME results showed that the most significant motifs identified were not the same using $1x10^3$, $1x10^4$ or $1x10^5$ control sequences (Table 5.3). However, motifs identified in DHA-altered sequences using $1x10^4$ and $1x10^5$ control sequences showed greater similarities (DHA = 5) than motifs identified using $1x10^3$ and $1x10^4$ (DHA = 0) or $1x10^3$ and $1x10^5$ controls sequences (DHA = 0). The latter was not identified in OA-altered sequences (Table 5.3).

Table 5.2: The three most significant DNA motifs in sequences close to a CpG site that changed DNA methylation by OA or DHA treatment using MEME tool. Analysis was carried out using $1x10^3$, $1x10^4$ or $1x10^5$ control sequences.

Group	Motif	Sequences with motif (%)		
		$1x10^3$	$1x10^4$	$1x10^5$
OA all	SSCBSSSVNGKKGCTGGGGNBRSVSGBGKG	19	-	-
	TTTTWNTWTTTTTWTTWKWKW	20	-	-
	GAGCYGAGATCACGCCACTRCACTCCAGC	1	-	-
	CGYRGTGGCTCACGCCTGTAATCCCAGCWM	-	3	-
	CCMSBBCHCSSCMCHSCCCCCCVSSCHSS	-	21	-
	AAAAAAAAWAAVAAMWMRAAA	-	14	-
	CCMSCVCCCCCMCSCCYRSSC	-	-	19
	CTGTARTCCCAGCWMYTYGGGAGGCYRAG	-	-	3
	AAAAWAAAAAAAAMRWARAAW	-	-	13
OA ↓	GVVGSMSBVGGDGBSTGKGRGSGSRSSGGG	22[a]	22[a]	-
	CTYNGCCTCCCAANKWGCTGGGAYTRCAG	2	2	-
	GVKGSCBSGSGGKSBGKGSDSGGGSCKGG	-	-	17
OA ↑	CGYRGTGGCTCACGCCTGTAATCCCAGCWC	4[f]	-	4[f]
	CHSCASBSAGCCSVGVCCMCBCCSSBGCMC	16[c]	-	16[c]
	TTDTTTTTTTWTTTT	19[d]	18[d]	-
	SCCBSSBNVRGDGCTGGGVKKRSRGGSRBG	-	27	-
	ASWCCAGCCTGGGBDACAGAGYGAGACYC	-	3	-
	TTBTWTTHTTTTTTTHTTTTT	-	-	16
DHA all	GGCYRGGCGTGGTGGCTCACGCCTGTAA	2	-	-
	RCACACACACRCACRCACRCACACACRCAC	2	-	-
	TCRGCCTCCCAAAGTGCTGGG	2	-	-
	RCCTGTAATCCCAGCACTTTGGGAGGCYGA	-	2	2
	GYGTGYGYGTGTGTGTGYSTGTGTGTGTGT	-	2[b]	2[b]
	TTKTTTTNTTTTBTTWTWTWW	-	10	-
	SCKSSYCBMSCYBCCSSCKCCCYVGYCYS	-	-	8
DHA ↓	GCYRGGCRYGGTGGCTCACGCCTGTAATC	3	-	-
	GGGRGSBBGGGGSRSSVSSVGSRSNYSDGG	11	-	-
	CCAGCACTTTGGGAGGCYGAG	2	-	-
	GGCRTGGTGGCTCACGCCTGTAATCCCAGC	-	2	2
	BSCBGGCGCCCBSCBCCNSCCCCGSSCC	-	7	7
	TTTGGGAGGCYGAGGCRGGHG	-	2	2
DHA ↑	GMSGSGGSGGYVSKGGSRGGSWGGSNRS	18	-	-
	CTGTAATCCCAGCWMYTYGGGAGGCTGAGG	2	-	-
	GCTGGGATTACAGGYGTGMGCCACCRCGCC	-	2	2
	GMSGBGGSGGHVSNGGSGVGSWGGRBRSSB	-	14[e]	18[e]

The symbol '↓' indicates that only sequences near a CpG site that decreased DNA methylation were analysed. The symbol '↑' indicates that only sequences near a CpG site that increased DNA methylation were analysed. K = G or T; Y = C or T; S = C or G; W = A or T; R = A or G; M = A or C; B = not A; D = Not C; H = Not G; V = Not T; N or X = any base. Superscripts indicate that motifs have a mismatch in 2 = [a,b], 4 = [c,d], 7 = [e] bases or a difference in length of 6 bases = [f].

Table 5.3: The three most significant DNA motifs in sequences close to a CpG site that changed DNA methylation by OA or DHA treatment using DREME tool. Analysis was carried out using $1x10^3$, $1x10^4$ or $1x10^5$ control sequences.

Group	Motif	Sequences with motif (%)					
		$1x10^3$		$1x10^4$		$1x10^5$	
		Target	CTRL	Target	CTRL	Target	CTRL
OA all	AHAWA	74	49	-	-	-	-
	WTAW	57	36	-	-	59	41
	ANAWAA	-	-	57	33	-	-
	WAWAW	-	-	63	43	-	
	AAWAW	-	-	-	-	66	43
OA ↓	AHAWA	74	49	79	52	79	52
	WATW	59	35	-	-	-	-
OA ↑	AAAAWD	49	24	49	26	-	-
	ATWWT	-	-	-	-	58	34
DHA all	TAHWW	78	56	-	-	-	-
	TWWW	79	62	-	-	-	-
	ATTWW	-	-	63	41	-	-
	ATWW	-	-	74	56	70	52
	TWWA	-	-	43	29	44	30
	WATWW	-	-	-	-	67	45
DHA ↓	TAWHW	81	57	-	-	-	-
	WAAW	79	62	-	-	-	-
	WATWW	-	-	70	45	70	45
	WTTWW	-	-	61	40	61	40
	WTWW	-	-	74	59	-	-
	ASWWA	-	-	-	-	70	55
DHA ↑	KAAAW	-	-	72	52	72	53

The symbol '↓' indicates that only sequences near a CpG site that decreased DNA methylation were analysed. The symbol '↑' indicates that only sequences near a CpG site that increased DNA methylation were analysed. K = G or T; Y = C or T; S = C or G; W = A or T; R = A or G; M = A or C; B = not A; D = Not C; H = Not G; V = Not T; N or X = any base.

Overall, MEME and DREME results showed a low agreement between motifs identified using a different number of control sequences. Besides, both tools showed a higher agreement between motifs identified in DHA-altered sequences using $1x10^4$ and 10^5 control sequences. Such evidence suggested that motifs were dependent on the number of sequences used as control, at least in part. In order to increase the reliability of results motif analysis was continued using only the greatest number of control sequences. Therefore, motif analysis was continued using only $1x10^5$ control sequences. This was the greater number it was possible to work with according to the number of sequences included in the DNA Methylation BeadArray.

The same motif analysis that was previously carried out was then performed grouping sequences by genomic regions (promoter, body and intergenic region). There were motifs identified in each genomic region except in promoter sequences containing a CpG site differentially methylated by OA treatment (data not shown). After this, motifs analysis was performed using HOMER tool with the aim to replicate the significant motifs identified by MEME and DREME analyses. Only those motifs that were similar between MEME or DREME and HOMER tool (E-value < 0.05) were considered in this work as significantly enriched motifs. Such motifs were then compared (aligned) with known response elements in order to identify possible transcription factors that may bind to them (Table 5.4, 5.5 and 5.6). All other DNA motifs that were not common between MEME and HOMER analyses or between DREME and HOMER analyses were discarded and are not shown.

Common DNA motifs by MEME and HOMER analyses were identified in sequences containing CpG sites differentially methylated by OA treatment with some exceptions. The exceptions were sequences that decreased methylation in the body or intergenic regions and all gene promoter sequences. The majority of DNA motifs identified were significantly similar to response elements (E-value < 0.05) of mainly zinc-finger transcription factors (Table 5.4). In addition to the common DNA motifs identified by MEME and HOMER, there were also common DNA motifs identified by DREME and HOMER analyses. Common short DNA motifs by DREME and HOMER tools were essentially identified only by analyses carried out using sequences regardless of the genomic location. In all instances, the significantly enriched short DNA motifs were A/T-rich (Table 5.6).

MEME and HOMER tools also identified common significantly enriched motifs in sequences proximal to CpG sites differentially methylated by DHA treatment with some exceptions. The exceptions were sequences that decrease methylation in the body or those that increase DNA methylation in the promoter, body and intergenic regions (Table 5.5). The majority of DNA motifs identified were significantly similar to response elements (E-value < 0.05) of mainly zinc-finger transcription factors. DNA motifs identified using only promoter sequences regardless of the direction of change in methylation were similar to response elements that were not predicted in any of the other genomic locations. Such response elements identified were similar to those of forkhead box J3 (FOXJ3), PR/SET domain 6 (PRDM6), androgen receptor (AR) and sex determining region Y (SRY) (Table 5.5). Common short DNA motifs by DREME and HOMER analyses were identified essentially in all genomic locations analysed except in sequences that increase methylation in the promoter, body or intergenic regions. Besides, there were not identified common DNA motifs in promoter sequences when the analysis was carried out regardless of the direction of change of methylation. Similar to DNA motifs in OA-altered sequences, significantly enriched short DNA motifs in the sequences altered by DHA were A/T-rich (Table 5.6).

Table 5.4: List of DNA motifs identified in sequences altered by OA which were significantly similar between MEME and HOMER analysis (E-value < 0.05). Identified DNA motifs were compared with known motifs using HOMOCOCO v11.

Group	Motifs by MEME or HOMER	Similar to binding site of
OA any all	CCNSNNCCCCCNNNCCYNSNC[a] ANCTCYTGYNMSSMASGTCTS[b]	SP2[a] , SP3[a], SP1[a], ZN467[a] WT1[a], MAZ[a], KLF3[a], PATZ1[a]
OA any ↓	GNKGSCNSNNNSKSNGKGSNSNGNSNKGG[a] CTNNNAGNATGCCGGGTGGCGGTGTGGA[b]	SP1[a], SP2[a], SP3[ab], ZN281[b]
OA any ↑	CNGCNSNSAGCCNNNNNCNNNCCNSNNCMC[a] ACKNYCYSGGGSCSGSCRCSTSGCCGCYCC[b]	SP2[ab], SP3[ab], KLF3[a] USF2[b], SP1[b]
	ARKTGCTGGGATTACAGGCGTGAGCCAC[a] GNCAASCNGNNGGGTGNNGGNKAARNGCCG[b]	-
OA body all	SNNCNNCCNNGNCNNNCCNSNCYNCNS[a] NNNANYCCNGNNGTNWGNNYCCGMNTTCC[b]	SP1[a], SP2[a], SP3[a], PATZ1[a], ZN467[a], MAZ[ac], WT1[a], VEZF1[a], KLF15[a], KLF9[a] KLF3[a]
OA body ↑	GNRGKNAGSNNRGNGSAGG[a] GCANTSARSNGAGANCANNYY[b]	VEZF1[a], ZN467[a], ZN341[a], KLF3[a], SP2[a], PATZ1[a] SP3[a], WT1[a], MAZ[a]
OA int all	GYGGTGGNKCRYRCCTGTARTCCCAGC[a] NGGAKTNKANCTGNAGNCNTWNSNANNA[b]	-
	NNSNNYCNNCNGCCNSNSCSYCCMNRN[a] NTAMTACNTNTNNCCYNCCCCYNNCMNN[b]	ZN770[a], WT1[a], SP3[a]
OA int ↑	YTYGGGAGGCYRAGGCRGRCGGRTCRCKT[a] SCNGNSWGGGANGNGNGNGGNGCCNCTGN[b]	ZN770[a], WT1[ab]
	GGGATTACAGGCGYGAGCCACYRC[a] MRGNNTRRANMTNYAKRMCTKWNYANNNR[b]	-
	GYRGTGGCTCRCGCCTGTAATCCC[a] ATGRMNWATNYCTGTCWNWMNMNN[b]	-

All DNA motifs shown were those identified by MEME or HOMER tool in sequences located in any genomic region (any), the promoter (prom), the body (body) or the intergenic region (int) which showed an expected (E)-value < 0.05 using STAMP tool. The E-value indicated the number of better alignments expected to match by chance. [a] = data by MEME analysis; [b] = data by HOMER analysis. All similarities between DNA motifs and response elements were significant (P < 0.0001, E-value < 0.05 and q-value < 0.05). The code for A, C, G and T nucleotides with the different symbols are the same as Table 5.3 and 5.2. Name and details of transcription factors shown here are described in Table 5.7

Table 5.5: List of DNA motifs identified in sequences altered by DHA which were significantly similar between MEME and HOMER analysis (E-value < 0.05). Identified DNA motifs were compared with known motifs using HOMOCOCO v11.

Group	Motifs by MEME or HOMER	Similar to binding site of
DHA any all	SNNSNNSNNSCYNCCNNCNCCCNNGNCNC[a] ASKGCNGGCASNGKGSCYNCCASCACNNNM[b]	SP1[a], SP2[a], SP3[a], MAZ[a] PATZ1[a], ZN467[a], ZN341[a] KLF15[a], VEZF1[a], ZBT17[a]
DHA any ↓	GGNSNGGGGSNGGNGSNGGGSNCNNGG[a] RGAGGNGGNNGNGGMGGGAGN[b]	SP1[ab], SP2[a], SP3[a], SP4[b] ZN263[b], ZN467[ab], ZN341[b], ZN770[b], WT1[ab], MAZ[b], KLF3[a], KLF15[ab], PATZ1[ab], TAF1[ab]
	CNCCYGCCTCGGCCTCCCAAA[a] NCTCCCKCCNCNNCCNCCTCY[b]	SP1[b], ZN770[ab], ZN263[b], ZN341[b] , ZN467[b], PATZ1[b], KLF15[b], WT1[b], EGR1[b], TAF1[b], MAZ[b]
	GCTGGGATTACAGGCGTGAGCCACCACGCC[a] NGCAATACTGATATGACNCCC[b]	-
DHA any ↑	GGCGYGGTGGCTCACRCCTGTAATCCCAGC[a] NARYCCAGMNNCYGGRNCWYNNCTGRRRN[b]	-
	CCNCCNNSYCNSNNCNNCCNNSNS[a] NARYCCAGMNNCYGGRNCWYNNCTGRRRN[b]	SP1[a], SP2[a], SP3[a], PATZ1[a], ZN281[a], ZN341[a], ZN467[a], MAZ[a], WT1[a], VEZF1[a], KLF15[a], ZBT17[a]
DHA body all	GCTCAYRCCTGTAATCCCAGCACTTTGGGA[a] NYAGNCACNNNNANNCYCNNCTMNNNAGAN[b]	ZN250[a]
DHA int all	CCTCCCAAAGTGCTGGGATTACAGGCGTG[a] TGNGNGNCGNAGGNCNCCGTGCCCGNCNT[b]	ZN250[a], IKZF1[a]
	CSNNNNCNNSCCCNCRSSNCNNNNNNS[a] AGCACSNSNCTSTCYCANCNNMMNYCCCN[b]	SP1[a], SP2[a], SP3[a], MAZ[ab], ZN467[ab], EGR1[a], PATZ1[ab], WT1[a], VEZF1[ab], KLF1[a]
DHA int ↓	GGCKNACGCCTGTAATCCCAGCWMTTTGGG[a] NGNNTGTMATANCANTANNNYNNKNGWNA[b]	-
DHA prom all	AAWAAAAWANANAAMAWWNAA[a] NNNNNNNNNNNAAAAAAANNAANNAAAANN[b]	FOXJ3[ab], PRDM6[ab], AR[ab], SRY[a]
DHA prom ↓	GNNNNSNNGNSGGGSGNGGGRGNNNNSNSS[a] GMGMCSAKNAGGGRCRANGSNNCMAGRGGC[b]	SP1[a], SP2[a], SP3[a], ZN467[a], PATZ1[a]

All DNA motifs shown were those identified by MEME or HOMER tool in sequences located in any genomic region (any), the promoter (prom), the body (body) or the intergenic region (int) which showed an expected (E)-value < 0.05 using STAMP tool. The E-value indicated the number of better alignments expected to match by chance. [a] = data by MEME analysis; [b] = data by HOMER analysis. All similarities between DNA motifs and response elements were significant (P < 0.0001, E-value < 0.05 and q-value < 0.05). The code for A, C, G and T nucleotides with the different symbols are the same as Table 5.3 and 5.2. Name and details of transcription factors shown here are described in Table 5.7

Table 5.6: List of DNA motifs identified in sequences altered by OA or DHA which were significantly similar between DREME and HOMER analysis (E-value < 0.05).

Group	Motifs in common	Group	Motifs in common
OA any all	AAWAW[a] AAAAA[b] TTAW[a] TTAA[b]	DHA any all	WATTW[a] AATTT[b] WAAT[a] AAATT[b]
OA any ↓	TWTNT[a] TTTTT[b] TWTNT[a] TATAT[b]	DHA any ↓	WAATW[a] NTATA[b] TTTTW[a] TTTTA[b]
OA any ↑	AAAAT[a] AAAAT[b] ATTTT[a] TTTTT[b]	DHA any ↑	KAAAW[a] TMAAA[b] WTTTM[a] AATTT[b]
OA body all	ARAAWA[a] AAAAAA[b] - -	DHA body all	TTAWN[a] TTATA[b] ATTT[a] ATTT[b]
OA body ↓	- - - -	DHA body ↓	NWTAA[a] TATAA[b] AATW[a] AAATW[b]
OA body ↑	ARAAWA[a] AARAAA[b] - -	DHA body ↑	- - - -
OA int all	- - - -	DHA int all	ATTTW[a] ATTTA[b] TAAA[a] TAAAT[b]
OA int ↓	- - - -	DHA int ↓	ATTTW[a] AATTT[b] TTTKA[a] TTTTA[b]
OA int ↑	- - - -	DHA int ↑	- - - -
OA prom all	- - - -	DHA prom all	- - - -
OA prom ↓	- - - -	DHA prom ↓	WATTNT[a] AATNTT[b] WATTNT[a] ATTTAT[b]
OA prom ↑	- - - -	DHA prom ↑	- - - -

All DNA motifs shown were those identified by DREME or HOMER tool in sequences located in any genomic region (any), the promoter (prom), the body (body) or the intergenic region (int) which showed an expected (E)-value < 0.05 using STAMP tool. The E-value indicated the number of better alignments expected to match by chance. [a] = data by DREME analysis; [b] = data by HOMER analysis. All similarities between DNA motifs and response elements were significant (P < 0.0001, E-value < 0.05 and q-value < 0.05). The code for A, C, G and T nucleotides with the different symbols are the same as Table 5.2 and 5.3.

Table 5.7: List of DNA-binding proteins which response elements were significantly similar to motifs identified in sequences close to CpG sites that changed DNA methylation by OA or DHA treatment.

Name	Symbol	Significant by	Domains able to bind DNA[a]
Androgen receptor	AR	DHA	ZF-C4
Early growth response 1	EGR1	DHA	ZF-C2H2
Forkhead box J3	FOXJ3	DHA	Fork-head
IKAROS family zinc finger 1	IKZF1	DHA	ZF-C2H2
Kruppel-like factor 1	KLF1	DHA	ZF-C2H2
Kruppel-like factor 3	KLF3	OA or DHA	ZF-C2H2
Kruppel-like factor 9	KLF9	OA	ZF-C2H2
Kruppel-like factor 15	KLF15	OA or DHA	ZF-C2H2
MYC associated zinc finger protein	MAZ	OA or DHA	ZF-C2H2
POZ/BTB and AT hook containing zinc finger 1	PATZ1	OA or DHA	A.T. hook, ZF-C2H2
PR/SET domain 6	PRDM6	DHA	ZF-C2H2
Sp1 transcription factor	SP1	OA or DHA	ZF-C2H2
Sp2 transcription factor	SP2	OA or DHA	ZF-C2H2
Sp3 transcription factor	SP3	OA or DHA	ZF-C2H2
Sp4 transcription factor	SP4	DHA	ZF-C2H2
Sex determining region Y	SRY	DHA	HMG box
TATA-box binding protein associated factor 1	TAF1	DHA	HMG box
Upstream transcription factor 2, C-fos interacting	USF2	OA	bHLH and L-Z
Vascular endothelial zinc finger 1	VEZF1	OA or DHA	ZF-C2H2
Wilms tumour 1	WT1	OA or DHA	ZF-C2H2
Zinc finger and BTB domain containing 17	ZBT17	DHA	ZF-C2H2
Zinc finger protein 250	ZN250	DHA	ZF-C2H2
Zinc finger protein 263	ZN263	DHA	ZF-C2H2
Zinc finger protein 281	ZN281	OA or DHA	ZF-C2H2
Zinc finger protein 341	ZN341	OA or DHA	ZF-C2H2
Zinc finger protein 467	ZN467	OA or DHA	ZF-C2H2
Zinc finger protein 770	ZN770	OA or DHA	ZF-C2H2

ZF-C4, zinc finger type Cys4; ZF-C2H2, zinc finger type Cys2-His2; A.T. hook, adenine-thymine hook; HMG box, high mobility group box; bHLH, basic helix-loop-helix; L-Z, leucine-zipper. [a] = data from UniProt Knowledgebase (UniProtKB) using only manually annotated records extracted from literature and further computational analysis.

5.3.3 Does H3K4me3 enrichment is altered on CpG sites that showed altered DNA methylation?

All CpG sites that significantly changed DNA methylation by OA or DHA treatment were mapped together with the H3K4me3 occupancy, specifically in Jurkat cells, using ENCODE. The analysis showed that 6.4% (36/563) of the CpG sites that were differentially methylated by OA treatment overlapped with H3K4me3 occupancy (23/36 increased). Analysis of each genomic location showed that there was a higher overlap between altered CpG sites and H3K4me3 in the promoter region (23.2%, 19/82) compared with the gene body (5.1%, 13/253) or intergenic regions (2.7%, 2/218) (Figure 5.11). 10 CpG sites with altered DNA methylation by OA were not included in this analysis because there was not identified a consensus location of those CpG sites.

Similar to OA, 7% (123/1596) of CpG sites that were differentially methylated by DHA treatment overlapped with H3K4me3 occupancy (55/123 increased). Analysis of each genomic location showed that there was a higher overlap between altered CpG sites and H3K4me3 occupancy in the promoter region (22.4%, 41/183) compared with the gene body (9.6%, 61/772) or intergenic regions (4.8%, 16/608) (Figure 5.11). 33 CpG sites with altered DNA methylation by DHA were not included in this analysis because there was not identified a consensus location of those CpG sites.

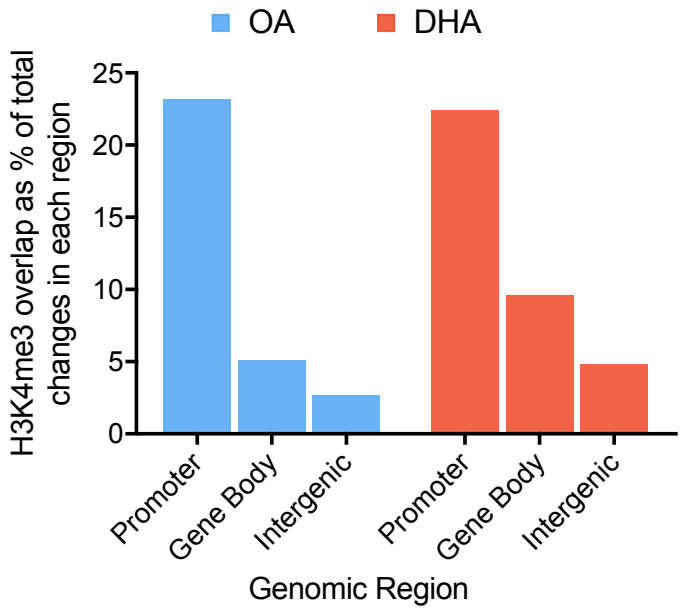

Figure 5.11: Overlap between CpG sites that were differentially methylated by OA or DHA treatment and H3K4me3 occupancy in Jurkat cells according to ENCODE. Data are percentages of the number of differentially methylated CpG sites that showed an overlap with H3K4me3 occupancy in comparison to the total number of altered CpG sites in each genomic region.

In order to validate the overlap between altered CpG sites with H3K4me3 and to further explore if H3K4me3 enrichment was altered, immunoprecipitation of the chromatin was carried out targeting H3K4me3. Optimisation of the method showed that the best time for enzymatic shearing of the chromatin was 20 minutes as this time produced brighter bands of size around 150 base pairs (Figure 5.12). Besides, optimisation showed that H3K4me3-immunoprecipitated chromatin amplified *GAPDH* gene which was used as positive control of ChIP reactions (Figure 5.13). Because of the latter, the RNA polymerase II immunoprecipitation, which is usually employed as positive control, was not carried out in the actual samples. Instead, *GAPDH* amplification in H3K4me3-immunoprecipitated chromatin was used as a positive control for ChIP reactions.

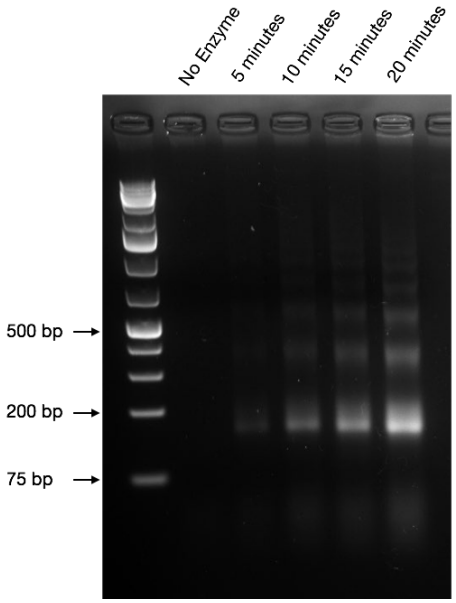

Figure 5.12: Optimisation of the time needed for chromatin shearing was addressed by enzymatic incubation for 5, 10, 15 or 20 minutes at 37 °C. A no control enzyme was also performed in the same conditions for 10 minutes. All samples were mixed by vortex every 2 minutes during the incubation. Reverse cross-linking was then performed and samples run in an 1% agarose:TAE gel (w/v).

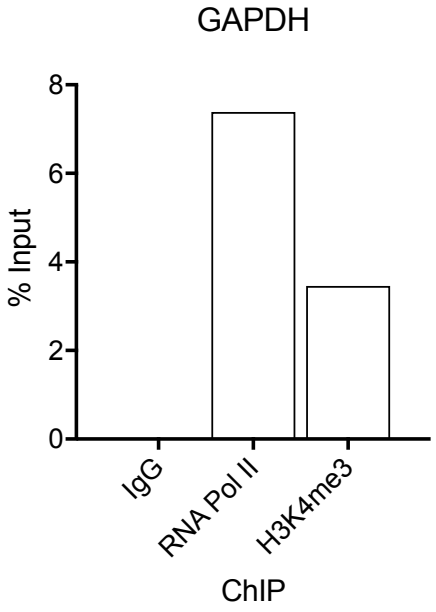

Figure 5.13: Antibody testing for chromatin immunoprecipitation assays was performed using IgG as a negative control, RNA Pol II as a positive control or H3K4me3 antibody. RNA Pol II and H3K4me3 immunoprecipitated samples showed a higher *GAPDH* amplification by qPCR according to the % input (n = 1 per antibody). The qPCR was performed in triplicate and averaged in each sample.

After optimisation, ChIP was then performed in Jurkat cells treated with 15 μM OA or 15 μM DHA for 8 days. Immunoprecipitated chromatin was then used as template to carry out qPCR in 5 candidate regions which showed the greatest H3K4me3 enrichment according to ENCONDE. Candidate regions analysed included 2 regions containing a CpG site with altered DNA methylation by OA and 4 regions containing a CpG site with altered DNA methylation by DHA. Genomic details of the candidate loci analysed and the respective change in the DNA methylation of the CpG sites within such loci are shown in Table 5.8.

Table 5.8: Details of candidate regions analysed by ChIP experiments

Primers ID	Genomic region	Altered CpG site[a]	Change in DNAm[a]	Change induced by[a]
cg17058565	Promoter of POLQ	cg17058565	+6	OA
cg15707568	Promoter of ATP5J	cg15707568	+6	DHA
cg17016559	Promoter of ATXN10	cg17016559	-6	OA or DHA
cg07203320	Promoter of COPB2	cg07203320	-5	DHA
cg18492804	Body of CGRRF1	cg18492804	-9	DHA

[a] = according to DNA methylation BeadArray results. POLQ, DNA Polymerase Theta; ATP5J, ATP Synthase Peripheral Stalk Subunit F6; ATXN10, Ataxin 10; COPB2, Coatomer Protein Complex Subunit Beta 2; CGRRF1, Cell Growth Regulator With Ring Finger Domain 1

ChIP-qPCR results showed that treatment with OA decreased H3K4me3 enrichment in the proximity of the 2 regions analysed. However, none of them reached statistical significance (Figure 5.14 A and C). One of the candidate regions examined contained a CpG site that increased while the other a CpG site that decreased DNA methylation by OA treatment (Table 5.8).

DHA-treated cells also showed decreased H3K4me3 enrichment in all 4 regions analysed. Only 3 changes were statistically significant. One of the significant changes overlapped with a CpG site that increased DNA methylation whereas the other two significant changes overlapped with CpG sites that decreased DNA methylation by DHA treatment (Figure 5.14 B, D, E, Table 5.8).

Both OA or DHA treatment amplified *GAPDH* positive control primers without any statistically significant difference (Figure 5.14).

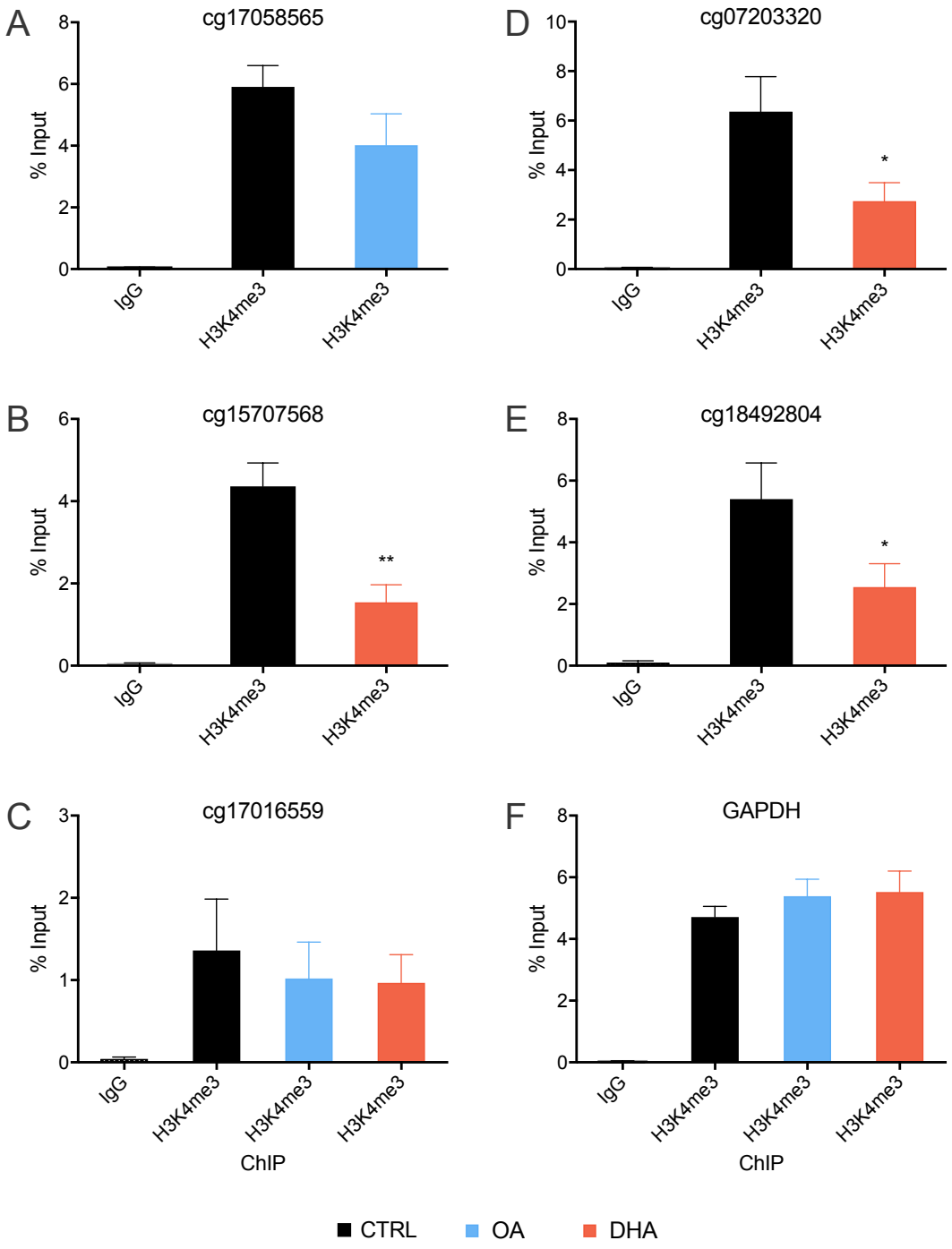

Figure 5.14: H3K4me3 enrichment in the proximity of 2 CpG sites that increased (A, B) and 3 CpG sites that decreased (C, D, E) DNA methylation by OA (A, C) or DHA treatment (B, C, D, E). *GAPDH* amplification (F) served as positive control in the same samples analysed. Data are means of 8 culture replicates per treatment ± standard error of the mean. Treatments versus controls means were compared by Student's T-test (A, B, D, E) or by one-way ANOVA with Dunnett's post-hoc test (C, F) and those which differed significantly are indicated by *P $<$ 0.05, **P $<$ 0.01, ***P $<$ 0.001.

5.4 Discussion

Three possible mechanisms to explain how fatty acids may alter the DNA methylome were evaluated in this Chapter. Results suggested that PPARα activity did not mediate the DNA methylation changes induced by DHA treatment. However, a relationship was identified between the altered DNA methylation induced by OA or DHA with DNA motifs and H3K4me3 enrichment.

5.4.1 The relationship between DNA methylation changes and PPARα activity

There is evidence that PPARα activity mediates the effect of arachidonic acid, but not OA, on the global DNA methylation of THP-1 monocytes[229]. This suggests that different fatty acids may use different mechanisms to induce altered DNA methylation of cells. Currently, it is unknown if PPARα activity mediates the effect of DHA on DNA methylation of cells because this has not been tested. To address this, Jurkat cells were treated with PPARα agonist and PPARα antagonist and the DNA methylation measured by pyrosequencing in candidate CpG sites previously identified to alter DNA methylation status by DHA treatment.

Treatment of cells with a PPARα-specific agonist failed to show any significant change in the DNA methylation of all 5 CpG sites that were analysed. Besides, co-treatment of cells with DHA plus a PPARα antagonist did not block DHA effects on the DNA methylation. Such results indicated that PPARα activity may not be involved in the altered DNA methylation induced by DHA treatment at these CpG sites. The 5 candidate CpG sites that were analysed here may not be representative of all 1596 differentially methylated CpG sites by DHA treatment. Thus, results do not discard the possibility that methylation levels of others CpGs may be mediated by PPARα. Overall, the current findings suggest that PPARα activity alone does not account for all DNA methylation changes by DHA treatment.

5.4.2 The relationship between DNA methylation changes and DNA motifs

The sequences containing a CpG site with altered DNA methylation by OA treatment were enriched with different DNA motifs. Such DNA motifs were identified in all genomic regions analysed except for promoter regions. Besides, there was not identified any DNA motif in those sequences which contained CpG sites that decreased DNA methylation in the intergenic and body regions. Therefore, motif analyses suggested that there was specificity in the genomic regions where DNA motifs may possibly influence DNA methylation changes by OA. The DNA motifs identified in the present

work supports the hypothesis that DNA sequence may influence DNA methylation patterns [323].

The sequences containing CpG sites with altered DNA methylation induced by DHA were also enriched in some DNA motifs. Analyses showed that DNA motifs were not present in all genomic regions. Therefore, this suggested again some specificity in the location of the DNA motifs identified. DNA motifs in sequences with CpG sites differentially methylated by DHA showed some similarities with those DNA motifs identified in sequences differentially methylated by OA. Nevertheless, promoter sequences with altered DNA methylation by DHA showed enrichment of DNA motifs very different from those identified in intergenic or body regions. DNA motifs in promoters were similar to response elements of FOXJ3, PRDM6, AR and SRY. These data suggested activity of such transcription factors may be related to DHA specificity on DNA methylation.

The majority of response elements identified in OA or DHA-altered sequences were zinc-finger proteins belonging to the Sp/KLF family. The most studied member of the family in human cells is the ubiquitously expressed SP1. There is evidence that this transcription factor can physically interact with DNMT1 [204]. Thus, it is possible that SP1 may direct this DNA methyltransferase to SP1 response elements (Figure 5.15). This mechanism may explain, at some extent, the specificity of fatty acids on the DNA methylation and the enrichment of SP1-like response elements identified in the proximity of such changes.

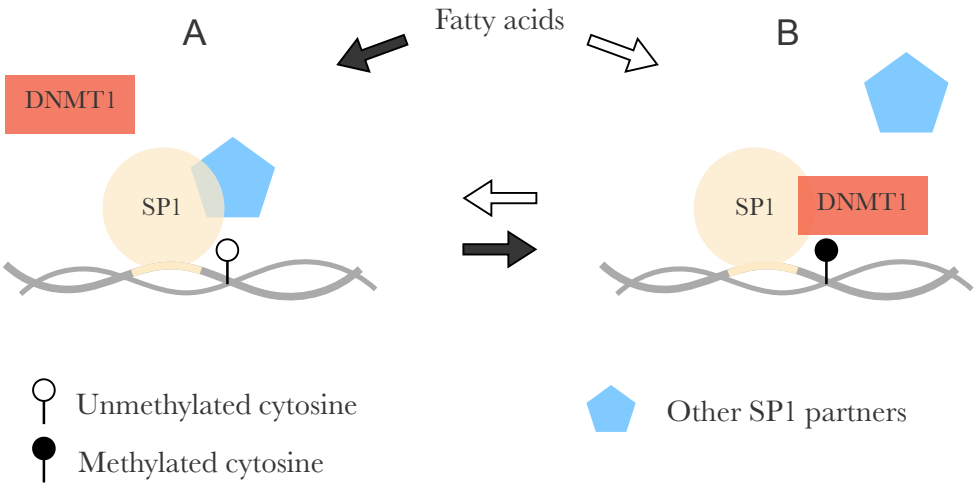

Figure 5.15: A possible mechanism to explain altered DNA methylation induced by OA or DHA according to motif analysis may involved SP1 activity and other proteins that physically interact with it. Increased DNA methylation by fatty acid treatment (A) may involve a swap of SP1 partners for DNA methyltranferase 1 (DNMT1). The reverse process may explain the decreased DNA methylation (B).

It has been shown that SP1 activity can be regulated by post-translational modifications and interactions with other proteins such as protein 53 (TP53 or P53)[349]. Mutations of TP53 that leads to gain of function have been shown to regulate fatty acid metabolism by modulation of 5' adenosine monophosphate-activated protein kinase (AMPK) in human cancer cell lines[350]. This is in agreement with animal studies that show a role of TP53 in the modulation of fatty acid metabolism[351;352]. AMPK serves as an energy sensor in cells[353] which has been shown to be regulated by palmitic acid in rat L6 muscle cells[354]. If AMPK regulation by palmitic acid was mediated by TP53 was not addressed in the study. At present, it is not well understood how these pathways may interact each other after fatty acid exposure on human cells. Moreover, it has not been tested how fatty acids may influence SP1-TP53 or SP1-DNMT1 interactions or another mechanism that may alter SP1 activity. Such experiments may provide some information about how fatty acids may modify the DNA methylation of cells.

5.4.3 The relationship between altered DNA methylation and decreased H3K4me3 enrichment induced by fatty acids

There is evidence that fatty acids can alter post-translational modifications of histones[249;250]. Studies addressing this have been focused on histone acetylation[245] while relatively little is known about the effect on histone methylation. Specifically in H3K4, a decrease in global H3K4me2 levels has been observed after incubation with 30 μM DHA for 2 days using human neuroblastoma M17 cells[248]. Results in the current work are in agreement with such evidence and indicate that besides H3K4me2, H3K4me3 mark is also decreased by DHA treatment in human cells.

There is a possibility that the decreased H3K4me3 enrichment on the 5 candidate regions analysed here led to complete demethylation of the lysine residue (H3K4me0). Unmethylated H3K4 may then provide a docking site for DNMT3A which can directly recognise and bind to H3K4me0, but not H3K4me3[325]. This process has been well described *in vitro* at the structural level for human DNMT3A[131] and may explain the increased DNA methylation by fatty acids in regions rich in H3K4me3 mark (Figure 5.16 A). This scenario implies that demethylation of H3K4me3 to H3K4me0 was the first step to induce changes on DNA methylation in cells. The possibility that DNMT3A mediates the altered DNA methylation by fatty acids may also explain why the majority of altered CpG sites did not overlap mainly with H3K4me3 mark. Current results support that H3K4me3 histone mark may protect the chromatin from DNA methylation changes as it has been suggested[131;328].

The possible DNA methylation changes mediated by DNMT3A activity does not explain the decreased H3K4me3 enrichment in regions containing CpG sites that decreased DNA methylation. This suggests that there may be more than one way in

which DNA methylation and chromatin modifications induced by fatty acids interact. At present, there is no direct evidence to explain the decreased DNA methylation alongside decreased H3K4me3 levels. Nevertheless, it is known that H3K4 can be acetylated (H3K4ac) instead of methylated and cumulative evidence has been shown that fatty acids may increase acetylation of histones[247]. Global acetylation of H3 and H4 have been shown an inverse relationship with DNA methylation *in vitro* using human cells[355;356]. This inverse relationship may be explained by methyl-CpG binding domain (MBD) proteins recruitment to the methylated CpG sites that in turn recruit histone deacetylases[357–359]. Acetylation and methylation of the same lysine residue are mutually exclusive marks. Therefore, it is possible that fatty acids may increase acetylation of histones which in turn decreases H3K4me3 enrichment by depleting H3K4 residues. If a probable increase in histone acetylation may be a cause or consequence of decreased DNA methylation by fatty acids is unknown.

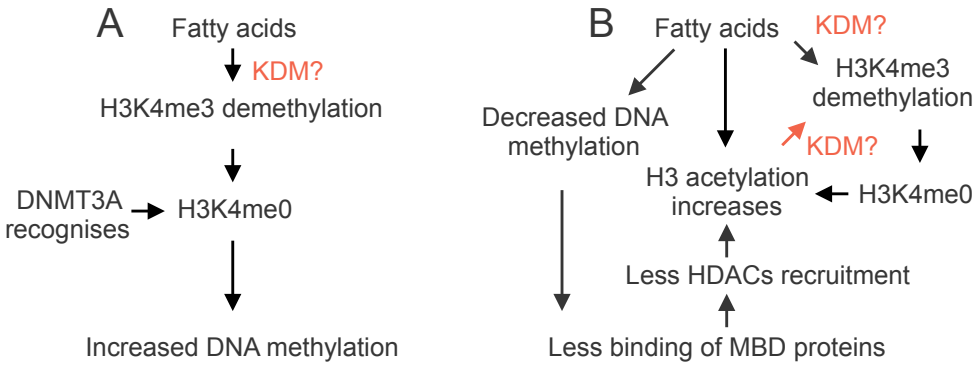

.

Figure 5.16: Possible mechanisms to explain the altered DNA methylation and reduced H3K4me3 enrichment by OA or DHA in Jurkat cells may be related to (A) recognition of H3K4me0, but not H3K4me3 by DNMT3A[131;248;325] or (B) increased levels of acetylation of histone 3 (H3) induce by fatty acids[247] which may decrease H3K4me3 indirectly by depleting free unmodified H3K4 residues. The diagram shows the current evidence (in black) couple with possible mechanisms involved (in red). KDM, Lysine Demethylase; DNMT3A, DNA Methyltransferase 3 Alpha; HDACs, histone deacetylases; MBD, methyl-CpG binding domain.

In the present work, OA or DHA treatment decreased, not abolish, H3K4me3 enrichment in the candidate regions that were analysed. If the degree of altered DNA methylation and H3K4me3 enrichment such regions were enough to induce an effect on genes that are close remains unknown.

5.4.4 Limitations of the experiments

Luciferase experiments showed little difference on the relative firefly/*Renilla* luminescence between the negative control compared with control treatment (vector ethanol). This made luciferase assays not suitable to test the effectiveness of the PPARα antagonist GW6471 in our experiments. The antagonistic effect of GW6471 has been shown to be mediated by the increase binding of PPARα with nuclear receptor corepressor (NCOR) 1 and NCOR2[252]. The PPARα antagonist GW6471 was used and stored accordingly to manufacturer's instructions.

Motif analysis was carried out using the sequences of the Infinium MethylationEPIC BeadChip. The sequences analysed by this BeadArray are not random sequences in the genome. There is a possibility that there are other DNA motifs that may influence the DNA methylation induced by fatty acids which were not predicted in the current work. The predicted binding of transcription factors should be interpreted as a possibility, and further work is needed to validate this experimentally as any other *in silico* analysis.

5.5 Conclusions

The effect on DNA methylation induced by DHA in Jurkat cells may be independent of PPARα activity. However, the effect on DNA methylation induced by both, OA or DHA treatment, showed a relationship with decreased H3K4me3 mark and enrichment of DNA motifs. Results suggest that decreased enrichment of H3K4me3 may be associated with DNMT3A activity and possibly with histone acetylation that may occur in the same lysine residue. DNA motifs identified were GC-rich and similar to response elements of transcription factors that were mostly members of the Sp/KLF family. The data suggest that the activity of some transcription factors may be involved in the epigenetic effect of fatty acids. One approach to asses the activity of transcription factors on a genome-wide scale is analysing changes in the transcriptome. Thus, to further explore the epigenetic effect of OA or DHA treatment, the expression of the transcriptome was assessed and will be discussed in the next Chapter.

Chapter 6

The Effect of OA or DHA Treatment on the Transcriptome and its Relation with the DNA Methylome.

6.1 Introduction

In the previous Chapter,analyses indicated that sequences proximal to CpG sites that changed DNA methylation by OA or DHA treatment were enriched with some DNA motifs. Such motifs were similar to the core binding site of some transcription factors which were, in the majority, members of the Sp/KLF family. Thus, this evidence suggested that activity of transcription factors may be related to the epigenetic effect of fatty acids. This hypothesis is supported by *in vitro* evidence which has shown that some transcription factors identified here by DNA motifs analysis, such as SP1, can physically interact with DNMTs[360]. SP1 has been shown to bind the promoter region and downregulate MYC associated zinc finger protein (MAZ) gene expression in a DNA methylation-dependent manner using human cell lines[360]. Therefore, evidence suggests that activity of transcription factors may direct DNA methyltransferases to the their response elements. Which transcription factors were altered in Jurkat cells by OA or DHA treatment? This is unknown.

Currently, it is well known that fatty acids can modulate the expression of the transcriptome. Transcriptome changes may be used to assess the altered activity of transcription factors genome-wide *in silico*. Furthermore, little is known about the relationship between the transcriptome and DNA methylome changes induced by fatty acids. The genome-wide studies addressing this relationship have included DNA me-

thylation data with confounding factors[242] or have not reached statistically significance results[229;287]. Therefore, there is still uncertainty in the possible relationship between the transcriptome and DNA methylome changes induced by fatty acids.

This Chapter aimed to assess the transcriptome changes induced by fatty acids using BeadArrays. Altered transcripts allowed to address the genome-wide relationship between altered DNA methylation and altered gene expression by OA or DHA treatment. To further explore this relationship, similarities in the biological function of genes with altered DNA methylation and altered expression by fatty acids was sought by comparisons of pathways analyses. Finally, transcriptome changes by fatty acid treatments were analysed to predict transcription regulators of such changes. The differentially expressed transcripts by BeadArray analysis were validated by qPCR in candidate genes.

6.2 Materials and methods

Cell cultures and treatments of Jurkat cells were carried out as described in section 2.2.1. Extraction of RNA was carried out as described in section 2.3.1. Quantity and quality of RNA was assessed by NanoDrop and agarose gel electrophoresis as indicated in sections 2.3.3 and 2.3.4, respectively. BeadArray analysis of gene expression was carried out as describe below (section 6.2.1). Validation of BeadArray results was performed by RT-qPCR as detailed in section 6.2.2.

6.2.1 BeadArray analysis of gene expression

Analysis of gene expression was determined using the Illumina HumanHT-12 v4 Expression BeadChip covering more than 47,000 transcripts per sample. An overview of the analysis that was carried out is shown in Figure 6.1.

6.2.1.1 Samples and sample quality assessment

RNA samples from different culture replicates treated with control, OA or DHA for 8 days were selected (n = 9 per treatment) and pooled using the same amount of RNA (n = 3 pooled samples per treatment). Pooled samples were then diluted to 50 ($\pm$5) ng/μl concentration. The integrity of samples was assessed by capillary electrophoresis by Dr Bastiaan Moesker at Southampton General Hospital, United Kingdom, using an Agilent 2100 Bioanalyzer (Agilent Technologies). The capillary electrophoresis generated an electropherogram for each sample (Figure 6.2) that was used to asses samples quality. This was given by the automated calculation of a RNA integrity number (RIN) score ranging from 0 to 10, being 10 the least degraded[361]. The RIN score was

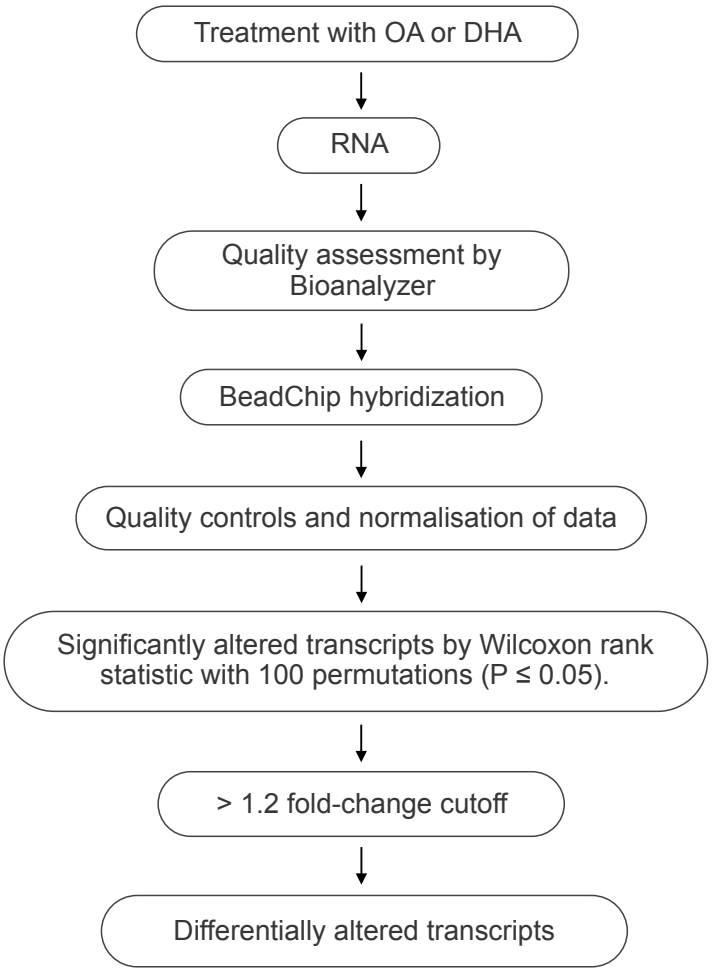

Figure 6.1: Illumina HumanHT-12 v4 Expression BeadChip; overview of analysis workflow.

calculated using the 28S/18S rRNA ratio, the absence of transcripts between the 18S and 5S rRNA and other parameters not publicly available. This procedure allowed a standardised and automated evaluation of the integrity of RNA in samples.

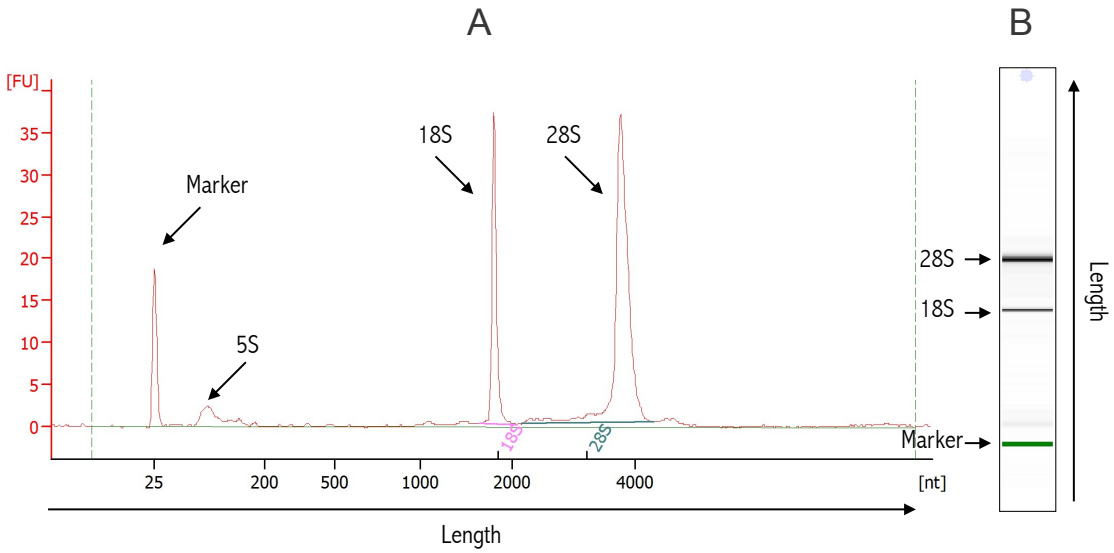

Figure 6.2: A typical electropherogram run of RNA (A) shows the length in nucleotides (nt) in ascending order in the x-axis and fluorescence (FU) in the y-axis. The area of the peaks are proportional to the quantity of RNA of a specific size. (B) Representation of how the electropherogram would look like on an agarose gel.

6.2.1.2 Expression BeadChip hybridisation

After quality assessment of RNA, samples were sent for BeadArray analysis to the Genome Centre at the Barts and The London School of Medicine and Dentistry, London, United Kingdom. In accordance with the company's quality control procedures RNA samples were processed for hybridisation using Illumina® TotalPrep™ RNA Amplification Kit. This included all reagents to perform reverse transcription of the mRNA fraction, second-strand synthesis and *in vitro* transcription using biotinylated uridine triphosphates following the manufacturer's instructions. The complementary RNA (cRNA) synthesised after *in vitro* transcription was hybridised to beads on BeadChip containing the complementary transcript-specific sequences. Serial washes at high temperature, room temperature, using ethanol and a second wash at room temperature were carried out to remove unspecific hybridization. Cy3-conjugated streptavidin was then added to samples and bound to biotin-labelled cRNA. The fluorescence of Cy3 in each bead of the Expression BeadChip was then measured. Such fluorescence was proportional to transcript levels. All samples were analysed using a single BeadChip to avoid batch effects.

6.2.1.3 Quality controls and normalisation

Quality controls and normalisation were carried out by the Genome Centre at the Barts and The London School of Medicine and Dentistry. At the sample level, the background, high hybridisation and all genes intensity quality controls were performed. At the probe level, the number of detected genes either at 0.05 or 0.01 significance were evaluated. The raw expression values were normalised using quantile normalisation. This method was implemented to make gene expression distributions of each sample the same length and was used because it has shown to reduce the non-biological origin variation[362].

6.2.1.4 Statistical analysis of BeadArray data

Expression values provided by the Genome Centre were analysed in-house to identify differentially expressed transcripts and the expression fold change difference. Analyses were carried out with the R package SAM 5.0 (Significance Analysis of Microarrays)[363] using RStudio Version 0.99.491 (2009-2015 RStudio, Inc. for Mac). The normalised expression values of transcripts were tested using two class unpaired Wilcoxon rank statistic permuting 100 times to obtain differentially expressed transcripts. Because of the small number of samples tested in each group (n = 3), the false discovery rate (FDR) was not considered as a cutoff. This is because the FDR by its nature is linked to the P-value resulted of a statistical test[364], which can not reach high enough significant values using an n = 3 to implement FDR. Instead of the FDR, a fold change cutoff > 1.2 was used to increase confidence in the results. A non-parametric test was selected for analysis as this has been shown to perform better for obtaining differentially expressed genes[365]. This is because the frequent presence of outliers in gene expression experiments can alter the mean and diminished the sensitivity of parametric tests[365]. In addition, gene expression has been shown to be not normally distributed[261]. Thus, the assumption of normality of parametric tests would not be fulfilled.

6.2.1.5 Validation of results

Significantly altered genes identified by Illumina HumanHT-12 v4 Expression BeadChip were validated by reverse transcription (RT) followed by quantitative polymerase chain reaction (qPCR) as described below 6.2.2.

6.2.2 RT-qPCR

6.2.2.1 Reverse transcription

The RNA was extracted, quantify and quality assessed as described in section 2.3.1, 2.3.3 and 2.3.4, respectively. In a 10 μl final volume reaction, 1 μg of each RNA sample was treated with 1 unit of DNase I for 15 minutes at room temperature using 1x reaction buffer (200 mM Tris-HCl pH 8.3, 20 mM $MgCl_2$) to avoid any possible DNA contamination. The reaction was then stopped by addition of 1 μl stop solution (EDTA 50 mM) and denaturation of DNase I at 70 °C for 10 minutes using a thermal cycler (Veriti 96, Applied Biosystems). The use of EDTA avoided RNA hydrolysis catalysed by metal ions (Mg) present in the reaction buffer[366]. After enzyme inactivation, 1 μl of 9-base oligodeoxynucleotides with random sequences (random nonamers) were added to samples and incubated at 70 °C for 10 minutes to prime the mRNAs using a thermal cycler (Veriti 96, Applied Biosystems). Samples were chilled on ice straight after incubation to avoid secondary structure formation of mRNAs. Samples were then reverse transcribed using Moloney-murine leukaemia virus (M-MLV) reverse transcriptase kit which provided all reagents. Following the manufacturers' instructions, the RT was then carried out in a 25 μl final volume reaction using 200 units of M-MLV, 1x reaction buffer (50 mM Tris-HCl pH 8.3 at 25 °C, 75 mM KCl, 3 mM $MgCl_2$ and 10 mM DTT), adenine, cytosine, guanine and thymidine triphosphates at 0.5 mM/each and the DNA- and RNA-free water to adjust volume. The retrotranscription of samples was achieved after serial incubations at 21 °C for 10 minutes, 37 °C for 50 minutes and 90 °C for 10 minutes. cDNA was chilled on ice and diluted with DNA- and RNA-free water to a concentration of 5 ng/μl (1 μg/200 μl).

6.2.2.2 Selection of reference genes

Selection of appropriate reference genes for Jurkat cells treated with vector ethanol, OA or DHA was achieved using the geNorm[367]. 6 candidate reference genes were analysed in 9 samples including control (vector ethanol), OA and DHA treatments. Manufacturer's instructions were followed with modifications in reaction volume, dye, and DNA polymerase used as described (section 2.4.2). Primers used in geNorm were provided by the kit with no available information about locations of the PCR amplicons. After qPCR was performed (section 2.4), the Ct values were analysed in qbasePLUS (Biogazelle) version 3.0 to evaluate the gene expression variations across treatments. Genes tested were commonly used reference genes in lymphocytes[368;369].

6.2.2.3 Quantitative PCR

qPCR, primers used and data analysis was carried out as indicated in section 2.4.

6.3 Results

6.3.1 Quality control of samples and BeadArray processing

RNA samples from 9 biological replicates per treatment (control, OA or DHA) were pooled into different mixes which included 3 replicates per mix. Pooled RNA samples (n = 3 per treatment) showed a RIN score above 9.4 in all instances (Figure 6.3).

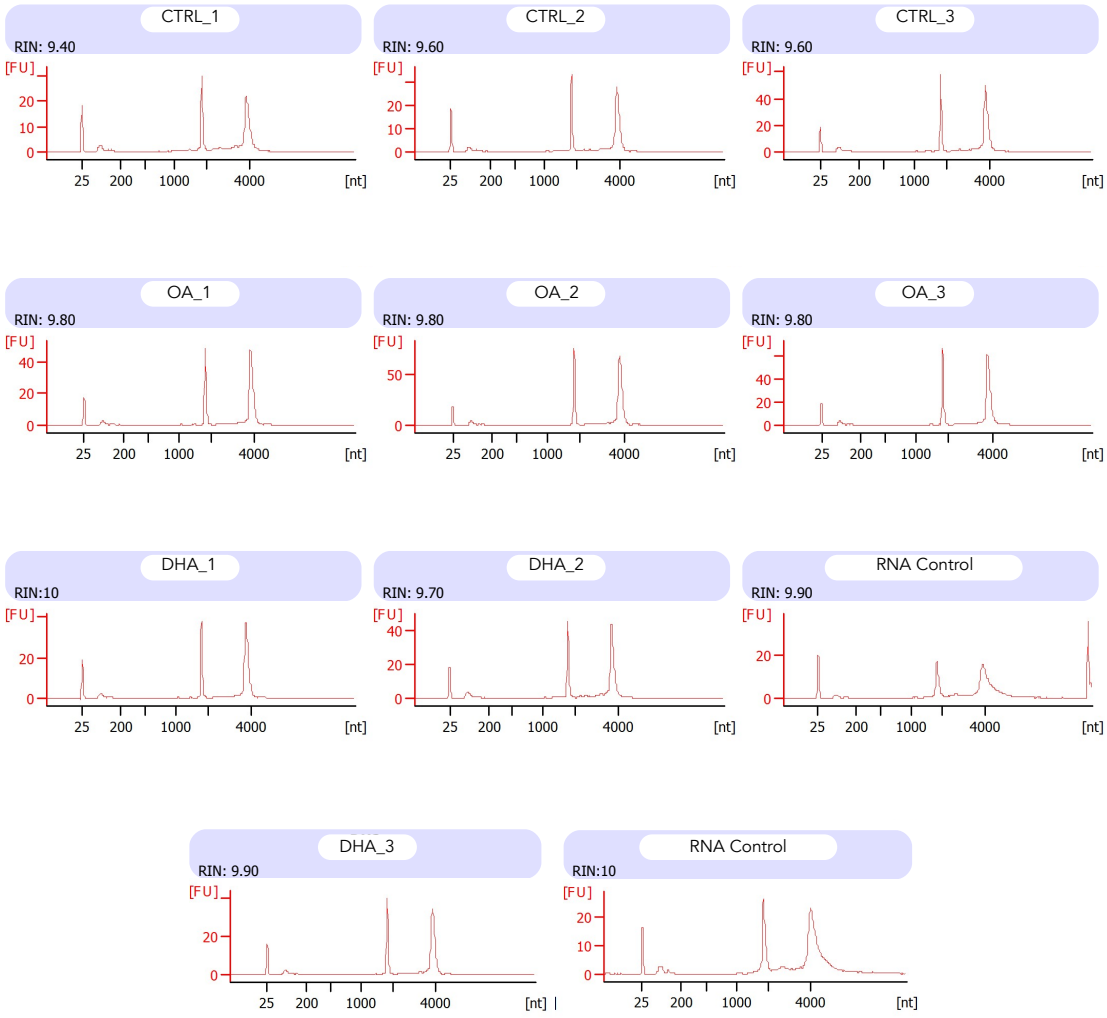

Figure 6.3: RIN score of pooled-samples used for gene expression BeadArray. Samples were named after treatments with suffix _1, _2, _3, that corresponded to a specific pool. Except for DHA_3, pooled samples were run in the same chip. The length in nucleotides (nt) is shown in the x-axis whereas fluorescence (FU) in the y-axis.

RNA samples were sent off for transcriptome analysis and the normalised intensity values returned. The background, high hybridisation and intensity of all genes quality controls showed consistent hybridization signals across all samples which is expected in array experiments[370] (Figure 6.4). The number of genes detected in all samples

with a detection p-value < 0.05 or < 0.01 were also similar in all treatments.

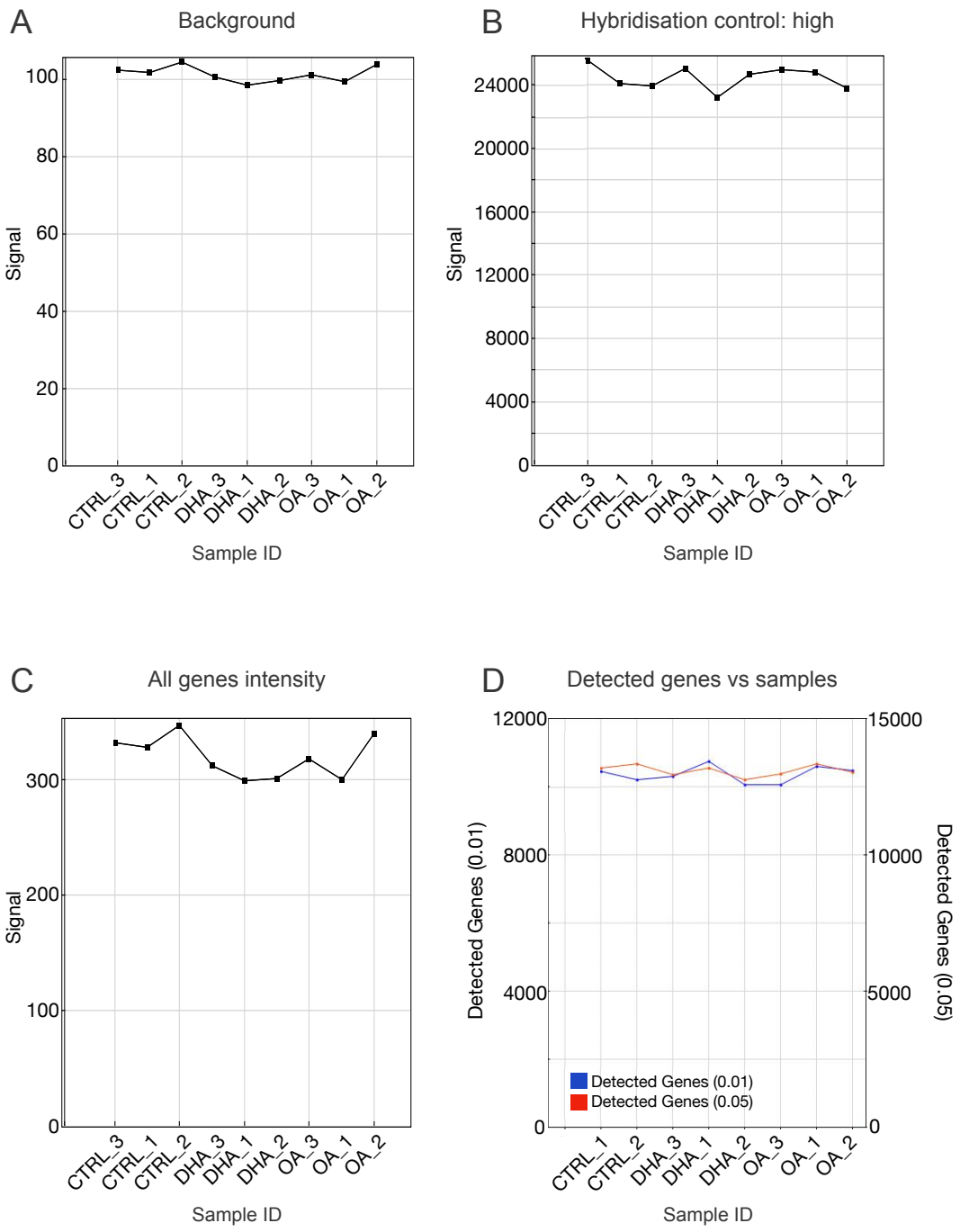

Figure 6.4: Gene expression BeadArray; quality report. Samples were named after treatments with suffix _1, _2, _3, that corresponded to a specific pooled sample. At the sample level, background, high hybridisation controls and all genes intensity showed to be similar in samples. At the probe level, the total number of genes detected within samples showed also to be similar. Analysis was performed by the Genome Centre at the Barts and The London School of Medicine and Dentistry (London, UK).

The raw signal distributions of expression values in samples were similar in the unnormalised data. An improvement in the distribution of expression values was observed after data was normalised using quantile normalisation (Figure 6.5). All quality controls and normalisation of the data was carried out by the Genome Centre at the Barts and The London School of Medicine and Dentistry (London, UK).

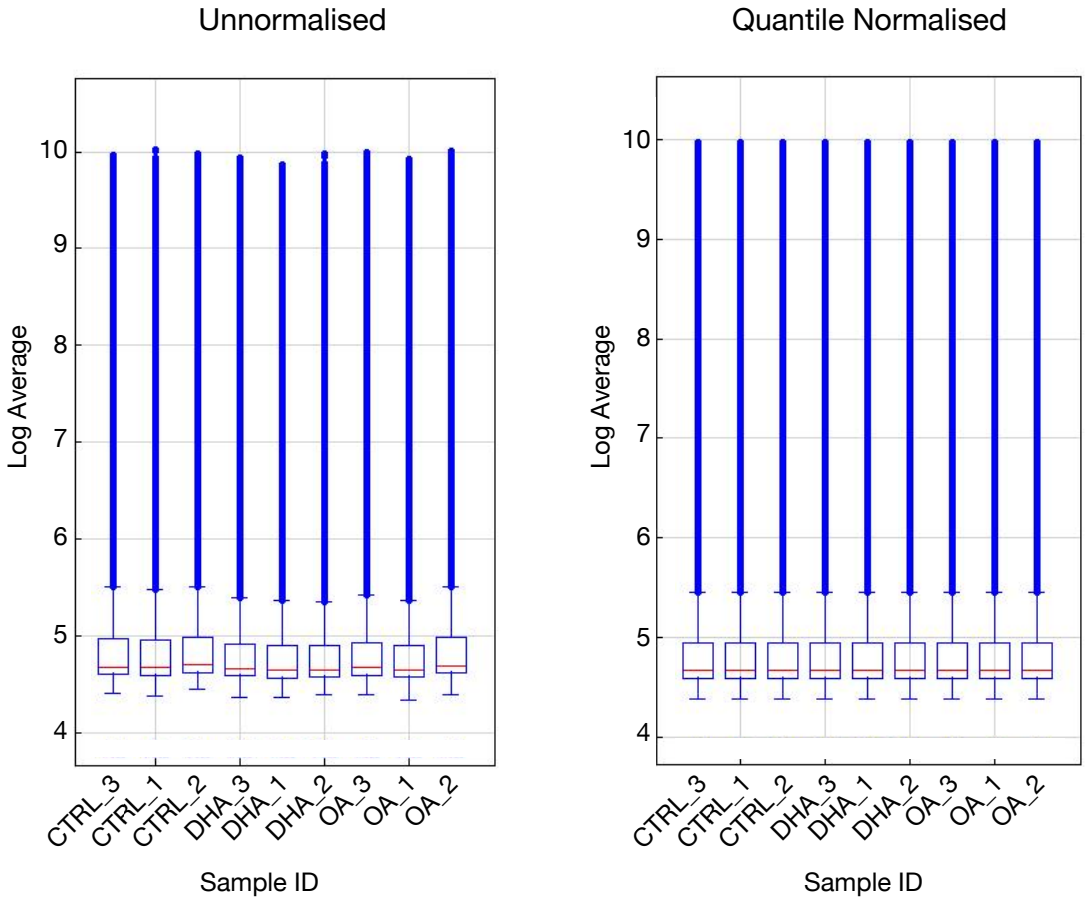

Figure 6.5: Gene expression BeadArray; normalisation of data. Samples were named after treatments with suffix _1, _2, _3, that corresponded to a specific pool. Figure shows the median values of the natural-logarithm averaged signal intensity before (left) and after (right) quantile normalisation. Normalisation was performed by the Genome Centre at the Barts and The London School of Medicine and Dentistry (London, UK).

6.3.2 Do OA or DHA treatment induce the same effect on the transcriptome?

Treatment with OA significantly altered the mRNA expression levels of 97 transcripts. The 51% (50/97) of the altered transcripts showed increased gene expression (Figure 6.6).

Treatment with DHA significantly altered the gene expression of five times more transcripts (502) compared with OA (97). Of these, 49% (248/502) showed increased expression levels (Figure 6.6).

The expression of 36 transcripts showed to be altered by both treatments. Such transcripts represented 37% (36/97) of total changes induced by OA or 7% (36/502) by DHA treatment. All 36 transcripts showed altered gene expression with the same direction of change, either increase or decrease, by OA or DHA. The 39% (14/36) of the altered transcripts by both treatments showed increased expression while the expression of the remaining 61% (22/36) was decreased (Figure 6.6).

The name and magnitude of change in expression (fold change) of all differentially altered transcripts by OA or DHA is shown in Appendix B.

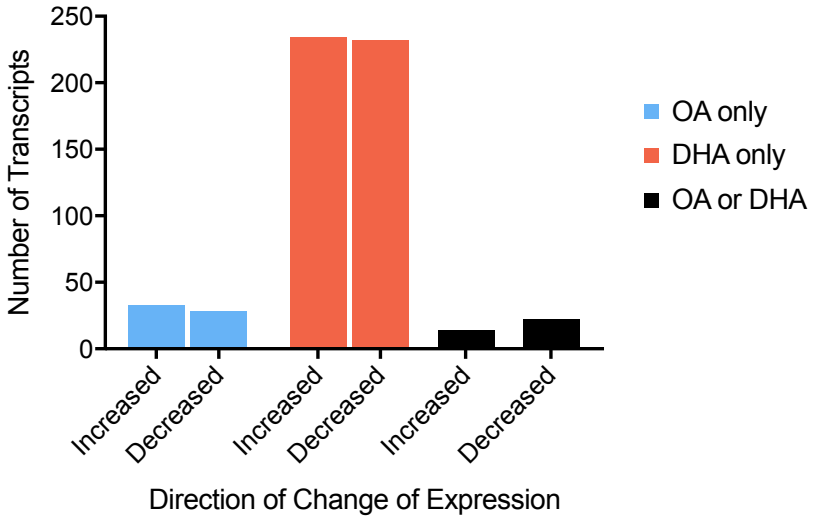

Figure 6.6: Number and direction of change of transcripts with altered gene expression after treatment with OA or DHA for 8 days. OA or DHA alone increased the expression of 33 or 234 loci whereas decreased the expression of 28 or 232 transcripts, respectively. Both treatments increased the expression of 14 transcripts and decreased the expression of 22 transcripts.

The total number of mRNA transcripts with altered expression by OA or DHA were analysed using IPA® to determine the possible biological functions altered in cells. From the total number of altered transcripts by OA or DHA only 82 and 445 genes, respectively, were mapped by the software and used for pathways analysis.

The genes with altered expression induced by OA were significantly enriched (-log(P-value) > 1.3) in "Sulfate Activation for Sulfonation", "Interferon Signalling" and "Rac Signalling" canonical pathways among others (Figure 6.7). The analysis of the same genes using as reference molecular associations of clinical pathology endpoints (ToxList) showed that "Glutation Depletion - CYP Induction and Reactive Metabolites" was the only category significantly enriched specifically by OA treatment (Figure 6.7). Ultimately, the list of genes with altered expression by OA treatment was also analysed to identify possible downstream effects according to the biological functions of the altered genes. Analysis showed that "Concentration of Phosphatidylcholine", "Quantity of Carbohydrate" and "Viral Infection" were the top three downstream effects significantly decreased, among others, by OA treatment (Figure 6.7).

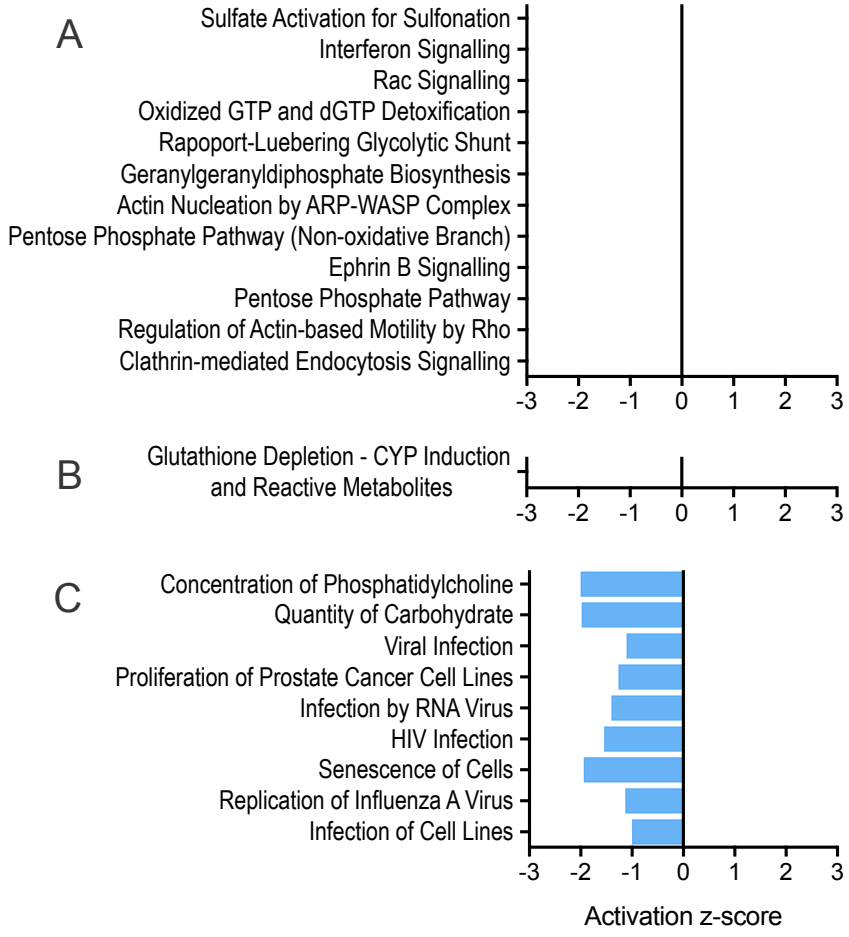

Figure 6.7: Canonical pathways (A), ToxList categories (B) and downstream effects (C) related exclusively to the altered gene expression by OA. All pathways/categories shown have a -log(P-value) > 1.3 by descending order from top to bottom calculated by a Fisher's exact test. The activation z-score indicates a predicted pathway activation (> 1) or inhibition (< -1) accordingly to the altered expression of genes in each pathway/category.

The genes with altered expression induced by DHA were significantly enriched in "Cell Cycle: G2/M DNA Damage Checkpoint Regulation", "Hypoxia Signalling in the Cardiovascular System" and "AMPK Signalling" canonical pathways among others (Figure 6.8). The analysis of the same genes using ToxList showed that "Cell Cycle: G2/M DNA Damage Checkpoint Regulation", "Fatty Acid Metabolism" and "Cardiac Necrosis / Cell Death" were the top three categories enriched specifically by DHA altered genes (Figure 6.8). Ultimately, downstream effects analysis showed that "Cell Proliferation of Tumour Cell Lines", "Cell Death" and "Apoptosis" were the top three downstream effects significantly altered (Figure 6.9).

The genes with altered mRNA expression induced by both, OA or DHA treatment, were significantly enriched mainly in "Superpathway of Cholesterol Biosynthesis" and other canonical pathways related to fatty acid synthesis (Figure 6.8). For both treatments, such lipid-related pathways were the most significantly altered canonical pathways of all. ToxList analysis showed that ""Cholesterol Biosynthesis", ""LXR/RXR Activation" and "Aryl Hydrocarbon Receptor Signalling" were the categories enriched by both treatments. The only downstream effect predicted on cells by both treatments was the decreased in the "Concentration of Lipid" (Figure 6.8).

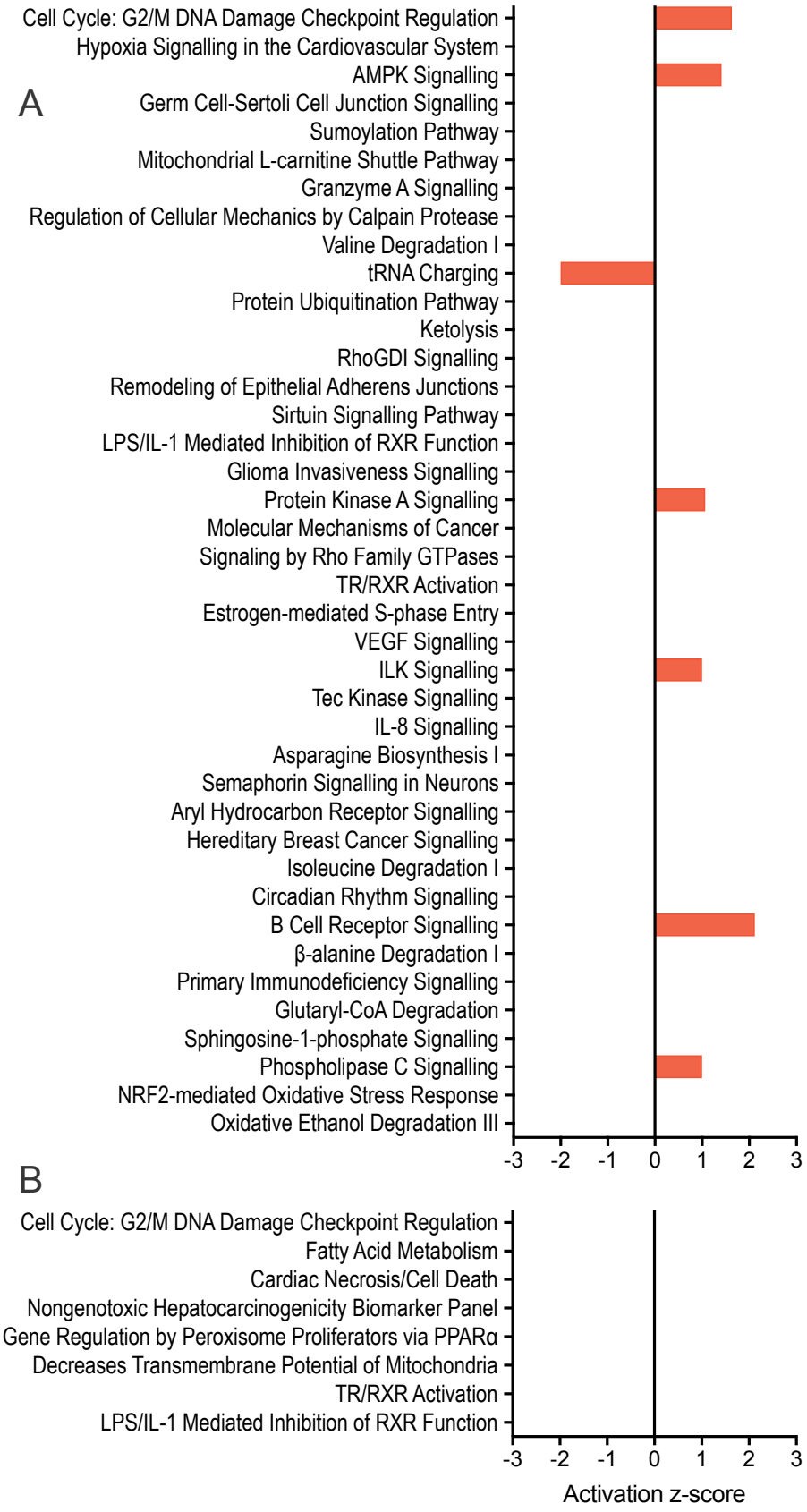

Figure 6.8: Canonical pathways (A) and ToxList categories (B) related exclusively to the altered gene expression by DHA treatment. All pathways/categories shown have a -log(P-value) > 1.3 by descending order from top to bottom calculated by a Fisher's exact test. The activation z-score indicates a predicted pathway activation (> 1) or inhibition (< -1) accordingly to the altered expression of genes in each pathway/category.

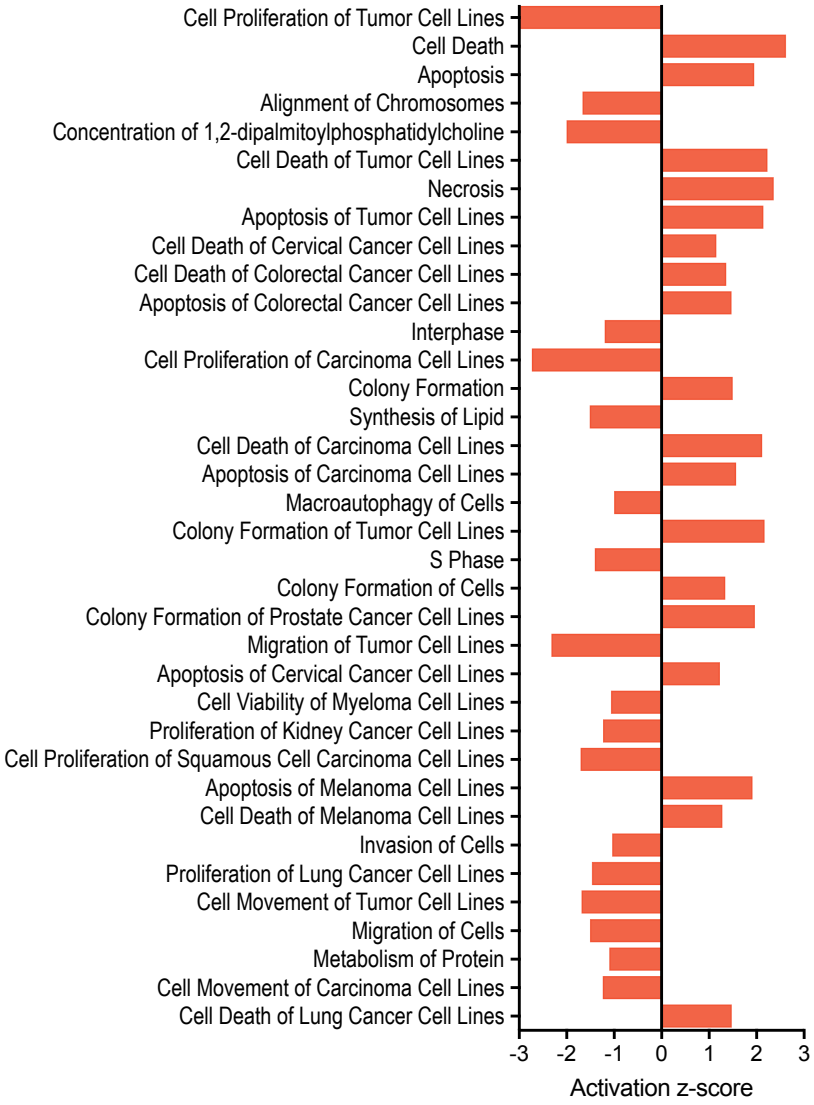

Figure 6.9: Downstream effects related exclusively to the altered gene expression by DHA treatment. All pathways shown have a -log(P-value) > 1.3 by descending order from top to bottom calculated by a Fisher's exact test. The activation z-score indicates a predicted pathway activation (> 1) or inhibition (< -1) accordingly to the altered expression of genes in each pathway/category.

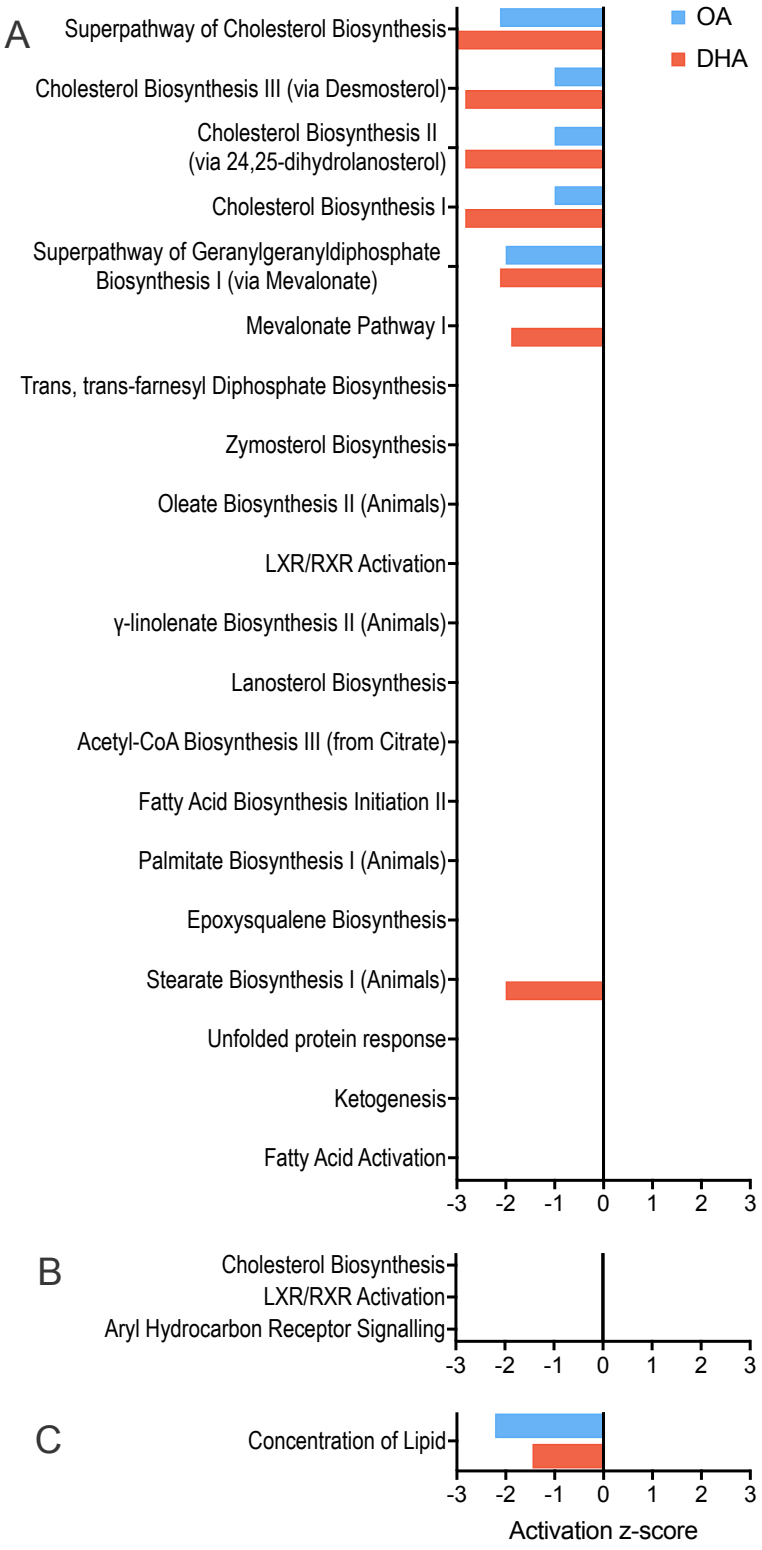

Figure 6.10: Canonical pathways (A), ToxList categories (B) and downstream effects (C) related to the altered gene expression by both, OA or DHA treatment. All pathways shown have a -log(P-value) $>$ 1.3 by descending order from top to bottom calculated by a Fisher's exact test. The activation z-score indicates a predicted pathway activation ($>$ 1) or inhibition ($<$ -1) accordingly to the altered expression of genes in each pathway/category.

6.3.3 Do OA or DHA treatment induced changes in the expression of transcription regulators?

Treatment with OA significantly altered the mRNA expression level of 5 transcription regulators. In contrast, treatment with DHA significantly altered the mRNA expression level of 41 transcription regulators, including SP3 (Table 6.1).

Both treatments significantly altered the mRNA expression level of only two transcription regulators. These were amino-terminal enhancer of split (*AES*), which showed upregulation, while SUB1 homolog, transcription regulator (*SUB1*) showed downregulation by both OA or DHA treatment (Table 6.1). The classification of an specific gene into a transcription regulator category was according with IPA® database.

Table 6.1: Transcription regulators that showed altered expression by OA or DHA treatment.

Gene Name	Gene Symbol	Exp[a]	By
Actinin alpha 1	ACTN1	1.2	DHA
Amino-terminal enhancer of split	AES	1.3[b]	OA/DHA
AF4/FMR2 family member 3	AFF3	1.21	DHA
Ankyrin repeat and SOCS box containing 8	ASB8	1.2	DHA
Activating transcription factor 5	ATF5	1.3	DHA
Basic leucine zipper ATF-like transcription factor 3	BATF3	1.25	DHA
Bromodomain containing 7	BRD7	-1.22	DHA
Basic transcription factor 3	BTF3	1.21	OA
Cullin associated and neddylation dissociated 1	CAND1	-1.23	DHA
CCAAT/enhancer binding protein epsilon	CEBPE	1.5	DHA
Cytosolic iron-sulfur assembly component 1	CIAO1	1.23	DHA
Cytoskeleton associated protein 5	CKAP5	-1.21	DHA
cAMP responsive element binding protein 3 like 3	CREB3L3	1.24	DHA
CREB binding protein	CREBBP	1.29	DHA
Deltex E3 ubiquitin ligase 1	DTX1	-1.34	DHA
E2F transcription factor 5	E2F5	-1.31	DHA
Eomesodermin	EOMES	-1.24	DHA
ETS proto-oncogene 1, transcription factor	ETS1	-1.25	DHA
Fem-1 homolog C	FEM1C	-1.25	DHA
Far upstream element binding protein 3	FUBP3	-1.2	DHA
General transcription factor IIE subunit 1	GTF2E1	-1.27	DHA
General transcription factor IIIC subunit 3	GTF3C3	-1.22	DHA

Helicase like transcription factor	HLTF	-1.21	DHA
High mobility group box 2	HMGB2	-1.22	OA
Heterogeneous nuclear ribonucleoprotein K	HNRNPK	1.21	OA
Inhibitor of DNA binding 1, HLH protein	ID1	-1.64	DHA
Inhibitor of DNA binding 3, HLH protein	ID3	-1.45	DHA
Interferon gamma inducible protein 16	IFI16	-1.23	DHA
Interferon regulatory factor 7	IRF7	1.3	DHA
LRR binding FLII interacting protein 1	LRRFIP1	1.44	DHA
Mediator complex subunit 7	MED7	-1.2	DHA
N(alpha)-acetyltransferase 15, NatA auxiliary subunit	NAA15	-1.22	DHA
Nuclear receptor corepressor 2	NCOR2	1.21	DHA
Nuclear factor, erythroid 2 like 2	NFE2L2	-1.21	DHA
NK3 homeobox 1	NKX3-1	1.73	DHA
Period circadian regulator 2	PER2	1.46	DHA
Proteasome 26S subunit, non-ATPase 10	PSMD10	-1.23	DHA
RB transcriptional corepressor 1	RB1	-1.28	DHA
Small nuclear RNA activating complex polypeptide 4	SNAPC4	1.2	DHA
Sp3 transcription factor	SP3	-1.22	DHA
SUB1 homolog, transcriptional regulator	SUB1	-1.3[c]	OA/DHA
TATA-box binding protein associated factor 9	TAF9	1.2	OA
TOX high mobility group box family member 2	TOX2	1.74	DHA
Teashirt zinc finger homeobox 3	TSHZ3	1.31	DHA
X-box binding protein 1	XBP1	-1.21	OA
Zinc finger protein 593	ZNF593	1.27	DHA
Zinc finger protein 91	ZNF91	1.25	DHA
Zinc ribbon domain containing 1	ZNRD1	1.21	DHA

[a] = expression fold change; [b] = 1.31 by OA or 1.33 by DHA; [c] = -1.32 by OA or -1.24 by DHA.

6.3.4 Do OA or DHA treatment induced changes in the activity of transcription regulators?

IPA® software allowed to predict the possible activity of transcription regulators (TR) using enrichment of altered genes which are known to be regulated by a specific TR and the activation z-score. This analysis was carried out in the transcriptome data, but not on DNA methylation data, as the fold change in expression is needed to predict the activity of the putative TRs.

The expression changes induced by OA treatment showed an enrichment on genes regulated by Synoviolin 1 (SYVN1). The activity of SYVN1 was predicted to be decreased (Figure 6.11).

The expression changes induced by DHA treatment showed an enrichment on genes regulated by 42 different TRs. The three most significant were "Tumour protein P53 (TP53)", "RAB, member RAS oncogene family-like 6 (RABL6)", and "lysine demethylase 5B (KDM5B)". The activity of TP53 and KDM5B was predicted to be increased while the activity of RABL6 decreased (Figure 6.11).

Three TRs were predicted to be altered by the expression changes induced by both, OA and DHA treatment. The activity of "Natriuretic peptide B (NPPB)" and "meningioma expressed antigen 5 (hyaluronidase) (MGEA5)" were predicted to be increased while the activity of "mitogen-activated protein kinase 9 (MAPK9)" was decreased (Figure 6.11).

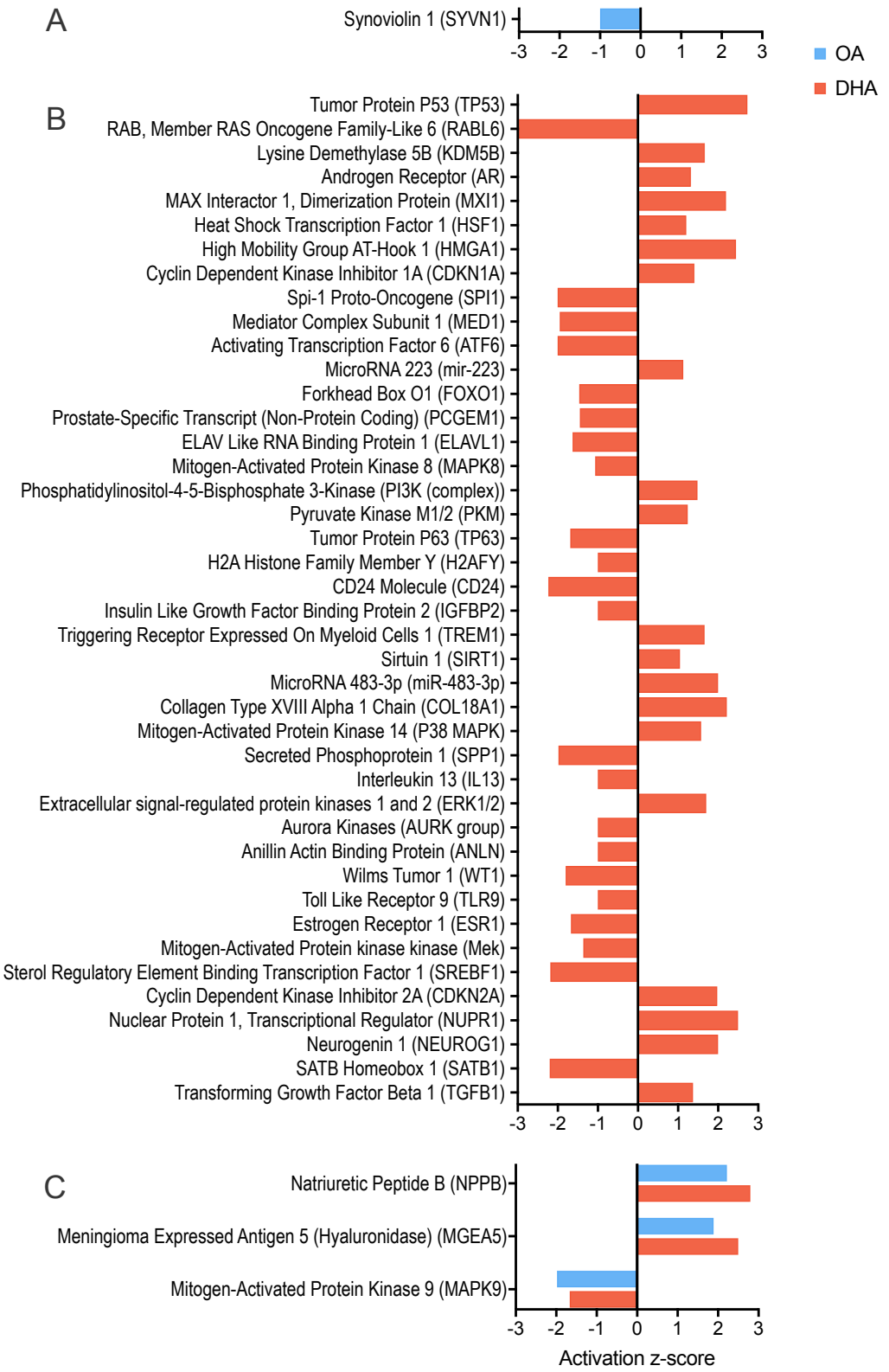

Figure 6.11: Possible transcription regulators of expression changes induced by OA, DHA or both treatment. The transcription regulators shown have a -log(P-value) > 1.3 by descending order from top to bottom calculated by a Fisher's exact test. The activation z-score indicates a predicted pathway activation (> 1) or inhibition (< -1) accordingly to the increased or decreased expression of the genes.

6.3.5 Do genes with altered expression change also DNA methylation?

Treatment with OA altered both, the expression and DNA methylation of only one gene while treatment with DHA altered the expression and DNA methylation of 10 genes (Table 6.2).

Table 6.2: Genes that showed altered expression and altered DNA methylation by OA or DHA treatment.

Gene Name	Gene Symbol	Accession Number	Exp[a]	Met[b]	Locus[c]	By
Acetyl-CoA carboxylase alpha	*ACACA*	NM_198836	-1.39	-5.22	Body	DHA
Argininosuccinate synthase 1	*ASS1*	NM_000050	1.31	5.38	5'UTR	DHA
Chromosome 6 open reading frame 223	*C6ORF223*	NM_153246	-1.3	5.01	Body	DHA
Coiled-coil domain containing 125	*CCDC125*	NM_176816	1.34	5.41	Body	DHA
Chloride intracellular channel 4	*CLIC4*	NM_013943	-1.24	-7.14	Body	DHA
EPH receptor A3	*EPHA3*	NM_005233	-1.38	5.12	TSS200	DHA
Heat shock protein family A (Hsp70) member 4	*HSPA4*	NM_002154	-1.27	-5.9	Body	DHA
Protocadherin 19	*PCDH19*	NM_020766	-1.2	-5.24	1st Exon	DHA
RAP1 GTPase activating protein	*RAP1GAP*	NM_002885	1.23	5.23	5'UTR	DHA
Septin 5	*SEPT5*	NM_002688	1.22	5.5	Body	DHA
Transmembrane protein 170B	*TMEM170B*	NM_001100829	-1.21	6.81	Body	OA

[a] = Expression fold change, [b] = Δ Methylation (%), [c] = Locus that showed a change in DNA methylation by fatty acids.

6.3.6 Do predicted pathways by transcriptome changes are also predicted by DNA methylome changes?

Treatment with OA altered mRNA expression and DNA methylation of genes that belong to "Clathrin-mediated Endocytosis Signalling" canonical pathway and the "Aryl Hydrocarbon Receptor Signalling" ToxList category. The downstream effect that showed enrichment according to genes with altered expression and altered DNA methylation by OA was only "Viral Infection" (Figure 6.12).

Treatment with DHA altered the mRNA expression and DNA methylation of genes that belong to "Protein Kinase A Signalling", "Phospholipase C Signalling" and "Signalling by Rho Family GTPases" canonical pathways. In addition, ToxList analysis showed an enrichment of genes in the "Mechanism of Gene Regulation by Peroxisome Proliferators via PPAR". The downstream effects that showed enrichment according to genes with altered expression and altered methylation by DHA were "Cell Death", "Apoptosis" and "Colony Formation of Tumour Cell Lines" (Figure 6.13).

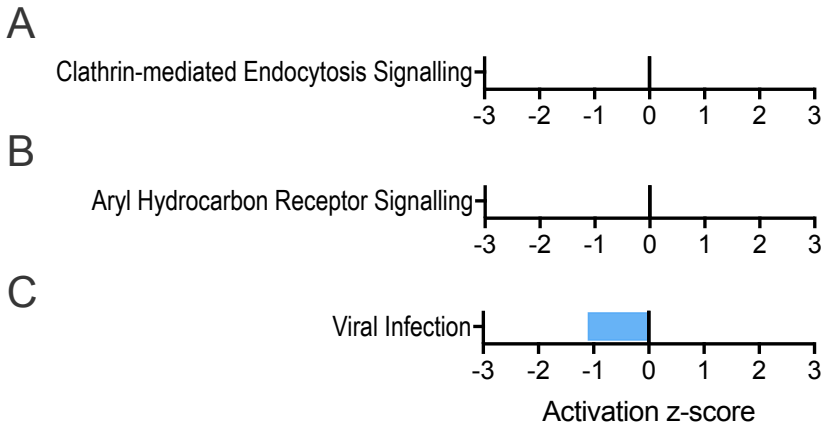

Figure 6.12: Canonical pathways (A), ToxList categories (B) and downstream effects (C) predicted by gene expression and DNA methylation changes by OA. Data shown have a -log(P-value) > 1.3. The activation z-score indicates a predicted pathway activation (> 1) or inhibition (< -1) accordingly to the increased or decreased expression of genes.

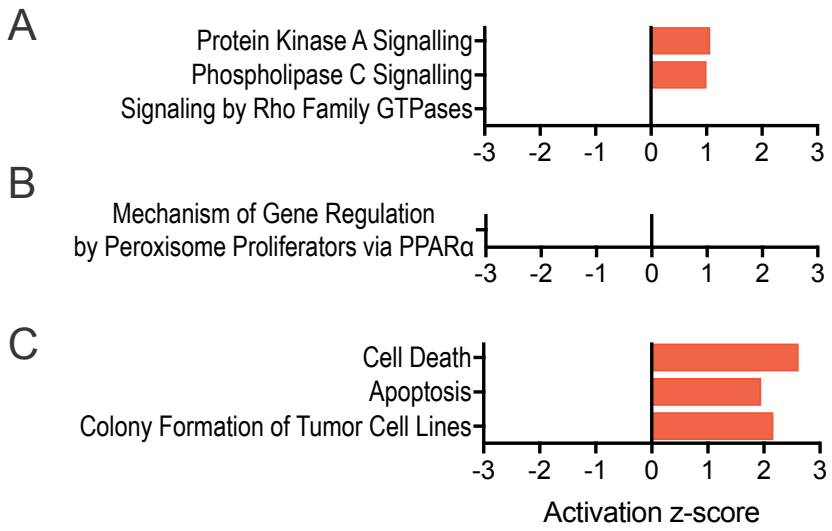

Figure 6.13: Canonical pathways (A), ToxList categories (B) and downstream effects (C) predicted by gene expression and DNA methylation changes by DHA. Data shown have a -log(P-value) > 1.3 by descending order from top to bottom calculated by a Fisher's exact test. The activation z-score indicates a predicted pathway activation (> 1) or inhibition (< -1) accordingly to the increased or decreased expression of genes.

6.3.7 BeadArray validation

The first step to validate the expression BeadArray was the selection of suitable reference genes. The genes tested were commonly used reference genes in lymphocytes[368;369] and included human actin beta (*ACTB*), beta-2-microglobulin (*B2M*), eukaryotic translation initiation factor 4A2 (*EIF4A2*), ribosomal protein L13a (*RPL13A*), ribosomal protein S18 (*RPS18*) and succinate dehydrogenase complex flavoprotein subunit A (*SDHA*).

geNorm analysis showed that all genes tested were stable (average geNorm M $\leq$ 0.5) and therefore suitable to use as reference genes[367;371] (Figure 6.14). Results recommended the use of only two reference genes, the minimum allowed, as the used of more did not represent an increase in stability (geNorm V $<$ 0.15) (Figure 6.15). Transcripts with the major stability denoted by the lower geNorm M in ascending order were *RPL13A*, *SDHA*, *B2M*, *RPS18*, *ACTB* and *EIF4A2* (Figure 6.14). However, some transcript variants of *SDHA* and *B2M* showed changes in expression according to BeadArray results. The changes in *SDHA* and *B2M* detected in the BeadArray were significant, although the fold change was lower than the 1.2 cutoff (data not shown). Because of this, the next more stable gene was used. *RPL13A* and *RPS18* were selected as the reference for all qPCR experiments for mRNA expression.

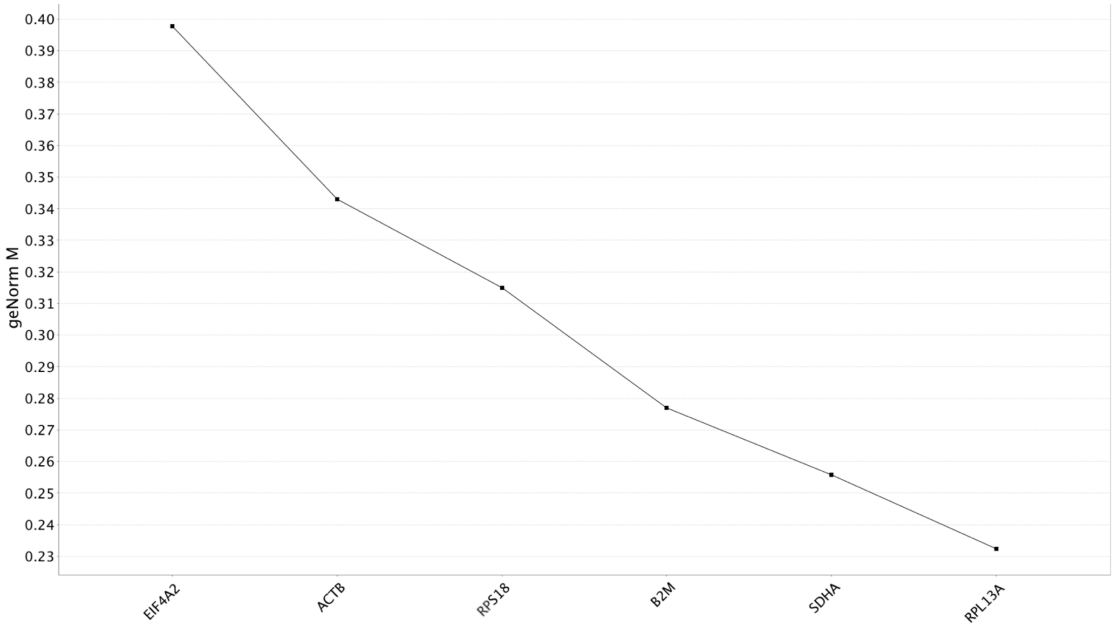

Figure 6.14: Average expression stability of reference genes tested in control, OA or DHA-treated cells (n = 3 cultures replicated per treatment). geNorm M value denoted the average pairwise variation of expression of each gene with all other genes analysed. The lower M value, the more stable the transcript was among samples.

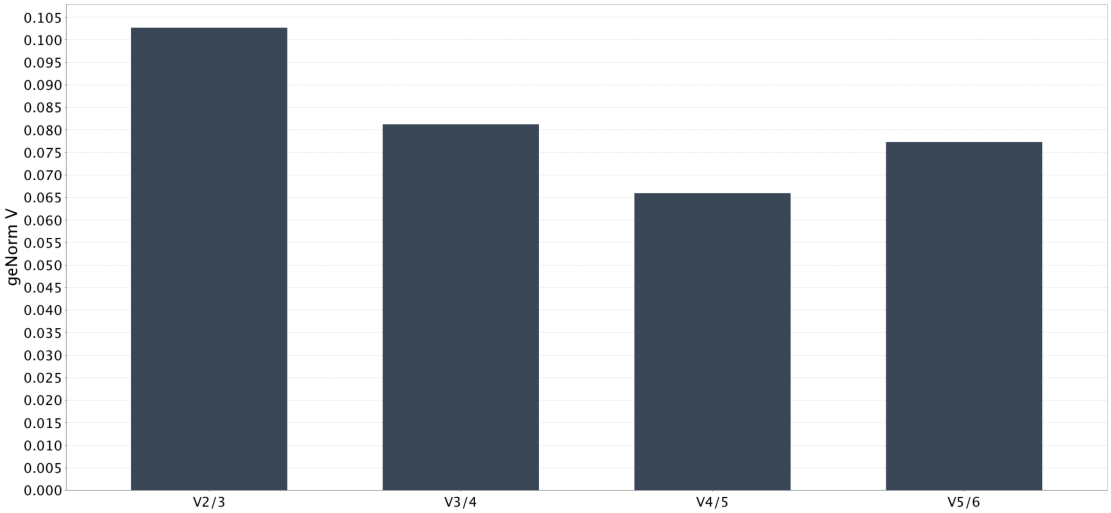

Figure 6.15: Optimal number of reference genes. Reference genes analysed were ranked from 1 to 6 according to geNorm M value. The geometric mean variation of the two more stable was compared with the mean of the three more stable (V2/3). The same was done for the third and fourth (V3/4), fourth and fifth (V4/5), fifth and sixth (V5/6) more stable genes. Two reference genes showed to be enough to obtain a geNorm V difference < 0.15.

After the selection of reference genes, bespoke primers were either bought or design. The annealing temperature of designed primers was optimised by a temperature gradient (Figure 6.16). The annealing temperature of purchased primers was already optimised by the provider (QuantiTect®, QIAGEN). The specificity of all primers was checked by a single melting curve in every qPCR amplification (Figure 6.17).

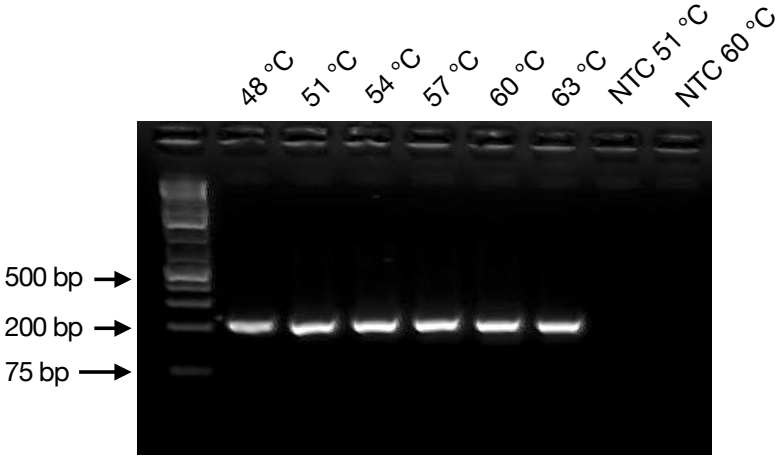

Figure 6.16: Example of primer optimisation by PCR gradient. PCR gradient amplicons of *RPS18* gene were run in an 2% (w/v) agarose/TAE gel supplemented with GelRed (7 μl/100 ml). PCR showed primers specificity as only one single amplicon was observed around the size expected (205 bp). No template controls (NTC) were performed only at 51 °C and 60 °C. The same gradient was carried out for all other primers that were designed.

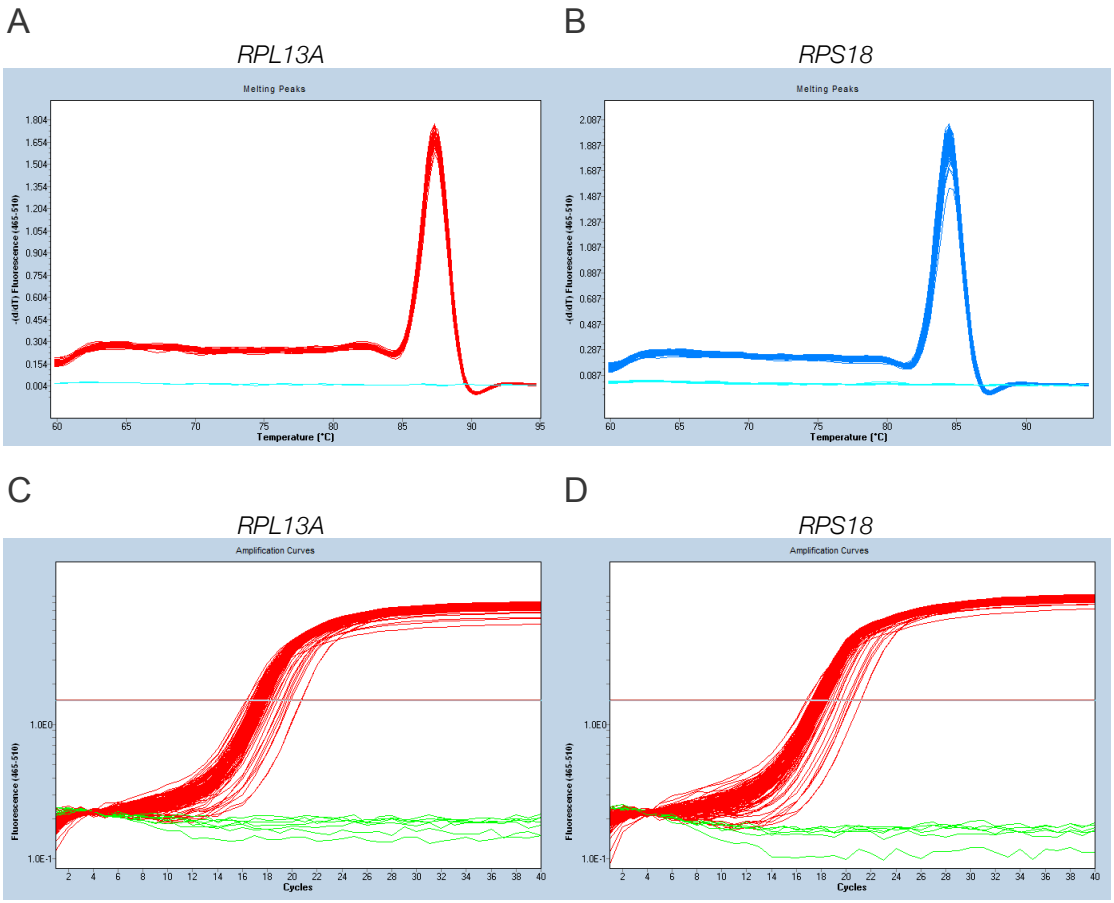

Figure 6.17: Example of melting and amplification curves of *RPL13A* (A, C) and *RPS18* (B, D). Melting curves (A, B) that showed a single peak were indicative of primer specificity. The horizontal line in amplification curves (C, D) indicated the background or noise band where the Ct values were obtained. The noise band was manually set at the same level for all genes analysed.

Once annealing temperatures were optimised and primer specificity was tested, qRT-PCR in pooled samples was performed on 5 transcripts that showed upregulation and 5 transcripts that showed downregulation by OA or DHA treatment. The selection of transcripts included the top altered genes and transcripts with different fold changes in expression. In total, 13 transcript changes were tested. The expression fold change by qPCR showed the same direction of change that the BeadArray in all 13 transcripts analysed, although only 10 reached statistical significance (Table 6.3).

Table 6.3: Candidate genes used to validate the gene expression BeadArray.

Gene Symbol	BeadArray Fold Change		qRT-PCR Fold Change	
	OA	DHA	OA	DHA
GZMA	-	2.3*	-	4.6**
CD79A	-	1.8*	-	1.8**
TOX2	-	1.7*	-	2.2**
PER2	-	1.5*	-	3.2**
IGF2R	-	1.3*	-	1.3*
HMGCS1	-1.4*	-2.1*	-1.8*	-1.8*
HMGCR	-	-1.6*	-	-1.5**
ID1	-	-1.6*	-	-1.6*
LSS	-1.4*	-1.5*	-1.2	-1.2
MSMO1	-1.3*	-1.7*	-1.2	-1.6**

Treatment versus control means (n = 3 pooled samples per treatment) were compared by one-way ANOVA with Dunnett's post hoc test on the log transformed data and those which differed significantly indicated by *, P <0.05; **, P <0.01; ***, P <0.001. Only the fold change expression of significantly altered transcripts on BeadArray analysis are shown in Table. *GZMA*, granzyme A; *CD79A*, CD79a molecule; *TOX2*, TOX high mobility group box family member 2; *PER2*, period circadian clock 2; *IGF2R*, insulin like growth factor 2 receptor; *HMGCS1*, 3-hydroxy-3-methylglutaryl-CoA synthase 1; *HMGCR*, 3-hydroxy-3-methylglutaryl-CoA reductase; *ID1*, inhibitor of DNA binding 1, HLH protein; *LSS*, lanosterol synthase; *MSMO1*, methylsterol monooxygenase 1.

6.4 Discussion

Treatment with OA or DHA altered the transcriptome of Jurkat cells in a treatment-specific manner. Genes that changed mRNA expression included different transcription factors. Besides, pathway analysis suggested that OA or DHA altered the activity some transcription regulators. The genes with altered transcription by OA or DHA treatment essentially did not show DNA methylation changes induced by the same treatments.

6.4.1 The effects of OA or DHA on Jurkat cells' transcriptome

It is well documented that fatty acids can change the expression of cells. In agreement with the literature, analysis support that OA has a lower effect on the transcriptome than other fatty acids such as DHA at the same concentration. Also, data supports that transcriptome changes by fatty acids are treatment-specific[111]. This specificity may arise by the fatty acids themselves as they have been shown to activate nuclear receptors (e.g. PPARs or RXRs) with different potencies[307;314]. Thus, fatty acids may alter the expression of particular genes by binding nuclear receptors differently, which in turn would induce different effects on cells. On the contrary, the specificity of gene expression changes may also be due to the different effects that OA or DHA have on cells. For instance, DHA, but not OA, has been shown to serve as a precursor of eicosanoids *in vitro*[100]. DHA-derived eicosanoids and even the epoxy-metabolites have shown to induce changes in gene expression of cells, although the exact mechanism is still not well understood[372;373]. Together, differences in the nuclear receptor binding and altered functions in cells may explain the treatment-specific transcriptome changes induced by OA or DHA treatment.

In this work, treatment with OA altered genes that showed a relationship with decreased infection of cells. It has been described that HIV infection[374], influenza A infection[375] and overall infection of human cells induce stress, apoptosis and cell death[376;377]. This suggests that the mid-to-low concentration of OA treatment may boost a good state of Jurkat cells at the gene expression level. This is further supported by the predicted decrease in the senescence of cells as a downstream effect of the expression changes. Besides, OA has been shown to be essential for the optimal *in vitro* growth of human primary lymphocytes stimulated with Concanavalin A[378] and to enable the growth of the Jurkat cell line[379]. The current results suggest that the reported optimal growth of Jurkat cells induced by OA treatment may be mediated, at least in part, at the gene expression level.

Treatment with DHA altered genes that were associated with three times more pathways compared with OA. This may be probably a reflection of the five times more number of altered transcripts in the DHA-treated cells. Analysis showed that the

most significantly enriched transcription regulators of transcriptome changes by DHA were TP53 and RABL6. TP53 is a tumour suppressor gene which is one of the most frequently altered genes in human cancers[380;381]. This gene can be activated upon cell damage among other factors to promote arrest of the cell cycle and apoptosis, which pathways were also predicted to be altered by DHA treatment[382]. TP53 and other proteins such as MAPKs (predicted as upstream regulator as well) have previously been reported to be involved in the effect that DHA has on cancer cells[383–385]. Therefore, the current results support this and suggest that TP53, more than a protein involved, may be the major contributor to the decreased proliferation and survival of cancer cells induced by DHA treatment in Jurkat cells (discussed in Chapter 3).

The second most significant transcription regulator of altered genes by DHA treatment was RABL6. The activity of RABL6 was decreased according to the pathway analysis carried out. Knockdown of RABL6 has shown that this protein is essential for the proliferation and survival of human osteosarcoma[386] and pancreatic cancer[387]. Mutations in RABL6 gene were recently identified as a cause of steroid resistance in T-cell pediatric acute lymphoblastic leukemia[388]. At present, there is no available information about how DHA may change the expression of genes that are controlled by RABL6. Given RABL6 function, there is a possibility that RABL6 may be also involved in the decreased proliferation induced by DHA treatment in Jurkat cells. This hypothesis has yet to be tested.

Both fatty acid treatments altered the expression of genes which biological function is involved in cholesterol and fatty acid biosynthesis. These pathways were the most significantly enriched pathways of all identified in OA or DHA-treated cells. Pathway analysis suggested that cells sensed the addition of OA or DHA to the cell media and counteracted this by decreasing endogenous lipid biosynthesis. This has been previously reported and there is evidence that such decreased is mediated by regulating gene expression and proteolytic activation of SREBFs[389]. Here, the activity of SREBF1 decreased by DHA treatment according to the pathway analysis performed. Altogether, transcriptome results are in agreement with reports that have been shown a decrease in mRNA expression and proteolytic activation of SREBP-1 by unsaturated fatty acids[390].

6.4.2 Relationship between transcriptome and DNA methylome changes

There were identified 11 genes with altered gene expression and altered DNA methylation by fatty acid treatments. This low co-occurrence between expression and methylation changes in genes is contrary to what has been suggested previously at a genome-wide level[229;287]. The difference may arise due to the different cell types used, the concentration of the fatty acid treatments, the time of exposure and the different ap-

proaches used for data analysis. Previous studies analysed the *ex vitro* treatment of human pancreatic cells with 1000 μM palmitate for 2 days[287] and the *in vitro* treatment of THP-1 cells with 100 μM OA or 100 μM AA for 1 day[229]. Such studies addressed the genome-wide association of gene expression with DNA methylation using BeadArray results that were not statistically significant[229] or that were not validated[287]. In the current study Jurkat cells were treated with 15 μM OA or 15 μM DHA for 8 days and only statistically significant changes (p-value < 0.05, q-value < 0.05) greater than 5% change on DNA methylation were included in the analysis. All these factors may influence the differences found in this study compared with previous reports. The results in the present work suggest that DNA methylation changes induced by OA or DHA are not directly associated with the expression of genes.

Besides the 11 genes that showed altered DNA methylation and gene expression, there were identify some similarities in the pathways altered by the fatty acid treatments. For instance, DHA treatment showed to alter independently the DNA methylation and mRNA expression of genes which function is related to "Cell Death" and "Apoptosis" as a downstream effect. However, individual genes that altered DNA methylation were not the same as those genes that altered mRNA expression. The same was observed in all canonical pathways, ToxList categories and downstream effects. At present, there is no evidence of such type of association between gene expression and DNA methylation changes induced by fatty acids. The cause of this relationship is unknown.

Transcriptome analysis showed that the mRNA expression of different transcription regulators was altered by OA or DHA treatment. For instance, the transcription factor SP3 was decreased by DHA treatment. SP3 response elements were identified near CpG sites with altered DNA methylation induced by OA or DHA treatment (discussed in Chapter 5). SP3 has been shown to physically interact with DNMT1[204]. Therefore, evidence suggests that SP3 may participate in the DNA methylation changes induced by fatty acids. The possible mechanism is described in the final discussion.

Finally, another possible relationship between altered gene expression and altered DNA methylation may be mediated by KDM5B. This was the third most significant transcription regulator of genes that showed altered expression by DHA treatment. KDM5B is lysine-specific demethylase and has been shown to act on H3K4me/2/3[391;392]. In mammals, the H3K4me3 histone mark is associated with CpG islands[393–395], which are usually free of DNA methylation and located in approximately 74% of human promoters[181;396]. Because of this, H3K4me3 is considered as a mark of actively transcribed genes. The results suggest that DHA treatment increased in some way KDM5B activity that in turn induced altered expression of KDM5B target genes. Given the function of KDM5B, altered gene expression induced by KDM5B may be mediated by H3K4me3 demethylation. Unmethylated H3K4 can be recognised by DNMT3A and promote, in theory, DNA methylation[325] as reviewed in Chapter 5. This hypothesis

is further supported by ChIP experiments that showed a decrease in H3K4me3 enrichment on regions proximal to CpG sites with altered DNA methylation (Chapter 5).

6.4.3 Limitations of the BeadArray analysis

BeadArray analyses usually implement a correction for multiple testing such as the false discovery rate (FDR). The nature of the FDR is linked to the P-value, result from a statistical test[364]. Because of the P-values that can be achievable by a statistical test with a sample size n = 3, the use of FDR as a cutoff was not suitable for the analysis. To deal with the problem of small samples sizes in BeadArray experiments, new alternatives have been proposed[397;398]. In the current work, samples from 9 cultures replicates were pooled to obtain 3 samples in each treatment which were analysed using expression BeadArrays. There is evidence showing that pooling may account for some of the variations in gene expression by reducing the noise[399]. Because of this, in addition to statistical significance (P-value < 0.05) only a threshold of 1.2 in the fold change expression was used as a cutoff. The lack of a multiple testing correction suggests that there is a possibility that some transcription changes reported here may be false positives. Yet, there is confidence in the results as these were validated by qPCR. Besides, genes with altered mRNA expression identified here are in agreement with reported evidence showing the effects of fatty acids on cells.

6.5 Conclusions

Fatty acid treatments altered the expression of the transcriptome in a treatment-specific manner. Overall, OA treatment altered the expression of genes associated with the basal growth of cells while DHA altered the expression of genes related to apoptotic pathways. Analysis showed that genes with altered expression were not essentially the same genes that changed DNA methylation. However, there was identified that OA or DHA altered the expression of genes with similar biological functions to those genes which changed DNA methylation. Transcriptome analysis suggests that the expression and activity of different transcription factors were altered by OA or DHA treatment. Such transcription factors included KDM5B, which may account for the decreased H3K4me3 enrichment previously observed in ChIP experiments, and SP3 whose response elements were identified in sequences proximal to CpG sites with altered DNA methylation. Thus, transcriptome data supports the hypothesis that activity of different transcription factors may participate in the effect that OA or DHA have on DNA methylation in Jurkat cells.

Chapter 7

Final Discussion, Conclusions and Future Work

7.1 Final discussion

The experiments carried out in this work aimed to expand our current understanding of the mechanisms involved in the effect of fatty acids on DNA methylation. In order to do so, a combination of *in vitro* and *in silico* analyses were performed using Jurkat cells treated with OA or DHA as a model. Overall, the effects of fatty acids showed specificity in terms of the number and location of altered CpG loci. DNA methylation changed after the 3rd day of treatment suggesting an indirect mechanism in which H3K4me3, but not PPARα, may be involved. Furthermore, a number of transcription factors which possibly participate in the DNA methylation changes induced by OA or DHA were identified .

7.1.1 Specificity of altered DNA methylation by OA or DHA treatment

The specificity of fatty acids to induce DNA methylation changes has been reported before in candidate genes[233;240]. *In vitro* experiments have shown that 100 μM EPA, but not 100 μM OA treatment, induced demethylation of a single CpG in the promoter of CCAAT/enhancer-binding protein delta using the human U937 leukaemia cell line[233]. *In vivo*, supplementation with olive or fish oil for 12 weeks has shown to differentially alter specific-locus DNA methylation levels of two candidates genes analysed in human PBMCs[240]. The specificity identified in candidate genes has also been suggested to occur at the DNA methylome level as treatment of THP-1 monocytes with 100 μM OA or 100 μM AA showed to induce a global DNA hypomethylation or hypermethylation, respectively. However, global DNA methylation changes or

in candidate genes do not provide details about genome-wide patterns. Experiments carried out in the current work addressed this. Results were in agreement with current evidence that shows specificity in the effect that different fatty acids have on DNA methylation. OA treatment induced DNA methylation changes in a different and lower number of CpG sites compared with DHA treatment. Besides, altered CpG sites by OA were located mainly in different genes of those CpG sites altered by DHA treatment. Despite these differences, both fatty acids altered mostly intergenic regions. The preference of OA and DHA to alter the methylation status of intergenic regions has not been reported before. Altered methylation of intergenic regions raises questions about their possible function. Are fatty acids changing the expression of non-coding RNAs? Regulatory regions? Future work will need to address such questions. Altogether, the findings in this work support the hypothesis that the genome-wide effect on the DNA methylation induced by fatty acids at the locus-specific level shows specificity.

The reason underlying OA or DHA specificity on DNA methylation is currently unknown. OA is a MUFA of 18 carbons compared with DHA which is a PUFA of 22 carbons. Thus, it is possible that specificity may be associated with the chemical structure of fatty acids. Other possibility is that specificity on the DNA methylation changes identified was related to the differential effects that OA and DHA have been shown on cells. For instance, only DHA treatment induced a decrease in Jurkat's cell viability and proliferation in a time-dependent manner. Pyrosequencing of candidate CpG sites showed that DHA treatment altered DNA methylation also in a time-dependent manner. Therefore, it is probable that decreased cell viability and proliferation may be associated with the effects on DNA methylation, at least to some extent. A relationship between cell viability or/and cell proliferation with DNA methylation changes is further supported by the low number of altered CpG sites by OA treatment, which did not alter cell viability or proliferation. At the same time, the DNA methylation changes identified in OA-treated cells indicated that an effect on cell viability or proliferation was not essential for the epigenetic effect of fatty acids.

Another possibility to explain the different DNA methylation changes induced by OA or DHA may be related to the differential gene expression induced by the same fatty acids. In this work, DHA treatment showed to alter the gene expression of five-times more genes compared with OA treatment. Similarly, DHA altered DNA methylation of almost three-times more number of CpG sites compared with OA treatment. Besides the number of CpG sites, genes with altered expression or DNA methylation by DHA treatment were mainly different from those genes altered by OA treatment. Thus, it is possible that some of the altered genes may lead to locus-specific DNA methylation changes in a way still not understood.

Finally, there is a possibility that incubation of Jurkat cells with more than 15 μM OA may induce similar effects on DNA methylation as 15 μM DHA treatment. This

has been reported for the cell viability and proliferation effect on cells by OA or DHA treatment [264]. At present, a relative potency of fatty acids to alter DNA methylation has not been addressed. Effects of fatty acids on DNA methylation is a relatively new field of study of which not much is known. In the present work, the same dose of OA or DHA was used as an initial approach. Specific effects of OA or DHA should be considered in such a context. Further experiments will need to address if specific effects on DNA methylation induced by OA or DHA treatment may be related to a relative potency of such fatty acids.

7.1.2 Time required by OA or DHA to induce DNA methylation changes in Jurkat cells

In vitro studies that have been addressed DNA methylation changes induced by fatty acids usually use 24-hour treatments [229–231;233;303;400]. Such studies have identified significant changes on DNA methylation in specific CpG sites of candidate genes or changes at the global level. Thus, reported evidence suggests that altered DNA methylation induced by fatty acids can be achieved since 24-hours after treatments.

In this work, pyrosequencing of five candidate CpG sites suggested that DNA methylation changes by 15 μM DHA treatment were time-dependent. This is because three of the CpG sites reached a statistical significance difference only after the 3$^{\text{rd}}$ day while the other two after the 6$^{\text{th}}$ day of treatment. In all five CpG sites analysed, the most significant change in DNA methylation was identified after the 8$^{\text{th}}$ day of treatment. The majority of the reported evidence showing a change in DNA methylation *in vitro* after 24 hours used 100 μM fatty acid concentrations [229;233;303;400]. In contrast, in the present work 15 μM OA or DHA was used. Therefore, there is a possibility that the longer time required for fatty acids to alter DNA methylation identified here was related to a lower concentration of fatty acids used. However, there is one study showing that 3 μM AA treatment decrease DNA methylation of the *KDR* promoter region after 24 hours incubation in human umbilical vein endothelial cells [231]. Thus, it is possible that the concentration of the fatty acid treatments may not account for the time required for some CpG sites to change their DNA methylation status. Alternatively, there is a possibility that particular fatty acids may need different times to alter DNA methylation. This is still unclear. Altogether, current evidence suggests that some CpG sites may change DNA methylation quicker than others. The different time required for some CpG sites to change DNA methylation supports the hypothesis that there is not a single mechanism (transcription factor, enzyme, pathway, etc.) by which fatty acids induce altered DNA methylation.

7.1.3 Possible transcription factors and pathways involved on the altered DNA methylation by OA or DHA

In the current project, pyrosequencing of five candidate CpG sites after treatment with DHA, 0.2 μM PPARα agonist GW7647, 2 μM PPARα inhibitor GW6471 or DHA plus 2 μM GW6471 showed no significant effect of PPARα activity on DNA methylation changes induced by DHA. Therefore, evidence suggested that similar to what has previously been reported for OA[229], PPARα does not mediate altered DNA methylation by DHA treatment. Instead of PPARα, other transcription factors were associated with the effect of DHA on DNA methylation. *In silico* experiments showed that sequences up to 60 bp next to CpG sites with altered DNA methylation were enriched with response elements of different transcription factors. The majority of them were members of the protein/Krüppel-like factor family which included SP1 and SP3. Determination of transcriptome changes identified that SP3, but not SP1, was significantly downregulated by DHA treatment. SP1 and SP3 share over 90% homology in their linear sequences[349] and both have shown to physically interact with DNMT1 through a conserved motif using HEK293 and Jurkat cells extracts, respectively[204]. Besides, there is evidence that SP1 interacts with tumour protein 53 (P53 or TP53) while DNMT1 can also interact with TP53 *in vivo* in human cells[203]. TP53 interaction with DNMT1 and SP1 requires different domains[203;204] suggesting that TP53 can interact with both proteins at the same time.

Results in this work suggest that interaction between SP1/SP3, TP53 and DNMT1 may be one of the primary mechanism mediating altered DNA methylation by DHA, similar to what has been observed in the survivin gene *in vitro*[203;204]. The latter hypothesis is supported by transcriptome data which indicated that TP53 activity was increased while *SP3* mRNA was downregulated in DHA-treated cells. Furthermore, there was identified an enrichment of SP1 and SP3 binding sites near CpG sites that showed altered DNA methylation by DHA treatment. A model to explain DNA methylation changes by DHA is shown in Figure 7.1. However, further work needs to address the direct participation of SP1, SP3, TP53 and DNMT1 as mediators of altered DNA methylation induced by DHA. As an added note, there was not identified any significant change in DNA methylation or expression of the survivin gene in the current experiments.

In the case of OA treatment, the only clear evidence related to mechanisms was the identification of response elements in the proximity of CpG sites with altered DNA methylation. The majority of response elements identified in OA-treated cells were similar to those detected in DHA-treated cells. However, there was not enough information in the literature to generate a particular model to explain specifically DNA methylation changes induced by OA treatment.

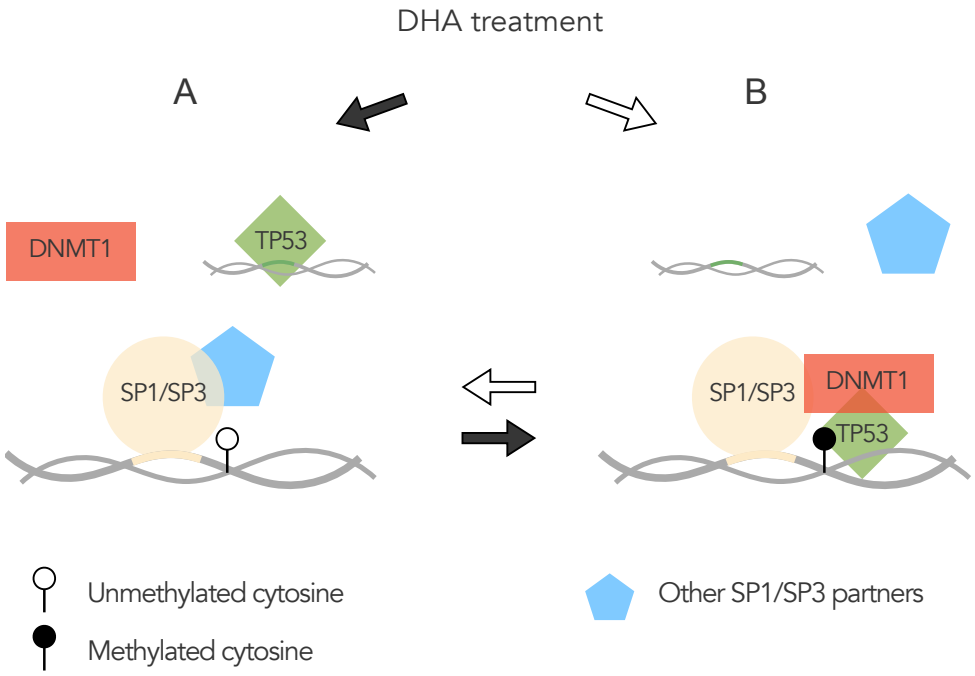

Figure 7.1: Proposed mechanism underlying the altered DNA methylation induced by DHA in Jurkat cells involves a crosstalk between SP1/SP3-TP53-DNMT1. Under normal conditions transcription factors such as SP1/SP3 or TP53 can modulate the expression of their targeted genes (A). However, under DHA stimulation SP1/SP3 or TP53 may bind to genomic regions other than their usual and/or recruit DNMT1, thus, increasing DNA methylation on site (B). The opposite process (B to A) may explain also the DHA-induced demethylation. The model is based on the *in vitro* regulation of the survivin gene by doxorubicin treatment [203;204] and the increased activity of TP53, the mRNA downregulation of SP3 and the enrichment of SP1 and SP3 response elements in sequences close to CpG sites with altered DNA methylation by DHA identified in the current work.

As final remarks, DHA treatment also showed to alter DNA methylation of promoter sequences enriched with the androgen receptor (AR) binding site. Pathway analysis of transcriptome changes indicated that AR increased its activity after DHA treatment. Therefore, data suggested that AR may participate in the altered DNA methylation induced by DHA specifically at promoter regions. Similarly, sequences that changed DNA methylation by OA or DHA treatment showed enrichment of Wilms tumour 1 (WT1) response element which activity was predicted to decrease in DHA-treated cells. This suggested again that the activity of transcription factors may be related to the DNA methylation changes induced by fatty acids. How the activity of AR and WT1 may mediate DNA methylation changes is currently unknown.

Pathway analysis of transcriptome changes also predicted an increased activity of SIRT1 by DHA treatment. This histone deacetylase showed to be required for the effect of OA or AA on the global DNA methylation of MEFs [229]. Furthermore, SIRT1 has been shown to deacetylate DNMT1 *in vitro* and *in vivo* [305]. Deacetylation of

DNMT1 has been shown to increase or decrease its methyltransferase activity depending on the residue that is deacetylated[305]. Results in this work are in agreement with current evidence and support the hypothesis that SIRT1 may participate in the DNA methylation changes induced by fatty acids in human cells.

7.1.4 Relationship between altered DNA methylation and decreased H3K4me3 enrichment by OA or DHA

Current evidence shows that fatty acids can alter specific histone marks *in vitro* and *in vivo* using mouse cells[249;250]. In human cells, modification of histone marks by fatty acids has only been reported *in vitro* so far by one study[248]. The study showed that H3K4me2 enrichment decreased after 30 μM DHA treatment for two days using the neuroblastoma M17 cell line[248]. Nevertheless, altered DNA methylation and altered histones marks at the same genomic region by any fatty acid has not been addressed in human cells. Here, ChIP assays showed that 15 μM DHA treatment significantly decreased H3K4me3 enrichment in 3 candidate regions with altered DNA methylation induced by the same treatment. OA treatment showed the same trend to decrease H3K4me3 enrichment on the 2 candidate regions analysed, but none of them reached statistical significance. *In silico* analysis of all CpG sites that changed DNA methylation by OA or DHA showed that only the 6% (36/563) or 7% (123/1596) of these, respectively, overlapped with H3K4me3 occupancy according to ENCODE data. Therefore, experiments carried out in this work suggest that altered DNA methylation and reduce H3K4me3 enrichment induced by fatty acids may relate to a low degree.

Transcriptome changes induced by DHA suggested that lysine demethylase 5B (KDM5B) activity, but not mRNA expression, was increased. Increased *Kdm5b* mRNA expression has been reported in mouse hepatocytes after the *in vitro* treatment with 40 μM oleate plus 40 μM palmitate for 24 hours[249]. Thus, there is a possibility that 15 μM DHA treatment may induce a small increase in *KDM5B* mRNA beyond the detection limits of the BeadArray. Another possibility is that DHA may induce just a change in KDM5B activity rather than alter *KDM5B* expression. KDM5B overexpression has been shown to demethylate H3K4me3/2/1, but not H3K9me3/2/1 or H3K36me3/2/1, *in vivo* using Hela cells[401]. The increased activity of KDM5B induced by DHA treatment may explain the decreased levels of H3K4me3 identified in regions with altered DNA methylation by the same treatment. If H3K4me3 demethylation induced by DHA showed genome-wide specificity remains unknown.

As discussed in detail in Chapter 5, decreased H3K4me3 may play a role in the DNA methylation changes induced by OA or DHA. Such a hypothesis is based on *in vitro* evidence suggesting that H3K4me0, but not H3K4me3, may be recognised by DNMT3A[131;325]. Thus, there is a possibility that decreased H3K4me3 enrichment identified here may increase H3K4me0 which in turn recruits DNMT3A to methylate the DNA.

7.2 Conclusions

Experiments carried out in this thesis project showed that OA or DHA treatment at the same concentration modified fatty acid composition, gene expression and DNA methylation in a treatment-specific manner in Jurkat cells. Pyrosequencing of five candidate CpG sites showed that the DNA methylation changes were established after the 3rd day of DHA treatment. PPARα did not mediate the altered DNA methylation of such candidate CpG sites. However, there is still unclear if the methylation status of some other CpG sites was mediated by PPARα activity in DHA-treated cells.

In silico analysis carried out to identify other possible mechanisms by which OA or DHA altered the DNA methylation showed that DNA motifs and differential activity and/or expression of different transcription factors may be involved. The genome-wide approach that was employed here allowed the detection of different candidate mechanisms. Available evidence suggests that the most feasible mechanism by which OA or DHA induced changes on DNA methylation may involve crosstalk between SP1/SP3-DNMT1-TP53 (Figure 7.1). Altogether, data support the hypothesis that DNA methylation changes induced by OA or DHA treatments were associated with the activity of different transcription factors.

Apart from transcription factors, altered DNA methylation induced by OA or DHA showed a relationship with decreased H3K4me3 enrichment on candidate regions analysed. This suggested that there may be an interplay between altered DNA methylation and H3K4me3 changes induced by fatty acids. If one epigenetic mark was needed for the other to take place should be assessed in future work.

At present, some of the most important public health problems in adults are non-communicable diseases. Dietary fats have been shown a relationship with some of them such as diabetes, cancer and atherosclerosis. The same non-communicable diseases have also been shown to alter DNA methylation patterns in cells. Understanding the underlying mechanisms by which fatty acids induce altered DNA methylation may help to elucidate the functional consequences of these. Furthermore, the latter may address the possible connection between altered DNA methylation patterns in diseases with the effect of fatty acids on DNA methylation. Such information may be useful for better dietary recommendations in order to improve human health.

7.3 Future work

7.3.1 To investigate the possible cause of the fatty acid specificity on the DNA methylome

Current evidence shows that different fatty acids induce diverse effects on DNA methylation at the global level or candidate genes[229;233;234;240]. In this work, it was shown that such specificity is also observed at the genome-wide level for OA and DHA. To explore the cause of such specificity, treatments with other fatty acids at the same concentration and assessment of the DNA methylation changes using BeadArrays can be carried out. The usage of palmitic (16:0), stearic (18:0), AA (20:4n-6) and EPA (20:5n-3) in the first instance may indicate if specificity is related to the chemical structure of fatty acids. Based on the hypothesis that the chemical structure is related to the specificity of fatty acids it would be expected that palmitic and stearic acid, both saturated, may alter similar CpG sites compared with EPA or DHA treatments. Similarities and differences between treatments may indicate if the number of double bonds, the position of double bonds or the number of carbons are associated with the specificity of fatty acids to alter the DNA methylome. Also, as palmitic, stearic, AA, EPA and DHA, but not OA, have shown to decrease cell viability of Jurkat cells at the same concentration[264], such type of experiments may allow determining if decreased viability by DHA was related to the greater number of CpG sites altered in the current experiments.

Similarly, determination of transcriptome changes induced by palmitic, stearic, AA, and EPA would indicate if the number and/or specific altered transcripts show a relationship with the DNA methylation changes induced by the same treatments. The implementation of RNA-seq to determine transcriptome changes may serve also to evaluate if fatty acid treatments alter the expression of non-coding RNAs.

It is possible to carry out the previously mentioned experiments using supplementation in humans. However, animal models or *in vitro* experiments still have some advantages considering the relatively little current knowledge in the subject. For instance, processing and metabolism of fats may be different between humans which may impact the outcomes. Besides, reported evidence have shown that altered DNA methylation occurred after 6 to 12 weeks of human supplementation with fatty acids[240;242]. The use of animal models can improve the control of metabolic differences but still, it should be considered that treatments should last around 9 weeks which is the time implemented in previous reports[234]. Here, experiments showed that 8 days was enough time to induce DNA methylation change by fatty acids. *In vitro* experiments may be preferable until further characterisation of the system is accomplished.

7.3.2 To characterise the time needed for fatty acids to induce DNA methylation changes

Results of this work showed that 15 μM DHA required more than 3 days to significantly alter DNA methylation of the five candidate CpG sites that were analysed. In contrast, reported evidence has been shown that 100 μM OA, AA or EPA treatments alter the DNA methylation after 24 hours *in vitro*[229;233;303;400]. There is only one report that has shown DNA methylation changes after 24 hours incubation using 3 μM AA treatment[231]. Therefore, it is unclear if the time required for DHA to altered the DNA methylation was due to an intrinsic characteristic of the CpG sites analysed, the different concentrations used in treatments or a particularity of DHA. To address this, Jurkat cell treatments with DHA at different concentrations may be carried out for 8 days. After every 24 hours of incubation, DNA methylation by pyrosequencing can be determined in the five CpG sites that were shown here to change DNA methylation by DHA treatment. The implementation of concentrations higher than 15 μM DHA showed a small but significant decrease in cell viability in a time-dependent manner in our experimental model. Thus, concentration recommended for treatments would be 5, 15, 30 and 60 μM DHA as a maximum. The possible decreased in cell viability by 30 and 60 μM DHA treatments may also allow identifying if an effect on viability is involved in the DNA methylation changes by DHA treatment.

Jurkat cells can be treated with different concentrations of EPA or AA, which have been shown to modify the DNA methylation status of the *CEBPD* or *KDR* promoter, respectively[231;233]. Results would reaffirm if concentrations of fatty acid treatments are associated or not with the time required to induce altered DNA methylation. Besides, the comparison of the results may allow determining if the time needed for DHA to alter DNA methylation is specific for this fatty acid.

After evaluation of results at least two different times of treatments, a short one and longer one, may be selected to carry out DNA methylation BeadArrays or reduced representation bisulphite sequencing (RRBS). Analysis of the data may indicate how frequent is the time-dependent DNA methylation changes at the genome-wide level. This information may be useful to also identify candidate CpG sites with an early response to fatty acid treatment. Currently, animal and human studies have been shown altered DNA methylation after 6 weeks of fatty acids supplementation[234;240;242]. CpG sites with an early response to fatty acid treatment can be used as biomarkers in animal or human studies to assess quicker the DNA methylation changes by fatty acid supplementation. The reduction in the duration of human clinical trials can make financing of future projects more efficient.

7.3.3 To identify the possible SP1/SP3-DNMT1-TP53 crosstalk induced by fatty acid treatments

Firstly, the characterisation of *SP3* mRNA downregulation by DHA can be performed. Western blotting can be used to detect if altered *SP3* mRNA levels correlate with altered protein levels. Treatment of Jurkat cells using different times of incubation and/or different concentrations of DHA can examine if SP3 is regulated in time and/or a dose-dependent manner at the mRNA and protein levels.

There is evidence suggesting that the activity of the SP family can be altered by post-translational modifications such as phosphorylation, acetylation, glycosylation and sumoylation[402]. In this work, DHA treatment showed to alter PKA, MAPK (kinase) pathways and SIRT1 (deacetylase) activity. Therefore, there is a possibility that phosphorylation and acetylation of SP1 or SP3 were altered by DHA treatment. To test phosphorylation changes, enzyme-linked immunosorbent assays (ELISA) can be performed in immunoprecipitated SP1 or SP3 complexes after DHA treatment. A detection antibody specific for phosphorylation may allow the identification of phosphorylation levels in immunoprecipitates using colourimetric or fluorometric methods. To test acetylation changes, Jurkat cells can be co-treated with DHA and [^{3}H]acetate or just [^{3}H]acetate. After treatments, immunoprecipitation of SP1 or SP3 and subsequent measurement of radioactivity levels may indicate acetylation differences between DHA-treated cells compared with control cells treated with only [^{3}H]acetate.

Knockout cells can be used to corroborate if crosstalk of SP1/SP3-DNMT1-TP53 is involved in the effect of fatty acids on DNA methylation. Because of evidence showing that SP1 and SP3 have redundancy in their target genes[349], and both transcription factors can interact with DNMT1[204], the use of SP1 and SP3 double-knockout cells may be preferable than single knockouts. Thus, fatty acids treatments can be carried out in SP1-SP3 double-knockout or TP53 knockout cells and the DNA methylation measured by BeadArrays. The difference between altered DNA methylation between wild-type and knockout cells may provide to support SP1/SP3 or TP53 participation in the mechanisms by which fatty acids alter the DNA methylation. The CpG sites identified can then serve as candidate regions to study if DNMT1 catalyses DNA methylation changes in such regions. To do this, fatty acid treatments can be performed again in wild type or knockout cells using this time the specific DNMT1 inhibitor (procainamide) or unspecific DNMT1 inhibitor (5-aza-2deoxycytidine). After treatments, the DNA methylation can be measured in candidate regions by *MspI* and *HpaII* restriction enzymes or by pyrosequencing. Analysis of the results may provide evidence to suggest if there is SP1/SP3-DNMT1-TP53 crosstalk and if this is required for the altered DNA methylation by fatty acid treatments.

Another approach to identifying SP1/SP3-DNMT1-TP53 crosstalk would be using ChIP-seq assays. DNMT1 can be co-immunoprecipitated with SP1, SP3 or TP53 to

obtained all DNA regions that possibly changed the occupancy of these proteins in treated cells compared with untreated cells. After ChIP-seq analysis, the methylation status of some candidate regions that change DNMT1-SP1, DNMT1-SP3 or DNMT1-TP53 occupancy can be identified by *MspI* and *HpaII* restriction enzymes or by pyrosequencing. Such results may indicate if the regions changing DNMT1 occupancy also change DNA methylation.

7.3.4 To examine H3K4me3 relationship with DNA methylation changes induced by fatty acids

The current work showed decreased H3K4me3 enrichment within candidate regions that showed altered DNA methylation by 15 μM DHA treatment. Besides, results suggested that DHA treatment increased the activity of KDM5B, a lysine demethylase that has shown to demethylate the H3K4 residue specifically[401]. If H3K4me3 demethylation or KDM5B activity participate in the altered DNA methylation by DHA treatment is currently unknown. To address this, KDM5B cDNA can be cloned, transfected and ectopically expressed in Jurkat cells to induce an overexpression. Cells transfected with an empty vector (control cells) or KDM5B cDNA can be treated with DHA to look for differences in the DNA methylation patterns induced by the treatment. As a first approach, genomic DNA can be treated with *MspI* and *HpaII* restriction enzymes as both cut at 5'-CCGG-3' sequences[403]. Nevertheless, HpaII cleavage is blocked by the presence of 5-methylcytosine in the sequence while the activity of MspI is not sensible to the methylation status of the sequence[403]. Therefore, differences on DNA methylation should create a different pattern of fragments. Furthermore, DNA methylation BeadArrays can be carried out to examine the possible differences at the locus-specific level.

Overexpression of KDM5B would allow determining if decreased H3K4me3 has an effect on DNA methylation induced by DHA. On the contrary, to explore if DNA methylation induced by DHA treatment promotes a decrease in H3K4me3 enrichment, Jurkat cells can be co-treated with DHA and the inhibitor of DNA methylation 5-aza-2-deoxycytidine. If DNA methylation is not needed for the decreased H3K4me3 induced by DHA, co-treatment of DHA plus 5-aza-2-deoxycytidine should show the same decreased in H3K4me3 as cells treated with DHA only.

To further characterise the H3K4me3 relationship with the altered DNA methylation induced by DHA treatment, ChIP-seq assays can be carried out. Sequencing of the immunoprecipitated DNA using an H3K4me3 antibody can provide evidence of the genomic locations where H3K4me3 decreased. The mapping of such regions with CpG sites that showed altered DNA methylation by the same DHA treatment (BeadArrays or RRBS) can provide evidence of the degree of relationship between both epigenetic marks.

Appendices

A DNA methylation changes after 8-day incubation with 15 μM OA or DHA assessed by the Infinium MethylationEPIC BeadChip

Table 1: Genome-wide DNA methylation changes after 8-day incubation with 15 μM OA or DHA assessed by Illumina Human MethylationEPIC BeadChip. All changes shown were significantly different compared with controls ($P < 0.05$) and passed FDR threshold ($q < 0.05$).

BeadChip ID	Chr	Position	Strand	CpGi	Genes	Intragenic	OA	DHA
cg02401415	chr14	22968476	+	OpenSea	no_gene	no_gene	-0.25	-0.23
cg14718695	chr14	22573370	-	OpenSea	no_gene	no_gene	-	-0.21
cg25254444	chr9	21408013	+	OpenSea	IFNA8	TSS1500	-	-0.17
cg00940972	chr14	22954575	-	OpenSea	no_gene	no_gene	-	-0.15
cg20507742	chr14	22966633	+	OpenSea	no_gene	no_gene	-	-0.15
cg17564498	chr7	133247477	+	OpenSea	EXOC4	Body	-	-0.15
cg26292058	chr1	192544252	-	OpenSea	RGS1	TSS1500	-0.07	-0.14
cg19301109	chr14	22943953	+	OpenSea	no_gene	no_gene	-	-0.14
cg05475386	chr12	65723693	-	OpenSea	MSRB3	Body	-	-0.13
cg04574083	chr5	6765204	-	OpenSea	no_gene	no_gene	-0.12	-0.13
cg10841253	chr4	10531768	+	OpenSea	CLNK	Body	-0.17	-0.12
cg05147200	chr9	22446830	-	Island	DMRTA1	TSS200	-0.11	-0.12
cg02481176	chr12	62749148	-	OpenSea	USP15	Body	-	-0.12
cg27188282	chr11	104780712	-	OpenSea	no_gene	no_gene	-	-0.11
cg18037846	chr5	112901383	-	OpenSea	YTHDC2	Body	-	-0.11

cg09918394	chr12	50523625	-	OpenSea	LASS5	3'UTR	-	-0.11
cg01819696	chr1	179708928	+	N_Shelf	no_gene	no_gene	-	-0.11
cg14047008	chr1	173887011	+	OpenSea	SERPINC1	TSS1500	-	-0.11
cg08600356	chr5	1562829	+	OpenSea	no_gene	no_gene	-	-0.11
cg09139559	chr4	69443819	+	OpenSea	no_gene	no_gene	-	-0.11
cg18173044	chr10	114535504	+	OpenSea	VTI1A	Body	-	-0.11
cg03640465	chr4	10042842	-	OpenSea	SLC2A9	TSS1500	-	-0.11
cg23350744	chr5	122422098	+	N_Shelf	no_gene	no_gene	-	-0.11
cg03939903	chr2	180662010	-	OpenSea	ZNF385B	5'UTR	-	-0.1
cg07321467	chr4	81960704	-	OpenSea	BMP3	Body	-0.08	-0.1
cg17658874	chr3	29456667	-	OpenSea	RBMS3	Body	-	-0.1
cg07314952	chr6	137822153	+	S_Shelf	no_gene	no_gene	-	-0.1
cg06031737	chr1	193112478	-	OpenSea	CDC73	Body	-	-0.1
cg01981108	chr8	146020112	+	S_Shore	no_gene	no_gene	-	-0.1
cg16535298	chr4	70518959	+	OpenSea	UGT2A1	NC	-	-0.1
cg07543138	chr21	16434067	-	N_Shelf	NRIP1	5'UTR	-	-0.1
cg17420463	chr3	185046594	-	OpenSea	MAP3K13	NC	-0.06	-0.1
cg02432263	chr10	18943063	-	S_Shelf	no_gene	no_gene	-	-0.1
cg14697125	chr6	168972044	-	N_Shore	SMOC2	Body	-	-0.1
cg09997714	chr6	166061418	+	OpenSea	PDE10A	NC	-	-0.1
cg22345964	chr12	26766956	+	OpenSea	ITPR2	Body	-	-0.1
cg17796599	chr12	91506404	-	OpenSea	LUM	TSS1500	-	-0.1
cg10960421	chr7	80008161	+	OpenSea	no_gene	no_gene	-	-0.1
cg23790478	chr4	134075898	-	S_Shelf	PCDH10	Body	-	-0.1
cg09357417	chr3	29108748	-	OpenSea	no_gene	no_gene	-	-0.09
cg16637554	chr5	72183175	-	OpenSea	TNPO1	Body	-	-0.09
cg07120174	chr8	41351213	-	S_Shelf	GOLGA7	Body	-	-0.09
cg26958509	chr18	12478776	-	OpenSea	SPIRE1	Body	-	-0.09
cg01199603	chr12	65718113	+	OpenSea	MSRB3	Body	-	-0.09
cg20318580	chr15	51398457	-	OpenSea	TNFAIP8L3	TSS1500	-	-0.09

cg02741177	chr4	71263061	+	OpenSea	PROL1	TSS1500	-	-0.09
cg12969902	chr11	89983939	-	OpenSea	DISC1FP1	TSS1500	-	-0.09
cg23865516	chr18	52363291	-	OpenSea	no_gene	no_gene	-	-0.09
cg08376643	chr10	64880766	-	OpenSea	no_gene	no_gene	-	-0.09
cg02190928	chr8	90427508	+	OpenSea	no_gene	no_gene	-	-0.09
cg13184811	chr9	107368897	+	OpenSea	OR13C2	TSS1500	-	-0.09
cg05662386	chr12	48406233	+	OpenSea	no_gene	no_gene	-	-0.09
cg19869212	chr11	76790769	-	OpenSea	CAPN5	5'UTR	-	-0.09
cg00947236	chr8	29020165	+	OpenSea	KIF13B	Body	-0.07	-0.09
cg13871684	chr2	119133353	+	OpenSea	no_gene	no_gene	-	-0.09
cg06899044	chr8	65294586	+	S_Shelf	no_gene	no_gene	-	-0.09
cg17241353	chr20	53868015	+	OpenSea	no_gene	no_gene	-	-0.09
cg19831946	chr15	68552396	-	OpenSea	no_gene	no_gene	-	-0.09
cg01372911	chr6	46759861	+	OpenSea	MEP1A	TSS1500	-	-0.09
cg18492804	chr14	54976994	+	Island	CGRRF1	Body	-	-0.09
cg21694873	chr3	45451677	+	OpenSea	LARS2	Body	-	-0.09
cg21548021	chr8	15873055	+	OpenSea	no_gene	no_gene	-0.08	-0.09
cg11599793	chr2	151284413	+	OpenSea	no_gene	no_gene	-	-0.09
cg10500749	chr6	8437152	-	S_Shore	SLC35B3	TSS1500	-	-0.09
cg02354913	chr14	45580008	+	OpenSea	PRPF39	NC	-	-0.09
cg17585208	chr4	120484257	-	OpenSea	PDE5A	Body	-	-0.09
cg02541672	chr14	22579700	+	OpenSea	no_gene	no_gene	-	-0.09
cg16663341	chr18	42327562	-	S_Shelf	SETBP1	Body	-	-0.09
cg09746078	chr12	56966920	-	OpenSea	RBMS2	Body	-0.07	-0.09
cg17752959	chr22	17906941	-	OpenSea	CECR2	5'UTR	-	-0.09
cg00550721	chr9	21986062	+	N_Shelf	CDKN2A	Body	-0.08	-0.09
cg16073236	chr7	107789943	+	OpenSea	NRCAM	3'UTR	-	-0.09
cg03687953	chr17	40834511	-	N_Shore	NC	NC	-0.08	-0.09
cg10312158	chr1	159044349	-	OpenSea	AIM2	5'UTR	-	-0.09
cg12932285	chr15	71272858	-	OpenSea	LRRC49	Body	-	-0.09

cg07532576	chr2	179544947	+	OpenSea	TTN	Body	-	-0.09
cg24377204	chr21	37817626	+	OpenSea	no_gene	no_gene	-	-0.09
cg21858680	chr4	85020829	+	OpenSea	no_gene	no_gene	-	-0.09
cg20875344	chrX	8907196	-	OpenSea	no_gene	no_gene	-	-0.08
cg23019611	chr8	23458336	-	OpenSea	no_gene	no_gene	-0.07	-0.08
cg14260304	chr18	61256157	+	OpenSea	SERPINB13	Body	-	-0.08
cg14472778	chr1	11867308	-	S_Shore	CLCN6	Body	-	-0.08
cg07121165	chr9	19967557	-	OpenSea	no_gene	no_gene	-	-0.08
cg03644541	chr14	35157273	+	OpenSea	no_gene	no_gene	-0.07	-0.08
cg24073674	chr2	202980510	+	OpenSea	KIAA2012	Body	-	-0.08
cg18306115	chr4	159441477	+	OpenSea	RXFP1	TSS1500	-	-0.08
cg11503396	chr2	25419761	-	OpenSea	no_gene	no_gene	-	-0.08
cg08997191	chr8	133788834	-	S_Shore	PHF20L1	5'UTR	-0.09	-0.08
cg06873652	chr11	82961275	-	OpenSea	ANKRD42	Body	-	-0.08
cg15467112	chr14	75489610	-	OpenSea	MLH3	Body	-	-0.08
cg20586750	chr6	2413556	+	OpenSea	no_gene	no_gene	-	-0.08
cg04504559	chr12	4918152	-	N_Shore	KCNA6	TSS200	-	-0.08
cg25046866	chr8	48680661	+	S_Shelf	no_gene	no_gene	-	-0.08
cg22329828	chrX	46834722	+	OpenSea	JADE3	5'UTR	-	-0.08
cg15237829	chr3	171102373	+	OpenSea	TNIK	Body	-0.11	-0.08
cg07107116	chr8	43097631	-	N_Shelf	no_gene	no_gene	-	-0.08
cg18217910	chr2	179756050	-	OpenSea	CCDC141	Body	-	-0.08
cg09203501	chr7	5271545	-	S_Shelf	WIPI2	3'UTR	-	-0.08
cg17467670	chr3	116173328	+	OpenSea	no_gene	no_gene	-	-0.08
cg00659910	chr8	64617139	-	OpenSea	no_gene	no_gene	-0.05	-0.08
cg00644508	chr4	138728775	+	OpenSea	no_gene	no_gene	-	-0.08
cg07026953	chr8	51306102	-	OpenSea	SNTG1	5'UTR	-	-0.08
cg04732840	chr5	12615428	+	OpenSea	no_gene	no_gene	-	-0.08
cg04560372	chr18	61173718	+	OpenSea	no_gene	no_gene	-	-0.08
cg24096977	chr16	12705506	-	OpenSea	no_gene	no_gene	-	-0.08

cg20805999	chr4	119606266	+	N_Shore	METTL14	TSS1500	-	-0.08
cg00576421	chr14	66806636	+	OpenSea	no_gene	no_gene	-	-0.08
cg07436354	chr4	155198629	+	OpenSea	DCHS2	Body	-	-0.08
cg19272419	chr15	51988314	-	OpenSea	SCG3	Body	-	-0.08
cg14781735	chrX	122319974	+	S_Shore	GRIA3	Body	-	-0.08
cg14006320	chr4	5889332	+	Island	CRMP1	Body	-	-0.08
cg13198116	chr2	5920502	+	OpenSea	no_gene	no_gene	-	-0.08
cg24042978	chr2	167344458	-	OpenSea	SCN7A	TSS1500	-0.06	-0.08
cg16510342	chrX	71505747	-	OpenSea	no_gene	no_gene	-	-0.08
cg23894215	chr6	133016633	+	OpenSea	VNN1	Body	-	-0.08
cg22736930	chr5	89784871	-	OpenSea	POLR3G	Body	-	-0.08
cg00380954	chr1	194803708	-	OpenSea	no_gene	no_gene	-	-0.08
cg22623133	chr7	27195960	+	Island	HOXA7	1stExon	-	-0.08
cg07274922	chrX	55102690	+	OpenSea	PAGE2B	Body	-	-0.08
cg05316006	chr10	114879619	-	OpenSea	TCF7L2	Body	-	-0.08
cg03088475	chr8	145981210	+	Island	ZNF251	TSS1500	-	-0.08
cg08593949	chr5	17218308	-	Island	NC	NC	-	-0.08
cg00303335	chr7	101385620	-	N_Shore	no_gene	no_gene	-	-0.08
cg02358456	chr4	4167048	+	OpenSea	no_gene	no_gene	-	-0.08
cg02578184	chr3	29563260	+	OpenSea	RBMS3	Body	-	-0.08
cg04011758	chr1	79048111	-	OpenSea	no_gene	no_gene	-	-0.08
cg03450794	chr15	21183212	+	OpenSea	no_gene	no_gene	-	-0.08
cg13554489	chr1	21835685	+	Island	ALPL	TSS200	-	-0.08
cg25831752	chr2	67299624	-	OpenSea	no_gene	no_gene	-	-0.08
cg05137251	chrX	50542290	+	OpenSea	SHROOM4	Body	-	-0.08
cg06059360	chr3	42657618	-	OpenSea	NKTR	Body	-	-0.08
cg17647823	chr2	47290974	-	OpenSea	TTC7A	Body	-	-0.08
cg03766407	chr2	38176669	-	OpenSea	FAM82A1	NC	-	-0.08
cg10569790	chr11	16274134	+	OpenSea	SOX6	Body	-	-0.08
cg17598713	chr6	33265534	+	N_Shore	RGL2	Body	-	-0.08

cg04711998	chr10	7708869	-	OpenSea	ITIH5	NC	-	-0.08
cg26463402	chr14	74003851	+	N_Shore	HEATR4	5'UTR	-0.08	-0.08
cg23630568	chr1	78960610	+	S_Shelf	PTGFR	Body	-	-0.08
cg19878120	chr7	105655497	-	OpenSea	CDHR3	Body	-0.06	-0.08
cg02972486	chr15	59980548	+	N_Shore	BNIP2	Body	-	-0.08
cg25848520	chr11	32619691	+	OpenSea	EIF3M	Body	-	-0.08
cg07831969	chr15	95806407	-	OpenSea	no_gene	no_gene	-	-0.08
cg06819082	chr9	16726627	-	N_Shore	BNC2	Body	-0.08	-0.08
cg04604050	chr5	150007561	-	S_Shelf	SYNPO	Body	-	-0.08
cg16158407	chrX	106449030	-	Island	CXorf41	TSS1500	-	-0.08
cg25740652	chr4	41361623	+	N_Shore	LIMCH1	TSS1500	-	-0.08
cg14262357	chr11	102444955	+	OpenSea	no_gene	no_gene	-	-0.08
cg10249637	chr7	157655436	+	N_Shelf	PTPRN2	Body	-	-0.08
cg05401575	chr3	63428587	-	OpenSea	SYNPR	NC	-0.06	-0.08
cg01737284	chr6	686506	+	OpenSea	EXOC2	NC	-	-0.08
cg23434461	chr8	119803683	+	OpenSea	no_gene	no_gene	-	-0.08
cg04294285	chr8	82620994	+	OpenSea	ZFAND1	Body	-	-0.08
cg14784293	chr15	101812904	-	OpenSea	SELS	3'UTR	-	-0.08
cg21141571	chr3	180260335	+	OpenSea	no_gene	no_gene	-	-0.08
cg02327501	chr14	93389472	-	Island	CHGA	NC	-	-0.08
cg27301645	chr2	88667670	+	OpenSea	no_gene	no_gene	-0.06	-0.08
cg13914982	chr2	190235654	-	OpenSea	no_gene	no_gene	-	-0.08
cg23619970	chr4	148686219	-	OpenSea	ARHGAP10	Body	-	-0.08
cg24907862	chr12	26112480	-	OpenSea	RASSF8	5'UTR	-0.06	-0.08
cg02694446	chr3	168887926	-	OpenSea	MECOM	NC	-	-0.08
cg10605687	chr7	82764087	-	OpenSea	PCLO	Body	-	-0.08
cg13795666	chr1	200618279	-	OpenSea	DDX59	Body	-	-0.08
cg11998579	chr9	78216643	-	OpenSea	MIR548H3	Body	-	-0.08
cg27244703	chr4	97074923	+	OpenSea	no_gene	no_gene	-	-0.08
cg15066837	chr7	79775261	-	OpenSea	GNAI1	Body	-	-0.08

cg14835057	chr3	71802959	-	Island	EIF4E3	5'UTR	-	-0.08
cg10306925	chr3	153161634	+	OpenSea	no_gene	no_gene	-	-0.08
cg24836671	chr5	148029901	+	N_Shelf	HTR4	NC	-	-0.08
cg16472334	chr17	77721757	+	Island	no_gene	no_gene	-	-0.08
cg07037583	chr12	72452357	+	OpenSea	no_gene	no_gene	-0.05	-0.08
cg21617583	chrX	55209265	-	OpenSea	MTRNR2L10	TSS1500	-	-0.08
cg05571912	chr16	87714601	-	Island	JPH3	Body	-	-0.07
cg17233998	chr6	169105683	+	OpenSea	no_gene	no_gene	-	-0.07
cg16927242	chr2	66664667	-	S_Shelf	MEIS1	Body	-	-0.07
cg27017707	chr12	80905121	-	OpenSea	PTPRQ	Body	-	-0.07
cg25350798	chr3	29891518	-	OpenSea	RBMS3	Body	-	-0.07
cg26711011	chr4	87683990	-	OpenSea	PTPN13	Body	-	-0.07
cg27448124	chr14	37669932	-	S_Shelf	MIPOL1	5'UTR	-	-0.07
cg05659160	chr4	86490880	+	OpenSea	ARHGAP24	5'UTR	-	-0.07
cg20223392	chr8	328499	+	OpenSea	no_gene	no_gene	-	-0.07
cg22725764	chr1	218766377	-	OpenSea	MIR548F3	Body	-	-0.07
cg20477705	chrX	11682132	+	N_Shore	ARHGAP6	Body	-	-0.07
cg04064987	chr9	12640151	-	OpenSea	no_gene	no_gene	-	-0.07
cg05795596	chr4	154170783	+	S_Shore	TRIM2	NC	-	-0.07
cg13738068	chr2	64193191	+	OpenSea	VPS54	Body	-	-0.07
cg02297335	chr8	87102011	-	OpenSea	no_gene	no_gene	-	-0.07
cg19107974	chr8	123715888	+	OpenSea	no_gene	no_gene	-	-0.07
cg12405098	chr3	178275369	-	OpenSea	KCNMB2	NC	-0.06	-0.07
cg13135449	chr7	86832969	+	OpenSea	TMEM243	Body	-	-0.07
cg07815324	chr4	43135729	-	OpenSea	no_gene	no_gene	-0.05	-0.07
cg06368141	chr12	54393838	-	Island	NC	TSS200	-	-0.07
cg24334048	chr2	169787256	+	OpenSea	ABCB11	Body	-	-0.07
cg05090036	chr18	42605240	+	OpenSea	SETBP1	Body	-	-0.07
cg15860114	chr10	88133956	+	N_Shelf	no_gene	no_gene	-	-0.07
cg08621893	chr4	123841798	-	N_Shore	NUDT6	NC	-	-0.07

cg20972857	chrX	47468321	+	OpenSea	SYN1	Body	-0.06	-0.07
cg12418190	chr15	37403304	-	S_Shore	no_gene	no_gene	-	-0.07
cg09222993	chr1	144913803	-	OpenSea	PDE4DIP	Body	-	-0.07
cg21195620	chr3	15838030	-	OpenSea	ANKRD28	NC	-0.07	-0.07
cg17181586	chr3	186377713	+	OpenSea	no_gene	no_gene	-	-0.07
cg25893414	chr10	32668805	+	OpenSea	EPC1	TSS1500	-	-0.07
cg12682607	chr3	32634705	+	OpenSea	no_gene	no_gene	-	-0.07
cg12901574	chr12	130931970	-	N_Shelf	RIMBP2	Body	-	-0.07
cg07516958	chr5	57536159	+	OpenSea	no_gene	no_gene	-	-0.07
cg24578404	chr14	25538050	-	OpenSea	no_gene	no_gene	-	-0.07
cg02304425	chr6	7324108	-	OpenSea	no_gene	no_gene	-	-0.07
cg00375389	chr1	225836351	+	N_Shelf	ENAH	Body	-	-0.07
cg10221590	chr10	111765251	-	N_Shore	NC	NC	-	-0.07
cg04628328	chr6	150956939	+	OpenSea	PLEKHG1	5'UTR	-	-0.07
cg15457495	chr7	107388396	-	S_Shelf	CBLL1	Body	-	-0.07
cg03592903	chr5	33737936	+	OpenSea	ADAMTS12	Body	-	-0.07
cg11970327	chr7	40529988	-	OpenSea	SUGCT	Body	-	-0.07
cg16191307	chr12	63754169	-	OpenSea	no_gene	no_gene	-	-0.07
cg25092881	chr10	84574204	-	OpenSea	NRG3	Body	-	-0.07
cg20411036	chr2	189676438	-	OpenSea	no_gene	no_gene	-	-0.07
cg26069299	chr5	140207247	-	N_Shore	PCDHA6	Body	-	-0.07
cg26700386	chr11	10878528	+	N_Shore	ZBED5	5'UTR	-	-0.07
cg16755924	chrX	25041099	-	Island	no_gene	no_gene	-	-0.07
cg09488352	chr6	53950838	-	OpenSea	C6orf142	Body	-	-0.07
cg05818000	chr21	16387536	+	OpenSea	NRIP1	5'UTR	-	-0.07
cg07366871	chr7	95313466	-	OpenSea	no_gene	no_gene	-	-0.07
cg06577144	chr2	33763831	-	OpenSea	RASGRP3	Body	-	-0.07
cg07152070	chrX	135386840	+	OpenSea	ADGRG4	5'UTR	-	-0.07
cg12196858	chrX	9000717	+	OpenSea	FAM9B	Body	-	-0.07
cg15283352	chr6	94595920	+	OpenSea	no_gene	no_gene	-	-0.07

cg19828382	chr4	112851899	-	OpenSea	no_gene	no_gene	-	-0.07
cg19751670	chr8	23088262	-	OpenSea	LOC389641	Body	-	-0.07
cg00637745	chr2	121497334	-	N_Shore	no_gene	no_gene	-	-0.07
cg17985493	chr1	25102228	-	OpenSea	CLIC4	Body	-	-0.07
cg05098943	chr3	24493821	-	OpenSea	THRB	5'UTR	-	-0.07
cg23853291	chr3	101817497	-	OpenSea	no_gene	no_gene	-	-0.07
cg12210824	chrX	120069108	+	N_Shore	NC	Body	-	-0.07
cg19866352	chr12	60517322	+	OpenSea	no_gene	no_gene	-	-0.07
cg10176345	chr2	66775051	-	OpenSea	MEIS1	Body	-	-0.07
cg26777925	chrX	109978710	-	OpenSea	CHRDL1	Body	-	-0.07
cg07047731	chr3	36218374	+	OpenSea	no_gene	no_gene	-	-0.07
ch.1.200256956R	chr1	201990333	+	OpenSea	no_gene	no_gene	-	-0.07
cg05875516	chr2	66930551	-	OpenSea	LOC101927577	TSS200	-	-0.07
cg12849734	chr20	36298899	+	OpenSea	no_gene	no_gene	-	-0.07
cg10009870	chr1	65944241	-	OpenSea	LEPR	5'UTR	-	-0.07
cg00071622	chr4	108814109	+	OpenSea	SGMS2	TSS1500	-	-0.07
cg01632300	chr6	152957223	+	N_Shore	SYNE1	5'UTR	-	-0.07
cg15165735	chr3	99389480	-	OpenSea	COL8A1	5'UTR	-	-0.07
cg11567854	chr12	52427143	+	Island	no_gene	no_gene	-	-0.07
cg15164276	chr3	168269445	+	OpenSea	NC	NC	-	-0.07
cg16589861	chr12	66457341	+	OpenSea	no_gene	no_gene	-	-0.07
cg05383271	chrX	135387028	-	OpenSea	ADGRG4	NC	-	-0.07
cg23102762	chr6	121252563	+	OpenSea	no_gene	no_gene	-	-0.07
cg17446488	chr6	6772111	+	OpenSea	no_gene	no_gene	-	-0.07
cg01750221	chr12	109985316	+	OpenSea	no_gene	no_gene	-	-0.07
cg17326336	chr6	46657943	+	S_Shore	TDRD6	1stExon	-	-0.07
cg02045559	chr21	43540621	-	OpenSea	UMODL1	Body	-	-0.07
cg11252004	chr10	111196813	+	OpenSea	no_gene	no_gene	-	-0.07
cg11824124	chr3	20895788	-	OpenSea	no_gene	no_gene	-	-0.07
cg03072786	chr13	59707460	-	OpenSea	no_gene	no_gene	-	-0.07

cg03744796	chr18	42277045	-	OpenSea	SETBP1	5'UTR	-	-0.07
cg00319034	chr6	162670883	+	OpenSea	PARK2	Body	-	-0.07
cg17120120	chr13	73798709	-	OpenSea	no_gene	no_gene	-	-0.07
cg17348722	chr17	7588137	+	N_Shore	TP53	5'UTR	-	-0.07
cg08310364	chr9	21369542	+	OpenSea	IFNA13	TSS1500	-	-0.07
cg27525731	chr7	47343605	+	OpenSea	TNS3	Body	-	-0.07
cg27196695	chr10	134571377	-	OpenSea	INPP5A	Body	-	-0.07
cg03962846	chr7	39053253	+	OpenSea	POU6F2	Body	-	-0.07
cg05445398	chr18	587097	-	OpenSea	no_gene	no_gene	-	-0.07
cg22468974	chr5	165036317	+	OpenSea	no_gene	no_gene	-	-0.07
cg24859854	chr3	167619765	+	OpenSea	LINC01330	Body	-	-0.07
cg27353099	chr4	88500875	+	OpenSea	no_gene	no_gene	-	-0.07
cg11219547	chr2	103066509	-	OpenSea	IL18RAP	Body	-	-0.07
cg23506331	chr14	63786048	+	OpenSea	GPHB5	TSS1500	-	-0.07
cg23935630	chr2	136396139	-	OpenSea	R3HDM1	Body	-	-0.07
cg03146533	chr4	74587910	-	OpenSea	no_gene	no_gene	-	-0.07
cg12828313	chr6	28744086	-	OpenSea	no_gene	no_gene	-	-0.07
cg11964772	chr13	76585950	-	OpenSea	no_gene	no_gene	-	-0.07
cg11150240	chr12	103698917	+	S_Shelf	C12orf42	Body	-	-0.07
cg02203420	chr9	19786951	+	N_Shore	SLC24A2	TSS200	-	-0.07
cg02076869	chr7	155301917	+	N_Shore	CNPY1	5'UTR	-	-0.07
cg07047532	chr4	166435972	+	OpenSea	no_gene	no_gene	-	-0.07
cg19702945	chrX	13612989	+	OpenSea	EGFL6	Body	-	-0.07
cg03777697	chr13	32921647	-	OpenSea	BRCA2	Body	-	-0.07
cg19618601	chr2	6644914	+	OpenSea	no_gene	no_gene	-	-0.07
cg26014594	chrX	107920300	+	OpenSea	COL4A5	Body	-	-0.07
cg07200490	chr6	138550505	+	OpenSea	KIAA1244	Body	-	-0.07
cg21187265	chr1	26127185	-	OpenSea	SEPN1	Body	-	-0.07
cg13943333	chr4	87959251	-	OpenSea	AFF1	Body	-	-0.07
cg19366091	chr12	44292779	+	OpenSea	TMEM117	Body	-0.06	-0.07

cg03881289	chr14	86334011	+	OpenSea	no_gene	no_gene	-	-0.07
cg00799619	chr4	39458346	-	N_Shore	RPL9	Body	-	-0.07
cg26379583	chr22	18399002	+	OpenSea	MICAL3	5'UTR	-	-0.07
cg01822559	chr7	67581481	-	OpenSea	no_gene	no_gene	-	-0.07
cg17558093	chr7	77039902	+	OpenSea	GSAP	Body	-	-0.07
cg27177112	chr18	58221283	+	OpenSea	no_gene	no_gene	-	-0.07
cg19688957	chr2	67147346	-	OpenSea	LOC101060019	Body	-	-0.07
cg07882863	chr6	132858438	-	OpenSea	TAAR9	TSS1500	-	-0.07
cg02621217	chrX	38020673	+	OpenSea	SRPX	Body	-	-0.07
cg13873305	chr5	174995026	+	OpenSea	no_gene	no_gene	-	-0.07
cg03095028	chr12	62222128	-	OpenSea	FAM19A2	Body	-	-0.07
cg13396038	chr6	141766970	-	OpenSea	no_gene	no_gene	-0.06	-0.07
cg11903155	chr20	14517564	-	OpenSea	MACROD2	Body	-	-0.07
cg12601520	chr3	78079090	-	OpenSea	no_gene	no_gene	-	-0.07
cg00638797	chr15	52447793	+	OpenSea	GNB5	Body	-	-0.07
cg16728241	chr4	106851879	+	OpenSea	NPNT	Body	-	-0.07
cg11774469	chr9	8888118	-	OpenSea	PTPRD	5'UTR	-	-0.07
cg26554253	chr3	79081833	-	OpenSea	ROBO1	Body	-	-0.07
cg19152851	chr12	38941731	+	OpenSea	no_gene	no_gene	-	-0.07
cg06722433	chr4	57238016	+	OpenSea	AASDH	Body	-	-0.07
cg27466454	chr1	212474113	-	OpenSea	PPP2R5A	NC	-	-0.07
cg20494215	chr7	40743543	-	OpenSea	SUGCT	Body	-	-0.07
cg14153112	chr18	3846438	-	OpenSea	DLGAP1	Body	-	-0.07
cg05308498	chr10	62174599	-	OpenSea	ANK3	Body	-	-0.07
cg01234248	chr12	26150045	+	OpenSea	RASSF8	5'UTR	-	-0.07
cg24789231	chr2	154720727	-	OpenSea	no_gene	no_gene	-	-0.07
cg26602760	chr4	69299485	-	OpenSea	no_gene	no_gene	-	-0.07
cg15551284	chr4	161240040	+	OpenSea	no_gene	no_gene	-	-0.07
cg07367602	chr7	115963592	-	OpenSea	no_gene	no_gene	-	-0.07
cg23067676	chrX	40141241	-	OpenSea	LOC101927476	Body	-0.05	-0.07

cg06494218	chr3	149359618	+	OpenSea	WWTR1	Body	-	-0.07
cg08912801	chr1	3399260	-	OpenSea	no_gene	no_gene	-	-0.07
cg08434621	chr13	28860661	-	OpenSea	PAN3	Body	-	-0.07
cg23497644	chr2	170654835	+	N_Shore	SSB	TSS1500	-	-0.07
cg25834692	chr3	29535414	+	OpenSea	RBMS3	Body	-	-0.07
cg09747456	chr10	91405300	-	S_Shore	PANK1	TSS200	-	-0.07
cg15406387	chr4	111397332	-	N_Shore	ENPEP	NC	-	-0.07
cg12423935	chr7	39126804	+	OpenSea	POU6F2	Body	-	-0.07
cg06477289	chr2	191400034	+	S_Shore	NEMP2	TSS1500	-	-0.07
cg26740119	chrX	4183329	+	OpenSea	no_gene	no_gene	-	-0.07
cg23213876	chr1	53924164	+	N_Shore	DMRTB1	TSS1500	-	-0.07
cg20073272	chr14	59650772	-	N_Shelf	no_gene	no_gene	-	-0.07
cg10226239	chr4	159985743	-	OpenSea	no_gene	no_gene	-	-0.07
cg22508969	chr6	55444091	-	Island	HMGCLL1	TSS200	-	-0.07
cg18291443	chr3	157178134	+	OpenSea	VEPH1	Body	-	-0.07
cg11472725	chr6	138938931	-	OpenSea	no_gene	no_gene	-	-0.07
cg03208936	chr1	98515087	-	N_Shelf	no_gene	no_gene	-	-0.07
cg20387884	chr14	80326076	+	N_Shore	NRXN3	Body	-	-0.07
cg12697186	chrX	71353459	+	S_Shore	NHSL2	Body	-	-0.07
cg21157357	chr5	140851830	-	N_Shelf	PCDHGA11	Body	-	-0.07
cg14360133	chr11	115378277	-	S_Shelf	no_gene	no_gene	-	-0.07
cg11944980	chr13	39625057	-	OpenSea	no_gene	no_gene	-	-0.07
cg24876314	chr5	60457326	+	N_Shore	NC	NC	-	-0.07
cg01914621	chr7	155260474	-	Island	no_gene	no_gene	-	-0.07
cg22180958	chr6	29055509	+	OpenSea	OR2B3	TSS1500	-	-0.07
cg23826993	chr8	58168222	+	N_Shelf	no_gene	no_gene	-	-0.07
cg26879773	chr2	121405238	-	OpenSea	no_gene	no_gene	-	-0.07
cg12235136	chr20	16727967	+	OpenSea	OTOR	TSS1500	-	-0.07
cg04523769	chr7	115445758	-	OpenSea	no_gene	no_gene	-	-0.07
cg13169954	chr1	52681425	-	OpenSea	ZFYVE9	5'UTR	-	-0.07

cg00963496	chr6	32154023	-	OpenSea	PBX2	3'UTR	-	-0.07
cg10508780	chr2	150681878	-	OpenSea	no_gene	no_gene	-	-0.07
cg06066032	chr13	48369175	-	OpenSea	no_gene	no_gene	-	-0.07
cg16030541	chr21	20716658	-	OpenSea	no_gene	no_gene	-	-0.07
cg19183436	chr16	67207740	-	N_Shore	NOL3	5'UTR	-	-0.07
cg19149664	chr4	125351027	-	OpenSea	no_gene	no_gene	-	-0.07
cg14375976	chr13	29098268	+	OpenSea	no_gene	no_gene	-0.05	-0.07
cg00793432	chr20	7997443	+	N_Shelf	TMX4	Body	-	-0.07
cg16296210	chr8	18541785	+	OpenSea	PSD3	Body	-	-0.07
cg23549892	chr4	20542259	+	OpenSea	SLIT2	Body	-	-0.07
cg12294112	chr12	77556843	-	OpenSea	no_gene	no_gene	-	-0.07
cg01446393	chr3	58563609	-	OpenSea	FAM107A	TSS200	-	-0.07
cg21614686	chr4	86352691	+	OpenSea	no_gene	no_gene	-	-0.07
cg11639001	chr11	117198156	-	N_Shore	CEP164	TSS1500	-	-0.07
cg02638458	chr7	155301811	+	N_Shore	CNPY1	5'UTR	-	-0.07
cg00994784	chr5	111566245	-	OpenSea	NC	Body	-	-0.07
cg03971661	chr2	139657512	+	N_Shelf	no_gene	no_gene	-	-0.07
cg11493571	chr7	83638285	-	OpenSea	SEMA3A	Body	-	-0.07
cg07902059	chr4	104013139	+	OpenSea	BDH2	Body	-	-0.07
cg13885150	chr4	91155076	-	OpenSea	CCSER1	NC	-	-0.07
cg22462983	chr6	133561756	+	N_Shore	EYA4	TSS1500	-	-0.07
cg23052520	chr11	18244784	-	OpenSea	no_gene	no_gene	-	-0.07
cg07366579	chr4	70254835	-	OpenSea	no_gene	no_gene	-	-0.07
cg00806644	chr10	126889815	+	OpenSea	no_gene	no_gene	-	-0.06
cg23759400	chr11	107187006	+	OpenSea	no_gene	no_gene	-	-0.06
cg18265579	chr12	76231691	+	OpenSea	no_gene	no_gene	-	-0.06
cg01647019	chrX	14547618	+	OpenSea	GLRA2	NC	-	-0.06
cg05478168	chr3	70255988	+	OpenSea	no_gene	no_gene	-	-0.06
cg17085774	chr3	160394526	-	OpenSea	ARL14	TSS1500	-	-0.06
cg05198817	chrX	122995701	-	S_Shore	XIAP	5'UTR	-	-0.06

cg15066656	chr2	172861329	+	N_Shelf	no_gene	no_gene	-	-0.06
cg05395403	chr13	28496641	+	N_Shore	PDX1	Body	-	-0.06
cg02784102	chr1	206317510	-	OpenSea	CTSE	NC	-	-0.06
cg18153989	chrX	113949673	+	OpenSea	NC	NC	-	-0.06
cg16612422	chr3	29738084	+	OpenSea	RBMS3	Body	-	-0.06
cg21827947	chr8	86255324	-	OpenSea	CA1	5'UTR	-	-0.06
cg20116513	chr12	16237483	-	OpenSea	no_gene	no_gene	-	-0.06
cg22035312	chr7	116212568	+	OpenSea	LINC01510	Body	-	-0.06
cg05632718	chr20	49066839	-	OpenSea	no_gene	no_gene	-	-0.06
cg05216534	chr8	29945944	-	OpenSea	MIR548O2	Body	-	-0.06
cg12565985	chr2	220291396	-	OpenSea	DES	3'UTR	-	-0.06
cg11122255	chr10	24995583	+	OpenSea	ARHGAP21	Body	-0.05	-0.06
cg13059737	chr21	16315109	+	OpenSea	no_gene	no_gene	-	-0.06
cg19238325	chr3	51988425	-	N_Shore	GPR62	TSS1500	-	-0.06
cg17266282	chr6	112294532	-	OpenSea	no_gene	no_gene	-	-0.06
cg03185698	chr3	164841471	+	OpenSea	no_gene	no_gene	-	-0.06
cg12018865	chr2	38406881	+	OpenSea	C2orf58	Body	-	-0.06
cg15423200	chr8	52589863	-	OpenSea	PXDNL	Body	-0.08	-0.06
cg05797854	chr6	155739835	-	OpenSea	NOX3	Body	-	-0.06
cg08958149	chr18	58735951	+	OpenSea	no_gene	no_gene	-	-0.06
cg27652723	chr17	67172872	-	OpenSea	ABCA10	Body	-	-0.06
cg00329695	chr14	37643265	-	S_Shore	SLC25A21	TSS1500	-	-0.06
cg09734394	chr7	20818887	+	S_Shore	no_gene	no_gene	-	-0.06
cg19508967	chr5	1840347	+	OpenSea	no_gene	no_gene	-0.05	-0.06
cg21232023	chr6	137820393	+	S_Shore	no_gene	no_gene	-	-0.06
cg03567055	chr9	84108400	+	OpenSea	no_gene	no_gene	-	-0.06
cg16630085	chr6	132580009	-	OpenSea	no_gene	no_gene	-	-0.06
cg11981328	chr9	138501333	-	OpenSea	no_gene	no_gene	-	-0.06
cg16172906	chr21	47707096	-	S_Shore	YBEY	Body	-	-0.06
cg23004862	chr5	175669020	-	S_Shelf	C5orf25	Body	-	-0.06

cg25669309	chr4	184826324	-	Island	STOX2	TSS200	-	-0.06
cg05895665	chr7	20818725	+	S_Shore	no_gene	no_gene	-	-0.06
cg09529310	chr14	51955743	-	OpenSea	NC	NC	-	-0.06
cg05920182	chr1	187411929	+	OpenSea	no_gene	no_gene	-	-0.06
cg26488672	chr7	24301747	+	OpenSea	no_gene	no_gene	-	-0.06
cg18141622	chr2	238525524	-	OpenSea	no_gene	no_gene	-	-0.06
cg13515095	chr10	70482115	-	S_Shore	CCAR1	5'UTR	-	-0.06
cg11195065	chr10	119292371	+	N_Shore	EMX2OS	Body	-0.05	-0.06
cg03271936	chr19	31557649	-	OpenSea	no_gene	no_gene	-	-0.06
cg24445278	chr7	79613751	-	OpenSea	no_gene	no_gene	-	-0.06
cg09671227	chr6	149511213	-	OpenSea	no_gene	no_gene	-	-0.06
cg09408520	chr2	157188965	+	N_Shore	NR4A2	5'UTR	-	-0.06
cg08495884	chr3	181614260	+	OpenSea	no_gene	no_gene	-	-0.06
cg26422223	chr4	124858308	+	OpenSea	no_gene	no_gene	-	-0.06
cg16132580	chr16	21028167	+	OpenSea	DNAH3	Body	-	-0.06
cg05915658	chrX	132552653	+	S_Shelf	no_gene	no_gene	-	-0.06
cg11978435	chr4	21546545	+	OpenSea	KCNIP4	NC	-	-0.06
cg17016559	chr22	46067508	+	Island	ATXN10	TSS200	-0.05	-0.06
cg01445130	chr21	16545422	-	OpenSea	no_gene	no_gene	-	-0.06
cg14160394	chr11	83563280	+	OpenSea	DLG2	Body	-	-0.06
cg02071806	chr15	69857379	-	OpenSea	DRAIC	Body	-	-0.06
cg03863606	chr7	12687574	+	OpenSea	SCIN	Body	-	-0.06
cg22919173	chr1	78356538	+	S_Shore	NEXN	5'UTR	-	-0.06
cg00927151	chr6	155146530	-	OpenSea	SCAF8	Body	-	-0.06
cg16663059	chr18	20420224	-	OpenSea	no_gene	no_gene	-	-0.06
cg02405813	chr6	83072522	+	N_Shore	TPBG	TSS1500	-	-0.06
cg01403803	chr5	123987218	-	N_Shore	ZNF608	Body	-	-0.06
cg04635364	chr4	138889982	+	OpenSea	no_gene	no_gene	-	-0.06
cg01171456	chr7	2726646	+	N_Shore	AMZ1	5'UTR	-	-0.06
cg20537521	chr12	52538433	-	OpenSea	no_gene	no_gene	-	-0.06

cg15941800	chr2	231126785	-	OpenSea	SP140	Body	-	-0.06
cg20628209	chr11	31326672	+	OpenSea	DCDC1	Body	-	-0.06
cg08466256	chr2	189957139	+	OpenSea	COL5A2	Body	-	-0.06
cg07582229	chr12	22171966	-	OpenSea	no_gene	no_gene	-	-0.06
cg24578769	chr2	8692174	-	OpenSea	no_gene	no_gene	-	-0.06
cg01116383	chr10	60410566	-	OpenSea	BICC1	Body	-	-0.06
cg24981400	chr2	100047526	+	OpenSea	REV1	Body	-	-0.06
cg22587673	chr8	36746190	+	OpenSea	KCNU1	Body	-	-0.06
cg04799002	chr8	117862551	+	OpenSea	RAD21	Body	-	-0.06
cg10075774	chr5	127626430	-	OpenSea	FBN2	NC	-	-0.06
cg11839719	chr21	44525367	+	N_Shore	U2AF1	Body	-	-0.06
cg08250990	chr16	49630178	+	OpenSea	ZNF423	Body	-	-0.06
cg07016258	chr15	83953929	+	Island	BNC1	TSS1500	-	-0.06
cg08531298	chr11	15515888	-	OpenSea	no_gene	no_gene	-0.07	-0.06
cg15727409	chrX	38079723	-	Island	SRPX	Body	-	-0.06
cg26103798	chr6	146660979	+	OpenSea	GRM1	Body	-	-0.06
cg02818728	chr4	189079272	+	N_Shore	no_gene	no_gene	-	-0.06
cg27295143	chr3	32986923	+	OpenSea	no_gene	no_gene	-	-0.06
cg00628674	chr9	108311552	+	OpenSea	FSD1L	3'UTR	-	-0.06
cg05040622	chr6	144142565	+	OpenSea	PHACTR2	Body	-	-0.06
cg06529747	chr1	183884763	-	OpenSea	RGL1	Body	-	-0.06
cg20577102	chr20	39966297	-	N_Shelf	no_gene	no_gene	-	-0.06
cg02228046	chr6	28950633	-	OpenSea	no_gene	no_gene	-	-0.06
cg16351410	chr11	49049039	-	OpenSea	no_gene	no_gene	-	-0.06
cg08870977	chr2	168292014	+	OpenSea	no_gene	no_gene	-	-0.06
cg04147741	chr3	64991635	-	OpenSea	no_gene	no_gene	-	-0.06
cg22875510	chr12	39600456	+	OpenSea	no_gene	no_gene	-	-0.06
cg18011088	chr6	28740611	-	OpenSea	no_gene	no_gene	-	-0.06
cg25076678	chr4	4172379	-	OpenSea	no_gene	no_gene	-	-0.06
cg08988226	chr3	133191851	-	OpenSea	BFSP2	Body	-	-0.06

cg10480476	chr19	47918372	-	N_Shelf	MEIS3	NC	-	-0.06
cg06684183	chr7	45601714	-	OpenSea	no_gene	no_gene	-	-0.06
cg01352526	chr2	66930502	-	OpenSea	LOC101927577	TSS200	-	-0.06
cg09160330	chr6	46760919	-	OpenSea	MEP1A	TSS200	-0.07	-0.06
cg14336221	chrX	47566479	-	OpenSea	CXXC1P1	TSS200	-	-0.06
cg00036045	chrX	49945417	+	OpenSea	no_gene	no_gene	-	-0.06
cg17952980	chr1	63687655	-	OpenSea	no_gene	no_gene	-	-0.06
cg16639417	chr3	192660793	+	OpenSea	no_gene	no_gene	-	-0.06
cg15355800	chr10	120895864	+	OpenSea	FAM45A	Body	-	-0.06
cg25721442	chrX	133478225	+	OpenSea	no_gene	no_gene	-	-0.06
cg09719772	chr9	102065912	-	OpenSea	no_gene	no_gene	-	-0.06
cg08179308	chr2	21442643	-	OpenSea	no_gene	no_gene	-	-0.06
cg20737242	chr4	126311441	+	OpenSea	FAT4	Body	-	-0.06
cg00688756	chr6	30706518	+	N_Shelf	FLOT1	Body	-	-0.06
cg10366596	chr3	28768725	-	OpenSea	LINC00693	Body	-	-0.06
cg01833895	chr4	106819158	-	S_Shore	NPNT	NC	-	-0.06
cg18211258	chr2	32779043	-	OpenSea	BIRC6	Body	-	-0.06
cg25006998	chr11	119897638	+	OpenSea	no_gene	no_gene	-	-0.06
cg01074318	chr3	191823430	-	OpenSea	no_gene	no_gene	-	-0.06
cg19808663	chr12	69978651	+	N_Shore	CCT2	TSS1500	-	-0.06
cg18597321	chr4	124737893	+	OpenSea	LINC01091	Body	-	-0.06
cg15332173	chr6	76074059	-	OpenSea	FILIP1	Body	-	-0.06
cg11502844	chr2	15731364	-	N_Shore	DDX1	TSS1500	-	-0.06
cg12993838	chr6	163608472	-	OpenSea	PACRG	Body	-	-0.06
cg04837483	chr3	52303959	+	OpenSea	WDR82	Body	-	-0.06
cg14451560	chr9	140499397	-	N_Shore	ARRDC1	TSS1500	-	-0.06
cg00661732	chr3	61860646	+	OpenSea	PTPRG	Body	-	-0.06
cg02993094	chr16	87110195	+	OpenSea	no_gene	no_gene	-	-0.06
cg00693710	chr8	102313771	+	OpenSea	no_gene	no_gene	-	-0.06
cg03467813	chr6	3851047	+	Island	FAM50B	3'UTR	-	-0.06

cg26808134	chr8	87385911	-	OpenSea	WWP1	5'UTR	-	-0.06
cg19868125	chr7	4153919	+	S_Shore	SDK1	Body	-	-0.06
cg03570708	chr5	133135701	+	OpenSea	no_gene	no_gene	-0.05	-0.06
cg10822948	chr4	107462541	+	OpenSea	no_gene	no_gene	-	-0.06
cg03425379	chr7	38734128	+	OpenSea	no_gene	no_gene	-	-0.06
cg08940326	chrX	39511706	+	OpenSea	no_gene	no_gene	-	-0.06
cg13683848	chr3	40960648	+	OpenSea	no_gene	no_gene	-	-0.06
cg10289926	chr22	45961452	-	OpenSea	FBLN1	NC	-	-0.06
cg11701367	chr5	56644736	-	OpenSea	no_gene	no_gene	-	-0.06
cg07392324	chr7	107645340	-	S_Shore	no_gene	no_gene	-	-0.06
cg24056365	chr1	110834615	+	OpenSea	no_gene	no_gene	-	-0.06
cg24533720	chr7	6099233	-	S_Shore	EIF2AK1	TSS1500	-	-0.06
cg14287794	chr2	163034394	+	OpenSea	FAP	Body	-	-0.06
cg09439867	chr10	120018076	+	OpenSea	no_gene	no_gene	-	-0.06
cg21219617	chr7	115201712	+	OpenSea	no_gene	no_gene	-	-0.06
cg09858004	chr22	19654413	-	OpenSea	no_gene	no_gene	-	-0.06
cg24602066	chr1	238769374	-	OpenSea	no_gene	no_gene	-	-0.06
cg05148629	chr6	168230116	-	S_Shore	MLLT4	Body	-	-0.06
cg03974621	chr12	129637133	-	OpenSea	TMEM132D	Body	-	-0.06
cg21621826	chr3	152974586	-	OpenSea	no_gene	no_gene	-	-0.06
cg25008317	chr8	75839311	+	OpenSea	no_gene	no_gene	-	-0.06
cg10542266	chr8	125893601	+	OpenSea	no_gene	no_gene	-	-0.06
cg13988558	chr1	14347415	-	OpenSea	no_gene	no_gene	-	-0.06
cg04089420	chr10	1378575	-	N_Shelf	ADARB2	Body	-	-0.06
cg06719949	chr15	39448875	-	OpenSea	no_gene	no_gene	-	-0.06
cg15949396	chr8	57837978	+	OpenSea	no_gene	no_gene	-	-0.06
cg03130663	chr10	37965751	-	N_Shelf	no_gene	no_gene	-	-0.06
cg18190286	chr2	54067920	+	OpenSea	GPR75-ASB3	Body	-	-0.06
cg11190953	chr8	6229904	+	OpenSea	no_gene	no_gene	-	-0.06
cg14531751	chr4	74374150	+	OpenSea	LOC728040	TSS1500	-	-0.06

cg05245650	chr2	37900205	+	S_Shore	CDC42EP3	TSS1500	-	-0.06
cg26469220	chr13	75736246	+	OpenSea	no_gene	no_gene	-	-0.06
cg21780117	chr6	49874487	+	OpenSea	no_gene	no_gene	-	-0.06
cg07214954	chr5	123997879	+	OpenSea	ZNF608	Body	-	-0.06
cg13781574	chrX	69675294	+	Island	DLG3	Body	-	-0.06
cg11683013	chr4	26824269	-	OpenSea	no_gene	no_gene	-	-0.06
cg09038569	chr5	89240289	+	OpenSea	no_gene	no_gene	-	-0.06
cg06397011	chr1	66379189	-	OpenSea	PDE4B	Body	-	-0.06
cg26387064	chr2	189599296	+	OpenSea	DIRC1	3'UTR	-	-0.06
cg06351537	chr22	49798750	-	Island	no_gene	no_gene	-	-0.06
cg05089090	chr13	37005570	+	N_Shore	CCNA1	TSS1500	-	-0.06
cg15803972	chr2	171319056	-	OpenSea	MYO3B	Body	-	-0.06
cg22672403	chr5	39730454	+	OpenSea	no_gene	no_gene	-	-0.06
cg12440885	chrX	57164610	+	S_Shore	SPIN2A	TSS1500	-	-0.06
cg14383480	chr2	168043663	-	OpenSea	XIRP2	Body	-0.05	-0.06
cg18211686	chr5	125929591	+	N_Shore	ALDH7A1	Body	-	-0.06
cg14690386	chrX	8726232	+	OpenSea	no_gene	no_gene	-	-0.06
cg25166271	chr13	71034012	+	OpenSea	no_gene	no_gene	-	-0.06
cg00182781	chr18	58377732	-	OpenSea	no_gene	no_gene	-	-0.06
cg07306737	chr6	33247141	-	S_Shore	WDR46	Body	-	-0.06
cg12403591	chr17	68763247	+	OpenSea	no_gene	no_gene	-	-0.06
cg00013952	chr11	66563344	-	OpenSea	C11orf80	Body	-	-0.06
cg04117798	chr14	47238968	-	OpenSea	no_gene	no_gene	-	-0.06
cg15498667	chr8	93889931	-	OpenSea	no_gene	no_gene	-	-0.06
cg04167096	chr2	227001602	+	OpenSea	no_gene	no_gene	-	-0.06
cg18701707	chr3	178560988	-	OpenSea	KCNMB2	3'UTR	-	-0.06
cg19243860	chr5	34841961	-	S_Shelf	TTC23L	Body	-	-0.06
cg22732561	chr2	28791389	+	S_Shore	PLB1	Body	-	-0.06
cg00488445	chr1	74929641	-	OpenSea	FPGT-TNNI3K	Body	-	-0.06
cg00967261	chr3	171392505	-	OpenSea	PLD1	Body	-	-0.06

cg15378061	chr7	93638064	-	OpenSea	no_gene	no_gene	-	-0.06
cg04104541	chr4	68996142	-	OpenSea	TMPRSS11F	TSS1500	-	-0.06
cg23614428	chr1	172498191	+	N_Shelf	no_gene	no_gene	-	-0.06
cg06813871	chr11	68325629	-	OpenSea	PPP6R3	Body	-	-0.06
cg21803428	chr12	59317318	+	S_Shelf	no_gene	no_gene	-	-0.06
cg18052369	chr5	99970791	+	OpenSea	no_gene	no_gene	-0.05	-0.06
cg19969391	chr18	24167674	+	OpenSea	KCTD1	NC	-	-0.06
cg09331881	chrX	102840170	+	N_Shore	TCEAL4	TSS1500	-	-0.06
cg27208212	chrX	30743534	-	OpenSea	GK	Body	-	-0.06
cg06551230	chr13	35714053	-	OpenSea	NBEA	Body	-	-0.06
cg12644411	chr2	240202361	+	OpenSea	HDAC4	Body	-	-0.06
cg16591450	chr4	165670119	+	OpenSea	no_gene	no_gene	-	-0.06
cg00250948	chr11	9514702	-	OpenSea	ZNF143	Body	-	-0.06
cg03969721	chr5	132437251	-	OpenSea	HSPA4	Body	-	-0.06
cg00526629	chr1	187378159	-	OpenSea	no_gene	no_gene	-	-0.06
cg00572889	chr1	230493461	+	S_Shore	PGBD5	Body	-	-0.06
cg11134322	chr5	40759194	+	S_Shelf	no_gene	no_gene	-	-0.06
cg00016418	chr5	82840805	+	OpenSea	VCAN	Body	-	-0.06
cg03127229	chr22	28277279	-	OpenSea	PITPNB	Body	-	-0.06
cg21157319	chr11	64636635	-	OpenSea	EHD1	Body	-	-0.06
cg26033657	chr17	66507816	-	Island	PRKAR1A	TSS1500	-	-0.06
cg04452501	chr6	53882728	-	OpenSea	MLIP	TSS1500	-	-0.06
cg13798000	chr20	7239807	-	OpenSea	no_gene	no_gene	-	-0.06
cg12923242	chr11	2994562	+	OpenSea	NAP1L4	Body	-	-0.06
cg26568330	chr5	60040736	+	S_Shore	no_gene	no_gene	-	-0.06
cg02110991	chr1	66370373	-	OpenSea	PDE4B	5'UTR	-	-0.06
cg08665687	chr5	143408198	+	OpenSea	no_gene	no_gene	-	-0.06
cg19519721	chr13	74070925	-	OpenSea	no_gene	no_gene	-	-0.06
cg24922877	chr12	93095981	+	OpenSea	C12orf74	TSS1500	-	-0.06
cg18470350	chr1	90454939	-	OpenSea	no_gene	no_gene	-	-0.06

cg11362904	chr2	43861377	-	N_Shelf	no_gene	no_gene	-	-0.06
cg06068891	chrX	135228207	-	N_Shore	FHL1	TSS1500	-	-0.06
cg16777028	chr14	66976276	-	S_Shore	GPHN	Body	-	-0.06
cg27072333	chr3	100711638	+	OpenSea	ABI3BP	Body	-	-0.06
cg08933268	chrX	41783837	+	S_Shore	no_gene	no_gene	-	-0.06
cg05529123	chr2	66910386	+	OpenSea	no_gene	no_gene	-	-0.06
cg02087985	chr1	151665715	-	OpenSea	SNX27	Body	-	-0.06
cg06199692	chrX	67430298	+	OpenSea	OPHN1	Body	-	-0.06
cg11985492	chr4	86681976	-	OpenSea	ARHGAP24	Body	-	-0.06
cg11873772	chr1	186430252	-	OpenSea	NC	Body	-	-0.06
cg00226689	chr7	41259421	-	OpenSea	no_gene	no_gene	-0.07	-0.06
cg15416661	chr6	28725789	-	OpenSea	no_gene	no_gene	-0.06	-0.06
cg02090654	chr7	126698344	-	OpenSea	GRM8	Body	-	-0.06
cg03997658	chr6	53964271	-	OpenSea	MLIP	Body	-	-0.06
cg20021806	chrX	68350862	-	S_Shelf	no_gene	no_gene	-	-0.06
cg22292016	chrX	111390240	-	OpenSea	ZCCHC16	5'UTR	-	-0.06
cg05409693	chr12	78680140	+	OpenSea	no_gene	no_gene	-	-0.06
cg26155503	chrX	139049552	-	OpenSea	no_gene	no_gene	-	-0.06
cg03555477	chr3	145678138	+	OpenSea	no_gene	no_gene	-	-0.06
cg05215498	chr17	68227252	+	OpenSea	no_gene	no_gene	-	-0.06
cg04125341	chr3	139656251	-	S_Shore	CLSTN2	Body	-	-0.06
cg27064605	chr20	13527267	+	OpenSea	TASP1	Body	-	-0.06
cg24549158	chr3	191001320	+	OpenSea	UTS2B	5'UTR	-	-0.06
cg13730193	chr7	99149509	-	Island	C7orf38	NC	-	-0.06
cg19045344	chrX	84364350	+	OpenSea	SATL1	TSS1500	-	-0.06
cg14273518	chr19	50084415	+	S_Shore	NOSIP	TSS1500	-	-0.06
cg18589513	chr7	99766643	-	N_Shelf	GAL3ST4	TSS1500	-	-0.06
cg03216475	chr1	9066015	-	OpenSea	SLC2A7	Body	-	-0.06
cg22903908	chr10	64578919	-	S_Shore	EGR2	NC	-	-0.06
cg08576959	chr5	58160593	-	OpenSea	no_gene	no_gene	-	-0.06

cg10730208	chr12	58290540	+	S_Shore	no_gene	no_gene	-	-0.06
cg09516121	chr4	72904216	-	OpenSea	NPFFR2	TSS1500	-	-0.06
cg00108694	chr5	55598438	-	OpenSea	no_gene	no_gene	-	-0.06
cg12480180	chr2	190748200	-	OpenSea	no_gene	no_gene	-	-0.06
cg00022064	chrX	40906133	-	OpenSea	no_gene	no_gene	-	-0.06
cg08733374	chr14	37640922	+	N_Shore	SLC25A21	Body	-	-0.06
cg08942734	chr9	86585713	+	OpenSea	HNRNPK	Body	-	-0.06
cg19498356	chr18	9141063	+	S_Shelf	ANKRD12	5'UTR	-	-0.06
cg03539071	chr5	58351706	+	OpenSea	PDE4D	Body	-	-0.06
cg25667841	chr20	61051762	-	Island	GATA5	TSS1500	-	-0.06
cg18125814	chr11	49455214	+	N_Shore	no_gene	no_gene	-	-0.06
cg20819345	chr6	78590360	+	OpenSea	MEI4	Body	-	-0.06
cg05471616	chr12	29778034	-	OpenSea	TMTC1	Body	-	-0.06
cg02989453	chr10	995095	+	OpenSea	no_gene	no_gene	-	-0.06
cg21831931	chr3	5137953	+	Island	no_gene	no_gene	-	-0.06
cg21696987	chr6	33140459	+	OpenSea	COL11A2	Body	-	-0.06
cg02494440	chr13	86172218	-	OpenSea	no_gene	no_gene	-	-0.06
cg00829646	chr7	15758936	-	OpenSea	no_gene	no_gene	-	-0.06
cg00203409	chr9	72791817	-	OpenSea	MAMDC2	Body	-	-0.06
cg13895853	chr3	78937525	+	OpenSea	ROBO1	Body	-	-0.06
cg14805060	chr16	30640740	+	OpenSea	no_gene	no_gene	-	-0.06
cg00394180	chr8	97167170	-	N_Shelf	GDF6	Body	-	-0.06
cg17398515	chr8	102092795	-	Island	no_gene	no_gene	-	-0.06
cg09985226	chr8	18656716	+	OpenSea	PSD3	Body	-	-0.06
cg09078504	chr9	106763782	-	S_Shore	no_gene	no_gene	-	-0.06
cg19916413	chr8	91925160	+	OpenSea	NECAB1	Body	-	-0.06
cg04215359	chr2	153381623	-	OpenSea	FMNL2	Body	-	-0.06
cg17731524	chr3	27235572	-	OpenSea	NEK10	Body	-	-0.06
cg01853526	chr2	220555667	+	OpenSea	no_gene	no_gene	-	-0.06
cg00510330	chr6	39916111	-	OpenSea	no_gene	no_gene	-	-0.06

cg22901490	chr5	110087806	+	OpenSea	SLC25A46	Body	-	-0.06
cg16126754	chr10	133156058	-	OpenSea	no_gene	no_gene	-	-0.06
cg07298447	chr10	99625810	+	OpenSea	NC	NC	-	-0.06
cg00705653	chr6	132946634	+	OpenSea	TAAR2	TSS1500	-	-0.06
cg01472026	chrX	101187257	+	Island	ZMAT1	TSS1500	-	-0.06
cg13571540	chrX	23801624	-	Island	SAT1	Body	-	-0.06
cg11180750	chr12	21283013	-	OpenSea	SLCO1B1	TSS1500	-	-0.06
cg10239376	chr4	75799090	-	OpenSea	no_gene	no_gene	-	-0.06
cg06763829	chr20	61885236	-	Island	NC	NC	-	-0.06
cg12696750	chr1	38022466	-	Island	DNALI1	TSS200	-	-0.06
cg09233782	chr19	18343636	+	Island	PDE4C	Body	-	-0.06
cg04380229	chr5	1084931	+	N_Shore	SLC12A7	Body	-	-0.06
cg00613691	chr14	22966344	+	OpenSea	no_gene	no_gene	-	-0.06
cg16338924	chr12	39711436	+	OpenSea	KIF21A	Body	-	-0.06
cg27495951	chr6	170608479	-	S_Shelf	no_gene	no_gene	-	-0.06
cg00562641	chr5	68789255	+	Island	OCLN	5'UTR	-	-0.06
cg18326398	chr2	75328206	+	OpenSea	TACR1	Body	-	-0.06
cg00552874	chr17	42836594	-	Island	ADAM11	1stExon	-	-0.06
cg01424970	chr19	45116089	+	OpenSea	IGSF23	TSS1500	-	-0.06
cg18395615	chrX	103499807	-	Island	ESX1	TSS1500	-	-0.06
cg03701805	chr5	122452418	+	OpenSea	PRDM6	Body	-0.07	-0.06
cg25623035	chr1	176177166	+	S_Shore	RFWD2	TSS1500	-	-0.06
cg06968794	chr17	28403561	+	OpenSea	EFCAB5	Body	-	-0.06
cg00591556	chr13	96853578	-	OpenSea	HS6ST3	Body	-	-0.06
cg17122758	chr2	65804208	+	OpenSea	no_gene	no_gene	-	-0.06
cg08081256	chr6	142491267	-	OpenSea	VTA1	Body	-	-0.06
cg09558765	chr12	8725364	+	OpenSea	no_gene	no_gene	-	-0.06
cg03681657	chr2	47587609	+	OpenSea	no_gene	no_gene	-	-0.06
cg02647287	chr21	47011127	+	Island	no_gene	no_gene	-	-0.06
cg16077391	chr1	248112099	-	OpenSea	OR2L13	5'UTR	-	-0.06

cg14789142	chr6	148589223	-	OpenSea	no_gene	no_gene	-	-0.06
cg13125506	chr9	68299110	-	Island	no_gene	no_gene	-	-0.06
cg22371052	chr18	72021321	+	OpenSea	C18orf63	Body	-0.08	-0.06
cg24311236	chr1	73381117	+	OpenSea	no_gene	no_gene	-	-0.06
cg16476710	chr14	37304393	+	OpenSea	SLC25A21	Body	-	-0.06
cg09332121	chr6	12596312	+	OpenSea	no_gene	no_gene	-	-0.06
cg25376503	chr7	120942042	-	OpenSea	no_gene	no_gene	-	-0.06
cg11235259	chr19	47526657	-	S_Shore	NPAS1	Body	-	-0.06
cg11233105	chr7	39054495	-	OpenSea	POU6F2	Body	-	-0.06
cg26839117	chr7	116166214	-	Island	CAV1	Body	-	-0.06
cg03300099	chr4	71230539	+	OpenSea	SMR3A	Body	-	-0.06
cg26168802	chr8	105613902	-	OpenSea	no_gene	no_gene	-	-0.06
cg25692621	chr7	95115163	+	OpenSea	ASB4	TSS200	-	-0.06
cg22683377	chr8	28371364	-	OpenSea	FZD3	Body	-	-0.06
cg21985631	chr4	175138377	-	S_Shelf	no_gene	no_gene	-	-0.06
cg02120745	chr9	109426838	-	OpenSea	LINC01505	Body	-	-0.06
cg03546864	chr8	125720993	+	OpenSea	MTSS1	Body	-	-0.06
cg01009952	chr13	23441033	-	OpenSea	no_gene	no_gene	-	-0.06
cg23367683	chr5	180627941	+	N_Shelf	TRIM7	5'UTR	-	-0.06
cg24130271	chr11	33563654	+	OpenSea	KIAA1549L	TSS1500	-	-0.06
cg20845085	chr12	65728847	-	OpenSea	MSRB3	Body	-	-0.06
cg01266362	chr9	98265802	-	N_Shelf	PTCH1	5'UTR	-0.05	-0.06
cg12131804	chr6	150949078	-	OpenSea	PLEKHG1	5'UTR	-	-0.06
cg21066558	chr10	95790516	+	OpenSea	PLCE1	5'UTR	-	-0.06
cg09973699	chr10	70002872	+	OpenSea	no_gene	no_gene	-	-0.06
cg27199550	chr5	22212645	+	OpenSea	CDH12	5'UTR	-	-0.06
cg17512240	chr1	193657562	+	OpenSea	no_gene	no_gene	-	-0.06
cg06555521	chr7	116624942	-	OpenSea	ST7	Body	-	-0.06
cg15535313	chr16	72206322	-	OpenSea	PMFBP1	NC	-	-0.06
cg03580358	chr8	41981423	+	OpenSea	no_gene	no_gene	-	-0.06

cg04865290	chr3	52927548	+	N_Shelf	TMEM110	Body	-	-0.06
cg27600413	chr2	157446456	-	OpenSea	no_gene	no_gene	-	-0.06
cg16105070	chr2	167759806	-	OpenSea	XIRP2	5'UTR	-	-0.06
cg26049293	chr8	16460659	-	OpenSea	no_gene	no_gene	-	-0.06
cg09572920	chrX	39866872	+	Island	no_gene	no_gene	-	-0.06
cg13089400	chr10	3669124	+	OpenSea	LOC105376360	Body	-	-0.06
cg09704444	chr3	175144634	-	OpenSea	NC	Body	-	-0.06
cg17298239	chr18	3499253	-	Island	DLGAP1	Body	-	-0.06
cg24902067	chr1	100809070	+	OpenSea	no_gene	no_gene	-	-0.06
cg06614754	chr13	107569395	-	N_Shore	no_gene	no_gene	-	-0.06
cg03946922	chrX	49833666	-	OpenSea	CLCN5	Body	-	-0.06
cg03915752	chr1	66802205	-	OpenSea	PDE4B	Body	-	-0.06
cg18798669	chr8	143470686	+	N_Shore	TSNARE1	5'UTR	-	-0.06
cg15935333	chr4	69964573	+	OpenSea	UGT2B7	Body	-	-0.06
cg16868350	chr19	55064373	-	OpenSea	no_gene	no_gene	-	-0.06
cg21519092	chr15	47534201	+	OpenSea	no_gene	no_gene	-	-0.06
cg05285223	chr3	69965487	+	OpenSea	MITF	Body	-	-0.06
cg23431721	chr3	50387780	+	N_Shore	NC	NC	-	-0.06
cg16946840	chr3	150888616	-	OpenSea	MED12L	Body	-	-0.06
cg09856045	chr6	75076408	+	OpenSea	LOC101928516	Body	-	-0.06
cg10849016	chr5	169416192	-	OpenSea	DOCK2	Body	-	-0.06
cg19193517	chr2	45394833	-	N_Shore	no_gene	no_gene	-	-0.06
cg00123072	chr5	79330259	+	N_Shore	THBS4	TSS1500	-	-0.06
cg03522063	chr10	119302167	+	Island	EMX2	NC	-	-0.06
cg17641861	chr4	570361	+	Island	no_gene	no_gene	-	-0.06
cg14795163	chr1	74620779	-	OpenSea	LRRIQ3	Body	-	-0.06
cg03872088	chr12	60757108	-	OpenSea	no_gene	no_gene	-	-0.06
cg20371265	chr10	80400824	-	OpenSea	no_gene	no_gene	-	-0.06
cg17119559	chrX	19100990	+	OpenSea	GPR64	5'UTR	-	-0.06
cg13110623	chr14	62334031	+	S_Shelf	no_gene	no_gene	-	-0.06

cg11434471	chr7	116889125	+	OpenSea	no_gene	no_gene	-	-0.06
cg24074432	chr2	85505567	+	OpenSea	TCF7L1	Body	-	-0.06
cg14102731	chr4	9534062	+	Island	no_gene	no_gene	-	-0.06
cg23775364	chr6	57035982	-	N_Shore	NC	NC	-	-0.06
cg23692540	chr9	33637473	+	OpenSea	no_gene	no_gene	-	-0.06
cg25160605	chr11	21087846	-	OpenSea	NELL1	Body	-	-0.06
cg02524825	chr8	110007070	+	OpenSea	no_gene	no_gene	-	-0.06
cg01471539	chrX	24795720	-	OpenSea	POLA1	Body	-	-0.06
cg00181669	chr3	44000978	+	OpenSea	no_gene	no_gene	-	-0.06
cg06226014	chr9	31140621	+	OpenSea	no_gene	no_gene	-	-0.05
cg00871215	chr2	238472338	+	OpenSea	no_gene	no_gene	-	-0.05
cg06161698	chr22	38795492	+	S_Shore	LOC400927	TSS1500	-	-0.05
cg22600079	chr19	50528096	+	N_Shore	NC	NC	-	-0.05
cg04616075	chr5	161914917	+	OpenSea	no_gene	no_gene	-	-0.05
cg09969640	chr3	175484137	+	OpenSea	NAALADL2	Body	-	-0.05
cg22628699	chrX	15802814	+	OpenSea	CA5B	3'UTR	-	-0.05
cg04960987	chr11	34407496	+	OpenSea	no_gene	no_gene	-	-0.05
cg21631220	chr13	26233578	-	OpenSea	ATP8A2	Body	-	-0.05
cg27576968	chr4	122615133	-	N_Shelf	ANXA5	Body	-	-0.05
cg03460001	chr7	101460955	-	Island	CUX1	Body	-	-0.05
cg10232138	chr6	137315116	-	OpenSea	NHEG1	TSS1500	-	-0.05
cg21695476	chr4	23935895	+	OpenSea	no_gene	no_gene	-	-0.05
cg03543448	chr16	4384967	-	OpenSea	GLIS2	Body	-	-0.05
cg18294191	chr3	29366028	-	OpenSea	RBMS3	Body	-	-0.05
cg14565071	chr19	35999608	-	OpenSea	DMKN	Body	-	-0.05
cg24806812	chr4	72635202	+	OpenSea	GC	Body	-	-0.05
cg20677114	chr11	61822258	-	OpenSea	no_gene	no_gene	-	-0.05
cg16305860	chr11	87832599	-	OpenSea	no_gene	no_gene	-	-0.05
cg25673355	chr7	70641938	-	OpenSea	WBSCR17	Body	-	-0.05
cg13257664	chr9	122733457	-	OpenSea	no_gene	no_gene	-	-0.05

cg22487367	chr1	115902819	+	OpenSea	no_gene	no_gene	-	-0.05
cg08313842	chr11	1628362	-	OpenSea	HCCA2	Body	-	-0.05
cg21335509	chr7	123389943	+	S_Shore	WASL	TSS1500	-	-0.05
cg22374237	chr7	126891197	-	N_Shore	GRM8	5'UTR	-	-0.05
cg26651837	chr4	104695090	+	OpenSea	no_gene	no_gene	-	-0.05
cg18123675	chr2	78014953	-	OpenSea	LOC101927967	Body	-	-0.05
cg21623902	chr4	86671197	+	OpenSea	ARHGAP24	Body	-	-0.05
cg22401505	chr6	116893550	-	S_Shore	RWDD1	5'UTR	-	-0.05
cg08546765	chr6	144208148	+	OpenSea	ZC2HC1B	Body	-	-0.05
cg06671445	chr12	25671475	-	OpenSea	LMNTD1	Body	-	-0.05
cg26222748	chrX	70502568	+	N_Shore	NONO	TSS1500	-	-0.05
cg13521538	chr9	38392470	+	N_Shore	ALDH1B1	TSS1500	-	-0.05
cg12823328	chr1	60554478	+	OpenSea	no_gene	no_gene	-	-0.05
cg27658132	chr7	117434635	-	OpenSea	CTTNBP2	Body	-	-0.05
cg04885343	chr4	72670093	-	OpenSea	no_gene	no_gene	-	-0.05
cg19735514	chr1	161762739	+	OpenSea	ATF6	Body	-	-0.05
cg07964275	chr10	11574278	+	OpenSea	USP6NL	NC	-	-0.05
cg13038229	chr12	94007449	+	OpenSea	no_gene	no_gene	-	-0.05
cg16612072	chr3	53380856	-	N_Shore	DCP1A	Body	-	-0.05
cg03538663	chr12	88423137	+	OpenSea	C12orf50	NC	-	-0.05
cg03646270	chr6	13667368	+	OpenSea	RANBP9	Body	-	-0.05
cg22576612	chr18	42550084	+	OpenSea	NC	Body	-	-0.05
cg03380861	chr13	31810686	+	OpenSea	B3GLCT	Body	-	-0.05
cg09628244	chr11	82478136	+	OpenSea	no_gene	no_gene	-	-0.05
cg12543545	chr6	139975635	-	OpenSea	no_gene	no_gene	-	-0.05
cg20046119	chr8	145981207	+	Island	ZNF251	TSS1500	-	-0.05
cg26349461	chr18	58324042	+	OpenSea	no_gene	no_gene	-	-0.05
cg00301120	chr10	132740439	+	OpenSea	no_gene	no_gene	-	-0.05
cg26797522	chrX	67947545	+	OpenSea	no_gene	no_gene	-	-0.05
cg22269416	chr6	32068240	-	S_Shelf	TNXB	5'UTR	-	-0.05

cg16690356	chr6	29945948	-	S_Shore	HCG9	Body	-	-0.05
cg01949341	chr3	44239999	+	OpenSea	no_gene	no_gene	-	-0.05
cg19028058	chr18	40858181	-	OpenSea	SYT4	TSS1500	-	-0.05
cg18199386	chr1	152729200	+	N_Shelf	KPRP	TSS1500	-	-0.05
cg15847614	chr17	6348019	-	Island	FAM64A	5'UTR	-	-0.05
cg00745062	chr12	102241294	-	OpenSea	no_gene	no_gene	-	-0.05
cg00368414	chr3	27333542	+	OpenSea	NEK10	Body	-	-0.05
cg17596316	chr6	138820714	+	OpenSea	NHSL1	NC	-	-0.05
cg24301414	chr19	50663474	-	N_Shelf	C19orf41	Body	-	-0.05
cg22004053	chr1	170758474	-	OpenSea	no_gene	no_gene	-	-0.05
cg13199603	chr8	57640050	+	OpenSea	no_gene	no_gene	-	-0.05
cg27573493	chr13	80026237	+	OpenSea	no_gene	no_gene	-	-0.05
cg02524009	chr20	8166645	+	OpenSea	PLCB1	Body	-	-0.05
cg00766289	chr12	3311121	-	S_Shore	TSPAN9	Body	-	-0.05
cg14550506	chr3	77239618	-	OpenSea	ROBO2	Body	-	-0.05
cg24061425	chr7	22762053	+	OpenSea	no_gene	no_gene	-	-0.05
cg08935703	chr10	117162648	-	OpenSea	ATRNL1	Body	-	-0.05
cg01244601	chr4	120671846	+	OpenSea	no_gene	no_gene	-	-0.05
cg22977331	chrX	111292132	+	OpenSea	TRPC5	5'UTR	-	-0.05
cg04442806	chr3	39509081	+	OpenSea	MOBP	NC	-	-0.05
cg10620730	chr19	40257211	-	OpenSea	no_gene	no_gene	-	-0.05
cg02038360	chr2	189849583	-	OpenSea	COL3A1	Body	-	-0.05
cg15523879	chr4	73837725	+	OpenSea	no_gene	no_gene	-	-0.05
cg02229724	chr8	133811571	-	OpenSea	PHF20L1	Body	-	-0.05
cg19407748	chr8	40110688	-	OpenSea	no_gene	no_gene	-	-0.05
cg21570108	chr1	178542596	+	OpenSea	no_gene	no_gene	-	-0.05
cg03868353	chr14	28191405	-	OpenSea	no_gene	no_gene	-	-0.05
cg04479219	chr13	88326918	+	Island	SLITRK5	5'UTR	-	-0.05
cg03458633	chr10	4720663	+	OpenSea	LOC100216001	TSS1500	-	-0.05
cg07486487	chr2	152653546	+	OpenSea	no_gene	no_gene	-	-0.05

cg27488740	chr2	78928852	+	OpenSea	no_gene	no_gene	-	-0.05
cg19820601	chr5	173030725	+	OpenSea	no_gene	no_gene	-	-0.05
cg05606010	chrX	11288235	+	OpenSea	ARHGAP6	Body	-	-0.05
cg25963419	chr2	102618414	-	OpenSea	IL1R2	5'UTR	-	-0.05
cg23439008	chr12	117769760	+	OpenSea	NOS1	5'UTR	-	-0.05
cg23707006	chr12	55522515	+	OpenSea	OR9K2	TSS1500	-	-0.05
cg01296593	chr16	86599976	-	Island	FOXC2	TSS1500	-	-0.05
cg16577083	chr16	1271153	-	S_Shelf	CACNA1H	3'UTR	-	-0.05
cg14014796	chr2	45029977	-	Island	no_gene	no_gene	-	-0.05
cg03233444	chr19	17581966	+	S_Shore	SLC27A1	Body	-	-0.05
cg07807695	chr5	81608485	-	OpenSea	ATP6AP1L	Body	-	-0.05
cg07143733	chr21	26938557	+	S_Shelf	MIR155HG	Body	-	-0.05
cg14873818	chrX	83757652	+	OpenSea	HDX	TSS200	-	-0.05
cg04382878	chr11	64707920	+	OpenSea	C11orf85	Body	-	-0.05
cg04349815	chr10	21573608	-	OpenSea	no_gene	no_gene	-	-0.05
cg11292060	chr6	111532847	+	OpenSea	SLC16A10	Body	-	-0.05
cg23453610	chr2	195903085	+	OpenSea	no_gene	no_gene	-	-0.05
cg26433086	chr15	80282723	-	OpenSea	no_gene	no_gene	-	-0.05
cg19978318	chr2	215430983	-	OpenSea	VWC2L	Body	-	-0.05
cg06672736	chr7	87032850	+	OpenSea	ABCB4	Body	-	-0.05
cg07790338	chr2	237218275	-	OpenSea	no_gene	no_gene	-	-0.05
cg07933845	chr8	90265771	-	OpenSea	no_gene	no_gene	-	-0.05
cg17575050	chr14	71447988	-	OpenSea	PCNX	Body	-	-0.05
cg05708452	chr8	86377153	-	S_Shore	NC	NC	-	-0.05
cg17640684	chr4	151776137	-	OpenSea	LRBA	Body	-	-0.05
cg09677297	chr14	88510165	+	OpenSea	LINC01146	Body	-	-0.05
cg02895698	chr16	303165	-	OpenSea	ITFG3	5'UTR	-	-0.05
cg02725420	chr2	182089834	+	OpenSea	LOC101927156	Body	-	-0.05
cg25495776	chr7	110406870	+	OpenSea	IMMP2L	Body	-	-0.05
cg16711835	chr5	59558467	-	OpenSea	PDE4D	5'UTR	-	-0.05

cg22348290	chr8	72459499	+	N_Shore	no_gene	no_gene	-	-0.05
cg25364141	chr16	56198044	+	OpenSea	LOC283856	Body	-	-0.05
cg27515800	chr8	33423676	+	N_Shore	RNF122	Body	-	-0.05
cg25344969	chr5	93217325	-	OpenSea	FAM172A	Body	-	-0.05
cg15484721	chr5	95421056	+	OpenSea	LOC101929710	Body	-	-0.05
cg21575576	chr4	70033274	-	OpenSea	no_gene	no_gene	-	-0.05
cg08032407	chr6	112500866	-	OpenSea	LAMA4	Body	-	-0.05
cg13324779	chr4	86923558	-	OpenSea	ARHGAP24	3'UTR	-	-0.05
cg08462879	chr1	66458116	+	OpenSea	PDE4B	Body	-	-0.05
cg20939319	chr8	30707701	-	OpenSea	TEX15	TSS1500	-	-0.05
cg18279090	chr2	182607410	-	OpenSea	no_gene	no_gene	-	-0.05
cg18258770	chr4	90757814	+	N_Shore	SNCA	5'UTR	-	-0.05
cg09243569	chr6	132817424	+	OpenSea	STX7	Body	-	-0.05
cg08715725	chr4	184922433	-	OpenSea	STOX2	Body	-	-0.05
cg03084184	chr10	133981681	-	OpenSea	JAKMIP3	3'UTR	-	-0.05
cg21627728	chr21	16335810	+	OpenSea	NRIP1	3'UTR	-	-0.05
cg22164781	chr19	45448680	+	OpenSea	NC	NC	-	-0.05
cg01458821	chr5	121427834	+	OpenSea	no_gene	no_gene	-	-0.05
cg10441034	chr2	100158888	+	OpenSea	no_gene	no_gene	-	-0.05
cg08641506	chrX	36163134	-	OpenSea	CXorf59	3'UTR	-	-0.05
cg21424557	chr9	90925448	-	OpenSea	no_gene	no_gene	-	-0.05
cg18793631	chr6	72961032	+	OpenSea	RIMS1	Body	-	-0.05
cg27529205	chr2	173103502	-	S_Shelf	no_gene	no_gene	-	-0.05
cg17436134	chr1	119536288	+	S_Shore	no_gene	no_gene	-	-0.05
cg18135774	chr2	38343597	+	OpenSea	no_gene	no_gene	-	-0.05
cg12861602	chr8	99045811	+	OpenSea	MATN2	Body	-	-0.05
cg27639249	chr6	30016420	+	OpenSea	NCRNA00171	Body	-0.08	-0.05
cg15450349	chr8	42269042	-	S_Shore	no_gene	no_gene	-	-0.05
cg14269813	chr9	3899055	-	OpenSea	GLIS3	Body	-	-0.05
cg16205846	chr2	211539520	+	OpenSea	CPS1	Body	-	-0.05

cg12604569	chr4	88188107	-	OpenSea	no_gene	no_gene	-	-0.05
cg01800986	chr13	80298553	-	OpenSea	no_gene	no_gene	-	-0.05
cg19517931	chr3	97755601	+	OpenSea	GABRR3	TSS1500	-	-0.05
cg13980719	chr2	217725560	+	OpenSea	TNP1	TSS1500	-	-0.05
cg24794102	chr7	116132431	+	OpenSea	no_gene	no_gene	-	-0.05
cg12374021	chr9	132193932	+	OpenSea	no_gene	no_gene	-	-0.05
cg20831491	chr3	99442950	-	OpenSea	COL8A1	5'UTR	-	-0.05
cg05215549	chr2	66470263	-	OpenSea	no_gene	no_gene	-	-0.05
cg21331228	chr4	185874781	-	S_Shore	no_gene	no_gene	-	-0.05
cg02988673	chr12	90674723	-	OpenSea	no_gene	no_gene	-	-0.05
cg12869615	chrX	101906288	-	Island	GPRASP1	TSS200	-	-0.05
cg23714733	chr2	168639953	+	OpenSea	no_gene	no_gene	-	-0.05
cg26944725	chr2	149926738	-	OpenSea	LYPD6B	5'UTR	-	-0.05
cg23625388	chr14	93076432	+	OpenSea	RIN3	Body	-	-0.05
cg24073215	chr7	123487071	-	OpenSea	HYAL4	5'UTR	-	-0.05
cg12265878	chr7	41995442	+	OpenSea	no_gene	no_gene	-	-0.05
cg06634441	chr4	70514647	-	OpenSea	UGT2A1	TSS1500	-	-0.05
cg12555810	chr12	119187794	-	OpenSea	no_gene	no_gene	-	-0.05
cg10312447	chr12	120036581	-	S_Shelf	TMEM233	Body	-	-0.05
cg22026953	chr6	87763957	+	OpenSea	no_gene	no_gene	-	-0.05
cg07254667	chr10	87291812	+	OpenSea	no_gene	no_gene	-	-0.05
cg24017056	chr15	80366893	-	OpenSea	ZFAND6	5'UTR	-	-0.05
cg11109182	chrX	99661885	-	Island	PCDH19	1stExon	-	-0.05
cg08349646	chr15	30647452	+	OpenSea	no_gene	no_gene	-	-0.05
cg27519691	chr1	77333074	-	N_Shore	ST6GALNAC5	TSS200	-	-0.05
cg15860717	chr16	5194387	+	OpenSea	no_gene	no_gene	-	-0.05
cg24726122	chr4	140223869	+	S_Shore	NDUFC1	TSS200	-	-0.05
cg14807263	chr8	117036403	+	OpenSea	LINC00536	Body	-	-0.05
cg19478779	chr12	91349273	+	S_Shore	C12orf12	TSS1500	-	-0.05
cg25760424	chr4	138046216	-	OpenSea	no_gene	no_gene	-	-0.05

cg17035814	chr6	67776312	-	OpenSea	no_gene	no_gene	-	-0.05
cg07623780	chr14	44864223	-	OpenSea	no_gene	no_gene	-	-0.05
cg18090331	chr5	132111426	+	N_Shore	Sep-08	Body	-	-0.05
cg16626884	chr2	71693389	+	Island	DYSF	NC	-	-0.05
cg01076970	chr5	180455248	+	OpenSea	no_gene	no_gene	-	-0.05
cg26795061	chr4	71181511	-	OpenSea	no_gene	no_gene	-	-0.05
cg03459617	chr4	88528262	+	OpenSea	DSPP	TSS1500	-	-0.05
cg24349193	chr1	157998998	+	OpenSea	KIRREL	Body	-	-0.05
cg19267253	chr7	19750896	-	S_Shelf	no_gene	no_gene	-	-0.05
cg07660627	chr17	35481970	+	OpenSea	ACACA	Body	-	-0.05
cg05568014	chr4	186350340	-	S_Shelf	C4orf47	TSS1500	-	-0.05
cg18147366	chr1	207669544	-	N_Shore	CR1	NC	-	-0.05
cg03347163	chr12	119615508	-	OpenSea	HSPB8	TSS1500	-	-0.05
cg13431811	chr13	101108790	+	OpenSea	PCCA	Body	-	-0.05
cg03453585	chr17	72885567	+	N_Shelf	FADS6	Body	-	-0.05
cg21182911	chr2	67392095	-	OpenSea	NC	Body	-	-0.05
cg03465600	chr2	206272776	+	OpenSea	PARD3B	Body	-	-0.05
cg00869927	chr1	67051101	-	OpenSea	SGIP1	Body	-	-0.05
cg09209931	chr15	92193348	-	OpenSea	no_gene	no_gene	-	-0.05
cg13757024	chr12	95645659	-	OpenSea	VEZT	Body	-	-0.05
cg05306225	chr8	4848947	+	N_Shore	CSMD1	Body	-	-0.05
cg11370512	chr12	113796654	+	Island	PLBD2	1stExon	-	-0.05
cg02934347	chr6	17393628	-	OpenSea	CAP2	TSS200	-	-0.05
cg01450725	chr4	154714852	+	S_Shore	no_gene	no_gene	-	-0.05
cg06432119	chr11	281516	-	Island	NLRP6	Body	-	-0.05
cg15177686	chr4	185828927	-	OpenSea	no_gene	no_gene	-	-0.05
cg16016188	chr13	19169029	+	N_Shelf	no_gene	no_gene	-	-0.05
cg09475813	chr1	35250346	+	N_Shore	GJB3	5'UTR	-	-0.05
cg10801034	chr5	81763211	-	OpenSea	no_gene	no_gene	-	-0.05
cg04404701	chr4	71234736	+	OpenSea	no_gene	no_gene	-	-0.05

cg02641801	chr2	26213508	+	OpenSea	no_gene	no_gene	-	-0.05
cg15080430	chr6	70876494	-	OpenSea	COL19A1	Body	-	-0.05
cg18723623	chr10	23730227	-	S_Shore	OTUD1	NC	-	-0.05
cg11040916	chr5	57366460	-	OpenSea	no_gene	no_gene	-	-0.05
cg16279679	chrX	20469364	-	OpenSea	no_gene	no_gene	-	-0.05
cg09215282	chr16	811744	-	OpenSea	MSLN	5'UTR	-	-0.05
cg00852964	chr6	133035150	+	OpenSea	VNN1	1stExon	-	-0.05
cg19139358	chr5	111400717	+	OpenSea	no_gene	no_gene	-	-0.05
cg13338306	chr11	1456891	-	OpenSea	BRSK2	Body	-	-0.05
cg17399550	chr4	149913051	+	OpenSea	no_gene	no_gene	-	-0.05
cg27095776	chr16	68124194	-	OpenSea	NFATC3	Body	-	-0.05
cg02284587	chr1	64971218	-	N_Shore	CACHD1	Body	-	-0.05
cg01863495	chr3	190581232	-	S_Shore	GMNC	TSS1500	-	-0.05
cg14295659	chr8	38954671	-	OpenSea	ADAM9	Body	-	-0.05
cg20975354	chr6	31009289	+	OpenSea	no_gene	no_gene	-	-0.05
cg09442789	chr15	33009115	-	N_Shore	GREM1	TSS1500	-	-0.05
cg17460713	chr5	178461226	-	OpenSea	ZNF879	3'UTR	-	-0.05
cg14772615	chr6	33116235	+	OpenSea	no_gene	no_gene	-	-0.05
cg21781988	chr10	101287742	-	Island	no_gene	no_gene	-	-0.05
cg02315096	chr13	110522020	+	Island	no_gene	no_gene	-	-0.05
cg24981196	chr1	195723692	+	OpenSea	no_gene	no_gene	-	-0.05
cg03530940	chr12	2198113	-	OpenSea	CACNA1C	Body	-0.05	-0.05
cg25480082	chr5	58364671	-	OpenSea	PDE4D	Body	-	-0.05
cg07270235	chr9	1490381	+	OpenSea	no_gene	no_gene	-	-0.05
cg04677123	chr5	90466501	-	OpenSea	no_gene	no_gene	-	-0.05
cg10467968	chr6	31862499	-	N_Shelf	EHMT2	Body	-	-0.05
cg15191636	chr3	15216953	+	OpenSea	COL6A4P1	Body	-	-0.05
cg11729174	chr13	95368297	+	S_Shelf	no_gene	no_gene	-	-0.05
cg17865954	chr21	31469453	+	OpenSea	no_gene	no_gene	-	-0.05
cg02327563	chr2	119597586	+	N_Shore	no_gene	no_gene	-	-0.05

cg08642979	chr1	116905976	+	OpenSea	no_gene	no_gene	-	-0.05
cg11758280	chr20	9153867	-	OpenSea	PLCB4	5'UTR	-	-0.05
cg00914834	chrX	129009789	+	OpenSea	no_gene	no_gene	-	-0.05
cg21262449	chr1	248128496	+	OpenSea	OR2L13	5'UTR	-	-0.05
cg02867811	chr6	45295368	+	OpenSea	RUNX2	TSS1500	-	-0.05
cg11781127	chr5	159660276	+	OpenSea	FABP6	Body	-	-0.05
cg16778230	chr14	44639523	-	OpenSea	no_gene	no_gene	-	-0.05
cg05110133	chr20	3220565	-	Island	no_gene	no_gene	-	-0.05
cg22749105	chr5	94772490	+	OpenSea	FAM81B	NC	-	-0.05
cg17572324	chr7	158559488	+	OpenSea	ESYT2	Body	-	-0.05
cg23239274	chr11	86066507	+	OpenSea	no_gene	no_gene	-	-0.05
cg26837196	chr12	49908358	+	OpenSea	SPATS2	Body	-	-0.05
cg20375608	chr5	52405108	+	N_Shore	MOCS2	NC	-	-0.05
cg04693895	chr10	431095	+	OpenSea	DIP2C	Body	-	-0.05
cg05767768	chr2	217565529	+	OpenSea	no_gene	no_gene	-	-0.05
cg21974845	chr1	192845391	-	OpenSea	no_gene	no_gene	-	-0.05
cg27588012	chr21	31853712	-	OpenSea	KRTAP19-1	TSS1500	-	-0.05
cg13496392	chr10	15014484	+	OpenSea	MEIG1	Body	-	-0.05
cg21256046	chr13	106118023	-	OpenSea	DAOA	TSS1500	-	-0.05
cg19854953	chr2	104764283	+	OpenSea	no_gene	no_gene	-	-0.05
cg14586939	chr4	156130206	+	Island	NPY2R	NC	-	-0.05
cg26885442	chr7	107881507	+	OpenSea	NRCAM	5'UTR	-	-0.05
cg22971407	chr16	2416574	-	OpenSea	ABCA17P	Body	-	-0.05
cg08200621	chr17	56247036	+	OpenSea	OR4D2	1stExon	-	-0.05
cg17497965	chr6	17282606	-	S_Shore	RBM24	NC	-	-0.05

NC, no consensus

B Transcriptome changes after 8-day incubation with 15 μM OA or DHA assessed by Illumina HumanHT-12 v4 Expression BeadChip

Table 2: Genome-wide mRNA transcription changes after 8-day incubation with 15 μM OA or DHA assessed by Illumina HumanHT-12 v4 Expression BeadChip. All changes shown were significantly different compared with controls ($P < 0.05$).

Probe_ID	Gene Symbol	NCBI Reference	Gene Description	OA	DHA
ILMN_1797728	HMGCS1	NM_002130.4	Homo sapiens 3-hydroxy-3-methylglutaryl-Coenzyme A synthase 1 (soluble) (HMGCS1), transcript variant 2, mRNA.	-1.45	-2.06
ILMN_1776678	GIMAP7	NM_153236.3	Homo sapiens GTPase, IMAP family member 7 (GIMAP7), mRNA.	-	-1.82
ILMN_3268697	LOC100129882	XM_001716882.1	PREDICTED: Homo sapiens similar to mCG49427 (LOC100129882), mRNA.	-1.47	-1.73
ILMN_1720889	SC4MOL	NM_006745.3	Homo sapiens sterol-C4-methyl oxidase-like (SC4MOL), transcript variant 2, mRNA.	-1.29	-1.71
ILMN_1664861	ID1	NM_181353.1	Homo sapiens inhibitor of DNA binding 1, dominant negative helix-loop-helix protein (ID1), transcript variant 2, mRNA.	-	-1.64
ILMN_1657395	HMGCR	NM_000859.1	Homo sapiens 3-hydroxy-3-methylglutaryl-Coenzyme A reductase (HMGCR), mRNA.	-	-1.63
ILMN_1784871	FASN	NM_004104.4	Homo sapiens fatty acid synthase (FASN), mRNA.	-1.24	-1.62
ILMN_1698019	LGMN	NM_005606.5	Homo sapiens legumain (LGMN), transcript variant 2, mRNA.	-	-1.55
ILMN_1724708	RAB33A	NM_004794.2	Homo sapiens RAB33A, member RAS oncogene family (RAB33A), mRNA.	-	-1.55
ILMN_2056074	RGPD2	NM_001078170.1	Homo sapiens RANBP2-like and GRIP domain containing 2 (RGPD2), mRNA.	-	-1.54
ILMN_1715024	LSS	NM_002340.3	Homo sapiens lanosterol synthase (2,3-oxidosqualene-lanosterol cyclase) (LSS), transcript variant 1, mRNA.	-1.4	-1.53

ILMN_1795325	ACTG2	NM_001615.3	Homo sapiens actin, gamma 2, smooth muscle, enteric (ACTG2), mRNA.	-	-1.51
ILMN_1708672	ACAT2	NM_005891.1	Homo sapiens acetyl-Coenzyme A acetyltransferase 2 (ACAT2), mRNA.	-	-1.5
ILMN_1689842	SC4MOL	NM_006745.3	Homo sapiens sterol-C4-methyl oxidase-like (SC4MOL), transcript variant 1, mRNA.	-	-1.47
ILMN_1657550	MVD	NM_002461.1	Homo sapiens mevalonate (diphospho) decarboxylase (MVD), mRNA.	-1.33	-1.46
ILMN_1732296	ID3	NM_002167.2	Homo sapiens inhibitor of DNA binding 3, dominant negative helix-loop-helix protein (ID3), mRNA.	-	-1.45
ILMN_1714197	ACSS2	NM_139274.1	Homo sapiens acyl-CoA synthetase short-chain family member 2 (ACSS2), transcript variant 1, mRNA.	-	-1.43
ILMN_1741096	FDFT1	NM_004462.3	Homo sapiens farnesyl-diphosphate farnesyltransferase 1 (FDFT1), mRNA.	-1.34	-1.43
ILMN_1673673	PBK	NM_018492.2	Homo sapiens PDZ binding kinase (PBK), mRNA.	-	-1.42
ILMN_2350634	EFEMP1	NM_001039348.1	Homo sapiens EGF-containing fibulin-like extracellular matrix protein 1 (EFEMP1), transcript variant 2, mRNA.	-	-1.41
ILMN_2041293	SQLE	NM_003129.3	Homo sapiens squalene epoxidase (SQLE), mRNA.	-	-1.41
ILMN_1674411	CKAP2	NM_018204.2	Homo sapiens cytoskeleton associated protein 2 (CKAP2), transcript variant 2, mRNA.	-	-1.41
ILMN_1772241	SQLE	NM_003129.3	Homo sapiens squalene epoxidase (SQLE), mRNA.	-	-1.4
ILMN_1685045	CHI3L2	NM_001025199.1	Homo sapiens chitinase 3-like 2 (CHI3L2), transcript variant 3, mRNA.	-	-1.4
ILMN_2316173	AP1S1	NM_001283.2	Homo sapiens adaptor-related protein complex 1, sigma 1 subunit (AP1S1), transcript variant 1, mRNA.	-	-1.4
ILMN_2226415	LOC440145	NM_001071775.1	Homo sapiens similar to RIKEN cDNA 2410129H14 (LOC440145), mRNA.	-1.24	-1.4

ILMN_2331636	ACACA	NM_198836.1	Homo sapiens acetyl-Coenzyme A carboxylase alpha (ACACA), transcript variant 3, mRNA.	-	-1.39
ILMN_1781942	HMMR	NM_012485.1	Homo sapiens hyaluronan-mediated motility receptor (RHAMM) (HMMR), transcript variant 2, mRNA.	-	-1.39
ILMN_1658607	DLEU2	XR_001514.1	PREDICTED: Homo sapiens deleted in lymphocytic leukemia, 2 (DLEU2), misc RNA.	-	-1.38
ILMN_1775931	EPHA3	NM_005233.3	Homo sapiens EPH receptor A3 (EPHA3), transcript variant 1, mRNA.	-	-1.38
ILMN_1789702	GBE1	NM_000158.1	Homo sapiens glucan (1,4-alpha-), branching enzyme 1 (glycogen branching enzyme, Andersen disease, glycogen storage disease type IV) (GBE1), mRNA.	-	-1.38
ILMN_1793474	INSIG1	NM_005542.3	Homo sapiens insulin induced gene 1 (INSIG1), transcript variant 2, mRNA.	-1.24	-1.37
ILMN_2409220	HMMR	NM_012484.1	Homo sapiens hyaluronan-mediated motility receptor (RHAMM) (HMMR), transcript variant 1, mRNA.	-	-1.37
ILMN_1735877	EFEMP1	NM_004105.2	Homo sapiens EGF-containing fibulin-like extracellular matrix protein 1 (EFEMP1), transcript variant 1, mRNA.	-	-1.37
ILMN_3239771	DLGAP5	NM_014750.3	Homo sapiens discs, large (Drosophila) homolog-associated protein 5 (DLGAP5), mRNA.	-	-1.36
ILMN_1661599	DDIT4	NM_019058.2	Homo sapiens DNA-damage-inducible transcript 4 (DDIT4), mRNA.	-	-1.36
ILMN_2148668	RCBTB2	NM_001268.2	Homo sapiens regulator of chromosome condensation (RCC1) and BTB (POZ) domain containing protein 2 (RCBTB2), mRNA.	-	-1.36
ILMN_3242586	RHOU	NM_021205.4	Homo sapiens ras homolog gene family, member U (RHOU), mRNA.	-	-1.35
ILMN_1728048	LOC158160	NM_001031744.1	Homo sapiens hypothetical protein LOC158160 (LOC158160), transcript variant 1, mRNA.	-	-1.35

ILMN_1653292	PFKFB4	NM_004567.2	Homo sapiens 6-phosphofructo-2-kinase/fructose-2,6-biphosphatase 4 (PFKFB4), mRNA.	-	-1.35
ILMN_1755075	IDI1	NM_004508.2	Homo sapiens isopentenyl-diphosphate delta isomerase 1 (IDI1), mRNA.	-1.2	-1.35
ILMN_1788166	TTK	NM_003318.3	Homo sapiens TTK protein kinase (TTK), mRNA.	-	-1.34
ILMN_1710962	TMEM97	NM_014573.1	Homo sapiens transmembrane protein 97 (TMEM97), mRNA.	-	-1.34
ILMN_1803799	LOC649555	XM_945579.1	PREDICTED: Homo sapiens similar to eukaryotic translation initiation factor 4E, transcript variant 2 (LOC649555), mRNA.	-	-1.34
ILMN_1689329	SCD	NM_005063.4	Homo sapiens stearoyl-CoA desaturase (delta-9-desaturase) (SCD), mRNA.	-1.23	-1.34
ILMN_1689002	DTX1	NM_004416.2	Homo sapiens deltex homolog 1 (Drosophila) (DTX1), mRNA.	-	-1.34
ILMN_1733956	IARS	NM_002161.2	Homo sapiens isoleucyl-tRNA synthetase (IARS), transcript variant short, mRNA.	-	-1.33
ILMN_1847965	HS.250648	Hs.250648	full-length cDNA clone CS0DC013YI10 of Neuroblastoma Cot 25-normalized of Homo sapiens (human)	-	-1.33
ILMN_1728024	TUBG1	XM_938498.1	Homo sapiens tubulin, gamma 1 (TUBG1), mRNA.	-	-1.33
ILMN_3218820	LOC645387	XR_016424.2	PREDICTED: Homo sapiens misc_RNA (LOC645387), miscRNA.	-	-1.33
ILMN_1786823	ICAM2	NM_000873.2	Homo sapiens intercellular adhesion molecule 2 (ICAM2), transcript variant 1, mRNA.	-	-1.33
ILMN_2165867	DHCR7	NM_001360.2	Homo sapiens 7-dehydrocholesterol reductase (DHCR7), transcript variant 1, mRNA.	-	-1.33
ILMN_1722127	RAD54B	NM_012415.2	Homo sapiens RAD54 homolog B (S. cerevisiae) (RAD54B), mRNA.	-	-1.33
ILMN_1712452	KIF20B	NM_016195.2	Homo sapiens kinesin family member 20B (KIF20B), mRNA.	-	-1.33
ILMN_1772123	ACACA	NM_000664.3	Homo sapiens acetyl-Coenzyme A carboxylase alpha (ACACA), transcript variant 2, mRNA.	-	-1.32
ILMN_2371379	ACLY	NM_198830.1	Homo sapiens ATP citrate lyase (ACLY), transcript variant 2, mRNA.	-	-1.32
ILMN_1786125	CCNA2	NM_001237.2	Homo sapiens cyclin A2 (CCNA2), mRNA.	-	-1.32

ILMN_1747016	CEP55	NM_018131.3	Homo sapiens centrosomal protein 55kDa (CEP55), mRNA.	-	-1.31
ILMN_1761486	C13ORF34	NM_024808.2	Homo sapiens chromosome 13 open reading frame 34 (C13orf34), mRNA.	-	-1.31
ILMN_1711414	MRPS27	NM_015084.1	Homo sapiens mitochondrial ribosomal protein S27 (MRPS27), nuclear gene encoding mitochondrial protein, mRNA.	-	-1.31
ILMN_1782897	CAPRIN1	NM_203364.2	Homo sapiens cell cycle associated protein 1 (CAPRIN1), transcript variant 2, mRNA.	-	-1.31
ILMN_1782551	E2F5	NM_001951.2	Homo sapiens E2F transcription factor 5, p130-binding (E2F5), transcript variant 1, mRNA.	-	-1.31
ILMN_1736555	ZNF280D	NM_001002844.1	Homo sapiens zinc finger protein 280D (ZNF280D), transcript variant 3, mRNA.	-	-1.31
ILMN_2132161	KIF18A	NM_031217.2	Homo sapiens kinesin family member 18A (KIF18A), mRNA.	-	-1.3
ILMN_2381758	G3BP2	NM_203504.1	Homo sapiens GTPase activating protein (SH3 domain) binding protein 2 (G3BP2), transcript variant 3, mRNA.	-	-1.3
ILMN_3238854	RGPD8	XM_001722279.1	PREDICTED: Homo sapiens RANBP2-like and GRIP domain containing 8 (RGPD8), mRNA.	-	-1.3
ILMN_3248091	C6ORF223	NM_153246.3	Homo sapiens chromosome 6 open reading frame 223 (C6orf223), mRNA.	-	-1.3
ILMN_1804150	HIBADH	NM_152740.2	Homo sapiens 3-hydroxyisobutyrate dehydrogenase (HIBADH), mRNA.	-	-1.29
ILMN_2144088	FDFT1	NM_004462.3	Homo sapiens farnesyl-diphosphate farnesyltransferase 1 (FDFT1), mRNA.	-	-1.29
ILMN_1778677	MRS2	NM_020662.1	Homo sapiens MRS2 magnesium homeostasis factor homolog (S. cerevisiae) (MRS2), mRNA.	-	-1.29

ILMN_1804248	FDPS	NM_002004.2	Homo sapiens farnesyl diphosphate synthase (farnesyl pyrophosphate synthetase, dimethylallyltranstransferase, geranyltranstransferase) (FDPS), mRNA.	-1.28	-1.29
ILMN_2105983	XRCC5	NM_021141.2	Homo sapiens X-ray repair complementing defective repair in Chinese hamster cells 5 (double-strand-break rejoining; Ku autoantigen, 80kDa) (XRCC5), mRNA.	-	-1.29
ILMN_1703697	LANCL1	NM_006055.1	Homo sapiens LanC lantibiotic synthetase component C-like 1 (bacterial) (LANCL1), mRNA.	-	-1.29
ILMN_1670134	FADS1	NM_013402.3	Homo sapiens fatty acid desaturase 1 (FADS1), mRNA.	-1.25	-1.29
ILMN_1815626	DHCR7	NM_001360.1	Homo sapiens 7-dehydrocholesterol reductase (DHCR7), mRNA.	-	-1.29
ILMN_3237850	C5ORF51	NM_175921.4	Homo sapiens chromosome 5 open reading frame 51 (C5orf51), mRNA.	-	-1.29
ILMN_1669905	DCP2	NM_152624.4	Homo sapiens DCP2 decapping enzyme homolog (S. cerevisiae) (DCP2), mRNA.	-	-1.29
ILMN_1795429	VCL	NM_003373.3	Homo sapiens vinculin (VCL), transcript variant 1, mRNA.	-	-1.28
ILMN_2320850	UBE2D3	NM_181890.1	Homo sapiens ubiquitin-conjugating enzyme E2D 3 (UBC4/5 homolog, yeast) (UBE2D3), transcript variant 6, mRNA.	-	-1.28
ILMN_2150019	SUCLA2	NM_003850.1	Homo sapiens succinate-CoA ligase, ADP-forming, beta subunit (SUCLA2), mRNA.	-	-1.28
ILMN_1813400	CBR4	NM_032783.3	Homo sapiens carbonyl reductase 4 (CBR4), mRNA.	-	-1.28
ILMN_1725906	C1ORF104	NM_173639.1	Homo sapiens chromosome 1 open reading frame 104 (C1orf104), mRNA.	-	-1.28
ILMN_2053415	LDLR	NM_000527.2	Homo sapiens low density lipoprotein receptor (familial hypercholesterolemia) (LDLR), mRNA.	-	-1.28
ILMN_1757186	GIMAP1	NM_130759.2	Homo sapiens GTPase, IMAP family member 1 (GIMAP1), mRNA.	-	-1.28
ILMN_1696591	RB1	NM_000321.1	Homo sapiens retinoblastoma 1 (RB1), mRNA.	-	-1.28
ILMN_1712803	CCNB1	NM_031966.2	Homo sapiens cyclin B1 (CCNB1), mRNA.	-	-1.28
ILMN_1774265	C2ORF82	NM_206895.1	Homo sapiens chromosome 2 open reading frame 82 (C2orf82), mRNA.	-	-1.28

ILMN_1656129	SLC39A10	NM_020342.1	Homo sapiens solute carrier family 39 (zinc transporter), member 10 (SLC39A10), mRNA.	-	-1.27
ILMN_1680955	AURKA	NM_198434.1	Homo sapiens aurora kinase A (AURKA), transcript variant 5, mRNA.	-	-1.27
ILMN_1655921	GTF2E1	NM_005513.1	Homo sapiens general transcription factor IIE, polypeptide 1 (alpha subunit, 56kD) (GTF2E1), mRNA.	-	-1.27
ILMN_2328280	ACTL6A	NM_004301.3	Homo sapiens actin-like 6A (ACTL6A), transcript variant 1, mRNA.	-	-1.27
ILMN_2357438	AURKA	NM_198434.1	Homo sapiens aurora kinase A (AURKA), transcript variant 3, mRNA.	-	-1.27
ILMN_2210129	PRIM1	NM_000946.2	Homo sapiens primase, DNA, polypeptide 1 (49kDa) (PRIM1), mRNA.	-	-1.27
ILMN_2112256	TNFRSF4	NM_003327.2	Homo sapiens tumor necrosis factor receptor superfamily, member 4 (TNFRSF4), mRNA.	-	-1.27
ILMN_1749829	DLGAP5	NM_014750.3	Homo sapiens discs, large (Drosophila) homolog-associated protein 5 (DLGAP5), mRNA.	-	-1.27
ILMN_1734814	HSPA4	NM_002154.3	Homo sapiens heat shock 70kDa protein 4 (HSPA4), mRNA.	-	-1.27
ILMN_1653871	NAMPT	NM_005746.1	Homo sapiens nicotinamide phosphoribosyltransferase (NAMPT), mRNA.	-	-1.26
ILMN_1766505	COMMD10	NM_016144.2	Homo sapiens COMM domain containing 10 (COMMD10), mRNA.	-	-1.26
ILMN_1685625	UCP2	NM_003355.2	Homo sapiens uncoupling protein 2 (mitochondrial, proton carrier) (UCP2), nuclear gene encoding mitochondrial protein, mRNA.	-	-1.26
ILMN_2111187	ELOVL6	NM_024090.1	Homo sapiens ELOVL family member 6, elongation of long chain fatty acids (FEN1/Elo2, SUR4/Elo3-like, yeast) (ELOVL6), mRNA.	-	-1.26
ILMN_1665049	SPG11	NM_025137.2	Homo sapiens spastic paraplegia 11 (autosomal recessive) (SPG11), transcript variant 1, mRNA.	-	-1.26
ILMN_1770692	WDR12	NM_018256.2	Homo sapiens WD repeat domain 12 (WDR12), mRNA.	-	-1.26
ILMN_2399328	COBRA1	NM_015456.2	Homo sapiens cofactor of BRCA1 (COBRA1), mRNA.	-	-1.26

ILMN_1815134	PI4K2B	NM_018323.2	Homo sapiens phosphatidylinositol 4-kinase type 2 beta (PI4K2B), mRNA.	-	-1.26
ILMN_1683598	ACSL4	NM_004458.1	Homo sapiens acyl-CoA synthetase long-chain family member 4 (ACSL4), transcript variant 1, mRNA.	-	-1.26
ILMN_2094905	COMMD10	NM_016144.2	Homo sapiens COMM domain containing 10 (COMMD10), mRNA.	-	-1.26
ILMN_1810176	MAP3K7	NM_145331.1	Homo sapiens mitogen-activated protein kinase kinase kinase 7 (MAP3K7), transcript variant B, mRNA.	-	-1.26
ILMN_1703692	LOC647000	XM_929980.1	PREDICTED: Homo sapiens similar to tubulin, beta 5 (LOC647000), mRNA.	-	-1.26
ILMN_1769810	ARL6IP5	NM_006407.3	Homo sapiens ADP-ribosylation-like factor 6 interacting protein 5 (ARL6IP5), mRNA.	-	-1.26
ILMN_1653026	PLAC8	NM_016619.1	Homo sapiens placenta-specific 8 (PLAC8), mRNA.	-	-1.26
ILMN_1682264	DCAF7	NM_005828.2	Homo sapiens DDB1 and CUL4 associated factor 7 (DCAF7), mRNA.	-	-1.26
ILMN_1794782	ABCG1	NM_004915.3	Homo sapiens ATP-binding cassette, sub-family G (WHITE), member 1 (ABCG1), transcript variant 2, mRNA.	-	-1.25
ILMN_1703330	FEM1C	NM_020177.2	Homo sapiens fem-1 homolog c (C. elegans) (FEM1C), mRNA.	-	-1.25
ILMN_1783023	C5ORF51	NM_175921.4	Homo sapiens chromosome 5 open reading frame 51 (C5orf51), mRNA.	-	-1.25
ILMN_3201115	LOC440043	XR_015812.2	PREDICTED: Homo sapiens misc_RNA (LOC440043), miscRNA.	-	-1.25
ILMN_1809889	CCDC117	NM_173510.1	Homo sapiens coiled-coil domain containing 117 (CCDC117), mRNA.	-	-1.25
ILMN_1800540	CD55	NM_000574.2	Homo sapiens CD55 molecule, decay accelerating factor for complement (Cromer blood group) (CD55), mRNA.	-	-1.25
ILMN_3213573	LOC645715	XR_017484.1	PREDICTED: Homo sapiens misc_RNA (LOC645715), miscRNA.	-	-1.25
ILMN_1720442	NCBP2	NM_007362.2	Homo sapiens nuclear cap binding protein subunit 2, 20kDa (NCBP2), transcript variant 1, mRNA.	-	-1.25
ILMN_2124951	RBMX	NM_002139.2	Homo sapiens RNA binding motif protein, X-linked (RBMX), mRNA.	-	-1.25
ILMN_1670079	OMA1	NM_145243.3	Homo sapiens OMA1 homolog, zinc metallopeptidase (S. cerevisiae) (OMA1), mRNA.	-	-1.25

ILMN_2326273	CHI3L2	NM_004000.2	Homo sapiens chitinase 3-like 2 (CHI3L2), transcript variant 1, mRNA.	-	-1.25
ILMN_2228732	CCNG2	NM_004354.1	Homo sapiens cyclin G2 (CCNG2), mRNA.	-	-1.25
ILMN_1687538	ETS1	NM_005238.2	Homo sapiens v-ets erythroblastosis virus E26 oncogene homolog 1 (avian) (ETS1), mRNA.	-	-1.25
ILMN_1806634	NNT	NM_182977.1	Homo sapiens nicotinamide nucleotide transhydrogenase (NNT), nuclear gene encoding mitochondrial protein, transcript variant 1, mRNA.	-	-1.25
ILMN_1675085	UBA6	NM_018227.3	Homo sapiens ubiquitin-like modifier activating enzyme 6 (UBA6), mRNA.	-1.21	-1.25
ILMN_2138435	MRPS27	NM_015084.1	Homo sapiens mitochondrial ribosomal protein S27 (MRPS27), nuclear gene encoding mitochondrial protein, mRNA.	-	-1.25
ILMN_2202948	BUB1	NM_004336.2	Homo sapiens BUB1 budding uninhibited by benzimidazoles 1 homolog (yeast) (BUB1), mRNA.	-	-1.24
ILMN_1736054	SUB1	NM_006713.2	Homo sapiens SUB1 homolog (S. cerevisiae) (SUB1), mRNA.	-1.32	-1.24
ILMN_2364828	OGT	NM_181672.1	Homo sapiens O-linked N-acetylglucosamine (GlcNAc) transferase (UDP-N-acetylglucosamine:polypeptide-N-acetylglucosaminyl transferase) (OGT), transcript variant 1, mRNA.	-	-1.24
ILMN_3288830	LOC100132918	XR_039697.1	PREDICTED: Homo sapiens misc_RNA (LOC100132918), miscRNA.	-	-1.24
ILMN_1746699	SGOL2	NM_152524.3	Homo sapiens shugoshin-like 2 (S. pombe) (SGOL2), mRNA.	-	-1.24
ILMN_1657862	AHCY	NM_000687.1	Homo sapiens S-adenosylhomocysteine hydrolase (AHCY), mRNA.	-	-1.24
ILMN_1771903	NUP37	NM_024057.2	Homo sapiens nucleoporin 37kDa (NUP37), mRNA.	-	-1.24
ILMN_1741264	MRPS33	NM_016071.2	Homo sapiens mitochondrial ribosomal protein S33 (MRPS33), nuclear gene encoding mitochondrial protein, transcript variant 1, mRNA.	-	-1.24
ILMN_2376108	PSMB9	NM_002800.4	Homo sapiens proteasome (prosome, macropain) subunit, beta type, 9 (large multifunctional peptidase 2) (PSMB9), transcript variant 1, mRNA.	-	-1.24

ILMN_1720422	G3BP2	NM_012297.3	Homo sapiens GTPase activating protein (SH3 domain) binding protein 2 (G3BP2), transcript variant 3, mRNA.	-	-1.24
ILMN_2332964	LGMN	NM_001008530.1	Homo sapiens legumain (LGMN), transcript variant 2, mRNA.	-	-1.24
ILMN_1660787	SUCLA2	NM_003850.1	Homo sapiens succinate-CoA ligase, ADP-forming, beta subunit (SUCLA2), mRNA.	-	-1.24
ILMN_2351611	UBQLN1	NM_053067.1	Homo sapiens ubiquilin 1 (UBQLN1), transcript variant 2, mRNA.	-	-1.24
ILMN_3208330	LOC100132797	XR_036994.1	PREDICTED: Homo sapiens misc_RNA (LOC100132797), miscRNA.	-	-1.24
ILMN_1767837	GOLT1B	NM_016072.2	Homo sapiens golgi transport 1 homolog B (S. cerevisiae) (GOLT1B), mRNA.	-	-1.24
ILMN_1760509	EOMES	NM_005442.2	Homo sapiens eomesodermin homolog (Xenopus laevis) (EOMES), mRNA.	-	-1.24
ILMN_2063586	CLIC4	NM_013943.1	Homo sapiens chloride intracellular channel 4 (CLIC4), nuclear gene encoding mitochondrial protein, mRNA.	-	-1.24
ILMN_1768050	SCOC	NM_032547.1	Homo sapiens short coiled-coil protein (SCOC), mRNA.	-1.22	-1.23
ILMN_3292224	LOC100131609	XR_038433.1	PREDICTED: Homo sapiens misc_RNA (LOC100131609), miscRNA.	-	-1.23
ILMN_3306482	LOC730107	XM_001721064.1	PREDICTED: Homo sapiens similar to Glycine cleavage system H protein, mitochondrial (LOC730107), mRNA.	-1.21	-1.23
ILMN_1706873	RPL34	NM_000995.2	Homo sapiens ribosomal protein L34 (RPL34), transcript variant 1, mRNA.	-	-1.23
ILMN_1776102	PSMD10	NM_170750.1	Homo sapiens proteasome (prosome, macropain) 26S subunit, non-ATPase, 10 (PSMD10), transcript variant 1, mRNA.	-	-1.23
ILMN_1774028	MTFR1	NM_014637.2	Homo sapiens mitochondrial fission regulator 1 (MTFR1), nuclear gene encoding mitochondrial protein, mRNA.	-	-1.23
ILMN_1710937	IFI16	NM_005531.1	Homo sapiens interferon, gamma-inducible protein 16 (IFI16), mRNA.	-	-1.23
ILMN_1801928	YWHAZ	NM_003406.2	Homo sapiens tyrosine 3-monooxygenase/tryptophan 5-monooxygenase activation protein, zeta polypeptide (YWHAZ), transcript variant 1, mRNA.	-	-1.23

ILMN_1807925	GNG2	NM_053064.2	Homo sapiens guanine nucleotide binding protein (G protein), gamma 2 (GNG2), mRNA.	-	-1.23
ILMN_1777564	MAD2L1	NM_002358.2	Homo sapiens MAD2 mitotic arrest deficient-like 1 (yeast) (MAD2L1), mRNA.	-	-1.23
ILMN_1728225	KIAA1524	NM_020890.1	Homo sapiens KIAA1524 (KIAA1524), mRNA.	-1.21	-1.23
ILMN_1694589	PAQR8	NM_133367.2	Homo sapiens progestin and adipoQ receptor family member VIII (PAQR8), mRNA.	-	-1.23
ILMN_1744647	CAND1	NM_018448.2	Homo sapiens cullin-associated and neddylation-dissociated 1 (CAND1), mRNA.	-	-1.23
ILMN_1686811	LOC402644	XM_938297.1	PREDICTED: Homo sapiens similar to peptidylprolyl isomerase A isoform 1 (LOC402644), mRNA.	-	-1.23
ILMN_1785284	ALDH6A1	NM_005589.2	Homo sapiens aldehyde dehydrogenase 6 family, member A1 (ALDH6A1), nuclear gene encoding mitochondrial protein, mRNA.	-	-1.23
ILMN_2331735	AP2B1	NM_001282.2	Homo sapiens adaptor-related protein complex 2, beta 1 subunit (AP2B1), transcript variant 2, mRNA.	-	-1.23
ILMN_1851547	HS.86045	Hs.86045	Homo sapiens cDNA FLJ43676 fis, clone SYNOV4009129	-	-1.23
ILMN_1664153	SLC30A5	NM_022902.2	Homo sapiens solute carrier family 30 (zinc transporter), member 5 (SLC30A5), transcript variant 1, mRNA.	-	-1.23
ILMN_2048636	ME2	NM_002396.3	Homo sapiens malic enzyme 2, NAD(+)-dependent, mitochondrial (ME2), nuclear gene encoding mitochondrial protein, mRNA.	-	-1.23
ILMN_2131381	PDE3B	NM_000922.2	Homo sapiens phosphodiesterase 3B, cGMP-inhibited (PDE3B), mRNA.	-	-1.23
ILMN_3267670	LOC100130550	XR_037892.1	PREDICTED: Homo sapiens misc_RNA (LOC100130550), miscRNA.	-	-1.23
ILMN_1761083	HNRNPA3	NM_194247.1	Homo sapiens heterogeneous nuclear ribonucleoprotein A3 (HNRNPA3), mRNA.	-	-1.22
ILMN_1854241	HS.544884	Hs.544884	602571480F1 NIH_MGC_77 Homo sapiens cDNA clone IMAGE:4696170 5, mRNA sequence	-	-1.22

ILMN_1669142	NARG1	NM_057175.3	Homo sapiens NMDA receptor regulated 1 (NARG1), mRNA.	-	-1.22
ILMN_1789508	GTF3C3	NM_012086.1	Homo sapiens general transcription factor IIIC, polypeptide 3, 102kDa (GTF3C3), mRNA.	-	-1.22
ILMN_2360705	ACSL3	NM_203372.1	Homo sapiens acyl-CoA synthetase long-chain family member 3 (ACSL3), transcript variant 2, mRNA.	-1.23	-1.22
ILMN_3297455	LOC729082	XR_040993.1	PREDICTED: Homo sapiens misc_RNA (LOC729082), miscRNA.	-	-1.22
ILMN_3281599	LOC642741	XR_019077.2	PREDICTED: Homo sapiens misc_RNA (LOC642741), miscRNA.	-	-1.22
ILMN_1794165	PGD	NM_002631.2	Homo sapiens phosphogluconate dehydrogenase (PGD), mRNA.	-	-1.22
ILMN_1677607	SC5DL	NM_006918.3	Homo sapiens sterol-C5-desaturase (ERG3 delta-5-desaturase homolog, S. cerevisiae)-like (SC5DL), transcript variant 1, mRNA.	-	-1.22
ILMN_1696420	BRD7	NM_013263.2	Homo sapiens bromodomain containing 7 (BRD7), mRNA.	-	-1.22
ILMN_2406335	ANKRD17	NM_198889.1	Homo sapiens ankyrin repeat domain 17 (ANKRD17), transcript variant 2, mRNA.	-	-1.22
ILMN_1668012	SLC25A13	NM_014251.1	Homo sapiens solute carrier family 25, member 13 (citrin) (SLC25A13), mRNA.	-	-1.22
ILMN_1757317	LARS	NM_020117.8	Homo sapiens leucyl-tRNA synthetase (LARS), mRNA.	-	-1.22
ILMN_1656691	FBXO4	NM_012176.2	Homo sapiens F-box protein 4 (FBXO4), transcript variant 1, mRNA.	-	-1.22
ILMN_1776073	CCT4	NM_006430.2	Homo sapiens chaperonin containing TCP1, subunit 4 (delta) (CCT4), mRNA.	-	-1.22
ILMN_2143250	FAR1	NM_032228.4	Homo sapiens fatty acyl CoA reductase 1 (FAR1), mRNA.	-	-1.22
ILMN_1770515	UBE2V2	NM_003350.2	Homo sapiens ubiquitin-conjugating enzyme E2 variant 2 (UBE2V2), mRNA.	-	-1.22
ILMN_2139816	GPSM2	NM_013296.3	Homo sapiens G-protein signalling modulator 2 (AGS3-like, C. elegans) (GPSM2), mRNA.	-	-1.22
ILMN_1756942	SP3	NM_001017371.3	Homo sapiens Sp3 transcription factor (SP3), transcript variant 2, mRNA.	-	-1.22

ILMN_1654488	UTX	NM_021140.1	Homo sapiens ubiquitously transcribed tetratricopeptide repeat, X chromosome (UTX), mRNA.	-	-1.22
ILMN_1727540	C1ORF112	NM_018186.2	Homo sapiens chromosome 1 open reading frame 112 (C1orf112), mRNA.	-	-1.22
ILMN_2381753	G3BP2	NM_203504.1	Homo sapiens GTPase activating protein (SH3 domain) binding protein 2 (G3BP2), transcript variant 3, mRNA.	-	-1.22
ILMN_1690040	TM7SF2	NM_003273.1	Homo sapiens transmembrane 7 superfamily member 2 (TM7SF2), mRNA.	-	-1.22
ILMN_1762972	CHD9	NM_025134.3	Homo sapiens chromodomain helicase DNA binding protein 9 (CHD9), mRNA.	-	-1.22
ILMN_1692163	NSDHL	NM_015922.1	Homo sapiens NAD(P) dependent steroid dehydrogenase-like (NSDHL), mRNA.	-	-1.22
ILMN_3268880	C10ORF75	XR_041972.1	PREDICTED: Homo sapiens misc_RNA (C10orf75), miscRNA.	-	-1.22
ILMN_1769118	Sep-09	NM_006640.2	Homo sapiens septin 9 (SEPT9), mRNA.	-	-1.22
ILMN_2163796	RABGGTB	NM_004582.2	Homo sapiens Rab geranylgeranyltransferase, beta subunit (RABGGTB), mRNA.	-	-1.22
ILMN_1738572	USP48	NM_001032730.1	Homo sapiens ubiquitin specific peptidase 48 (USP48), transcript variant 2, mRNA.	-	-1.22
ILMN_2100458	RFESD	NM_173362.2	Homo sapiens Rieske (Fe-S) domain containing (RFESD), mRNA.	-	-1.22
ILMN_1733256	PSMD8	NM_002812.3	Homo sapiens proteasome (prosome, macropain) 26S subunit, non-ATPase, 8 (PSMD8), mRNA.	-	-1.21
ILMN_3226181	NUDT7	NM_001105663.1	Homo sapiens nudix (nucleoside diphosphate linked moiety X)-type motif 7 (NUDT7), transcript variant 1, mRNA.	-	-1.21
ILMN_2294431	CDC25C	NM_001790.3	Homo sapiens cell division cycle 25 homolog C (S. pombe) (CDC25C), transcript variant 1, mRNA.	-	-1.21
ILMN_1791097	RSBN1	NM_018364.3	Homo sapiens round spermatid basic protein 1 (RSBN1), mRNA.	-	-1.21
ILMN_1730611	RTN4	NM_007008.2	Homo sapiens reticulon 4 (RTN4), transcript variant 3, mRNA.	-	-1.21

ILMN_1659766	BAG3	NM_004281.3	Homo sapiens BCL2-associated athanogene 3 (BAG3), mRNA.	-	-1.21
ILMN_1794539	KIF11	NM_004523.2	Homo sapiens kinesin family member 11 (KIF11), mRNA.	-	-1.21
ILMN_1756572	COQ2	NM_015697.5	Homo sapiens coenzyme Q2 homolog, prenyltransferase (yeast) (COQ2), mRNA.	-	-1.21
ILMN_1696003	GNAI3	NM_006496.1	Homo sapiens guanine nucleotide binding protein (G protein), alpha inhibiting activity polypeptide 3 (GNAI3), mRNA.	-	-1.21
ILMN_1785795	METAP1	NM_015143.1	Homo sapiens methionyl aminopeptidase 1 (METAP1), mRNA.	-	-1.21
ILMN_1673820	HLTF	NM_003071.2	Homo sapiens helicase-like transcription factor (HLTF), transcript variant 2, mRNA.	-	-1.21
ILMN_2093343	PLAC8	NM_016619.1	Homo sapiens placenta-specific 8 (PLAC8), mRNA.	-	-1.21
ILMN_2344002	SIP1	NM_001009182.1	Homo sapiens survival of motor neuron protein interacting protein 1 (SIP1), transcript variant beta, mRNA.	-	-1.21
ILMN_1790909	NFE2L2	NM_006164.2	Homo sapiens nuclear factor (erythroid-derived 2)-like 2 (NFE2L2), mRNA.	-	-1.21
ILMN_3275672	LOC643873	XR_039149.1	PREDICTED: Homo sapiens misc_RNA (LOC643873), miscRNA.	-	-1.21
ILMN_1675186	ME2	NM_002396.3	Homo sapiens malic enzyme 2, NAD(+)-dependent, mitochondrial (ME2), nuclear gene encoding mitochondrial protein, mRNA.	-	-1.21
ILMN_1734476	KIF2A	NM_004520.1	Homo sapiens kinesin heavy chain member 2A (KIF2A), mRNA.	-	-1.21
ILMN_1748770	CKAP5	NM_001008938.1	Homo sapiens cytoskeleton associated protein 5 (CKAP5), transcript variant 1, mRNA.	-	-1.21
ILMN_3243441	EEF1AL7	NR_003586.1	Homo sapiens eukaryotic translation elongation factor 1 alpha-like 7 (EEF1AL7), non-coding RNA.	-	-1.21
ILMN_1761363	VAMP4	NM_003762.2	Homo sapiens vesicle-associated membrane protein 4 (VAMP4), mRNA.	-	-1.21
ILMN_2164081	KLHL12	NM_021633.2	Homo sapiens kelch-like 12 (Drosophila) (KLHL12), mRNA.	-	-1.21
ILMN_1801121	SENP2	NM_021627.2	Homo sapiens SUMO1/sentrin/SMT3 specific peptidase 2 (SENP2), mRNA.	-	-1.21

ILMN_1712888	HSPH1	NM_006644.2	Homo sapiens heat shock 105kDa/110kDa protein 1 (HSPH1), mRNA.	-	-1.21
ILMN_2181060	CKAP2	NM_018204.2	Homo sapiens cytoskeleton associated protein 2 (CKAP2), mRNA.	-	-1.21
ILMN_1781943	FAM83D	NM_030919.1	Homo sapiens family with sequence similarity 83, member D (FAM83D), mRNA.	-	-1.21
ILMN_1875342	HS.356079	Hs.356079	Homo sapiens cDNA FLJ42149 fis, clone THYMU1000692	-	-1.21
ILMN_1754421	NDUFAF1	NM_016013.2	Homo sapiens NADH dehydrogenase (ubiquinone) 1 alpha subcomplex, assembly factor 1 (NDUFAF1), mRNA.	-	-1.21
ILMN_1790978	ATG7	NM_006395.1	Homo sapiens ATG7 autophagy related 7 homolog (S. cerevisiae) (ATG7), mRNA.	-	-1.21
ILMN_1731484	RHOT1	NM_001033568.1	Homo sapiens ras homolog gene family, member T1 (RHOT1), transcript variant 1, mRNA.	-	-1.21
ILMN_2225718	CENPE	NM_001813.2	Homo sapiens centromere protein E, 312kDa (CENPE), mRNA.	-	-1.21
ILMN_1676191	DARS2	NM_018122.3	Homo sapiens aspartyl-tRNA synthetase 2, mitochondrial (DARS2), nuclear gene encoding mitochondrial protein, mRNA.	-	-1.21
ILMN_1720241	TRIP12	NM_004238.1	Homo sapiens thyroid hormone receptor interactor 12 (TRIP12), mRNA.	-	-1.21
ILMN_1794046	MTX2	NM_006554.3	Homo sapiens metaxin 2 (MTX2), transcript variant 1, mRNA.	-	-1.21
ILMN_1700202	TMEM135	NM_022918.2	Homo sapiens transmembrane protein 135 (TMEM135), mRNA.	-1.22	-1.21
ILMN_1711470	UBE2T	NM_014176.1	Homo sapiens ubiquitin-conjugating enzyme E2T (putative) (UBE2T), mRNA.	-	-1.21
ILMN_2354478	CYFIP2	NM_001037333.1	Homo sapiens cytoplasmic FMR1 interacting protein 2 (CYFIP2), transcript variant 1, mRNA.	-1.24	-1.2
ILMN_2335754	CD1E	NM_001042586.1	Homo sapiens CD1e molecule (CD1E), transcript variant 5, mRNA.	-	-1.2
ILMN_1791568	CEP57	NM_014679.3	Homo sapiens centrosomal protein 57kDa (CEP57), mRNA.	-	-1.2
ILMN_2353033	FUBP3	NM_003934.1	Homo sapiens far upstream element (FUSE) binding protein 3 (FUBP3), mRNA. XM_945904 XM_945906 XM_945907	-	-1.2

ILMN_1769665	RAB5C	NM_201434.1	Homo sapiens RAB5C, member RAS oncogene family (RAB5C), transcript variant 1, mRNA.	-	-1.2
ILMN_1835925	HS.576501	Hs.576501	602641695F1 NIH_MGC_61 Homo sapiens cDNA clone IMAGE:4772926 5, mRNA sequence	-	-1.2
ILMN_3177285	HNRNPR	NM_005826.3	Homo sapiens heterogeneous nuclear ribonucleoprotein R (HNRNPR), transcript variant 2, mRNA.	-	-1.2
ILMN_1800008	ACAT1	NM_000019.2	Homo sapiens acetyl-Coenzyme A acetyltransferase 1 (ACAT1), nuclear gene encoding mitochondrial protein, mRNA.	-	-1.2
ILMN_1805132	PCDH19	NM_020766.1	Homo sapiens protocadherin 19 (PCDH19), mRNA.	-	-1.2
ILMN_1666453	STK3	NM_006281.1	Homo sapiens serine/threonine kinase 3 (STE20 homolog, yeast) (STK3), mRNA.	-	-1.2
ILMN_1738712	GPR180	NM_180989.3	Homo sapiens G protein-coupled receptor 180 (GPR180), mRNA.	-	-1.2
ILMN_2412927	GMPPB	NM_021971.1	Homo sapiens GDP-mannose pyrophosphorylase B (GMPPB), transcript variant 2, mRNA.	-	-1.2
ILMN_1741976	SMARCAD1	NM_020159.1	Homo sapiens SWI/SNF-related, matrix-associated actin-dependent regulator of chromatin, subfamily a, containing DEAD/H box 1 (SMARCAD1), mRNA.	-	-1.2
ILMN_1732080	SUMO1P3	NR_002190.1	Homo sapiens SUMO1 pseudogene 3 (SUMO1P3), non-coding RNA.	-	-1.2
ILMN_1697024	LOC730432	XM_936257.1	PREDICTED: Homo sapiens similar to serine/threonine/tyrosine interacting protein, transcript variant 1 (LOC730432), mRNA.	-	-1.2
ILMN_1693220	AKAP11	NM_016248.2	Homo sapiens A kinase (PRKA) anchor protein 11 (AKAP11), mRNA.	-	-1.2
ILMN_1675669	IBTK	NM_015525.2	Homo sapiens inhibitor of Bruton agammaglobulinemia tyrosine kinase (IBTK), mRNA.	-	-1.2

ILMN_2405521	MTHFD2	NM_001040409.1	Homo sapiens methylenetetrahydrofolate dehydrogenase (NADP+ dependent) 2, methenyltetrahydrofolate cyclohydrolase (MTHFD2), nuclear gene encoding mitochondrial protein, transcript variant 2, mRNA.	-	-1.2
ILMN_2399893	RPS24	NM_001026.3	Homo sapiens ribosomal protein S24 (RPS24), transcript variant 2, mRNA.	-	-1.2
ILMN_1685480	TARS	NM_152295.3	Homo sapiens threonyl-tRNA synthetase (TARS), mRNA.	-1.2	-1.2
ILMN_1707695	IFIT1	NM_001548.2	Homo sapiens interferon-induced protein with tetratricopeptide repeats 1 (IFIT1), transcript variant 2, mRNA.	-	-1.2
ILMN_1656977	HIBCH	NM_014362.2	Homo sapiens 3-hydroxyisobutyryl-Coenzyme A hydrolase (HIBCH), nuclear gene encoding mitochondrial protein, transcript variant 2, mRNA.	-	-1.2
ILMN_2350114	TRIM13	NM_001007278.1	Homo sapiens tripartite motif-containing 13 (TRIM13), transcript variant 4, mRNA.	-	-1.2
ILMN_3229552	MED7	NM_001100816.1	Homo sapiens mediator complex subunit 7 (MED7), transcript variant 1, mRNA.	-	-1.2
ILMN_1691341	IL7R	XM_937367.1	PREDICTED: Homo sapiens interleukin 7 receptor (IL7R), mRNA.	-	1.2
ILMN_1764609	PWWP2B	NM_138499.2	Homo sapiens PWWP domain containing 2B (PWWP2B), transcript variant 1, mRNA.	-	1.2
ILMN_1684553	RHOH	NM_004310.2	Homo sapiens ras homolog gene family, member H (RHOH), mRNA.	-	1.2
ILMN_2232177	ACTN1	NM_001102.2	Homo sapiens actinin, alpha 1 (ACTN1), mRNA.	-	1.2
ILMN_2173740	ASB8	NM_024095.3	Homo sapiens ankyrin repeat and SOCS box-containing 8 (ASB8), mRNA.	-	1.2
ILMN_1727756	IDI2	NM_033261.2	Homo sapiens isopentenyl-diphosphate delta isomerase 2 (IDI2), mRNA.	-	1.2

ILMN_2379130	IRAK1	NM_001025243.1	Homo sapiens interleukin-1 receptor-associated kinase 1 (IRAK1), transcript variant 3, mRNA.	-	1.2
ILMN_3245688	DGCR6L	NM_033257.2	Homo sapiens DiGeorge syndrome critical region gene 6-like (DGCR6L), mRNA.	-	1.2
ILMN_1677484	SNAPC4	NM_003086.1	Homo sapiens small nuclear RNA activating complex, polypeptide 4, 190kDa (SNAPC4), mRNA.	-	1.2
ILMN_3248773	C7ORF40	NR_003697.1	Homo sapiens chromosome 7 open reading frame 40 (C7orf40), non-coding RNA.	-	1.2
ILMN_1667034	PDPR	NM_017990.3	PREDICTED: Homo sapiens pyruvate dehydrogenase phosphatase regulatory subunit (PDPR), mRNA.	-	1.2
ILMN_2365569	ICA1	NM_004968.2	Homo sapiens islet cell autoantigen 1, 69kDa (ICA1), transcript variant 2, mRNA.	-	1.2
ILMN_1693410	BRI3BP	XM_941876.1	PREDICTED: Homo sapiens BRI3 binding protein (BRI3BP), mRNA.	-	1.21
ILMN_2398587	ZNRD1	NM_014596.4	Homo sapiens zinc ribbon domain containing 1 (ZNRD1), transcript variant b, mRNA.	-	1.21
ILMN_1799856	NOMO2	NM_173614.2	Homo sapiens NODAL modulator 2 (NOMO2), transcript variant 2, mRNA.	-	1.21
ILMN_1672605	C7ORF41	NM_152793.1	Homo sapiens chromosome 7 open reading frame 41 (C7orf41), mRNA.	-	1.21
ILMN_1794213	ABHD14A	NM_015407.3	Homo sapiens abhydrolase domain containing 14A (ABHD14A), mRNA.	-	1.21
ILMN_3242818	RNU105C	NR_004385.1	Homo sapiens RNA, U105C small nucleolar (RNU105C), small nucleolar RNA.	-	1.21
ILMN_1672961	LOC652624	XM_942165.1	PREDICTED: Homo sapiens similar to 40S ribosomal protein SA (p40) (34/67 kDa laminin receptor) (LOC652624), mRNA.	-	1.21

ILMN_3249286	SNORD12C	NR_002433.1	Homo sapiens small nucleolar RNA, C/D box 12C (SNORD12C), small nucleolar RNA.	-	1.21
ILMN_1654262	ZMAT3	NM_152240.1	Homo sapiens zinc finger, matrin type 3 (ZMAT3), transcript variant 2, mRNA.	-	1.21
ILMN_1791232	SPRED2	NM_181784.1	Homo sapiens sprouty-related, EVH1 domain containing 2 (SPRED2), mRNA.	-	1.21
ILMN_2374164	HERPUD1	NM_001010990.1	Homo sapiens homocysteine-inducible, endoplasmic reticulum stress-inducible, ubiquitin-like domain member 1 (HERPUD1), transcript variant 3, mRNA.	-	1.21
ILMN_1654118	BCL2L1	NM_138578.1	Homo sapiens BCL2-like 1 (BCL2L1), nuclear gene encoding mitochondrial protein, transcript variant 1, mRNA.	-	1.21
ILMN_2206716	JTB	NM_006694.2	Homo sapiens jumping translocation breakpoint (JTB), mRNA.	-	1.21
ILMN_1880937	HS.153349	Hs.153349	xs48g03.x1 NCI_CGAP_Kid11 Homo sapiens cDNA clone IMAGE:2772916 3, mRNA sequence	-	1.21
ILMN_1716093	KRT10	NM_000421.2	Homo sapiens keratin 10 (epidermolytic hyperkeratosis; keratosis palmaris et plantaris) (KRT10), mRNA.	-	1.21
ILMN_2316104	IQCB1	NM_001023571.1	Homo sapiens IQ motif containing B1 (IQCB1), transcript variant 3, mRNA.	-	1.21
ILMN_1666280	COX11	NM_004375.2	Homo sapiens COX11 homolog, cytochrome c oxidase assembly protein (yeast) (COX11), nuclear gene encoding mitochondrial protein, mRNA.	-	1.21
ILMN_1695706	H3F3B	NM_005324.3	Homo sapiens H3 histone, family 3B (H3.3B) (H3F3B), mRNA.	-	1.21
ILMN_1773868	U2AF1L2	NM_005089.1	Homo sapiens U2(RNU2) small nuclear RNA auxiliary factor 1-like 2 (U2AF1L2), mRNA.	-	1.21
ILMN_1811117	LOC400986	NM_001010914.1	PREDICTED: Homo sapiens protein immuno-reactive with anti-PTH polyclonal antibodies (LOC400986), mRNA.	-	1.21

ILMN_1698419	NCOR2	NM_006312.2	Homo sapiens nuclear receptor co-repressor 2 (NCOR2), transcript variant 2, mRNA.	-	1.21
ILMN_1653856	STS-1	NM_032873.3	Homo sapiens Cbl-interacting protein Sts-1 (STS-1), mRNA.	-	1.21
ILMN_1660292	MRPS21	NM_018997.1	Homo sapiens mitochondrial ribosomal protein S21 (MRPS21), nuclear gene encoding mitochondrial protein, transcript variant 2, mRNA.	-	1.21
ILMN_1808769	C1ORF97	NM_032705.2	Homo sapiens chromosome 1 open reading frame 97 (C1orf97), mRNA.	-	1.21
ILMN_1701558	MAP1A	NM_002373.4	Homo sapiens microtubule-associated protein 1A (MAP1A), mRNA.	-	1.21
ILMN_2326713	CD151	NM_139030.3	Homo sapiens CD151 molecule (Raph blood group) (CD151), transcript variant 2, mRNA.	-	1.21
ILMN_1764500	C3ORF10	NM_018462.4	Homo sapiens chromosome 3 open reading frame 10 (C3orf10), mRNA.	-	1.21
ILMN_1775235	AFF3	NM_002285.2	Homo sapiens AF4/FMR2 family, member 3 (AFF3), transcript variant 2, mRNA.	-	1.21
ILMN_2143795	MGC4677	NM_052871.3	Homo sapiens hypothetical protein MGC4677 (MGC4677), mRNA.	-	1.21
ILMN_1709039	RPL13	NM_033251.1	Homo sapiens ribosomal protein L13 (RPL13), transcript variant 2, mRNA.	-	1.22
ILMN_2116714	SLC39A1	NM_014437.3	Homo sapiens solute carrier family 39 (zinc transporter), member 1 (SLC39A1), mRNA.	-	1.22
ILMN_1812297	CYP26B1	NM_019885.2	Homo sapiens cytochrome P450, family 26, subfamily B, polypeptide 1 (CYP26B1), mRNA.	-	1.22
ILMN_2398107	ASNS	NM_133436.1	Homo sapiens asparagine synthetase (ASNS), transcript variant 1, mRNA.	-	1.22
ILMN_3241554	KANK4	NM_181712.4	Homo sapiens KN motif and ankyrin repeat domains 4 (KANK4), mRNA.	-	1.22
ILMN_1707631	MED10	NM_032286.2	Homo sapiens mediator complex subunit 10 (MED10), mRNA.	-	1.22
ILMN_1789627	Sep-05	NM_000407.3	Homo sapiens septin 5 (SEPT5), mRNA.	-	1.22
ILMN_1674983	LOC387841	XM_932678.1	PREDICTED: Homo sapiens similar to ribosomal protein L13a, transcript variant 2 (LOC387841), mRNA.	-	1.22

ILMN_2177090	LOC200030	NM_183372.3	Homo sapiens neuroblastoma breakpoint family, member 11-like (LOC200030), mRNA.	-	1.22
ILMN_3246214	B3GNT1	NM_006876.2	Homo sapiens UDP-GlcNAc:betaGal beta-1,3-N-acetylglucosaminyltransferase 1 (B3GNT1), mRNA.	1.22	1.22
ILMN_2327860	MAL	NM_022440.1	Homo sapiens mal, T-cell differentiation protein (MAL), transcript variant d, mRNA.	1.34	1.22
ILMN_1713266	FAM46C	NM_017709.2	Homo sapiens family with sequence similarity 46, member C (FAM46C), mRNA.	-	1.22
ILMN_2325506	BCAS4	NM_017843.3	Homo sapiens breast carcinoma amplified sequence 4 (BCAS4), transcript variant 1, mRNA.	-	1.22
ILMN_1809750	TDRD1	NM_198795.1	Homo sapiens tudor domain containing 1 (TDRD1), mRNA.	-	1.22
ILMN_1665335	DIABLO	NM_138930.2	Homo sapiens diablo homolog (Drosophila) (DIABLO), nuclear gene encoding mitochondrial protein, transcript variant 2, mRNA.	-	1.22
ILMN_1714364	PTK2	NM_153831.2	Homo sapiens PTK2 protein tyrosine kinase 2 (PTK2), transcript variant 2, mRNA.	-	1.22
ILMN_1740185	TPMT	NM_000367.2	Homo sapiens thiopurine S-methyltransferase (TPMT), mRNA.	-	1.22
ILMN_2320330	MAL	NM_002371.2	Homo sapiens mal, T-cell differentiation protein (MAL), transcript variant a, mRNA.	1.41	1.22
ILMN_1688780	S100A4	NM_002961.2	Homo sapiens S100 calcium binding protein A4 (S100A4), transcript variant 2, mRNA.	-	1.22
ILMN_1814282	ISG20L1	NM_022767.2	Homo sapiens interferon stimulated exonuclease gene 20kDa-like 1 (ISG20L1), mRNA.	-	1.23
ILMN_1696316	CPT1A	NM_001876.2	Homo sapiens carnitine palmitoyltransferase 1A (liver) (CPT1A), nuclear gene encoding mitochondrial protein, transcript variant 2, mRNA.	-	1.23

ILMN_1658290	C16ORF68	NM_024109.1	Homo sapiens chromosome 16 open reading frame 68 (C16orf68), mRNA.	-	1.23
ILMN_2388070	TMEM44	NM_138399.3	Homo sapiens transmembrane protein 44 (TMEM44), transcript variant 1, mRNA.	-	1.23
ILMN_1706859	C22ORF32	NM_033318.3	Homo sapiens chromosome 22 open reading frame 32 (C22orf32), mRNA.	-	1.23
ILMN_1703153	N-PAC	NM_032569.2	Homo sapiens cytokine-like nuclear factor n-pac (N-PAC), mRNA.	1.26	1.23
ILMN_2115490	NBPF20	NM_001037675.1	Homo sapiens neuroblastoma breakpoint family, member 20 (NBPF20), mRNA.	-	1.23
ILMN_1697377	LOC649841	XM_938906.1	PREDICTED: Homo sapiens similar to protein immuno-reactive with anti-PTH polyclonal antibodies (LOC649841), mRNA.	-	1.23
ILMN_1776519	RAP1GAP	NM_002885.1	Homo sapiens RAP1 GTPase activating protein (RAP1GAP), mRNA.	-	1.23
ILMN_2415786	CD96	NM_005816.4	Homo sapiens CD96 molecule (CD96), transcript variant 2, mRNA.	-	1.23
ILMN_1802646	EPHB6	NM_004445.2	Homo sapiens EPH receptor B6 (EPHB6), mRNA.	-	1.23
ILMN_1710075	FAM89A	XM_939093.1	PREDICTED: Homo sapiens family with sequence similarity 89, member A (FAM89A), mRNA.	-	1.23
ILMN_1754795	FAT1	NM_005245.3	Homo sapiens FAT tumor suppressor homolog 1 (Drosophila) (FAT1), mRNA.	-	1.23
ILMN_2135798	NR2C2AP	NM_176880.4	Homo sapiens nuclear receptor 2C2-associated protein (NR2C2AP), mRNA.	-	1.23
ILMN_1669788	NUDT14	NM_177533.2	Homo sapiens nudix (nucleoside diphosphate linked moiety X)-type motif 14 (NUDT14), mRNA.	-	1.23
ILMN_3238785	SNHG9	NR_003142.2	Homo sapiens small nucleolar RNA host gene 9 (non-protein coding) (SNHG9), non-coding RNA.	-	1.23
ILMN_1806408	ACADVL	NM_000018.2	Homo sapiens acyl-Coenzyme A dehydrogenase, very long chain (ACADVL), nuclear gene encoding mitochondrial protein, transcript variant 2, mRNA.	1.2	1.23

ILMN_2048793	CIAO1	NM_004804.2	Homo sapiens cytosolic iron-sulfur protein assembly 1 homolog (S. cerevisiae) (CIAO1), mRNA.	-	1.23
ILMN_2082762	SNORD68	NR_002450.1	Homo sapiens small nucleolar RNA, C/D box 68 (SNORD68), small nucleolar RNA.	-	1.23
ILMN_2246548	GSTTP2	NR_003082.1	Homo sapiens glutathione S-transferase theta pseudogene 2 (GSTTP2), non-coding RNA. XM_941198 XM_945014 XM_945016	-	1.23
ILMN_3233229	SNHG7	NR_024542.1	Homo sapiens small nucleolar RNA host gene 7 (non-protein coding) (SNHG7), transcript variant 2, non-coding RNA.	-	1.23
ILMN_1692865	VPS37D	XM_376631.3	Homo sapiens vacuolar protein sorting 37 homolog D (S. cerevisiae) (VPS37D), mRNA.	-	1.23
ILMN_1659936	PPP1R15A	NM_014330.2	Homo sapiens protein phosphatase 1, regulatory (inhibitor) subunit 15A (PPP1R15A), mRNA.	-	1.24
ILMN_1779524	CREB3L3	NM_032607.1	Homo sapiens cAMP responsive element binding protein 3-like 3 (CREB3L3), mRNA.	-	1.24
ILMN_2396991	HCST	NM_014266.3	Homo sapiens hematopoietic cell signal transducer (HCST), transcript variant 1, mRNA.	-	1.24
ILMN_1741632	RAB3IL1	NM_013401.2	Homo sapiens RAB3A interacting protein (rabin3)-like 1 (RAB3IL1), mRNA.	-	1.24
ILMN_1797875	ALOX5AP	NM_001629.2	Homo sapiens arachidonate 5-lipoxygenase-activating protein (ALOX5AP), mRNA.	-	1.24
ILMN_2070043	PPM1K	NM_152542.2	Homo sapiens protein phosphatase 1K (PP2C domain containing) (PPM1K), mRNA.	-	1.24
ILMN_1739032	TMEM70	NM_017866.3	Homo sapiens transmembrane protein 70 (TMEM70), transcript variant 1, mRNA.	-	1.24
ILMN_2157510	BLOC1S1	NM_001487.1	Homo sapiens biogenesis of lysosome-related organelles complex-1, subunit 1 (BLOC1S1), mRNA.	-	1.24

ILMN_1664912	IL11RA	NM_004512.3	Homo sapiens interleukin 11 receptor, alpha (IL11RA), transcript variant 1, mRNA.	-	1.24
ILMN_2306540	PDE9A	NM_001001567.1	Homo sapiens phosphodiesterase 9A (PDE9A), transcript variant 2, mRNA.	-	1.24
ILMN_1679826	CST7	NM_003650.2	Homo sapiens cystatin F (leukocystatin) (CST7), mRNA.	-	1.24
ILMN_2140799	FAM24B	NM_152644.2	Homo sapiens family with sequence similarity 24, member B (FAM24B), mRNA.	-	1.24
ILMN_1779228	CDH2	NM_001792.2	Homo sapiens cadherin 2, type 1, N-cadherin (neuronal) (CDH2), mRNA.	-	1.24
ILMN_2164242	UBE2F	NM_080678.1	Homo sapiens ubiquitin-conjugating enzyme E2F (putative) (UBE2F), mRNA.	-	1.24
ILMN_1802053	ZNF91	NM_003430.1	Homo sapiens zinc finger protein 91 (ZNF91), mRNA.	-	1.25
ILMN_1691156	MT1A	NM_005946.2	Homo sapiens metallothionein 1A (MT1A), mRNA.	-	1.25
ILMN_2311989	CUTA	NM_001014840.1	Homo sapiens cutA divalent cation tolerance homolog (E. coli) (CUTA), transcript variant 5, mRNA.	-	1.25
ILMN_1763207	BATF3	NM_018664.1	Homo sapiens basic leucine zipper transcription factor, ATF-like 3 (BATF3), mRNA.	-	1.25
ILMN_3300353	LOC729920	NM_001101417.2	Homo sapiens notch1-induced protein (LOC729920), transcript variant 2, mRNA.	-	1.25
ILMN_1785037	SSR2	XM_945430.1	PREDICTED: Homo sapiens signal sequence receptor, beta (translocon-associated protein beta), transcript variant 4 (SSR2), mRNA.	-	1.25
ILMN_2393765	IGLL1	NM_020070.2	Homo sapiens immunoglobulin lambda-like polypeptide 1 (IGLL1), transcript variant 1, mRNA.	-	1.25
ILMN_1741131	CHRNB1	NM_000747.2	Homo sapiens cholinergic receptor, nicotinic, beta 1 (muscle) (CHRNB1), mRNA.	1.23	1.25
ILMN_1769782	LAX1	NM_017773.2	Homo sapiens lymphocyte transmembrane adaptor 1 (LAX1), mRNA.	-	1.25

ILMN_2384405	RTBDN	NM_031429.1	Homo sapiens retbindin (RTBDN), transcript variant 2, mRNA.	-	1.25
ILMN_2098947	LOC338799	NR_002809.1	Homo sapiens hypothetical locus LOC338799 (LOC338799), non-coding RNA.	-	1.25
ILMN_1775170	MT1X	NM_005952.2	Homo sapiens metallothionein 1X (MT1X), mRNA.	-	1.25
ILMN_1694514	ZDHHC11	NM_024786.1	Homo sapiens zinc finger, DHHC-type containing 11 (ZDHHC11), mRNA.	-	1.25
ILMN_1684306	S100A4	NM_002961.2	Homo sapiens S100 calcium binding protein A4 (S100A4), transcript variant 2, mRNA.	-	1.26
ILMN_1822307	HS.572649	Hs.572649	Homo sapiens cDNA FLJ46527 fis, clone THYMU3034853	-	1.26
ILMN_3286809	LOC100131139	XR_037336.1	PREDICTED: Homo sapiens misc_RNA (LOC100131139), miscRNA.	-	1.26
ILMN_2298860	HAGHL	NM_207112.1	Homo sapiens hydroxyacylglutathione hydrolase-like (HAGHL), transcript variant 1, mRNA.	-	1.26
ILMN_1675258	LOC441268	NM_001013725.1	Homo sapiens hypothetical gene supported by BC044942 (LOC441268), mRNA.	-	1.26
ILMN_1857081	HS.560357	Hs.560357	te46f04.x1 Soares_NhHMPu_S1 Homo sapiens cDNA clone IMAGE:2089759 3, mRNA sequence	-	1.26
ILMN_1654946	ZSCAN18	NM_023926.3	Homo sapiens zinc finger and SCAN domain containing 18 (ZSCAN18), mRNA.	-	1.26
ILMN_2277676	ERCC1	NM_001983.2	Homo sapiens excision repair cross-complementing rodent repair deficiency, complementation group 1 (includes overlapping antisense sequence) (ERCC1), transcript variant 2, mRNA.	-	1.26
ILMN_1772207	LOC653377	XM_929420.1	PREDICTED: Homo sapiens similar to family with sequence similarity 36, member A (LOC653377), mRNA.	-	1.26
ILMN_2300396	COMMD5	NM_014066.3	Homo sapiens COMM domain containing 5 (COMMD5), transcript variant 1, mRNA.	-	1.26
ILMN_1651378	AUP1	NM_012103.2	Homo sapiens ancient ubiquitous protein 1 (AUP1), mRNA.	-	1.26
ILMN_1658802	KRTCAP2	NM_173852.3	Homo sapiens keratinocyte associated protein 2 (KRTCAP2), mRNA.	-	1.26

ILMN_2330495	OCIAD1	NM_001079842.1	Homo sapiens OCIA domain containing 1 (OCIAD1), transcript variant 5, mRNA.	-	1.26
ILMN_1703441	ZNF593	NM_015871.2	Homo sapiens zinc finger protein 593 (ZNF593), mRNA.	-	1.27
ILMN_1811104	KTELC1	NM_020231.3	Homo sapiens KTEL (Lys-Tyr-Glu-Leu) containing 1 (KTELC1), mRNA.	-	1.27
ILMN_3240222	PRAGMIN	NM_001080826.1	Homo sapiens homolog of rat pragma of Rnd2 (PRAGMIN), mRNA.	-	1.27
ILMN_2404795	SULT1A1	NM_177530.1	Homo sapiens sulfotransferase family, cytosolic, 1A, phenol-preferring, member 1 (SULT1A1), transcript variant 3, mRNA.	-	1.27
ILMN_2383611	PTPRE	NM_130435.2	Homo sapiens protein tyrosine phosphatase, receptor type, E (PTPRE), transcript variant 2, mRNA.	-	1.27
ILMN_1713706	ZNF786	NM_152411.1	Homo sapiens zinc finger protein 786 (ZNF786), mRNA.	-	1.27
ILMN_3227023	SNHG7	NR_003672.2	Homo sapiens small nucleolar RNA host gene 7 (non-protein coding) (SNHG7), transcript variant 1, non-coding RNA.	-	1.27
ILMN_1815733	EIF5	NM_001969.3	Homo sapiens eukaryotic translation initiation factor 5 (EIF5), transcript variant 1, mRNA.	-	1.27
ILMN_3202024	LOC392437	XR_037197.1	PREDICTED: Homo sapiens misc_RNA (LOC392437), miscRNA.	-	1.27
ILMN_2152257	SSTR2	NM_001050.2	Homo sapiens somatostatin receptor 2 (SSTR2), mRNA.	-	1.27
ILMN_2093389	SNAPC1	NM_003082.2	Homo sapiens small nuclear RNA activating complex, polypeptide 1, 43kDa (SNAPC1), mRNA.	-	1.27
ILMN_1740165	C14ORF102	NM_017970.2	Homo sapiens chromosome 14 open reading frame 102 (C14orf102), transcript variant 1, mRNA.	-	1.28
ILMN_1721741	ATPBD1B	NM_018066.2	Homo sapiens ATP binding domain 1 family, member B (ATPBD1B), mRNA.	-	1.28
ILMN_1740466	FAM46A	NM_017633.1	Homo sapiens family with sequence similarity 46, member A (FAM46A), mRNA.	-	1.28
ILMN_1700074	SNORA62	NR_002324.1	Homo sapiens small nucleolar RNA, H/ACA box 62 (SNORA62), small nucleolar RNA.	-	1.28

ILMN_1773764	CECR7	XM_927968.1	PREDICTED: Homo sapiens cat eye syndrome chromosome region, candidate 7 (CECR7), mRNA.	-	1.28
ILMN_1730612	DBNDD2	NM_018478.2	Homo sapiens dysbindin (dystrobrevin binding protein 1) domain containing 2 (DBNDD2), transcript variant 3, mRNA.	-	1.28
ILMN_2391765	C6ORF48	NM_001040437.1	Homo sapiens chromosome 6 open reading frame 48 (C6orf48), transcript variant 1, mRNA.	-	1.28
ILMN_1857017	HS.551538	Hs.551538	Homo sapiens mRNA; cDNA DKFZp761E1721 (from clone DKFZp761E1721)	-	1.28
ILMN_1812552	PHCA	NM_018367.3	Homo sapiens phytoceramidase, alkaline (PHCA), mRNA.	-	1.28
ILMN_2230162	FLJ44124	NM_001039755.1	Homo sapiens hypothetical protein LOC641737 (FLJ44124), mRNA.	-	1.28
ILMN_2365484	SNX1	NM_003099.3	Homo sapiens sorting nexin 1 (SNX1), transcript variant 1, mRNA.	-	1.28
ILMN_2179726	C16ORF93	NM_001014979.1	Homo sapiens chromosome 16 open reading frame 93 (C16orf93), mRNA.	-	1.28
ILMN_3246401	AIF1L	NM_031426.2	Homo sapiens allograft inflammatory factor 1-like (AIF1L), transcript variant 1, mRNA.	-	1.28
ILMN_3206429	LOC646936	XR_039521.1	PREDICTED: Homo sapiens misc_RNA (LOC646936), miscRNA.	-	1.28
ILMN_1686664	MT2A	NM_005953.2	Homo sapiens metallothionein 2A (MT2A), mRNA.	-	1.29
ILMN_1796912	ARHGEF7	NM_003899.2	Homo sapiens Rho guanine nucleotide exchange factor (GEF) 7 (ARHGEF7), transcript variant 1, mRNA.	-	1.29
ILMN_1797693	BRI3BP	XM_941876.1	Homo sapiens BRI3 binding protein (BRI3BP), mRNA.	-	1.29
ILMN_3230608	NBPF8	XM_001726946.1	PREDICTED: Homo sapiens neuroblastoma breakpoint family, member 8 (NBPF8), mRNA.	-	1.29
ILMN_1762531	FGF9	NM_002010.1	Homo sapiens fibroblast growth factor 9 (glia-activating factor) (FGF9), mRNA.	-	1.29
ILMN_1704286	FXYD5	NM_014164.4	Homo sapiens FXYD domain containing ion transport regulator 5 (FXYD5), transcript variant 1, mRNA.	-	1.29

ILMN_1853167	HS.564874	Hs.564874	UI-H-DI0-auw-h-24-0-UI.s1 NCI_CGAP_DI0 Homo sapiens cDNA clone IMAGE:5875271 3, mRNA sequence	-	1.29
ILMN_1809583	CREBBP	NM_004380.1	Homo sapiens CREB binding protein (CREBBP), transcript variant 2, mRNA.	-	1.29
ILMN_1697308	LOC648405	NM_002285.2	PREDICTED: Homo sapiens hypothetical LOC648405 (LOC648405), mRNA.	-	1.29
ILMN_1669113	ATF5	NM_012068.2	Homo sapiens activating transcription factor 5 (ATF5), mRNA.	-	1.3
ILMN_1691747	KHDRBS3	NM_006558.1	Homo sapiens KH domain containing, RNA binding, signal transduction associated 3 (KHDRBS3), mRNA.	-	1.3
ILMN_1703178	SCG2	NM_003469.3	Homo sapiens secretogranin II (chromogranin C) (SCG2), mRNA.	-	1.3
ILMN_1697409	TNFRSF14	NM_003820.2	Homo sapiens tumor necrosis factor receptor superfamily, member 14 (herpesvirus entry mediator) (TNFRSF14), mRNA.	-	1.3
ILMN_1798181	IRF7	NM_004030.1	Homo sapiens interferon regulatory factor 7 (IRF7), transcript variant b, mRNA.	-	1.3
ILMN_1697448	TXNIP	NM_006472.1	Homo sapiens thioredoxin interacting protein (TXNIP), mRNA.	-	1.3
ILMN_2345898	SLA	NM_001045557.1	Homo sapiens Src-like-adaptor (SLA), transcript variant 2, mRNA.	-	1.3
ILMN_2155719	NBPF10	NM_001039703.1	Homo sapiens neuroblastoma breakpoint family, member 10 (NBPF10), mRNA.	1.26	1.3
ILMN_3232282	LOC100130445	XM_001715069.1	PREDICTED: Homo sapiens similar to AML-associated zinc finger protein (LOC100130445), mRNA.	-	1.3
ILMN_1743933	TSHZ3	NM_020856.1	Homo sapiens teashirt zinc finger homeobox 3 (TSHZ3), mRNA.	-	1.31
ILMN_1806908	PRKCB1	NM_002738.5	Homo sapiens protein kinase C, beta 1 (PRKCB1), transcript variant 2, mRNA.	-	1.31
ILMN_1708778	ASS1	NM_000050.3	Homo sapiens argininosuccinate synthetase 1 (ASS1), transcript variant 1, mRNA.	-	1.31
ILMN_1718766	MT1F	NM_005949.1	Homo sapiens metallothionein 1F (MT1F), mRNA.	-	1.31
ILMN_1680424	CTSG	NM_001911.2	Homo sapiens cathepsin G (CTSG), mRNA.	-	1.31

ILMN_1736178	AEBP1	NM_001129.3	Homo sapiens AE binding protein 1 (AEBP1), mRNA.	-	1.31
ILMN_1844464	HS.534427	Hs.534427	Human mRNA for T-cell specific protein	-	1.31
ILMN_3287996	LOC400446	XR_019205.2	PREDICTED: Homo sapiens misc_RNA (LOC400446), miscRNA.	-	1.32
ILMN_1807662	IGF2R	NM_000876.1	Homo sapiens insulin-like growth factor 2 receptor (IGF2R), mRNA.	-	1.32
ILMN_2134538	FTHL11	NR_002204.1	Homo sapiens ferritin, heavy polypeptide-like 11 (FTHL11) on chromosome 8.	-	1.32
ILMN_1731745	NINJ2	NM_016533.4	Homo sapiens ninjurin 2 (NINJ2), mRNA.	-	1.32
ILMN_1699521	KIAA1641	XM_944061.1	PREDICTED: Homo sapiens KIAA1641, transcript variant 7 (KIAA1641), mRNA.	-	1.33
ILMN_1748538	ALDH1A2	NM_170696.1	Homo sapiens aldehyde dehydrogenase 1 family, member A2 (ALDH1A2), transcript variant 3, mRNA.	-	1.33
ILMN_2359742	CTSB	NM_001908.3	Homo sapiens cathepsin B (CTSB), transcript variant 1, mRNA.	-	1.33
ILMN_1699931	HCST	NM_014266.3	Homo sapiens hematopoietic cell signal transducer (HCST), transcript variant 2, mRNA.	-	1.33
ILMN_2333107	AES	NM_198970.1	Homo sapiens amino-terminal enhancer of split (AES), transcript variant 3, mRNA.	1.31	1.33
ILMN_2048811	NUBPL	NM_025152.1	Homo sapiens nucleotide binding protein-like (NUBPL), mRNA.	-	1.33
ILMN_2409167	ANXA2	NM_001002858.1	Homo sapiens annexin A2 (ANXA2), transcript variant 1, mRNA.	-	1.33
ILMN_1677396	NDFIP2	NM_019080.1	Homo sapiens Nedd4 family interacting protein 2 (NDFIP2), mRNA.	-	1.34
ILMN_3244319	CCDC125	NM_176816.3	Homo sapiens coiled-coil domain containing 125 (CCDC125), mRNA.	-	1.34
ILMN_1900734	HS.580797	Hs.580797	MR1-GN0172-061100-005-h03 GN0172 Homo sapiens cDNA, mRNA sequence	-	1.34
ILMN_3227321	LOC731542	XR_015517.2	PREDICTED: Homo sapiens misc_RNA (LOC731542), miscRNA.	-	1.34
ILMN_1657011	LOC286208	XM_379668.3	PREDICTED: Homo sapiens hypothetical protein LOC286208, transcript variant 1 (LOC286208), mRNA.	-	1.35
ILMN_3240594	RNU4ATAC	NR_023343.1	Homo sapiens RNA, U4atac small nuclear (U12-dependent splicing) (RNU4ATAC), small nuclear RNA.	-	1.35

ILMN_2397028	SERPINB8	NM_002640.3	Homo sapiens serpin peptidase inhibitor, clade B (ovalbumin), member 8 (SERPINB8), transcript variant 1, mRNA.	-	1.36
ILMN_1720282	NQO1	NM_000903.2	Homo sapiens NAD(P)H dehydrogenase, quinone 1 (NQO1), transcript variant 1, mRNA.	-	1.36
ILMN_3300797	LOC729090	XR_015449.2	PREDICTED: Homo sapiens similar to Eukaryotic translation elongation factor 1 alpha 1 (LOC729090), mRNA.	-	1.37
ILMN_1812191	C12ORF57	NM_138425.2	Homo sapiens chromosome 12 open reading frame 57 (C12orf57), mRNA.	-	1.38
ILMN_2053538	RHBDL2	NM_017821.3	Homo sapiens rhomboid, veinlet-like 2 (Drosophila) (RHBDL2), mRNA.	1.23	1.38
ILMN_2150856	SERPINB2	NM_002575.1	Homo sapiens serpin peptidase inhibitor, clade B (ovalbumin), member 2 (SERPINB2), mRNA.	-	1.38
ILMN_1725441	NFATC2IP	XM_944125.1	Homo sapiens nuclear factor of activated T-cells, cytoplasmic, calcineurin-dependent 2 interacting protein (NFATC2IP), mRNA.	1.22	1.38
ILMN_1798270	C11ORF75	NM_020179.1	Homo sapiens chromosome 11 open reading frame 75 (C11orf75), mRNA.	-	1.39
ILMN_1757467	H1F0	NM_005318.2	Homo sapiens H1 histone family, member 0 (H1F0), mRNA.	-	1.39
ILMN_3243644	LOC100132564	XM_001713808.1	PREDICTED: Homo sapiens hypothetical protein LOC100132564 (LOC100132564), mRNA.	-	1.4
ILMN_1796430	PSMD3	NM_002809.2	Homo sapiens proteasome (prosome, macropain) 26S subunit, non-ATPase, 3 (PSMD3), mRNA.	1.38	1.4
ILMN_2173835	FTHL3	NR_002201.1	Homo sapiens ferritin, heavy polypeptide-like 3 (FTHL3), non-coding RNA.	-	1.41
ILMN_1659316	HEPACAM	NM_152722.3	Homo sapiens hepatocyte cell adhesion molecule (HEPACAM), mRNA.	-	1.41
ILMN_1683146	FTH1	NM_002032.2	Homo sapiens ferritin, heavy polypeptide 1 (FTH1), mRNA.	-	1.42
ILMN_1680279	USP49	NM_018561.3	Homo sapiens ubiquitin specific peptidase 49 (USP49), mRNA.	-	1.42

ILMN_2381537	CRCP	NM_014478.4	Homo sapiens CGRP receptor component (CRCP), transcript variant 1, mRNA.	-	1.43
ILMN_1886655	HS.554324	Hs.554324	full-length cDNA clone CS0DI056YK21 of Placenta Cot 25-normalized of Homo sapiens (human)	1.27	1.44
ILMN_2214997	LRRFIP1	NM_004735.2	Homo sapiens leucine rich repeat (in FLII) interacting protein 1 (LRRFIP1), mRNA.	-	1.44
ILMN_2276758	POFUT1	NM_015352.1	Homo sapiens protein O-fucosyltransferase 1 (POFUT1), transcript variant 1, mRNA.	-	1.45
ILMN_2150851	SERPINB2	NM_002575.1	Homo sapiens serpin peptidase inhibitor, clade B (ovalbumin), member 2 (SERPINB2), mRNA.	-	1.45
ILMN_1738095	PER2	NM_022817.1	Homo sapiens period homolog 2 (Drosophila) (PER2), mRNA.	-	1.46
ILMN_3176403	FTHL16	XR_041433.1	PREDICTED: Homo sapiens misc_RNA (FTHL16), miscRNA.	-	1.46
ILMN_1795089	RASAL3	XM_937586.1	Homo sapiens RAS protein activator like 3 (RASAL3), mRNA.	-	1.47
ILMN_1677691	LOC648852	XM_940430.1	PREDICTED: Homo sapiens hypothetical protein LOC648852 (LOC648852), mRNA.	-	1.47
ILMN_2352009	ACADVL	NM_000018.2	Homo sapiens acyl-Coenzyme A dehydrogenase, very long chain (ACADVL), nuclear gene encoding mitochondrial protein, transcript variant 1, mRNA.	1.27	1.48
ILMN_2262275	TRIM13	NM_001007278.1	Homo sapiens tripartite motif-containing 13 (TRIM13), transcript variant 4, mRNA.	-	1.48
ILMN_3232828	LOC728620	XR_037241.1	PREDICTED: Homo sapiens misc_RNA (LOC728620), miscRNA.	-	1.48
ILMN_1656920	CRIP1	NM_001311.3	Homo sapiens cysteine-rich protein 1 (intestinal) (CRIP1), mRNA.	-	1.48
ILMN_1780711	LOC390530	XM_372543.2	PREDICTED: Homo sapiens similar to Ig heavy chain V-I region HG3 precursor (LOC390530), mRNA.	-	1.48
ILMN_1718960	SERPINB8	NM_001031848.1	Homo sapiens serpin peptidase inhibitor, clade B (ovalbumin), member 8 (SERPINB8), transcript variant 2, mRNA.	-	1.49

ILMN_1779095	CEBPE	NM_001805.2	Homo sapiens CCAAT/enhancer binding protein (C/EBP), epsilon (CEBPE), mRNA.	-	1.5
ILMN_1715301	FXYD2	NM_021603.2	Homo sapiens FXYD domain containing ion transport regulator 2 (FXYD2), transcript variant b, mRNA.	-	1.5
ILMN_3236653	RNU1-5	NR_004400.1	Homo sapiens RNA, U1 small nuclear 5 (RNU1-5), small nuclear RNA.	-	1.51
ILMN_3235410	HIATL2	NR_002894.1	Homo sapiens hippocampus abundant transcript-like 2 (HIATL2), non-coding RNA.	-	1.51
ILMN_1773780	FAM173A	NM_023933.1	Homo sapiens family with sequence similarity 173, member A (FAM173A), mRNA.	-	1.52
ILMN_2234016	FTHL7	NR_002202.2	Homo sapiens ferritin, heavy polypeptide-like 7 (FTHL7) on chromosome 13.	-	1.54
ILMN_3241034	SNORD3C	NR_006881.1	Homo sapiens small nucleolar RNA, C/D box 3C (SNORD3C), small nucleolar RNA.	-	1.57
ILMN_1822458	HS.567472	Hs.567472	BX400436 Homo sapiens T CELLS (JURKAT CELL LINE) COT 10-NORMALIZED Homo sapiens cDNA clone CS0DJ011YK18 5-PRIME, mRNA sequence	-	1.57
ILMN_3278506	LOC148430	XR_038750.1	PREDICTED: Homo sapiens misc_RNA (LOC148430), miscRNA.	-	1.58
ILMN_1706013	FTHL11	NR_002204.1	Homo sapiens ferritin, heavy polypeptide-like 11 (FTHL11) on chromosome 8.	-1.2	1.59
ILMN_3227315	LOC729009	XR_042330.1	PREDICTED: Homo sapiens misc_RNA (LOC729009), miscRNA.	-	1.63
ILMN_3245678	RNU1A3	NR_004430.1	Homo sapiens RNA, U1A3 small nuclear (RNU1A3), small nuclear RNA.	-	1.64
ILMN_3242315	SNORD3D	NR_006882.1	Homo sapiens small nucleolar RNA, C/D box 3D (SNORD3D), small nucleolar RNA.	-	1.64

ILMN_1696911	FTHL8	NR_002203.1	Homo sapiens ferritin, heavy polypeptide-like 8 (FTHL8) on chromosome X.	-	1.65
ILMN_3261439	LOC100128098	XM_001721625.1	PREDICTED: Homo sapiens hypothetical protein LOC100128098 (LOC100128098), mRNA.	-	1.65
ILMN_2073235	FTHL12	NR_002205.1	Homo sapiens ferritin, heavy polypeptide-like 12 (FTHL12) on chromosome 9.	-	1.65
ILMN_1746525	FTHL2	NR_002200.1	Homo sapiens ferritin, heavy polypeptide-like 2 (FTHL2) on chromosome 1.	-	1.66
ILMN_1873034	HS.546375	Hs.546375	Homo sapiens T cell receptor alpha locus, mRNA (cDNA clone MGC:88342 IMAGE:30352166), complete cds	-	1.67
ILMN_2235745	GRIPAP1	NM_207672.1	Homo sapiens GRIP1 associated protein 1 (GRIPAP1), transcript variant 2, mRNA.	-	1.67
ILMN_1793628	SERPINA10	NM_016186.1	Homo sapiens serpin peptidase inhibitor, clade A (alpha-1 antiproteinase, antitrypsin), member 10 (SERPINA10), transcript variant 1, mRNA.	-	1.71
ILMN_2154322	SEMA3E	NM_012431.1	Homo sapiens sema domain, immunoglobulin domain (Ig), short basic domain, secreted, (semaphorin) 3E (SEMA3E), mRNA.	-	1.72
ILMN_1667162	NKX3-1	NM_006167.2	Homo sapiens NK3 homeobox 1 (NKX3-1), mRNA.	-	1.73
ILMN_2082209	C20ORF100	NM_032883.1	Homo sapiens chromosome 20 open reading frame 100 (C20orf100), mRNA.	-	1.74
ILMN_1750278	FTHL12	NR_002205.1	Homo sapiens ferritin, heavy polypeptide-like 12 (FTHL12) on chromosome 9.	-	1.75
ILMN_3239574	SNORD3A	NR_006880.1	Homo sapiens small nucleolar RNA, C/D box 3A (SNORD3A), small nucleolar RNA.	-	1.76
ILMN_1795963	OKL38	NM_013370.2	Homo sapiens pregnancy-induced growth inhibitor (OKL38), transcript variant 1, mRNA.	-	1.78

ILMN_1742163	LOC441087	NM_001013716.1	Homo sapiens hypothetical gene supported by AK125735 (LOC441087), mRNA.	-	1.78
ILMN_1734878	CD79A	NM_001783.2	Homo sapiens CD79a molecule, immunoglobulin-associated alpha (CD79A), transcript variant 2, mRNA.	-	1.8
ILMN_1779324	GZMA	NM_006144.2	Homo sapiens granzyme A (granzyme 1, cytotoxic T-lymphocyte-associated serine esterase 3) (GZMA), mRNA.	-	2.27
ILMN_1786242	LOC649821	XM_942212.1	PREDICTED: Homo sapiens similar to 60S ribosomal protein L14 (CAG-ISL 7), transcript variant 1 (LOC649821), mRNA.	-1.39	-
ILMN_2092536	HSPE1	NM_002157.1	Homo sapiens heat shock 10kDa protein 1 (chaperonin 10) (HSPE1), mRNA.	-1.38	-
ILMN_1686989	INSIG1	NM_198336.1	Homo sapiens insulin induced gene 1 (INSIG1), transcript variant 2, mRNA.	-1.35	-
ILMN_2116556	LSM5	NM_012322.1	Homo sapiens LSM5 homolog, U6 small nuclear RNA associated (S. cerevisiae) (LSM5), mRNA.	-1.31	-
ILMN_1789614	TPT1	NM_003295.1	Homo sapiens tumor protein, translationally-controlled 1 (TPT1), mRNA.	-1.26	-
ILMN_1771149	MRPL19	NM_014763.2	Homo sapiens mitochondrial ribosomal protein L19 (MRPL19), nuclear gene encoding mitochondrial protein, mRNA.	-1.26	-
ILMN_3290100	LOC645157	XR_016770.2	PREDICTED: Homo sapiens misc_RNA (LOC645157), miscRNA.	-1.25	-
ILMN_1738150	SUMO2	NM_001005849.1	Homo sapiens SMT3 suppressor of mif two 3 homolog 2 (S. cerevisiae) (SUMO2), transcript variant 2, mRNA.	-1.25	-
ILMN_1657153	ACTR3	NM_005721.3	Homo sapiens ARP3 actin-related protein 3 homolog (yeast) (ACTR3), mRNA.	-1.24	-
ILMN_1749014	ACLY	NM_198830.1	Homo sapiens ATP citrate lyase (ACLY), transcript variant 1, mRNA.	-1.24	-
ILMN_1656111	MYLIP	NM_013262.3	Homo sapiens myosin regulatory light chain interacting protein (MYLIP), mRNA.	-1.24	-
ILMN_3280020	LOC441506	XR_017565.2	PREDICTED: Homo sapiens misc_RNA (LOC441506), miscRNA.	-1.23	-

ILMN_1778321	SLC2A6	NM_017585.2	Homo sapiens solute carrier family 2 (facilitated glucose transporter), member 6 (SLC2A6), mRNA.	-1.23	-
ILMN_1676523	CCDC91	NM_018318.3	Homo sapiens coiled-coil domain containing 91 (CCDC91), mRNA.	-1.23	-
ILMN_3246805	LOC100134364	XM_001713810.1	PREDICTED: Homo sapiens hypothetical protein LOC100134364 (LOC100134364), mRNA.	-1.22	-
ILMN_1763539	IER3IP1	NM_016097.2	Homo sapiens immediate early response 3 interacting protein 1 (IER3IP1), mRNA.	-1.22	-
ILMN_3272424	LOC100128836	XR_038689.1	PREDICTED: Homo sapiens misc_RNA (LOC100128836), miscRNA.	-1.22	-
ILMN_2219712	HMGB2	NM_002129.2	Homo sapiens high-mobility group box 2 (HMGB2), mRNA.	-1.22	-
ILMN_2224103	PAPSS1	NM_005443.4	Homo sapiens 3'-phosphoadenosine 5'-phosphosulfate synthase 1 (PAPSS1), mRNA.	-1.21	-
ILMN_3206132	LOC388076	XM_001722259.1	PREDICTED: Homo sapiens hypothetical LOC388076 (LOC388076), mRNA.	-1.21	-
ILMN_3236428	TMEM170B	NM_001100829.1	Homo sapiens transmembrane protein 170B (TMEM170B), mRNA.	-1.21	-
ILMN_1681998	AP2B1	NM_001282.2	Homo sapiens adaptor-related protein complex 2, beta 1 subunit (AP2B1), transcript variant 2, mRNA.	-1.21	-
ILMN_1792138	UQCRH	NM_006004.1	Homo sapiens ubiquinol-cytochrome c reductase hinge protein (UQCRH), mRNA.	-1.21	-
ILMN_2365465	XBP1	NM_001079539.1	Homo sapiens X-box binding protein 1 (XBP1), transcript variant 2, mRNA.	-1.21	-
ILMN_1663313	AMY1C	NM_001008219.1	Homo sapiens amylase, alpha 1C (salivary) (AMY1C), mRNA.	-1.21	-
ILMN_1791057	IFNAR2	NM_207585.1	Homo sapiens interferon (alpha, beta and omega) receptor 2 (IFNAR2), transcript variant 1, mRNA.	-1.2	-
ILMN_1743711	LOC650215	NM_007235.3	PREDICTED: Homo sapiens similar to Exportin-T (tRNA exportin) (Exportin(tRNA)) (LOC650215), mRNA.	-1.2	-
ILMN_1688158	CYB5R4	NM_016230.2	Homo sapiens cytochrome b5 reductase 4 (CYB5R4), mRNA.	-1.2	-

ILMN_3274671	LOC283481	XM_001133584.1	PREDICTED: Homo sapiens hypothetical protein LOC283481 (LOC283481), mRNA.	1.2	-
ILMN_1656372	PES1	NM_014303.2	Homo sapiens pescadillo homolog 1, containing BRCT domain (zebrafish) (PES1), mRNA.	1.2	-
ILMN_1778617	TAF9	NM_016283.4	Homo sapiens TAF9 RNA polymerase II, TATA box binding protein (TBP)-associated factor, 32kDa (TAF9), transcript variant 3, mRNA.	1.2	-
ILMN_1803110	SF3B3	NM_012426.3	Homo sapiens splicing factor 3b, subunit 3, 130kDa (SF3B3), mRNA.	1.21	-
ILMN_2245676	BTF3	NM_001037637.1	Homo sapiens basic transcription factor 3 (BTF3), transcript variant 1, mRNA.	1.21	-
ILMN_1715705	SSNA1	NM_003731.1	Homo sapiens Sjogren syndrome nuclear autoantigen 1 (SSNA1), mRNA.	1.21	-
ILMN_1681092	LOC651316	XM_940451.1	PREDICTED: Homo sapiens similar to T25G3.1 (LOC651316), mRNA.	1.21	-
ILMN_1810418	LBR	NM_002296.2	Homo sapiens lamin B receptor (LBR), transcript variant 1, mRNA.	1.21	-
ILMN_1712357	HNRPK	NM_031263.1	Homo sapiens heterogeneous nuclear ribonucleoprotein K (HNRPK), transcript variant 3, mRNA.	1.21	-
ILMN_1698323	PLEKHB2	NM_001031706.1	Homo sapiens pleckstrin homology domain containing, family B (evectins) member 2 (PLEKHB2), transcript variant 1, mRNA.	1.21	-
ILMN_2257432	RAD51	NM_002875.2	Homo sapiens RAD51 homolog (RecA homolog, E. coli) (S. cerevisiae) (RAD51), transcript variant 1, mRNA.	1.21	-
ILMN_1743655	TMED9	NM_017510.3	Homo sapiens transmembrane emp24 protein transport domain containing 9 (TMED9), mRNA.	1.21	-
ILMN_1736597	TKT	NM_001064.1	Homo sapiens transketolase (Wernicke-Korsakoff syndrome) (TKT), mRNA.	1.22	-
ILMN_1654068	NUDT1	NM_198954.1	Homo sapiens nudix (nucleoside diphosphate linked moiety X)-type motif 1 (NUDT1), transcript variant 4B, mRNA.	1.22	-

ILMN_1697652	PLEKHB2	NM_017958.1	Homo sapiens pleckstrin homology domain containing, family B (evectins) member 2 (PLEKHB2), transcript variant 2, mRNA.	1.23	-
ILMN_1679188	ATP5S	NM_015684.2	Homo sapiens ATP synthase, H+ transporting, mitochondrial F0 complex, subunit s (factor B) (ATP5S), nuclear gene encoding mitochondrial protein, transcript variant 2, mRNA.	1.23	-
ILMN_1764165	TRIM65	NM_173547.2	Homo sapiens tripartite motif-containing 65 (TRIM65), mRNA.	1.23	-
ILMN_1675156	CDC42	NM_044472.1	Homo sapiens cell division cycle 42 (GTP binding protein, 25kDa) (CDC42), transcript variant 3, mRNA.	1.23	-
ILMN_1730816	GPR162	NM_014449.1	Homo sapiens G protein-coupled receptor 162 (GPR162), transcript variant A-2, mRNA.	1.23	-
ILMN_1767006	PSMB8	NM_148919.3	Homo sapiens proteasome (prosome, macropain) subunit, beta type, 8 (large multifunctional peptidase 7) (PSMB8), transcript variant 2, mRNA.	1.23	-
ILMN_1661366	PGAM1	NM_002629.2	Homo sapiens phosphoglycerate mutase 1 (brain) (PGAM1), mRNA.	1.25	-
ILMN_3238570	EIF3CL	NM_001099661.1	Homo sapiens eukaryotic translation initiation factor 3, subunit C-like (EIF3CL), mRNA.	1.25	-
ILMN_1690063	LOC651143	XM_942536.1	PREDICTED: Homo sapiens hypothetical protein LOC651143, transcript variant 1 (LOC651143), mRNA.	1.27	-
ILMN_1657884	NME2	NM_002512.2	Homo sapiens non-metastatic cells 2, protein (NM23B) expressed in (NME2), transcript variant 1, mRNA.	1.27	-
ILMN_3237729	LOC100133551	XM_001721670.1	PREDICTED: Homo sapiens hypothetical protein LOC100133551 (LOC100133551), mRNA.	1.27	-
ILMN_1676719	LOC644330	XM_946163.1	PREDICTED: Homo sapiens similar to tropomyosin 3 isoform 2 (LOC644330), mRNA.	1.28	-
ILMN_1779258	LOC644774	XM_927868.1	PREDICTED: Homo sapiens similar to Phosphoglycerate kinase 1 (LOC644774), mRNA.	1.29	-

ILMN_1707493	SNHG3-RCC1	NM_001269.2	Homo sapiens SNHG3-RCC1 readthrough transcript (SNHG3-RCC1), transcript variant 1, mRNA.	1.3	-
ILMN_3247895	LOC728188	XM_001126103.2	PREDICTED: Homo sapiens similar to phosphoglycerate mutase processed protein (LOC728188), mRNA.	1.3	-
ILMN_1785711	NEDD8	NM_006156.1	Homo sapiens neural precursor cell expressed, developmentally down-regulated 8 (NEDD8), mRNA.	1.3	-
ILMN_1704702	MCM7	NM_005916.3	Homo sapiens minichromosome maintenance complex component 7 (MCM7), transcript variant 1, mRNA.	1.31	-
ILMN_3204734	LOC100134648	XM_001724681.1	PREDICTED: Homo sapiens similar to hCG2024106, transcript variant 2 (LOC100134648), mRNA.	1.34	-
ILMN_2222008	KIFC1	NM_002263.2	Homo sapiens kinesin family member C1 (KIFC1), mRNA.	1.48	-

References

[1] Moss GP, Smith PAS, Tavernier D. Glossary of Class Names of Organic-Compounds and Reactive Intermediates Based on Structure. Pure and Applied Chemistry. 1995;67(8-9):1307–1375.

[2] Fahy E, Subramaniam S, Murphy RC, Nishijima M, Raetz CR, Shimizu T, et al. Update of the LIPID MAPS comprehensive classification system for lipids. J Lipid Res. 2009;50 Suppl:S9–14.

[3] Rustan AC, Drevon CA. Fatty Acids: Structures and Properties. 2005;.

[4] Calder PC. Very long chain omega-3 (n-3) fatty acids and human health. European Journal of Lipid Science and Technology. 2014;116(10):1280–1300.

[5] Kihara A. Very long-chain fatty acids: elongation, physiology and related disorders. Journal of Biochemistry. 2012;152(5):387–395.

[6] Papamandjaris AA, MacDougall DE, Jones PJ. Medium chain fatty acid metabolism and energy expenditure: obesity treatment implications. Life Sci. 1998;62(14):1203–15.

[7] St-Onge MP, Bosarge A, Goree LLT, Darnell B. Medium Chain Triglyceride Oil Consumption as Part of a Weight Loss Diet Does Not Lead to an Adverse Metabolic Profile When Compared to Olive Oil. Journal of the American College of Nutrition. 2008;27(5):547–552.

[8] Tan HZ, O'Toole PW. Impact of diet on the human intestinal microbiota. Current Opinion in Food Science. 2015;2:71–77.

[9] Schonfeld P, Wojtczak L. Short- and medium-chain fatty acids in energy metabolism: the cellular perspective. J Lipid Res. 2016;57(6):943–54.

[10] Hinnebusch BF, Meng S, Wu JT, Archer SY, Hodin RA. The effects of short-chain fatty acids on human colon cancer cell phenotype are associated with histone hyperacetylation. J Nutr. 2002;132(5):1012–7.

[11] Hiltunen JK, Schonauer MS, Autio KJ, Mittelmeier TM, Kastaniotis AJ, Dieckmann CL. Mitochondrial fatty acid synthesis type II: more than just fatty acids. J Biol Chem. 2009;284(14):9011–5.

[12] Smith S, Witkowski A, Joshi AK. Structural and functional organization of the animal fatty acid synthase. Prog Lipid Res. 2003;42(4):289–317.

[13] White SW, Zheng J, Zhang YM, Rock. The structural biology of type II fatty acid biosynthesis. Annu Rev Biochem. 2005;74:791–831.

[14] Alberts AW, Greenspan MD. In: Numa S, editor. Chapter 2 Animal and bacterial fatty acid synthetase: structure, function and regulation. vol. 7 of New Comprehensive Biochemistry. Elsevier; 1984. p. 29 – 58.

[15] Jayakumar A, Tai MH, Huang WY, al Feel W, Hsu M, Abu-Elheiga L, et al. Human fatty acid synthase: properties and molecular cloning. Proc Natl Acad Sci U S A. 1995;92(19):8695–9.

[16] Jayakumar A, Huang WY, Raetz B, Chirala SS, Wakil SJ. Cloning and expression of the multifunctional human fatty acid synthase and its subdomains in Escherichia coli. Proc Natl Acad Sci U S A. 1996;93(25):14509–14.

[17] Sassa T, Kihara A. Metabolism of Very Long-Chain Fatty Acids: Genes and Pathophysiology. Biomolecules and Therapeutics. 2014;22(2):83–92.

[18] ALjohani AM, Syed DN, Ntambi JM. Insights into Stearoyl-CoA Desaturase-1 Regulation of Systemic Metabolism. Trends in Endocrinology and Metabolism. 2017;28(12):831–842.

[19] Wang J, Yu L, Schmidt RE, Su C, Huang X, Gould K, et al. Characterization of HSCD5, a novel human stearoyl-CoA desaturase unique to primates. Biochem Biophys Res Commun. 2005;332(3):735–42.

[20] Robichaud PP, Boulay K, Munganyiki JE, Surette ME. Fatty acid remodeling in cellular glycerophospholipids following the activation of human T cells. J Lipid Res. 2013;54(10):2665–77.

[21] Fujii M, Nakashima H, Tomozawa J, Shimazaki Y, Ohyanagi C, Kawaguchi N, et al. Deficiency of n-6 polyunsaturated fatty acids is mainly responsible for atopic dermatitis-like pruritic skin inflammation in special diet-fed hairless mice. Experimental Dermatology. 2013;22(4):272–277.

[22] Bjerve KS, Fischer S, Alme K. Alpha-Linolenic Acid Deficiency in Man - Effect of Ethyl Linolenate on Plasma and Erythrocyte Fatty-Acid Composition and Biosynthesis of Prostanoids. American Journal of Clinical Nutrition. 1987;46(4):570–576.

[23] Holman RT, Johnson SB, Hatch TF. A case of human linolenic acid deficiency involving neurological abnormalities. Am J Clin Nutr. 1982;35(3):617–23.

[24] Zensen R, Husmann H, Schneider R, Peine T, Weiss H. De novo synthesis and desaturation of fatty acids at the mitochondrial acyl-carrier protein, a subunit of NADH:ubiquinone oxidoreductase in Neurospora crassa. FEBS Lett. 1992;310(2):179–81.

[25] Wanders RJ, Waterham HR, Ferdinandusse S. Metabolic Interplay between Peroxisomes and Other Subcellular Organelles Including Mitochondria and the Endoplasmic Reticulum. Front Cell Dev Biol. 2015;3:83.

[26] Wanders RJA, Jansen GA, Skjeldal OH. Refsum disease, peroxisomes and phytanic acid oxidation: A review. Journal of Neuropathology and Experimental Neurology. 2001;60(11):1021–1031.

[27] Mihalik SJ, Morrell JC, Kim D, Sacksteder KA, Watkins PA, Gould SJ. Identification of PAHX, a Refsum disease gene. Nature Genetics. 1997;17(2):185–189.

[28] Wanders RJA, Jansen GA, Lloyd MD. Phytanic acid alpha-oxidation, new insights into an old problem: a review. Biochimica Et Biophysica Acta-Molecular and Cell Biology of Lipids. 2003;1631(2):119–135.

[29] Jansen GA, Ferdinandusse S, Ijlst L, Muijsers AO, Skjeldal OH, Stokke O, et al. Refsum disease is caused by mutations in the phytanoyl-CoA hydroxylase gene. Nature Genetics. 1997;17(2):190–193.

[30] Jansen GA, Hogenhout EM, Ferdinandusse S, Waterham HR, Ofman R, Jakobs C, et al. Human phytanoyl-CoA hydroxylase: resolution of the gene structure and the molecular basis of Refsum's disease. Hum Mol Genet. 2000;9(8):1195–200.

[31] Braverman N, Chen L, Lin P, Obie C, Steel G, Douglas P, et al. Mutation analysis of PEX7 in 60 probands with rhizomelic chondrodysplasia punctata and functional correlations of genotype with phenotype. Hum Mutat. 2002;20(4):284–97.

[32] van den Brink DM, Brites P, Haasjes J, Wierzbicki AS, Mitchell J, Lambert-Hamill M, et al. Identification of PEX7 as the second gene involved in Refsum disease. American Journal of Human Genetics. 2003;72(2):471–477.

[33] Hoch U, Zhang Z, Kroetz DL, Ortiz de Montellano PR. Structural determination of the substrate specificities and regioselectivities of the rat and human fatty acid omega-hydroxylases. Arch Biochem Biophys. 2000;373(1):63–71.

[34] Kawashima H, Naganuma T, Kusunose E, Kono T, Yasumoto R, Sugimura K, et al. Human fatty acid omega-hydroxylase, CYP4A11: determination of complete genomic sequence and characterization of purified recombinant protein. Arch Biochem Biophys. 2000;378(2):333–9.

[35] Christmas P, Jones JP, Patten CJ, Rock DA, Zheng Y, Cheng SM, et al. Alternative splicing determines the function of CYP4F3 by switching substrate specificity. J Biol Chem. 2001;276(41):38166–72.

[36] Sontag TJ, Parker RS. Cytochrome P450 omega-hydroxylase pathway of tocopherol catabolism. Novel mechanism of regulation of vitamin E status. J Biol Chem. 2002;277(28):25290–6.

[37] Hansson G, Lindgren JA, Dahlen SE, Hedqvist P, Samuelsson B. Identification and biological activity of novel omega-oxidized metabolites of leukotriene B4 from human leukocytes. FEBS Lett. 1981;130(1):107–12.

[38] Wanders RJA, Komen J, Kemp S. Fatty acid omega-oxidation as a rescue pathway for fatty acid oxidation disorders in humans. Febs Journal. 2011;278(2):182–194.

[39] Brenton DP, Krywawych S. 3-Methyladipate excretion in Refsum's disease. Lancet. 1982;1(8272):624.

[40] Wierzbicki AS, Mayne PD, Lloyd MD, Burston D, Mei G, Sidey MC, et al. Metabolism of phytanic acid and 3-methyl-adipic acid excretion in patients with adult Refsum disease. J Lipid Res. 2003;44(8):1481–8.

[41] Wanders RJ, Vreken P, Ferdinandusse S, Jansen GA, Waterham HR, van Roermund CW, et al. Peroxisomal fatty acid alpha- and beta-oxidation in humans: enzymology, peroxisomal metabolite transporters and peroxisomal diseases. Biochem Soc Trans. 2001;29(Pt 2):250–67.

[42] Schrader M, Fahimi HD. Peroxisomes and oxidative stress. Biochim Biophys Acta. 2006;1763(12):1755–66.

[43] Fransen M, Lismont C, Walton P. The Peroxisome-Mitochondria Connection: How and Why? Int J Mol Sci. 2017;18(6).

[44] Abdelmagid SA, Clarke SE, Nielsen DE, Badawi A, El-Sohemy A, Mutch DM, et al. Comprehensive Profiling of Plasma Fatty Acid Concentrations in Young Healthy Canadian Adults. Plos One. 2015;10(2).

[45] Hodson L, Skeaff CM, Fielding BA. Fatty acid composition of adipose tissue and blood in humans and its use as a biomarker of dietary intake. Progress in Lipid Research. 2008;47(5):348–380.

[46] Martinez M, Mougan I. Fatty acid composition of human brain phospholipids during normal development. J Neurochem. 1998;71(6):2528–33.

[47] Caslake MJ, Miles EA, Kofler BM, Lietz G, Curtis P, Armah CK, et al. Effect of sex and genotype on cardiovascular biomarker response to fish oils: the FINGEN Study. Am J Clin Nutr. 2008;88(3):618–29.

[48] Yao CH, Fowle-Grider R, Mahieu NG, Liu GY, Chen YJ, Wang R, et al. Exogenous Fatty Acids Are the Preferred Source of Membrane Lipids in Proliferating Fibroblasts. Cell Chem Biol. 2016;23(4):483–93.

[49] Browning LM, Walker CG, Mander AP, West AL, Madden J, Gambell JM, et al. Incorporation of eicosapentaenoic and docosahexaenoic acids into lipid pools when given as supplements providing doses equivalent to typical intakes of oily fish. Am J Clin Nutr. 2012;96(4):748–58.

[50] Hames KC, Morgan-Bathke M, Harteneck DA, Zhou L, Port JD, Lanza IR, et al. Very-long-chain omega-3 fatty acid supplements and adipose tissue functions: a randomized controlled trial. Am J Clin Nutr. 2017;105(6):1552–1558.

[51] Li Q, Wang M, Tan L, Wang C, Ma J, Li N, et al. Docosahexaenoic acid changes lipid composition and interleukin-2 receptor signaling in membrane rafts. J Lipid Res. 2005;46(9):1904–13.

[52] Gorjao R, Verlengia R, Lima TM, Soriano FG, Boaventura MF, Kanunfre CC, et al. Effect of docosahexaenoic acid-rich fish oil supplementation on human leukocyte function. Clin Nutr. 2006;25(6):923–38.

[53] Calder PC. The relationship between the fatty acid composition of immune cells and their function. Prostaglandins Leukot Essent Fatty Acids. 2008;79(3-5):101–8.

[54] McCollum EV, Davis M. The necessity of certain lipins in the diet during growth. J Biol Chem. 1913;15:167–175.

[55] Burr GO, Burr MM. A new deficiency disease produced by the rigid exclusion of fat from the diet. J Biol Chem. 1929;82:345–367.

[56] Neitzel JJ. Fatty Acid Molecules: Fundamentals and Role in Signaling. Nature Education. 2010;3(9):57.

[57] Bergstrom S. Prostaglandins: members of a new hormonal system. These physiologically very potent compounds of ubiquitous occurrence are formed from essential fatty acids. Science. 1967;157(3787):382–91.

[58] Van Dorp DA, Beerthuis RK, Nugteren DH, Vonkeman H. Enzymatic Conversion of All-cis-Polyunsaturated Fatty Acids into Prostaglandins. Nature. 1964;203:839–841.

[59] Bergstroem S, Danielsson H, Klenberg D, Samuelsson B. The Enzymatic Conversion of Essential Fatty Acids into Prostaglandins. J Biol Chem. 1964;239:PC4006–8.

[60] Bergstroem S, Danielsson H, Samuelsson B. The Enzymatic Formation of Prostaglandin E2 from Arachidonic Acid Prostaglandins and Related Factors 32. Biochim Biophys Acta. 1964;90:207–10.

[61] Odutuga AA. Reversal of brain essential fatty-acid deficiency in the rat by dietary linoleate, linolenate and arachidonate. Int J Biochem. 1981;13(9):1035–8.

[62] Kodas E, Vancassel S, Lejeune B, Guilloteau D, Chalon S. Reversibility of n-3 fatty acid deficiency-induced changes in dopaminergic neurotransmission in rats: critical role of developmental stage. J Lipid Res. 2002;43(8):1209–19.

[63] Kupiecki FP, Sekhar NC, Weeks JR. Effects of infusion of some prostaglandins in essential fatty acid-deficient and normal rats. J Lipid Res. 1968;9(5):602–5.

[64] Bjerve KS, Mostad IL, Thoresen L. Alpha-linolenic acid deficiency in patients on long-term gastric-tube feeding: estimation of linolenic acid and long-chain unsaturated n-3 fatty acid requirement in man. Am J Clin Nutr. 1987;45(1):66–77.

[65] Hansen AE, Wiese HF, Boelsche AN, Haggard ME, D ADJ, Davis H. Role of linoleic acid in infant nutrition : clinical and chemical study of 428 infants fed on milk mixtures varying in kind and amount of fat. Pedriatics. 1963;31:171–192.

[66] Forouhi NG, Krauss RM, Taubes G, Willett W. Dietary fat and cardiometabolic health: evidence, controversies, and consensus for guidance. BMJ. 2018;361:k2139.

[67] Siri-Tarino PW, Sun Q, Hu FB, Krauss RM. Meta-analysis of prospective cohort studies evaluating the association of saturated fat with cardiovascular disease. Am J Clin Nutr. 2010;91(3):535–46.

[68] Chowdhury R, Warnakula S, Kunutsor S, Crowe F, Ward HA, Johnson L, et al. Association of dietary, circulating, and supplement fatty acids with coronary risk: a systematic review and meta-analysis. Ann Intern Med. 2014;160(6):398–406.

[69] de Souza RJ, Mente A, Maroleanu A, Cozma AI, Ha V, Kishibe T, et al. Intake of saturated and trans unsaturated fatty acids and risk of all cause mortality, cardiovascular disease, and type 2 diabetes: systematic review and meta-analysis of observational studies. Bmj-British Medical Journal. 2015;351.

[70] Jakobsen MU, O'Reilly EJ, Heitmann BL, Pereira MA, Balter K, Fraser GE, et al. Major types of dietary fat and risk of coronary heart disease: a pooled analysis of 11 cohort studies. Am J Clin Nutr. 2009;89(5):1425–32.

[71] Mozaffarian D, Micha R, Wallace S. Effects on coronary heart disease of increasing polyunsaturated fat in place of saturated fat: a systematic review and meta-analysis of randomized controlled trials. PLoS Med. 2010;7(3):e1000252.

[72] Farvid MS, Ding M, Pan A, Sun Q, Chiuve SE, Steffen LM, et al. Dietary linoleic acid and risk of coronary heart disease: a systematic review and meta-analysis of prospective cohort studies. Circulation. 2014;130(18):1568–78.

[73] Kepler CR, Hirons KP, McNeill JJ, Tove SB. Intermediates and products of the biohydrogenation of linoleic acid by Butyrinvibrio fibrisolvens. J Biol Chem. 1966;241(6):1350–4.

[74] Willett WC, Stampfer MJ, Manson JE, Colditz GA, Speizer FE, Rosner BA, et al. Intake of trans fatty acids and risk of coronary heart disease among women. Lancet. 1993;341(8845):581–5.

[75] Mensink RP, Katan MB. Effect of Dietary Trans-Fatty-Acids on High-Density and Low-Density-Lipoprotein Cholesterol Levels in Healthy-Subjects. New England Journal of Medicine. 1990;323(7):439–445.

[76] Zock PL, Katan MB. Hydrogenation alternatives: effects of trans fatty acids and stearic acid versus linoleic acid on serum lipids and lipoproteins in humans. J Lipid Res. 1992;33(3):399–410.

[77] Gebauer SK, Destaillats F, Dionisi F, Krauss RM, Baer DJ. Vaccenic acid and trans fatty acid isomers from partially hydrogenated oil both adversely affect LDL cholesterol: a double-blind, randomized controlled trial. Am J Clin Nutr. 2015;102(6):1339–46.

[78] Tricon S, Burdge GC, Kew S, Banerjee T, Russell JJ, Jones EL, et al. Opposing effects of cis-9,trans-11 and trans-10,cis-12 conjugated linoleic acid on blood lipids in healthy humans. Am J Clin Nutr. 2004;80(3):614–20.

[79] Rubinstein A, Elorriaga N, Garay OU, Poggio R, Caporale J, Matta MG, et al. Eliminating artificial trans fatty acids in Argentina: estimated effects on the burden of coronary heart disease and costs. Bull World Health Organ. 2015;93(9):614–22.

[80] Restrepo BJ, Rieger M. Denmark's Policy on Artificial Trans Fat and Cardiovascular Disease. Am J Prev Med. 2016;50(1):69–76.

[81] Bang HO, Dyerberg J. Plasma lipids and lipoproteins in Greenlandic west coast Eskimos. Acta Med Scand. 1972;192(1-2):85–94.

[82] Bang HO, Dyerberg J, Hjoorne N. The composition of food consumed by Greenland Eskimos. Acta Med Scand. 1976;200(1-2):69–73.

[83] Byelashov OA, Sinclair AJ, Kaur G. Dietary sources, current intakes, and nutritional role of omega-3 docosapentaenoic acid. Lipid Technol. 2015;27(4):79–82.

[84] London B, Albert C, Anderson ME, Giles WR, Van Wagoner DR, Balk E, et al. Omega-3 fatty acids and cardiac arrhythmias: Prior studies and recommendations for future research - A report from the national heart, lung, and blood institute and office of dietary supplements omega-3 fatty acids and their role in cardiac arrhythmogenesis workshop. Circulation. 2007;116(10):E320–E335.

[85] Ascherio A, Rimm EB, Stampfer MJ, Giovannucci EL, Willett WC. Dietary-Intake of Marine N-3 Fatty-Acids, Fish Intake, and the Risk of Coronary-Disease among Men. New England Journal of Medicine. 1995;332(15):977–982.

[86] Nilsen DWT, Albrektsen G, Landmark K, Moen S, Aarsland T, Woie L. Effects of a high-dose concentrate of n-3 fatty acids or corn oil introduced early after an acute myocardial infarction on serum triacylglycerol and HDL cholesterol. American Journal of Clinical Nutrition. 2001;74(1):50–56.

[87] Calder PC. Functional Roles of Fatty Acids and Their Effects on Human Health. JPEN J Parenter Enteral Nutr. 2015;39(1 Suppl):18S–32S.

[88] Kris-Etherton PM, Harris WS, Appel LJ, Comm N. Fish consumption, fish oil, omega-3 fatty acids, and cardiovascular disease. Circulation. 2002;106(21):2747–2757.

[89] Stulnig TM, Berger M, Sigmund T, Raederstorff D, Stockinger H, Waldhausl W. Polyunsaturated fatty acids inhibit T cell signal transduction by modification of detergent-insoluble membrane domains. J Cell Biol. 1998;143(3):637–44.

[90] Stulnig TM, Huber J, Leitinger N, Imre EM, Angelisova P, Nowotny P, et al. Polyunsaturated eicosapentaenoic acid displaces proteins from membrane rafts by altering raft lipid composition. J Biol Chem. 2001;276(40):37335–40.

[91] Calder PC. Long-chain n-3 fatty acids and inflammation: potential application in surgical and trauma patients. Braz J Med Biol Res. 2003;36(4):433–46.

[92] Price PT, Nelson CM, Clarke SD. Omega-3 polyunsaturated fatty acid regulation of gene expression. Curr Opin Lipidol. 2000;11(1):3–7.

[93] Deckelbaum RJ, Worgall TS, Seo T. n-3 fatty acids and gene expression. Am J Clin Nutr. 2006;83(6 Suppl):1520S–1525S.

[94] Kelley DS, Taylor PC, Nelson GJ, Mackey BE. Arachidonic acid supplementation enhances synthesis of eicosanoids without suppressing immune functions in young healthy men. Lipids. 1998;33(2):125–130.

[95] Peterson LD, Jeffery NM, Thies F, Sanderson P, Newsholme EA, Calder PC. Eicosapentaenoic and docosahexaenoic acids alter rat spleen leukocyte fatty acid composition and prostaglandin E-2 production but have different effects on lymphocyte functions and cell-mediated immunity. Lipids. 1998;33(2):171–180.

[96] Faber J, Berkhout M, Vos AP, Sijben JW, Calder PC, Garssen J, et al. Supplementation with a fish oil-enriched, high-protein medical food leads to rapid incorporation of EPA into white blood cells and modulates immune responses within one week in healthy men and women. J Nutr. 2011;141(5):964–70.

[97] Kohli P, Levy BD. Resolvins and protectins: mediating solutions to inflammation. British Journal of Pharmacology. 2009;158(4):960–971.

[98] Serhan CN, Yang R, Martinod K, Kasuga K, Pillai PS, Porter TF, et al. Maresins: novel macrophage mediators with potent antiinflammatory and proresolving actions. J Exp Med. 2009;206(1):15–23.

[99] Fischer R, Konkel A, Mehling H, Blossey K, Gapelyuk A, Wessel N, et al. Dietary omega-3 fatty acids modulate the eicosanoid profile in man primarily via the CYP-epoxygenase pathway. Journal of Lipid Research. 2014;55(6):1150–1164.

[100] Dong L, Zou H, Yuan C, Hong YH, Kuklev DV, Smith WL. Different Fatty Acids Compete with Arachidonic Acid for Binding to the Allosteric or Catalytic Subunits of Cyclooxygenases to Regulate Prostanoid Synthesis. J Biol Chem. 2016;291(8):4069–78.

[101] Faber J, Berkhout M, Fiedler U, Avlar M, Witteman BJ, Vos AP, et al. Rapid EPA and DHA incorporation and reduced PGE2 levels after one week intervention with a medical food in cancer patients receiving radiotherapy, a randomized trial. Clin Nutr. 2013;32(3):338–45.

[102] Nakanishi M, Rosenberg DW. Multifaceted roles of PGE2 in inflammation and cancer. Semin Immunopathol. 2013;35(2):123–37.

[103] Lopez-Candales A, Hernandez Burgos PM, Hernandez-Suarez DF, Harris D. Linking Chronic Inflammation with Cardiovascular Disease: From Normal Aging to the Metabolic Syndrome. J Nat Sci. 2017;3(4).

[104] Bouwens M, Grootte Bromhaar M, Jansen J, Muller M, Afman LA. Postprandial dietary lipid-specific effects on human peripheral blood mononuclear cell gene expression profiles. Am J Clin Nutr. 2010;91(1):208–17.

[105] Tsunoda F, Lamon-Fava S, Asztalos BF, Iyer LK, Richardson K, Schaefer EJ. Effects of oral eicosapentaenoic acid versus docosahexaenoic acid on human peripheral blood mononuclear cell gene expression. Atherosclerosis. 2015;241(2):400–8.

[106] Myhrstad MC, Ottestad I, Gunther CC, Ryeng E, Holden M, Nilsson A, et al. The PBMC transcriptome profile after intake of oxidized versus high-quality fish oil: an explorative study in healthy subjects. Genes Nutr. 2016;11:16.

[107] Polus A, Zapala B, Razny U, Gielicz A, Kiec-Wilk B, Malczewska-Malec M, et al. Omega-3 fatty acid supplementation influences the whole blood transcriptome in women with obesity, associated with pro-resolving lipid mediator production. Biochim Biophys Acta. 2016;1861(11):1746–1755.

[108] Schmidt S, Stahl F, Mutz KO, Scheper T, Hahn A, Schuchardt JP. Different gene expression profiles in normo- and dyslipidemic men after fish oil supplementation: results from a randomized controlled trial. Lipids Health Dis. 2012;11:105.

[109] Rudkowska I, Paradis AM, Thifault E, Julien P, Tchernof A, Couture P, et al. Transcriptomic and metabolomic signatures of an n-3 polyunsaturated fatty acids supplementation in a normolipidemic/normocholesterolemic Caucasian population. J Nutr Biochem. 2013;24(1):54–61.

[110] Rudkowska I, Ponton A, Jacques H, Lavigne C, Holub BJ, Marette A, et al. Effects of a supplementation of n-3 polyunsaturated fatty acids with or without fish gelatin on gene expression in peripheral blood mononuclear cells in obese, insulin-resistant subjects. J Nutrigenet Nutrigenomics. 2011;4(4):192–202.

[111] Bouwens M, van de Rest O, Dellschaft N, Bromhaar MG, de Groot LC, Geleijnse JM, et al. Fish-oil supplementation induces antiinflammatory gene expression profiles in human blood mononuclear cells. Am J Clin Nutr. 2009;90(2):415–24.

[112] Dawson K, Zhao L, Adkins Y, Vemuri M, Rodriguez RL, Gregg JP, et al. Modulation of blood cell gene expression by DHA supplementation in hypertriglyceridemic men. J Nutr Biochem. 2012;23(6):616–21.

[113] Vedin I, Cederholm T, Freund-Levi Y, Basun H, Garlind A, Irving GF, et al. Effects of DHA-rich n-3 fatty acid supplementation on gene expression in blood mononuclear leukocytes: the OmegAD study. PLoS One. 2012;7(4):e35425.

[114] van Dijk SJ, Feskens EJ, Bos MB, de Groot LC, de Vries JH, Muller M, et al. Consumption of a high monounsaturated fat diet reduces oxidative phosphorylation gene expression in peripheral blood mononuclear cells of abdominally overweight men and women. J Nutr. 2012;142(7):1219–25.

[115] Myhrstad MC, Ulven SM, Gunther CC, Ottestad I, Holden M, Ryeng E, et al. Fish oil supplementation induces expression of genes related to cell cycle, endoplasmic reticulum stress and apoptosis in peripheral blood mononuclear cells: a transcriptomic approach. J Intern Med. 2014;276(5):498–511.

[116] Newell M, Baker K, Postovit LM, Field CJ. A Critical Review on the Effect of Docosahexaenoic Acid (DHA) on Cancer Cell Cycle Progression. Int J Mol Sci. 2017;18(8).

[117] Grossniklaus U, Kelly WG, Ferguson-Smith AC, Pembrey M, Lindquist S. Transgenerational epigenetic inheritance: how important is it? (vol 14, pg 228, 2013). Nature Reviews Genetics. 2013;14(11).

[118] Portela A, Esteller M. Epigenetic modifications and human disease. Nat Biotechnol. 2010;28(10):1057–68.

[119] Collins LJ, Schonfeld B, Chen XS. The Epigenetics of Non-coding RNA. Handbook of Epigenetics: The New Molecular and Medical Genetics. 2011;p. 49–61.

[120] Sado T, Fenner MH, Tan SS, Tam P, Shioda T, Li E. X inactivation in the mouse embryo deficient for Dnmt1: distinct effect of hypomethylation on imprinted and random X inactivation. Dev Biol. 2000;225(2):294–303.

[121] Yeo S, Jeong S, Kim J, Han JS, Han YM, Kang YK. Characterization of DNA methylation change in stem cell marker genes during differentiation of human embryonic stem cells. Biochem Biophys Res Commun. 2007;359(3):536–42.

[122] Wu TP, Wang T, Seetin MG, Lai Y, Zhu S, Lin K, et al. DNA methylation on N(6)-adenine in mammalian embryonic stem cells. Nature. 2016;532(7599):329–33.

[123] Xiao CL, Zhu S, He M, Chen, Zhang Q, Chen Y, et al. N(6)-Methyladenine DNA Modification in the Human Genome. Mol Cell. 2018;71(2):306–318 e7.

[124] Santi DV, Norment A, Garrett CE. Covalent Bond Formation between a DNA-Cytosine Methyltransferase and DNA Containing 5-Azacytosine. Proceedings of the National Academy of Sciences of the United States of America-Biological Sciences. 1984;81(22):6993–6997.

[125] Wu JC, Santi DV. Kinetic and Catalytic Mechanism of Hhai Methyltransferase. Journal of Biological Chemistry. 1987;262(10):4778–4786.

[126] Klimasauskas S, Kumar S, Roberts RJ, Cheng XD. Hhal Methyltransferase Flips Its Target Base out of the DNA Helix. Cell. 1994;76(2):357–369.

[127] Goyal R, Rathert P, Laser H, Gowher H, Jeltsch A. Phosphorylation of serine-515 activates the mammalian maintenance methyltransferase Dnmt1. Epigenetics. 2007;2(3):155–160.

[128] Cheng XD, Hashimoto H, Horton JR, Zhang X. Mechanisms of DNA Methylation, Methyl-CpG Recognition, and Demethylation in Mammals. Handbook of Epigenetics: The New Molecular and Medical Genetics. 2011;p. 9–24.

[129] Kumar S, Cheng XD, Klimasauskas S, Mi S, Posfai J, Roberts RJ, et al. The DNA (Cytosine-5) Methyltransferases. Nucleic Acids Research. 1994;22(1):1–10.

[130] Jeltsch A, Jurkowska RZ. New concepts in DNA methylation. Trends in Biochemical Sciences. 2014;39(7):310–318.

[131] Guo X, Wang L, Li J, Ding Z, Xiao J, Yin X, et al. Structural insight into autoinhibition and histone H3-induced activation of DNMT3A. Nature. 2015;517(7536):640–4.

[132] Chedin F. The DNMT3 Family of Mammalian De Novo DNA Methyltransferases. Modifications of Nuclear DNA and Its Regulatory Proteins. 2011;101:255–285.

[133] Robertson KD, Uzvolgyi E, Liang GN, Talmadge C, Sumegi J, Gonzales FA, et al. The human DNA methyltransferases (DNMTs) 1, 3a and 3b: coordinate mRNA expression in normal tissues and overexpression in tumors. Nucleic Acids Research. 1999;27(11):2291–2298.

[134] Robertson KD, Keyomarsi K, Gonzales FA, Velicescu M, Jones PA. Differential mRNA expression of the human DNA methyltransferases (DNMTs) 1,3a and 3b during the G(0)/G(1) to S phase transition in normal and tumor cells. Nucleic Acids Research. 2000;28(10):2108–2113.

[135] Glickman JF, Flynn J, Reich NO. Purification and characterization of recombinant baculovirus-expressed mouse DNA methyltransferase. Biochem Biophys Res Commun. 1997;230(2):280–4.

[136] Okano M, Xie S, Li E. Cloning and characterization of a family of novel mammalian DNA (cytosine-5) methyltransferases. Nat Genet. 1998;19(3):219–20.

[137] Bonfils C, Beaulieu N, Chan E, Cotton-Montpetit J, MacLeod AR. Characterization of the human DNA methyltransferase splice variant Dnmt1b. J Biol Chem. 2000;275(15):10754–60.

[138] Bostick M, Kim JK, Esteve PO, Clark A, Pradhan S, Jacobsen SE. UHRF1 plays a role in maintaining DNA methylation in mammalian cells. Science. 2007;317(5845):1760–4.

[139] Spada F, Haemmer A, Kuch D, Rothbauer U, Schermelleh L, Kremmer E, et al. DNMT1 but not its interaction with the replication machinery is required for maintenance of DNA methylation in human cells. J Cell Biol. 2007;176(5):565–71.

[140] Chen ZX, Mann JR, Hsieh CL, Riggs AD, Chedin F. Physical and functional interactions between the human DNMT3L protein and members of the de novo methyltransferase family. Journal of Cellular Biochemistry. 2005;95(5):902–917.

[141] Gowher H, Liebert K, Hermann A, Xu G, Jeltsch A. Mechanism of stimulation of catalytic activity of Dnmt3A and Dnmt3B DNA-(cytosine-C5)-methyltransferases by Dnmt3L. J Biol Chem. 2005;280(14):13341–8.

[142] Ooi SKT, Qiu C, Bernstein E, Li KQ, Jia D, Yang Z, et al. DNMT3L connects unmethylated lysine 4 of histone H3 to de novo methylation of DNA. Nature. 2007;448(7154):714–U13.

[143] Weber M, Hellmann I, Stadler MB, Ramos L, Paabo S, Rebhan M, et al. Distribution, silencing potential and evolutionary impact of promoter DNA methylation in the human genome. Nat Genet. 2007;39(4):457–66.

[144] Rondelet G, Dal Maso T, Willems L, Wouters J. Structural basis for recognition of histone H3K36me3 nucleosome by human de novo DNA methyltransferases 3A and 3B. J Struct Biol. 2016;194(3):357–67.

[145] Baubec T, Colombo DF, Wirbelauer C, Schmidt J, Burger L, Krebs AR, et al. Genomic profiling of DNA methyltransferases reveals a role for DNMT3B in genic methylation. Nature. 2015;520(7546):243–7.

[146] Li E, Bestor TH, Jaenisch R. Targeted Mutation of the DNA Methyltransferase Gene Results in Embryonic Lethality. Cell. 1992;69(6):915–926.

[147] Okano M, Bell DW, Haber DA, Li E. DNA methyltransferases Dnmt3a and Dnmt3b are essential for de novo methylation and mammalian development. Cell. 1999;99(3):247–257.

[148] Christman JK. 5-Azacytidine and 5-aza-2 '-deoxycytidine as inhibitors of DNA methylation: mechanistic studies and their implications for cancer therapy. Oncogene. 2002;21(35):5483–5495.

[149] Rougier N, Bourc'his D, Gomes DM, Niveleau A, Plachot M, Paldi A, et al. Chromosome methylation patterns during mammalian preimplantation development. Genes and Development. 1998;12(14):2108–2113.

[150] Mayer W, Niveleau A, Walter J, Fundele R, Haaf T. Embryogenesis - Demethylation of the zygotic paternal genome. Nature. 2000;403(6769):501–502.

[151] Guo HS, Zhu P, Yan LY, Li R, Hu BQ, Lian Y, et al. The DNA methylation landscape of human early embryos. Nature. 2014;511(7511):606–+.

[152] Chen CC, Wang KY, Shen CKJ. The Mammalian de Novo DNA Methyltransferases DNMT3A and DNMT3B Are Also DNA 5-Hydroxymethylcytosine Dehydroxymethylases. Journal of Biological Chemistry. 2012;287(40):33116–33121.

[153] Chen CC, Wang KY, Shen CKJ. DNA 5-Methylcytosine Demethylation Activities of the Mammalian DNA Methyltransferases. Journal of Biological Chemistry. 2013;288(13):9084–9091.

[154] Liutkeviciute Z, Kriukiene E, Licyte J, Rudyte M, Urbanaviciute G, Klimasauskas S. Direct decarboxylation of 5-carboxylcytosine by DNA C5-methyltransferases. J Am Chem Soc. 2014;136(16):5884–7.

[155] Wu SC, Zhang Y. Active DNA demethylation: many roads lead to Rome. Nat Rev Mol Cell Biol. 2010;11(9):607–20.

[156] Krokan HE, Bjoras M. Base excision repair. Cold Spring Harb Perspect Biol. 2013;5(4):a012583.

[157] Whitaker AM, Schaich MA, Smith MR, Flynn TS, Freudenthal BD. Base excision repair of oxidative DNA damage: from mechanism to disease. Front Biosci (Landmark Ed). 2017;22:1493–1522.

[158] He YF, Li BZ, Li Z, Liu P, Wang Y, Tang QY, et al. Tet-Mediated Formation of 5-Carboxylcytosine and Its Excision by TDG in Mammalian DNA. Science. 2011;333(6047):1303–1307.

[159] Maiti A, Drohat AC. Thymine DNA Glycosylase Can Rapidly Excise 5-Formylcytosine and 5-Carboxylcytosine: Potential Implications For Active Demethylation of CpG Sites. Journal of Biological Chemistry. 2011;286(41):35334–35338.

[160] Raiber EA, Murat P, Chirgadze DY, Beraldi D, Luisi BF, Balasubramanian S. 5-Formylcytosine alters the structure of the DNA double helix. Nat Struct Mol Biol. 2015;22(1):44–49.

[161] Bellon SF, Coleman JH, Lippard SJ. DNA Unwinding Produced by Site-Specific Intrastrand Cross-Links of the Antitumor Drug Cis-Diamminedichloroplatinum(Ii). Biochemistry. 1991;30(32):8026–8035.

[162] Bochtler M, Kolano A, Xu GL. DNA demethylation pathways: Additional players and regulators. Bioessays. 2017;39(1).

[163] Pena-Diaz J, Bregenhorn S, Ghodgaonkar M, Follonier C, Artola-Boran M, Castor D, et al. Noncanonical Mismatch Repair as a Source of Genomic Instability in Human Cells. Molecular Cell. 2012;47(5):669–680.

[164] Cheng YB, Fang DC, Yao P, Guo LP, Ning XY, Wang L. Demethylation of the hTERT promoter in normal human gastric mucosal epithelial cells following N-methyl-N '-nitro-N-nitrosoguanidine exposure. Biomedical Reports. 2015;3(2):176–178.

[165] Tahiliani M, Koh KP, Shen YH, Pastor WA, Bandukwala H, Brudno Y, et al. Conversion of 5-Methylcytosine to 5-Hydroxymethylcytosine in Mammalian DNA by MLL Partner TET1. Science. 2009;324(5929):930–935.

[166] Ito S, D'Alessio AC, Taranova OV, Hong K, Sowers LC, Zhang Y. Role of Tet proteins in 5mC to 5hmC conversion, ES-cell self-renewal and inner cell mass specification. Nature. 2010;466(7310):1129–U151.

[167] Ito S, Shen L, Dai Q, Wu SC, Collins LB, Swenberg JA, et al. Tet Proteins Can Convert 5-Methylcytosine to 5-Formylcytosine and 5-Carboxylcytosine. Science. 2011;333(6047):1300–1303.

[168] Chen JK, Guo L, Zhang L, Wu HY, Yang JQ, Liu H, et al. Vitamin C modulates TET1 function during somatic cell reprogramming. Nature Genetics. 2013;45(12):1504–U140.

[169] Thienpont B, Steinbacher J, Zhao H, D'Anna F, Kuchnio A, Ploumakis A, et al. Tumour hypoxia causes DNA hypermethylation by reducing TET activity. Nature. 2016;537(7618):63–68.

[170] Lewis J C A, Crayle J, Zhou S, Swanstrom R, Wolfenden R. Cytosine deamination and the precipitous decline of spontaneous mutation during Earth's history. Proc Natl Acad Sci U S A. 2016;113(29):8194–9.

[171] Ehrlich M, Gama-Sosa MA, Huang LH, Midgett RM, Kuo KC, McCune RA, et al. Amount and distribution of 5-methylcytosine in human DNA from different types of tissues of cells. Nucleic Acids Res. 1982;10(8):2709–21.

[172] Moyzis RK, Torney DC, Meyne J, Buckingham JM, Wu JR, Burks C, et al. The distribution of interspersed repetitive DNA sequences in the human genome. Genomics. 1989;4(3):273–89.

[173] Cordaux R, Batzer MA. The impact of retrotransposons on human genome evolution. Nat Rev Genet. 2009;10(10):691–703.

[174] Luo YT, Lu XM, Xie HH. Dynamic Alu Methylation during Normal Development, Aging, and Tumorigenesis. Biomed Research International. 2014;.

[175] Heartlein MW, Knoll JH, Latt SA. Chromosome instability associated with human alphoid DNA transfected into the Chinese hamster genome. Mol Cell Biol. 1988;8(9):3611–8.

[176] Su J, Shao X, Liu H, Liu S, Wu Q, Zhang Y. Genome-wide dynamic changes of DNA methylation of repetitive elements in human embryonic stem cells and fetal fibroblasts. Genomics. 2012;99(1):10–7.

[177] Jjingo D, Conley AB, Yi SV, Lunyak VV, Jordan IK. On the presence and role of human gene-body DNA methylation. Oncotarget. 2012;3(4):462–74.

[178] Hellman A, Chess A. Gene body-specific methylation on the active X chromosome. Science. 2007;315(5815):1141–3.

[179] Lister R, Pelizzola M, Dowen RH, Hawkins RD, Hon G, Tonti-Filippini J, et al. Human DNA methylomes at base resolution show widespread epigenomic differences. Nature. 2009;462(7271):315–322.

[180] Neri F, Rapelli S, Krepelova A, Incarnato D, Parlato C, Basile G, et al. Intragenic DNA methylation prevents spurious transcription initiation. Nature. 2017;543(7643):72–77.

[181] Saxonov S, Berg P, Brutlag DL. A genome-wide analysis of CpG dinucleotides in the human genome distinguishes two distinct classes of promoters. Proc Natl Acad Sci U S A. 2006;103(5):1412–7.

[182] Larsen F, Gundersen G, Lopez R, Prydz H. Cpg Islands as Gene Markers in the Human Genome. Genomics. 1992;13(4):1095–1107.

[183] Maatouk DM, Kellam LD, Mann MR, Lei H, Li E, Bartolomei MS, et al. DNA methylation is a primary mechanism for silencing postmigratory primordial germ cell genes in both germ cell and somatic cell lineages. Development. 2006;133(17):3411–8.

[184] Bae MG, Kim JY, Choi JK. Frequent hypermethylation of orphan CpG islands with enhancer activity in cancer. BMC Med Genomics. 2016;9 Suppl 1:38.

[185] Maunakea AK, Nagarajan RP, Bilenky M, Ballinger TJ, D'Souza C, Fouse SD, et al. Conserved role of intragenic DNA methylation in regulating alternative promoters. Nature. 2010;466(7303):253–7.

[186] Lee JH, Park SJ, Nakai K. Differential landscape of non-CpG methylation in embryonic stem cells and neurons caused by DNMT3s. Sci Rep. 2017;7(1):11295.

[187] Yu B, Dong X, Gravina S, Kartal O, Schimmel T, Cohen J, et al. Genome-wide, Single-Cell DNA Methylomics Reveals Increased Non-CpG Methylation during Human Oocyte Maturation. Stem Cell Reports. 2017;9(1):397–407.

[188] Ziller MJ, Muller F, Liao J, Zhang Y, Gu H, Bock C, et al. Genomic distribution and inter-sample variation of non-CpG methylation across human cell types. PLoS Genet. 2011;7(12):e1002389.

[189] Olova N, Krueger F, Andrews S, Oxley D, Berrens RV, Branco MR, et al. Comparison of whole-genome bisulfite sequencing library preparation strategies identifies sources of biases affecting DNA methylation data. Genome Biology. 2018;19.

[190] Thorvaldsen JL, Duran KL, Bartolomei MS. Deletion of the H19 differentially methylated domain results in loss of imprinted expression of H19 and Igf2. Genes Dev. 1998;12(23):3693–702.

[191] Bell AC, Felsenfeld G. Methylation of a CTCF-dependent boundary controls imprinted expression of the Igf2 gene. Nature. 2000;405(6785):482–5.

[192] Webber AL, Ingram RS, Levorse JM, Tilghman SM. Location of enhancers is essential for the imprinting of H19 and Igf2 genes. Nature. 1998;391(6668):711–715.

[193] Hark AT, Tilghman SM. Chromatin conformation of the H19 epigenetic mark. Human Molecular Genetics. 1998;7(12):1979–1985.

[194] Hark AT, Schoenherr CJ, Katz DJ, Ingram RS, Levorse JM, Tilghman SM. CTCF mediates methylation-sensitive enhancer-blocking activity at the H19/Igf2 locus. Nature. 2000;405(6785):486–489.

[195] Du MJ, Beatty LG, Zhou WJ, Lew J, Schoenherr C, Weksberg R, et al. Insulator and silencer sequences in the imprinted region of human chromosome 11p15.5. Human Molecular Genetics. 2003;12(15):1927–1939.

[196] Gicquel C, Rossignol S, Cabrol S, Houang M, Steunou V, Barbu V, et al. Epimutation of the telomeric imprinting center region on chromosome 11p15 in Silver-Russell syndrome. Nature Genetics. 2005;37(9):1003–1007.

[197] Bartholdi D, Krajewska-Walasek M, Ounap K, Gaspar H, Chrzanowska KH, Ilyana H, et al. Epigenetic mutations of the imprinted IGF2-H19 domain in Silver-Russell syndrome (SRS): results from a large cohort of patients with SRS and SRS-like phenotypes. Journal of Medical Genetics. 2009;46(3):192–197.

[198] Cerrato F, Sparago A, Verde G, De Crescenzo A, Citro V, Cubellis MV, et al. Different mechanisms cause imprinting defects at the IGF2/H19 locus in Beckwith-Wiedemann syndrome and Wilms' tumour. Human Molecular Genetics. 2008;17(10):1427–1435.

[199] Demars J, Shmela ME, Rossignol S, Okabe J, Netchine I, Azzi S, et al. Analysis of the IGF2/H19 imprinting control region uncovers new genetic defects, including mutations of OCT-binding sequences, in patients with 11p15 fetal growth disorders. Human Molecular Genetics. 2010;19(5):803–814.

[200] Kumar A, Kumar S, Vikram A, Hoffman TA, Naqvi A, Lewarchik CM, et al. Histone and DNA methylation-mediated epigenetic downregulation of endothelial Kruppel-like factor 2 by low-density lipoprotein cholesterol. Arterioscler Thromb Vasc Biol. 2013;33(8):1936–42.

[201] Lewis JD, Meehan RR, Henzel WJ, Maurerfogy I, Jeppesen P, Klein F, et al. Purification, Sequence, and Cellular-Localization of a Novel Chromosomal Protein That Binds to Methylated DNA. Cell. 1992;69(6):905–914.

[202] Okitsu CY, Hsieh CL. DNA methylation dictates histone H3K4 methylation. Molecular and Cellular Biology. 2007;27(7):2746–2757.

[203] Esteve PO, Chin HG, Pradhan S. Human maintenance DNA (cytosine-5)-methyltransferase and p53 modulate expression of p53-repressed promoters. Proc Natl Acad Sci U S A. 2005;102(4):1000–5.

[204] Esteve PO, Chin HG, Pradhan S. Molecular mechanisms of transactivation and doxorubicin-mediated repression of survivin gene in cancer cells. Journal of Biological Chemistry. 2007;282(4):2615–2625.

[205] Li W, Chen BF. Aberrant DNA methylation in human cancers. J Huazhong Univ Sci Technolog Med Sci. 2013;33(6):798–804.

[206] Davegardh C, Garcia-Calzon S, Bacos K, Ling C. DNA methylation in the pathogenesis of type 2 diabetes in humans. Mol Metab. 2018;.

[207] Hai Z, Zuo W. Aberrant DNA methylation in the pathogenesis of atherosclerosis. Clin Chim Acta. 2016;456:69–74.

[208] Bachman KE, Park BH, Rhee I, Rajagopalan H, Herman JG, Baylin SB, et al. Histone modifications and silencing prior to DNA methylation of a tumor suppressor gene. Cancer Cell. 2003;3(1):89–95.

[209] D'Alessio AC, Weaver ICG, Szyf M. Acetylation-induced transcription is required for active DNA demethylation in methylation-silenced genes. Molecular and Cellular Biology. 2007;27(21):7462–7474.

[210] Robin P, Fritsch L, Philipot O, Svinarchuk F, Ait-Si-Ali S. Post-translational modifications of histones H3 and H4 associated with the histone methyltransferases Suv39h1 and G9a. Genome Biol. 2007;8(12):R270.

[211] Mathis DJ, Oudet P, Wasylyk B, Chambon P. Effect of Histone Acetylation on Structure and Invitro Transcription of Chromatin. Nucleic Acids Research. 1978;5(10):3523–3547.

[212] Vidali G, Boffa LC, Bradbury EM, Allfrey VG. Butyrate Suppression of Histone Deacetylation Leads to Accumulation of Multiacetylated Forms of Histones H-3 and H-4 and Increased Dnase-I Sensitivity of Associated DNA Sequences. Proceedings of the National Academy of Sciences of the United States of America. 1978;75(5):2239–2243.

[213] Annunziato AT, Frado LLY, Seale RL, Woodcock CLF. Treatment with Sodium-Butyrate Inhibits the Complete Condensation of Interphase Chromatin. Chromosoma. 1988;96(2):132–138.

[214] Tse C, Sera T, Wolffe AP, Hansen JC. Disruption of higher-order folding by core histone acetylation dramatically enhances transcription of nucleosomal arrays by RNA polymerase III. Molecular and Cellular Biology. 1998;18(8):4629–4638.

[215] Pham TX, Lee J. Dietary regulation of histone acetylases and deacetylases for the prevention of metabolic diseases. Nutrients. 2012;4(12):1868–86.

[216] Serrano L, Vazquez BN, Tischfield J. Chromatin structure, pluripotency and differentiation. Exp Biol Med (Maywood). 2013;238(3):259–70.

[217] Flanagan JF, Mi LZ, Chruszcz M, Cymborowski M, Clines KL, Kim YC, et al. Double chromodomains cooperate to recognize the methylated histone H3 tail. Nature. 2005;438(7071):1181–1185.

[218] Gaspar-Maia A, Alajem A, Polesso F, Sridharan R, Mason MJ, Heidersbach A, et al. Chd1 regulates open chromatin and pluripotency of embryonic stem cells. Nature. 2009;460(7257):863–8.

[219] Barski A, Cuddapah S, Cui KR, Roh TY, Schones DE, Wang ZB, et al. High-resolution profiling of histone methylations in the human genome. Cell. 2007;129(4):823–837.

[220] Heintzman ND, Stuart RK, Hon G, Fu YT, Ching CW, Hawkins RD, et al. Distinct and predictive chromatin signatures of transcriptional promoters and enhancers in the human genome. Nature Genetics. 2007;39(3):311–318.

[221] Dunham I, Kundaje A, Aldred SF, Collins PJ, Davis C, Doyle F, et al. An integrated encyclopedia of DNA elements in the human genome. Nature. 2012;489(7414):57–74.

[222] Hyun K, Jeon J, Park K, Kim J. Writing, erasing and reading histone lysine methylations. Exp Mol Med. 2017;49(4):e324.

[223] Lee JH, Skalnik DG. CpG-binding protein (CXXC finger protein 1) is a component of the mammalian set1 histone H3-Lys(4) methyltransferase complex, the analogue of the yeast Set1/COMPASS complex. Journal of Biological Chemistry. 2005;280(50):41725–41731.

[224] Clouaire T, Webb S, Skene P, Illingworth R, Kerr A, Andrews R, et al. Cfp1 integrates both CpG content and gene activity for accurate H3K4me3 deposition in embryonic stem cells. Genes and Development. 2012;26(15):1714–1728.

[225] Voo KS, Carlone DL, Jacobsen BM, Flodin A, Skalnik DG. Cloning of a mammalian transcriptional activator that binds unmethylated CpG motifs and shares a CXXC domain with DNA methyltransferase, human trithorax, and methyl-CpG binding domain protein 1. Molecular and Cellular Biology. 2000;20(6):2108–2121.

[226] Lee JH, Skalnik DG. Wdr82 is a C-terminal domain-binding protein that recruits the Setd1A histone H3-Lys4 methyltransferase complex to transcription start sites of transcribed human genes. Molecular and Cellular Biology. 2008;28(2):609–618.

[227] Vermeulen M, Mulder KW, Denissov S, Pijnappel WWMP, van Schaik FMA, Varier RA, et al. Selective anchoring of TFIID to nucleosomes by trimethylation of histone H3 lysine 4. Cell. 2007;131(1):58–69.

[228] Lauberth SM, Nakayama T, Wu XL, Ferris AL, Tang ZY, Hughes SH, et al. H3K4me3 Interactions with TAF3 Regulate Preinitiation Complex Assembly and Selective Gene Activation. Cell. 2013;152(5):1021–1036.

[229] Silva-Martinez GA, Rodriguez-Rios D, Alvarado-Caudillo Y, Vaquero A, Esteller M, Carmona FJ, et al. Arachidonic and oleic acid exert distinct effects on the DNA methylome. Epigenetics. 2016;11(5):321–34.

[230] Kiec-Wilk B, Polus A, Mikolajczyk M, Mathers JC. Beta-carotene and arachidonic acid induced DNA methylation and the regulation of pro-chemotactic activity of endothelial cells and its progenitors. J Physiol Pharmacol. 2007;58(4):757–66.

[231] Kiec-Wilk B, Razny U, Mathers JC, Dembinska-Kiec A. DNA methylation, induced by beta-carotene and arachidonic acid, plays a regulatory role in the pro-angiogenic VEGF-receptor (KDR) gene expression in endothelial cells. J Physiol Pharmacol. 2009;60(4):49–53.

[232] Barres R, Osler ME, Yan J, Rune A, Fritz T, Caidahl K, et al. Non-CpG methylation of the PGC-1alpha promoter through DNMT3B controls mitochondrial density. Cell Metab. 2009;10(3):189–98.

[233] Ceccarelli V, Racanicchi S, Martelli MP, Nocentini G, Fettucciari K, Riccardi C, et al. Eicosapentaenoic acid demethylates a single CpG that mediates expression of tumor suppressor CCAAT/enhancer-binding protein delta in U937 leukemia cells. J Biol Chem. 2011;286(31):27092–102.

[234] Hoile SP, Irvine NA, Kelsall CJ, Sibbons C, Feunteun A, Collister A, et al. Maternal fat intake in rats alters 20:4n-6 and 22:6n-3 status and the epigenetic regulation of Fads2 in offspring liver. J Nutr Biochem. 2013;24(7):1213–20.

[235] Lee HS, Barraza-Villarreal A, Hernandez-Vargas H, Sly PD, Biessy C, Ramakrishnan U, et al. Modulation of DNA methylation states and infant immune system by dietary supplementation with omega-3 PUFA during pregnancy in an intervention study. Am J Clin Nutr. 2013;98(2):480–7.

[236] van Dijk SJ, Zhou J, Peters TJ, Buckley M, Sutcliffe B, Oytam Y, et al. Effect of prenatal DHA supplementation on the infant epigenome: results from a randomized controlled trial. Clin Epigenetics. 2016;8:114.

[237] Burdge GC. DHA supplementation during pregnancy and DNA methylation in cord blood leukocytes. Am J Clin Nutr. 2013;98(6):1594–5.

[238] Irahara N, Nosho K, Baba Y, Shima K, Lindeman NI, Hazra A, et al. Precision of pyrosequencing assay to measure LINE-1 methylation in colon cancer, normal colonic mucosa, and peripheral blood cells. J Mol Diagn. 2010;12(2):177–83.

[239] de la Rocha C, Perez-Mojica JE, Leon SZ, Cervantes-Paz B, Tristan-Flores FE, Rodriguez-Rios D, et al. Associations between whole peripheral blood fatty acids and DNA methylation in humans. Sci Rep. 2016;6:25867.

[240] Hoile SP, Clarke-Harris R, Huang RC, Calder PC, Mori TA, Beilin LJ, et al. Supplementation with N-3 long-chain polyunsaturated fatty acids or olive oil in men and women with renal disease induces differential changes in the DNA methylation of FADS2 and ELOVL5 in peripheral blood mononuclear cells. PLoS One. 2014;9(10):e109896.

[241] Tremblay BL, Guenard F, Rudkowska I, Lemieux S, Couture P, Vohl MC. Epigenetic changes in blood leukocytes following an omega-3 fatty acid supplementation. Clin Epigenetics. 2017;9:43.

[242] Perfilyev A, Dahlman I, Gillberg L, Rosqvist F, Iggman D, Volkov P, et al. Impact of polyunsaturated and saturated fat overfeeding on the DNA-methylation pattern in human adipose tissue: a randomized controlled trial. Am J Clin Nutr. 2017;105(4):991–1000.

[243] Morcillo S, Martin-Nunez GM, Garcia-Serrano S, Gutierrez-Repiso C, Rodriguez-Pacheco F, Valdes S, et al. Changes in SCD gene DNA methylation after bariatric surgery in morbidly obese patients are associated with free fatty acids. Scientific Reports. 2017;7.

[244] Benton MC, Johnstone A, Eccles D, Harmon B, Hayes MT, Lea RA, et al. An analysis of DNA methylation in human adipose tissue reveals differential modification of obesity genes before and after gastric bypass and weight loss. Genome Biol. 2015;16:8.

[245] Davie JR. Inhibition of histone deacetylase activity by butyrate. J Nutr. 2003;133(7 Suppl):2485S–2493S.

[246] Pougovkina O, te Brinke H, Ofman R, van Cruchten AG, Kulik W, Wanders RJA, et al. Mitochondrial protein acetylation is driven by acetyl-CoA from fatty acid oxidation. Human Molecular Genetics. 2014;23(13):3513–3522.

[247] Simithy J, Sidoli S, Yuan ZF, Coradin M, Bhanu NV, Marchione DM, et al. Characterization of histone acylations links chromatin modifications with metabolism. Nature Communications. 2017;8.

[248] Sadli N, Ackland ML, De Mel D, Sinclair AJ, Suphioglu C. Effects of zinc and DHA on the epigenetic regulation of human neuronal cells. Cell Physiol Biochem. 2012;29(1-2):87–98.

[249] Jun HJ, Kim J, Hoang MH, Lee SJ. Hepatic lipid accumulation alters global histone h3 lysine 9 and 4 trimethylation in the peroxisome proliferator-activated receptor alpha network. PLoS One. 2012;7(9):e44345.

[250] Masuyama H, Hiramatsu Y. Effects of a high-fat diet exposure in utero on the metabolic syndrome-like phenomenon in mouse offspring through epigenetic changes in adipocytokine gene expression. Endocrinology. 2012;153(6):2823–30.

[251] Brown PJ, Stuart LW, Hurley KP, Lewis MC, Winegar DA, Wilson JG, et al. Identification of a subtype selective human PPARalpha agonist through parallel-array synthesis. Bioorg Med Chem Lett. 2001;11(9):1225–7.

[252] Xu HE, Stanley TB, Montana VG, Lambert MH, Shearer BG, Cobb JE, et al. Structural basis for antagonist-mediated recruitment of nuclear co-repressors by PPARalpha. Nature. 2002;415(6873):813–7.

[253] Strober W. Trypan blue exclusion test of cell viability. Curr Protoc Immunol. 2001;Appendix 3:Appendix 3B.

[254] Chomczynski P, Sacchi N. Single-step method of RNA isolation by acid guanidinium thiocyanate-phenol-chloroform extraction. Anal Biochem. 1987;162(1):156–9.

[255] Boom R, Sol CJ, Salimans MM, Jansen CL, Wertheim-van Dillen PM, van der Noordaa J. Rapid and simple method for purification of nucleic acids. J Clin Microbiol. 1990;28(3):495–503.

[256] Koressaar T, Remm M. Enhancements and modifications of primer design program Primer3. Bioinformatics. 2007;23(10):1289–91.

[257] Untergasser A, Cutcutache I, Koressaar T, Ye J, Faircloth BC, Remm M, et al. Primer3–new capabilities and interfaces. Nucleic Acids Res. 2012;40(15):e115.

[258] Ye J, Coulouris G, Zaretskaya I, Cutcutache I, Rozen S, Madden TL. Primer-BLAST: a tool to design target-specific primers for polymerase chain reaction. BMC Bioinformatics. 2012;13:134.

[259] Porschke D. Cooperative Nonenzymic Base Recognition .2. Thermodynamics of Helix-Coil Transition of Oligoadenylic and Oligouridylic Acids. Biopolymers. 1971;10(10).

[260] Cikos S, Bukovska A, Koppel J. Relative quantification of mRNA: comparison of methods currently used for real-time PCR data analysis. BMC Molecular Biology. 2007;8(1):1–14.

[261] Hunter L, Taylor RC, Leach SM, Simon R. GEST: a gene expression search tool based on a novel Bayesian similarity metric. Bioinformatics. 2001;17 Suppl 1:S115–22.

[262] Kramer A, Green J, Pollard J J, Tugendreich S. Causal analysis approaches in Ingenuity Pathway Analysis. Bioinformatics. 2014;30(4):523–30.

[263] Kleiveland CR. In: Verhoeckx K, Cotter P, Lopez-Exposito I, Kleiveland C, Lea T, Mackie A, et al., editors. Peripheral Blood Mononuclear Cells. Cham (CH); 2015. p. 161–167.

[264] Lima TM, Kanunfre CC, Pompeia C, Verlengia R, Curi R. Ranking the toxicity of fatty acids on Jurkat and Raji cells by flow cytometric analysis. Toxicol In Vitro. 2002;16(6):741–7.

[265] Guieze R, Gyan E, Tournilhac O, Halty C, Veyrat-Masson R, Akil S, et al. Docosahexaenoic Acid Induces Apoptosis in Primary Chronic Lymphocytic Leukemia Cells. Hematol Rep. 2015;7(4):6043.

[266] Siddiqui RA, Jenski LJ, Harvey KA, Wiesehan JD, Stillwell W, Zaloga GP. Cell-cycle arrest in Jurkat leukaemic cells: a possible role for docosahexaenoic acid. Biochem J. 2003;371(Pt 2):621–9.

[267] Verlengia R, Gorjao R, Kanunfre CC, Bordin S, Martins De Lima T, Martins EF, et al. Comparative effects of eicosapentaenoic acid and docosahexaenoic acid on proliferation, cytokine production, and pleiotropic gene expression in Jurkat cells. J Nutr Biochem. 2004;15(11):657–65.

[268] Cury-Boaventura MF, Pompeia C, Curi R. Comparative toxicity of oleic acid and linoleic acid on Jurkat cells. Clin Nutr. 2004;23(4):721–32.

[269] Finstad HS, Myhrstad MC, Heimli H, Lomo J, Blomhoff HK, Kolset SO, et al. Multiplication and death-type of leukemia cell lines exposed to very long-chain polyunsaturated fatty acids. Leukemia. 1998;12(6):921–9.

[270] Aires V, Hichami A, Moutairou K, Khan NA. Docosahexaenoic acid and other fatty acids induce a decrease in pHi in Jurkat T-cells. Br J Pharmacol. 2003;140(7):1217–26.

[271] Grammatikos SI, Subbaiah PV, Victor TA, Miller WM. Diversity in the ability of cultured cells to elongate and desaturate essential (n-6 and n-3) fatty acids. Ann N Y Acad Sci. 1994;745:92–105.

[272] Folch J, Lees M, Sloane Stanley GH. A simple method for the isolation and purification of total lipides from animal tissues. J Biol Chem. 1957;226(1):497–509.

[273] Burdge GC, Wright P, Jones AE, Wootton SA. A method for separation of phosphatidylcholine, triacylglycerol, non-esterified fatty acids and cholesterol esters from plasma by solid-phase extraction. Br J Nutr. 2000;84(5):781–7.

[274] Terada S, Takizawa M, Yamamoto S, Ezaki O, Itakura H, Akagawa KS. Suppressive mechanisms of EPA on human T cell proliferation. Microbiol Immunol. 2001;45(6):473–81.

[275] D'Eliseo D, Velotti F. Omega-3 Fatty Acids and Cancer Cell Cytotoxicity: Implications for Multi-Targeted Cancer Therapy. J Clin Med. 2016;5(2).

[276] Germain E, Chajes V, Cognault S, Lhuillery C, Bougnoux P. Enhancement of doxorubicin cytotoxicity by polyunsaturated fatty acids in the human breast tumor cell line MDA-MB-231: relationship to lipid peroxidation. Int J Cancer. 1998;75(4):578–83.

[277] Siddiqui RA, Jenski LJ, Neff K, Harvey K, Kovacs RJ, Stillwell W. Docosahexaenoic acid induces apoptosis in Jurkat cells by a protein phosphatase-mediated process. Biochim Biophys Acta. 2001;1499(3):265–75.

[278] Roman AS, Schreher J, Mackenzie AP, Nathanielsz PW. Omega-3 fatty acids and decidual cell prostaglandin production in response to the inflammatory cytokine IL-1 beta. American Journal of Obstetrics and Gynecology. 2006;195(6):1693–1699.

[279] Landschulz KT, Jump DB, Macdougald OA, Lane MD. Transcriptional Control of the Stearoyl-Coa Desaturase-1 Gene by Polyunsaturated Fatty-Acids. Biochemical and Biophysical Research Communications. 1994;200(2):763–768.

[280] Guillou H, Zadravec D, Martin PG, Jacobsson A. The key roles of elongases and desaturases in mammalian fatty acid metabolism: Insights from transgenic mice. Prog Lipid Res. 2010;49(2):186–99.

[281] Moore SA, Hurt E, Yoder E, Sprecher H, Spector AA. Docosahexaenoic acid synthesis in human skin fibroblasts involves peroxisomal retroconversion of tetracosahexaenoic acid. J Lipid Res. 1995;36(11):2433–43.

[282] Gronn M, Christensen E, Hagve TA, Christophersen BO. Peroxisomal retroconversion of docosahexaenoic acid (22:6(n-3)) to eicosapentaenoic acid (20:5(n-3)) studied in isolated rat liver cells. Biochim Biophys Acta. 1991;1081(1):85–91.

[283] Itoyama A, Honsho M, Abe Y, Moser A, Yoshida Y, Fujiki Y. Docosahexaenoic acid mediates peroxisomal elongation, a prerequisite for peroxisome division. Journal of Cell Science. 2012;125(3):589–602.

[284] Calder PC. Marine omega-3 fatty acids and inflammatory processes: Effects, mechanisms and clinical relevance. Biochim Biophys Acta. 2015;1851(4):469–84.

[285] Walker CG, West AL, Browning LM, Madden J, Gambell JM, Jebb SA, et al. The Pattern of Fatty Acids Displaced by EPA and DHA Following 12 Months Supplementation Varies between Blood Cell and Plasma Fractions. Nutrients. 2015;7(8):6281–93.

[286] Chapkin RS, Akoh CC, Miller CC. Influence of dietary n-3 fatty acids on macrophage glycerophospholipid molecular species and peptidoleukotriene synthesis. J Lipid Res. 1991;32(7):1205–13.

[287] Hall E, Volkov P, Dayeh T, Bacos K, Ronn T, Nitert MD, et al. Effects of palmitate on genome-wide mRNA expression and DNA methylation patterns in human pancreatic islets. BMC Med. 2014;12:103.

[288] Zou Y, Jiang Y, Yang T, Hu P, Xu X. In: Oi-Ming L, Chin-Ping T, Casimir CA, editors. Minor Constituents of Palm Oil: Characterization, Processing, and Application. AOCS Press; 2012. .

[289] Buhule OD, Minster RL, Hawley NL, Medvedovic M, Sun G, Viali S, et al. Stratified randomization controls better for batch effects in 450K methylation analysis: a cautionary tale. Front Genet. 2014;5:354.

[290] Pidsley R, Zotenko E, Peters TJ, Lawrence MG, Risbridger GP, Molloy P, et al. Critical evaluation of the Illumina MethylationEPIC BeadChip microarray for whole-genome DNA methylation profiling. Genome Biol. 2016;17(1):208.

[291] Aryee MJ, Jaffe AE, Corrada-Bravo H, Ladd-Acosta C, Feinberg AP, Hansen KD, et al. Minfi: a flexible and comprehensive Bioconductor package for the analysis of Infinium DNA methylation microarrays. Bioinformatics. 2014;30(10):1363–9.

[292] Maksimovic J, Phipson B, Oshlack A. A cross-package Bioconductor workflow for analysing methylation array data. F1000Res. 2016;5:1281.

[293] Chen YA, Lemire M, Choufani S, Butcher DT, Grafodatskaya D, Zanke BW, et al. Discovery of cross-reactive probes and polymorphic CpGs in the Illumina Infinium HumanMethylation450 microarray. Epigenetics. 2013;8(2):203–9.

[294] Fortin JP, Labbe A, Lemire M, Zanke BW, Hudson TJ, Fertig EJ, et al. Functional normalization of 450k methylation array data improves replication in large cancer studies. Genome Biol. 2014;15(12):503.

[295] Johnson WE, Li C, Rabinovic A. Adjusting batch effects in microarray expression data using empirical Bayes methods. Biostatistics. 2007;8(1):118–27.

[296] Du P, Zhang X, Huang CC, Jafari N, Kibbe WA, Hou L, et al. Comparison of Beta-value and M-value methods for quantifying methylation levels by microarray analysis. BMC Bioinformatics. 2010;11:587.

[297] Benjamini Y, Hochberg Y. Controlling the False Discovery Rate - a Practical and Powerful Approach to Multiple Testing. Journal of the Royal Statistical Society Series B-Methodological. 1995;57(1):289–300.

[298] Jaffe AE, Murakami P, Lee H, Leek JT, Fallin MD, Feinberg AP, et al. Bump hunting to identify differentially methylated regions in epigenetic epidemiology studies. Int J Epidemiol. 2012;41(1):200–9.

[299] Ferrante A, Goh D, Harvey DP, Robinson BS, Hii CST, Bates EJ, et al. Neutrophil Migration-Inhibitory Properties of Polyunsaturated Fatty-Acids - the Role of Fatty-Acid Structure, Metabolism, and Possible 2nd Messenger Systems. Journal of Clinical Investigation. 1994;93(3):1063–1070.

[300] Yaqoob P. Monounsaturated fatty acids and immune function. Eur J Clin Nutr. 2002;56 Suppl 3:S9–S13.

[301] Shaikh SR, Dumaual AC, Castillo A, LoCascio D, Siddiqui RA, Stillwell W, et al. Oleic and docosahexaenoic acid differentially phase separate from lipid raft molecules: a comparative NMR, DSC, AFM, and detergent extraction study. Biophys J. 2004;87(3):1752–66.

[302] Shaikh SR, Rockett BD, Salameh M, Carraway K. Docosahexaenoic acid modifies the clustering and size of lipid rafts and the lateral organization and surface expression of MHC class I of EL4 cells. J Nutr. 2009;139(9):1632–9.

[303] Ceccarelli V, Valentini V, Ronchetti S, Cannarile L, Billi M, Riccardi C, et al. Eicosapentaenoic acid induces DNA demethylation in carcinoma cells through a TET1-dependent mechanism. FASEB J. 2018;p. fj201800245R.

[304] Altucci L, Leibowitz MD, Ogilvie KM, de Lera AR, Gronemeyer H. RAR and RXR modulation in cancer and metabolic disease. Nat Rev Drug Discov. 2007;6(10):793–810.

[305] Peng L, Yuan Z, Ling H, Fukasawa K, Robertson K, Olashaw N, et al. SIRT1 deacetylates the DNA methyltransferase 1 (DNMT1) protein and alters its activities. Mol Cell Biol. 2011;31(23):4720–34.

[306] O'Hagan HM, Wang W, Sen S, Destefano Shields C, Lee SS, Zhang YW, et al. Oxidative damage targets complexes containing DNA methyltransferases, SIRT1, and polycomb members to promoter CpG Islands. Cancer Cell. 2011;20(5):606–19.

[307] Lengqvist J, Mata De Urquiza A, Bergman AC, Willson TM, Sjovall J, Perlmann T, et al. Polyunsaturated fatty acids including docosahexaenoic and arachidonic acid bind to the retinoid X receptor alpha ligand-binding domain. Mol Cell Proteomics. 2004;3(7):692–703.

[308] Hassan HM, Kolendowski B, Isovic M, Bose K, Dranse HJ, Sampaio AV, et al. Regulation of Active DNA Demethylation through RAR-Mediated Recruitment of a TET/TDG Complex. Cell Reports. 2017;19(8):1685–1697.

[309] Song EA, Kim H. Docosahexaenoic Acid Induces Oxidative DNA Damage and Apoptosis, and Enhances the Chemosensitivity of Cancer Cells. Int J Mol Sci. 2016;17(8).

[310] Sarabi MM, Naghibalhossaini F. The impact of polyunsaturated fatty acids on DNA methylation and expression of DNMTs in human colorectal cancer cells. Biomed Pharmacother. 2018;101:94–99.

[311] Branzei D, Foiani M. Regulation of DNA repair throughout the cell cycle. Nature Reviews Molecular Cell Biology. 2008;9(4):297–308.

[312] Kang KS, Wang P, Yamabe N, Fukui M, Jay T, Zhu BT. Docosahexaenoic acid induces apoptosis in MCF-7 cells in vitro and in vivo via reactive oxygen species formation and caspase 8 activation. PLoS One. 2010;5(4):e10296.

[313] Sies H. Hydrogen peroxide as a central redox signaling molecule in physiological oxidative stress: Oxidative eustress. Redox Biology. 2017;11:613–619.

[314] Murakami K, Ide T, Suzuki M, Mochizuki T, Kadowaki T. Evidence for direct binding of fatty acids and eicosanoids to human peroxisome proliferators-activated receptor alpha. Biochem Biophys Res Commun. 1999;260(3):609–13.

[315] Levo M, Segal E. In pursuit of design principles of regulatory sequences. Nat Rev Genet. 2014;15(7):453–68.

[316] Pennacchio LA, Bickmore W, Dean A, Nobrega MA, Bejerano G. Enhancers: five essential questions. Nat Rev Genet. 2013;14(4):288–95.

[317] Petrykowska HM, Vockley CM, Elnitski L. Detection and characterization of silencers and enhancer-blockers in the greater CFTR locus. Genome Res. 2008;18(8):1238–46.

[318] Palazzo AF, Lee ES. Non-coding RNA: what is functional and what is junk? Front Genet. 2015;6:2.

[319] Long HK, King HW, Patient RK, Odom DT, Klose RJ. Protection of CpG islands from DNA methylation is DNA-encoded and evolutionarily conserved. Nucleic Acids Res. 2016;44(14):6693–706.

[320] Amir RE, Van den Veyver IB, Wan M, Tran CQ, Francke U, Zoghbi HY. Rett syndrome is caused by mutations in X-linked MECP2, encoding methyl-CpG-binding protein 2. Nature Genetics. 1999;23(2):185–188.

[321] De Felice C, Signorini C, Durand T, Ciccoli L, Leoncini S, D'Esposito M, et al. Partial rescue of Rett syndrome by omega-3 polyunsaturated fatty acids (PUFAs) oil. Genes Nutr. 2012;7(3):447–58.

[322] Leoncini S, De Felice C, Signorini C, Zollo G, Cortelazzo A, Durand T, et al. Cytokine Dysregulation in MECP2- and CDKL5-Related Rett Syndrome: Relationships with Aberrant Redox Homeostasis, Inflammation, and omega-3 PUFAs. Oxid Med Cell Longev. 2015;2015:421624.

[323] Quante T, Bird A. Do short, frequent DNA sequence motifs mould the epigenome? Nat Rev Mol Cell Biol. 2016;17(4):257–62.

[324] Hu JL, Zhou BO, Zhang RR, Zhang KL, Zhou JQ, Xu GL. The N-terminus of histone H3 is required for de novo DNA methylation in chromatin. Proceedings of the National Academy of Sciences of the United States of America. 2009;106(52):22187–22192.

[325] Zhang Y, Jurkowska R, Soeroes S, Rajavelu A, Dhayalan A, Bock I, et al. Chromatin methylation activity of Dnmt3a and Dnmt3a/3L is guided by interaction of the ADD domain with the histone H3 tail. Nucleic Acids Res. 2010;38(13):4246–53.

[326] Fuks F, Hurd PJ, Wolf D, Nan X, Bird AP, Kouzarides T. The methyl-CpG-binding protein MeCP2 links DNA methylation to histone methylation. J Biol Chem. 2003;278(6):4035–40.

[327] Sarraf SA, Stancheva I. Methyl-CpG binding protein MBD1 couples histone H3 methylation at lysine 9 by SETDB1 to DNA replication and chromatin assembly. Mol Cell. 2004;15(4):595–605.

[328] Rose NR, Klose RJ. Understanding the relationship between DNA methylation and histone lysine methylation. Biochimica Et Biophysica Acta-Gene Regulatory Mechanisms. 2014;1839(12):1362–1372.

[329] Cheng X. Structural and functional coordination of DNA and histone methylation. Cold Spring Harb Perspect Biol. 2014;6(8).

[330] Isomura H, Stinski MF. The human cytomegalovirus major immediate-early enhancer determines the efficiency of immediate-early gene transcription and viral replication in permissive cells at low multiplicity of infection. J Virol. 2003;77(6):3602–14.

[331] Bailey TL, Elkan C. Fitting a mixture model by expectation maximization to discover motifs in biopolymers. Proc Int Conf Intell Syst Mol Biol. 1994;2:28–36.

[332] Heinz S, Benner C, Spann N, Bertolino E, Lin YC, Laslo P, et al. Simple combinations of lineage-determining transcription factors prime cis-regulatory elements required for macrophage and B cell identities. Mol Cell. 2010;38(4):576–89.

[333] Bailey TL. DREME: motif discovery in transcription factor ChIP-seq data. Bioinformatics. 2011;27(12):1653–9.

[334] Mahony S, Auron PE, Benos PV. DNA familial binding profiles made easy: Comparison of various motif alignment and clustering strategies. Plos Computational Biology. 2007;3(3):578–591.

[335] Mahony S, Benos PV. STAMP: a web tool for exploring DNA-binding motif similarities. Nucleic Acids Research. 2007;35:W253–W258.

[336] Waterman MS, Smith TF, Beyer WA. Some Biological Sequence Metrics. Advances in Mathematics. 1976;20(3):367–387.

[337] Barton GJ, Sternberg MJE. A Strategy for the Rapid Multiple Alignment of Protein Sequences - Confidence Levels from Tertiary Structure Comparisons. Journal of Molecular Biology. 1987;198(2):327–337.

[338] Pietrokovski S. Searching databases of conserved sequence regions by aligning protein mutliple-alignments (vol 24, pg 3836, 1996). Nucleic Acids Research. 1996;24(21):4372–4372.

[339] Gupta S, Stamatoyannopoulos JA, Bailey TL, Noble WS. Quantifying similarity between motifs. Genome Biology. 2007;8(2).

[340] Kulakovskiy IV, Vorontsov IE, Yevshin IS, Sharipov RN, Fedorova AD, Rumynskiy EI, et al. HOCOMOCO: towards a complete collection of transcription factor binding models for human and mouse via large-scale ChIP-Seq analysis. Nucleic Acids Research. 2018;46(D1):D252–D259.

[341] Myers R, Pauli F. Myers Lab ChIP-seq Protocol, v041610.1 and v041610.2 [Document on Internet]; 2010.

[342] Hoffman EA, Frey BL, Smith LM, Auble DT. Formaldehyde crosslinking: a tool for the study of chromatin complexes. J Biol Chem. 2015;290(44):26404–11.

[343] Jackson V. Studies on histone organization in the nucleosome using formaldehyde as a reversible cross-linking agent. Cell. 1978;15(3):945–54.

[344] Allan J, Fraser RM, Owen-Hughes T, Keszenman-Pereyra D. Micrococcal nuclease does not substantially bias nucleosome mapping. J Mol Biol. 2012;417(3):152–64.

[345] Dingwall C, Lomonossoff GP, Laskey RA. High sequence specificity of micrococcal nuclease. Nucleic Acids Res. 1981;9(12):2659–73.

[346] Horz W, Altenburger W. Sequence specific cleavage of DNA by micrococcal nuclease. Nucleic Acids Res. 1981;9(12):2643–58.

[347] Zhou X, Maricque B, Xie M, Li D, Sundaram V, Martin EA, et al. The human epigenome browser at Washington University. Nature Methods;8(12):989–990.

[348] Thorvaldsdottir H, Robinson JT, Mesirov JP. Integrative Genomics Viewer (IGV): high-performance genomics data visualization and exploration. Brief Bioinform. 2013;14(2):178–92.

[349] O'Connor L, Gilmour J, Bonifer C. The Role of the Ubiquitously Expressed Transcription Factor Sp1 in Tissue-specific Transcriptional Regulation and in Disease. Yale J Biol Med. 2016;89(4):513–525.

[350] Zhou G, Wang J, Zhao M, Xie TX, Tanaka N, Sano D, et al. Gain-of-function mutant p53 promotes cell growth and cancer cell metabolism via inhibition of AMPK activation. Mol Cell. 2014;54(6):960–74.

[351] Yahagi N, Shimano H, Matsuzaka T, Najima Y, Sekiya M, Nakagawa Y, et al. p53 Activation in adipocytes of obese mice. J Biol Chem. 2003;278(28):25395–400.

[352] Buzzai M, Jones RG, Amaravadi RK, Lum JJ, DeBerardinis RJ, Zhao F, et al. Systemic treatment with the antidiabetic drug metformin selectively impairs p53-deficient tumor cell growth. Cancer Res. 2007;67(14):6745–52.

[353] Hardie DG, Pan DA. Regulation of fatty acid synthesis and oxidation by the AMP-activated protein kinase. Biochem Soc Trans. 2002;30(Pt 6):1064–70.

[354] Fediuc S, Gaidhu MP, Ceddia RB. Regulation of AMP-activated protein kinase and acetyl-CoA carboxylase phosphorylation by palmitate in skeletal muscle cells. J Lipid Res. 2006;47(2):412–20.

[355] Schubeler D, Lorincz MC, Cimbora DM, Telling A, Feng YQ, Bouhassira EE, et al. Genomic targeting of methylated DNA: influence of methylation on transcription, replication, chromatin structure, and histone acetylation. Mol Cell Biol. 2000;20(24):9103–12.

[356] Irvine RA, Lin IG, Hsieh CL. DNA methylation has a local effect on transcription and histone acetylation. Molecular and Cellular Biology. 2002;22(19):6689–6696.

[357] Jones PL, Veenstra GJ, Wade PA, Vermaak D, Kass SU, Landsberger N, et al. Methylated DNA and MeCP2 recruit histone deacetylase to repress transcription. Nat Genet. 1998;19(2):187–91.

[358] Nan X, Ng HH, Johnson CA, Laherty CD, Turner BM, Eisenman RN, et al. Transcriptional repression by the methyl-CpG-binding protein MeCP2 involves a histone deacetylase complex. Nature. 1998;393(6683):386–9.

[359] Kimura H, Shiota K. Methyl-CpG-binding protein, MeCP2, is a target molecule for maintenance DNA methyltransferase, Dnmt1. Journal of Biological Chemistry. 2003;278(7):4806–4812.

[360] Song J, Ugai H, Kanazawa I, Sun K, Yokoyama KK. Independent repression of a GC-rich housekeeping gene by Sp1 and MAZ involves the same cis-elements. J Biol Chem. 2001;276(23):19897–904.

[361] Schroeder A, Mueller O, Stocker S, Salowsky R, Leiber M, Gassmann M, et al. The RIN: an RNA integrity number for assigning integrity values to RNA measurements. BMC Mol Biol. 2006;7:3.

[362] Bolstad BM, Irizarry RA, Astrand M, Speed TP. A comparison of normalization methods for high density oligonucleotide array data based on variance and bias. Bioinformatics. 2003;19(2):185–93.

[363] Tusher VG, Tibshirani R, Chu G. Significance analysis of microarrays applied to the ionizing radiation response. Proc Natl Acad Sci U S A. 2001;98(9):5116–21.

[364] Higdon R, van Belle G, Kolker E. A note on the false discovery rate and inconsistent comparisons between experiments. Bioinformatics. 2008;24(10):1225–8.

[365] Gao X, Song PX. Nonparametric tests for differential gene expression and interaction effects in multi-factorial microarray experiments. BMC Bioinformatics. 2005;6:186.

[366] Wiame I, Remy S, Swennen R, Sagi L. Irreversible heat inactivation of DNase I without RNA degradation. Biotechniques. 2000;29(2):252–+.

[367] Vandesompele J, De Preter K, Pattyn F, Poppe B, Van Roy N, De Paepe A, et al. Accurate normalization of real-time quantitative RT-PCR data by geometric averaging of multiple internal control genes. Genome Biol. 2002;3(7):RESEARCH0034.

[368] Valceckiene V, Kontenyte R, Jakubauskas A, Griskevicius L. Selection of reference genes for quantitative polymerase chain reaction studies in purified B cells from B cell chronic lymphocytic leukaemia patients. Br J Haematol. 2010;151(3):232–8.

[369] Ledderose C, Heyn J, Limbeck E, Kreth S. Selection of reliable reference genes for quantitative real-time PCR in human T cells and neutrophils. BMC Res Notes. 2011;4:427.

[370] Illumina. Technical Note: RNA Analysis. Gene Expression Microarray Data Quality Control [Document on Internet]; 2010.

[371] Hellemans J, Mortier G, De Paepe A, Speleman F, Vandesompele J. qBase relative quantification framework and software for management and automated analysis of real-time quantitative PCR data. Genome Biol. 2007;8(2):R19.

[372] Schmid M, Gemperle C, Rimann N, Hersberger M. Resolvin D1 Polarizes Primary Human Macrophages toward a Proresolution Phenotype through GPR32. J Immunol. 2016;196(8):3429–37.

[373] Sapieha P, Stahl A, Chen J, Seaward MR, Willett KL, Krah NM, et al. 5-Lipoxygenase Metabolite 4-HDHA Is a Mediator of the Antiangiogenic Effect of omega-3 Polyunsaturated Fatty Acids. Science Translational Medicine. 2011;3(69).

[374] Alimonti JB, Ball TB, Fowke KR. Mechanisms of CD4+ T lymphocyte cell death in human immunodeficiency virus infection and AIDS. J Gen Virol. 2003;84(Pt 7):1649–61.

[375] Nichols JE, Niles JA, Roberts J N J. Human lymphocyte apoptosis after exposure to influenza A virus. J Virol. 2001;75(13):5921–9.

[376] Barber GN. Host defense, viruses and apoptosis. Cell Death Differ. 2001;8(2):113–26.

[377] Zhou X, Jiang W, Liu Z, Liu S, Liang X. Virus Infection and Death Receptor-Mediated Apoptosis. Viruses. 2017;9(11).

[378] Spieker-Polet H, Polet H. Requirement of a combination of a saturated and an unsaturated free fatty acid and a fatty acid carrier protein for in vitro growth of lymphocytes. J Immunol. 1981;126(3):949–54.

[379] Okazaki T, Iwasaki T, Fukuoka A, Suzuki M, Katagiri H, Okano T, et al. Effects of albumin-bound-fatty acids on the growth of the human T lymphoblastic cell line Jurkat. In Vitro Cell Dev Biol Anim. 2011;47(9):615–7.

[380] Olivier M, Hollstein M, Hainaut P. TP53 Mutations in Human Cancers: Origins, Consequences, and Clinical Use. Cold Spring Harbor Perspectives in Biology. 2010;2(1).

[381] Kandoth C, McLellan MD, Vandin F, Ye K, Niu BF, Lu C, et al. Mutational landscape and significance across 12 major cancer types. Nature. 2013;502(7471):333–+.

[382] Zilfou JT, Lowe SW. Tumor suppressive functions of p53. Cold Spring Harb Perspect Biol. 2009;1(5):a001883.

[383] Shin S, Jing K, Jeong S, Kim N, Song KS, Heo JY, et al. The omega-3 polyunsaturated fatty acid DHA induces simultaneous apoptosis and autophagy via mitochondrial ROS-mediated Akt-mTOR signaling in prostate cancer cells expressing mutant p53. Biomed Res Int. 2013;2013:568671.

[384] Sam MR, Tavakoli-Mehr M, Safaralizadeh R. Omega-3 fatty acid DHA modulates p53, survivin, and microRNA-16-1 expression in KRAS-mutant colorectal cancer stem-like cells. Genes Nutr. 2018;13:8.

[385] Jeong S, Jing K, Kim N, Shin S, Kim S, Song KS, et al. Docosahexaenoic acid-induced apoptosis is mediated by activation of mitogen-activated protein kinases in human cancer cells. Bmc Cancer. 2014;14.

[386] Tang HH, Ji F, Sun J, Xie Y, Xu YY, Yue HT. RBEL1 is required for osteosarcoma cell proliferation via inhibiting retinoblastoma 1. Molecular Medicine Reports. 2016;13(2):1275–1280.

[387] Hagen J, Muniz VP, Falls KC, Reed SM, Taghiyev AF, Quelle FW, et al. RABL6A promotes G1-S phase progression and pancreatic neuroendocrine tumor cell proliferation in an Rb1-dependent manner. Cancer Res. 2014;74(22):6661–70.

[388] Li Y, Buijs-Gladdines JG, Cante-Barrett K, Stubbs AP, Vroegindeweij EM, Smits WK, et al. IL-7 Receptor Mutations and Steroid Resistance in Pediatric T cell Acute Lymphoblastic Leukemia: A Genome Sequencing Study. PLoS Med. 2016;13(12):e1002200.

[389] Ye J, DeBose-Boyd RA. Regulation of cholesterol and fatty acid synthesis. Cold Spring Harb Perspect Biol. 2011;3(7).

[390] Hannah VC, Ou J, Luong A, Goldstein JL, Brown MS. Unsaturated fatty acids down-regulate srebp isoforms 1a and 1c by two mechanisms in HEK-293 cells. J Biol Chem. 2001;276(6):4365–72.

[391] Zhang Y, Yang H, Guo X, Rong N, Song Y, Xu Y, et al. The PHD1 finger of KDM5B recognizes unmodified H3K4 during the demethylation of histone H3K4me2/3 by KDM5B. Protein Cell. 2014;5(11):837–50.

[392] Johansson C, Velupillai S, Tumber A, Szykowska A, Hookway ES, Nowak RP, et al. Structural analysis of human KDM5B guides histone demethylase inhibitor development. Nat Chem Biol. 2016;12(7):539–45.

[393] Illingworth RS, Gruenewald-Schneider U, Webb S, Kerr AR, James KD, Turner DJ, et al. Orphan CpG islands identify numerous conserved promoters in the mammalian genome. PLoS Genet. 2010;6(9):e1001134.

[394] Mikkelsen TS, Ku M, Jaffe DB, Issac B, Lieberman E, Giannoukos G, et al. Genome-wide maps of chromatin state in pluripotent and lineage-committed cells. Nature. 2007;448(7153):553–60.

[395] Guenther MG, Levine SS, Boyer LA, Jaenisch R, Young RA. A chromatin landmark and transcription initiation at most promoters in human cells. Cell. 2007;130(1):77–88.

[396] Yang C, Bolotin E, Jiang T, Sladek FM, Martinez E. Prevalence of the initiator over the TATA box in human and yeast genes and identification of DNA motifs enriched in human TATA-less core promoters. Gene. 2007;389(1):52–65.

[397] Yang YH, Lin WY, Lee WC. A Fuzzy Permutation Method for False Discovery Rate Control. Sci Rep. 2016;6:28507.

[398] McCarthy DJ, Smyth GK. Testing significance relative to a fold-change threshold is a TREAT. Bioinformatics. 2009;25(6):765–71.

[399] Peng X, Wood CL, Blalock EM, Chen KC, Landfield PW, Stromberg AJ. Statistical implications of pooling RNA samples for microarray experiments. BMC Bioinformatics. 2003;4:26.

[400] Ceccarelli V, Nocentini G, Billi M, Racanicchi S, Riccardi C, Roberti R, et al. Eicosapentaenoic acid activates RAS/ERK/C/EBPbeta pathway through H-Ras intron 1 CpG island demethylation in U937 leukemia cells. PLoS One. 2014;9(1):e85025.

[401] Xiang Y, Zhu Z, Han G, Ye X, Xu B, Peng Z, et al. JARID1B is a histone H3 lysine 4 demethylase up-regulated in prostate cancer. Proceedings of the National Academy of Sciences of the United States of America. 2007;104(49):19226–19231.

[402] Waby JS, Bingle CD, Corfe BM. Post-translational control of sp-family transcription factors. Curr Genomics. 2008;9(5):301–11.

[403] Waalwijk C, Flavell RA. MspI, an isoschizomer of hpaII which cleaves both unmethylated and methylated hpaII sites. Nucleic Acids Res. 1978;5(9):3231–6.